Oncolytic Virotherapy for the Treatment of Non-Hodgkin Lymphoma

Matthew Holmes

Submitted in accordance with the requirements for the degree of Doctor of Philosophy

The University of Leeds

School of Medicine

November 2018

The candidate confirms that the work submitted is his own and that appropriate credit has been given where reference has been made to the work of others.

Chapter 1 Preface

1.1 Acknowledgements

I would like to extend my utmost gratitude to Drs Fiona Errington-Mais and Gina Scott, and Professor Alan Melcher for their guidance, advice and patience. Thank you for your help and for giving me so many opportunities to expand my career. I would also like to thank the members of Level 5 for their help, advice and friendship throughout the last 3 years. I would especially like to thank Rob Berkeley for making my time in the lab as enjoyable as the time outside. My best wishes to you and Vaila for the rest of your lives. Thank you to my family for all their support, especially during the write up. Lastly, thank you to Louise for making this PhD some of the best years of my life: *Utan dig skulle dagens känslor endast vara döda huden av gårdagens känslor*.

1.2 Abstract

Non-Hodgkin Lymphoma (NHL) is a diverse group of more than 80 predominantly B cell cancers of the lymphatic system. Poor survival rates in aggressive subsets, the transformation of indolent subsets into aggressive forms, and the emergence of therapy-resistance warrants research into novel therapies. Oncolytic viruses (OV) preferentially replicate in and kill malignant cells. Here we investigate the efficacy of two OV, reovirus Type 3 Dearing and Coxsackievirus Type A21 (CVA21), against NHL cell lines and primary patient samples, examine the role of the tumour microenvironment in virus susceptibility, characterise the cellular determinants of CVA21 infection of malignant cells and test the ability of both viruses to potentiate an immune response against NHL, alone or in combination with monoclonal antibodies (mAbs).

CD40L on T cells can signal through CD40 on NHL B cells, resulting in pro-survival signals that induce resistance to standard chemotherapy. CD40L stimulation induced vincristine resistance in NHL cell lines but enhanced CVA21-induced cell death, implying a role for CVA21 in targeting drug-resistant NHL cells. CD40L stimulation and had no effect on reovirus-induced cell death.

To investigate possible determinants of CVA21 susceptibility, the effects of the interferon (IFN) response and mTOR pathway on CVA21-induced cell death of NHL cells were investigated. Despite possessing an intact IFN response, NHL cell lines remained susceptible to CVA21 infection, suggesting that CVA21 may utilise mechanisms to subvert the antiviral IFN response. Moreover, mTOR inhibition by rapamycin reduced CVA21-induced cell death in NHL cell lines, demonstrating the importance of mTOR signalling for CVA21-induced cell death.

MAbs bind to their cognate antigen and mark cells for destruction by immune cells and have shown promising results in combination with OV in a variety of malignancies. Anti-CD20 antibodies, such as rituximab, target CD20 on NHL cells and are being investigated in combination with OV for haematological malignancies, such as Chronic Lymphocytic Leukaemia (CLL). CVA21, reovirus and our candidate anti-CD20 antibody, BHH2, induced NK cell recognition of NHL cell lines as single agents. This targeting was enhanced in some cell lines when either virus was used in combination with BHH2, outlining a potential role for an OV-mAb combination for the

treatment of NHL. Importantly, CD40L stimulation and the induction of a drug-resistant phenotype did not impair recognition of NHL cell lines by OV activated NK cells.

The results reported here outline a promising role for CVA21, but not reovirus, as a potent lytic agent against NHL cells. This data also implicates both reovirus and CVA21 as potent immunogenic agents that can induce NK cell targeting of NHL cell lines alone and in combination with anti-CD20 mAbs.

1.3 Table of Contents

1.4 List of Tables

1.5 Table of Figures

1.6 List of Abbreviations

Abbreviation	Definition
4EBP1	Eukaryotic translation initiation factor 4E-binding protein 1
ADCC	Antibody-Dependent Cellular Cytotoxicity
ADCP	Antibody-Dependent Cellular Phagocytosis
AID	Activation-Induced Cytidine Deaminase
AIDS	Acquired Immunodeficiency Syndrome
ALL	Acute Lymphocytic Leukaemia
ALTCL	Anaplastic Large T Cell Lymphoma
AML	Acute Myeloid Leukaemia
ANOVA	Analysis of Variance
APC	Allophycocyanin (fluorochrome)
APC	Antigen Presenting Cell
ATCC	American Type Culture Collection
ATM	Ataxia telangiectasia mutated
B-NHL	B cell Non-Hodgkin's Lymphoma
BCR	B Cell Receptor
BL	Burkitt's Lymphoma
BSA	Bovine Serum Albumin
CD	Cluster of Differentiation
CDC	Complement-dependent cytotoxicity
CFSE	Carboxyfluorescein Succinimidyl Ester
CHL	Classical Hodgkin Lymphoma
CHO	Chinese Hamster Ovary
CLL	Chronic Lymphocytic Leukaemia
CM	Conditioned media

CMC	Carboxymethylcellulose
CNS	Central Nervous System
CO_2	Carbon Dioxide
CPE	Cytopathic Effect
CVA21	Coxsackievirus Type A21
CVB3	Coxsackievirus Type B3
DAF	Decay-Accelerating Factor
DEPTOR	DEP domain-containing mTOR-interacting protein
DLBCL-ABC	Diffuse Large B Cell Lymphoma-Activated B cell subset
DLBCL-GCB	Diffuse Large B Cell Lymphoma-Germinal Centre B cell subset
DMEM	Dulbecco's Modified Eagles Medium
DMSO	Dimethyl sulphoxide
DNA	Deoxyribonucleic Acid
DNAM-1	DNAX Accessory Molecule-1
DSMZ	Deutsche Sammlung von Mikroorganismen und Zellkulturen
dsRNA	Double-stranded RNA
EBL	Endemic Burkitt's Lymphoma
EBV	Epstein-Barr Virus
ECTV	Ectromelia Virus
EGFr	Epidermal Growth Factor receptor
eIF4E	Eukaryotic translation initiation factor 4E
eIF4F	Eukaryotic initiation factor 4F
ELISA	Enzyme-Linked Immunosorbent Assay
FACS	Fluorescence Activated Cell Sorting
Fas	First apoptosis signal

FasL	Fas Ligand
Fc	Fragment Crystallizable
FCS	Foetal Calf Serum
FITC	Fluorescein Isothyocyanate (fluorochrome)
FIV	Feline Immunodeficiency Virus
FL	Follicular Lymphoma
FMDV	Foot and Mouth Disease Virus
FSC	Forward Scatter
g	Grams
g	Gravitational Force
G-CSF	Granulocyte Colony-Stimulating Factor
GC	Germinal Centre
GBM	Glioblastoma Multiforme
GM-CSF	Granulocyte-Macrophage Colony-Stimulating Factor
Gy	Gray
HBSS	Hanks Balanced Salt Solution
HeLa	Henrietta Lacks cells
HER2	Human Epidermal Growth Factor Receptor 2
HFMDV	Hand, Foot and Mouth Disease Virus
HIV	Human Immunodeficiency Virus
HLA	Human Leukocyte Antigen (see MHC)
HM	Haematological Malignancy
HMDS	Haematological Malignancy Diagnostic Service
HNSCC	Head and Neck Squamous Cell Carcinoma
HRP	Horseradish Peroxidase
hrs	Hours

HSV-1	Herpes Simplex Virus-1
HVEM	Herpesvirus Entry Mediator
ICAM-1	Intercellular Adhesion Molecule 1
ICP 34.5	Infected cell protein 34.5
ICP 6	Infected Cell Protein 6
IFN	Interferon
IFN-α	Interferon alpha
IFN-β	Interferon beta
IFN-γ	Interferon gamma
IL	Interleukin
IPS1	Induced by Phosphate Starvation1
IRF-7	Interferon Regulatory Factor 7
ISG	Interferon-Stimulated Genes
IT	Intratumoural
JAM-A	Junctional Adhesion Molecule-A
KIR	Killer cell Immunoglobulin-like Receptor
KL	Kit Ligand
LFA-1	Lymphocyte Function-associated Antigen 1
LICAP	Leeds Institute of Cancer and Pathology
LMP2A	Latent Membrane Protein 2A
LN	Lymph node
LN_2	Liquid Nitrogen
LNMC	Lymph Node Mononuclear Cell
M-CSF	Macrophage Colony-Stimulating Factor
mAb	Monoclonal Antibody
MAC	Membrane Attack Complex

MCL	Mantle Cell Lymphoma
MDA-5	Melanoma Differentiation-Associated protein 5
MICA/N	MHC class I polypeptide-related sequence
MIP-1α	Macrophage-Inhibitory Protein-1α
MFI	Mean Fluorescence Intensity
MHC	Major Histocompatibility Complex (see HLA)
mins	Minutes
mLST8	Mammalian Lethal with SEC13 Protein 8
mSIN1	Mammalian stress-activated protein kinase interacting protein 1
MTOR	Mechanistic Target of Rapamycin
MTORC1	Mechanistic Target of Rapamycin Complex 1
MTORC2	Mechanistic Target of Rapamycin Complex 2
MZL	Marginal Zone Lymphoma
NDV	Newcastle Disease Virus
NFκB	Nuclear Factor Kappa-Light-Chain-Enhancer of Activated B Cells
NHL	Non-Hodgkin Lymphoma
NK Cells	Natural Killer Cells
NSCLC	Non-small-cell lung carcinoma
OAS-1	Oligoadenylate synthetase 1
^{o}C	Degrees centigrade
OV	Oncolytic Virus(es)
P/S	Penicillin and Streptomycin
p-STAT1	Phosphorylated Signal Transducer and Activator of Transcription 1
PAMPs	Pathogen Associated Molecular Patterns

PBMC	Peripheral Blood Mononuclear Cell
PBS	Phosphate Buffered Saline
PCR	Polymerase Chain Reaction
PD-1	Programmed Death Receptor 1
PD-L1	Programmed Death Ligand 1
pDC	Plasmacytoid Dendritic cell
PE	Phycoerythrin (fluorochrome)
PERCP	Peridinin chlorophyll protein (fluorochrome)
PFA	Paraformaldehyde
PFU	Plaque Forming Units
PFU/mL	Plaque Forming Units per millilitre
pg/mL	Picograms per millilitre
PKC	Protein Kinase C
PKR	Protein Kinase R
PI	Propidium Iodide
PI3K	Phosphatidylinositol 3-Kinase
pNpp	P-nitrophenyl phosphate
PRAS40	Proline-rich AKT substrate of 40 kDa
PROTOR	Protein observed with Rictor
PRR	Pattern Recognition Receptor
PVR	Poliovirus Receptor
R-CHOP	Rituximab, Cyclophosphamide, Hydroxydaunorubicin, Oncovin, Prednisolone
Raptor	Regulatory-associated protein of mTOR
Ras	Rat sarcoma viral oncogene
Rb	Retinoblastoma protein

rhIFN-α	Recombinant Human IFN-α
RICTOR	Rapamycin-insensitive companion of mammalian target of rapamycin
RNA	Ribonucleic Acid
RPM	Rotations per Minute
RPMI 1640	Roswell Park Memorial Institute 1640 medium
RSV	Respiratory syncytial virus
S6K	S6 Kinase
SBL	Sporadic Burkitt's Lymphoma
SBS	St. James' Biomedical Service
SCC	Squamous Cell Carcinoma
SCID	Severe Combined Immunodeficiency
SEM	Standard Error of the Mean
SJUH	St. James University Hospital
SSC	Side Scatter
ssRNA	Single-stranded RNA
STAT	Signal Transducer and Activator of Transcription
STR	Short Tandem Repeat
T-VEC	Talimogene Laherparepvec
TBS	Tris-buffered saline
$TCID_{50}$	50% Tissue culture Infective Dose
TCR	T Cell Receptor
TLR	Toll-Like Receptor
TME	Tumour Microenvironment
TNF-α	Tumour Necrosis Factor-α
TRAIL	TNF-related apoptosis-inducing ligand

Treg	Regulatory T cell
TRIF	TIR-domain-containing adapter-inducing interferon-β
TRIM5α	Tripartite Motif-containing protein 5-α
UKCCCR	United Kingdom Co-ordinating Committee on Cancer Research
ULBP-1	UL16 binding protein 1
UV	Ultraviolet
v/v	volume/volume
VCAM-1	Vascular Cell Adhesion Molecule-1
VSV	Vesicular stomatitis virus
WST-1	Water-Soluble Tetrazolium 1

Chapter 2:
Introduction

Chapter 2

2.1 Haematopoiesis and B cell Development

The human body consists of a diverse range of cell types, each with specific characteristics and functions. Cells can form solid tissues such as muscle, skin and organs, or can exist individually in suspension, such as haematological (blood) cells. Blood is composed of red blood cells for transporting oxygen throughout the body, and white blood cells that are primarily responsible for defending the body from infection through innate mechanisms that can occur immediately upon contact with the infection, or adaptive mechanisms that require pre-exposure to the infection to allow the priming of a specific, targeted response. The human body can generate a diverse arsenal of blood cells from a common progenitor (haematopoietic stem cell) that must undergo a complex process of differentiation and maturation to become a specific cell type, such as B cells and T cells. These cells can undergo further maturation and differentiation, upon contact with specific pathogens or foreign material, resulting in clones of cells that are reactive to specific infections.

B cells are a vital member of the human immune system, that can differentiate into a multitude of cell clones that protect against specific pathogens through the recognition of pathogenic antigens. B cells exert their protective effect by producing huge quantities of proteins called antibodies or immunoglobulins (Igs), that bind to very specific regions on antigens. These antibodies can act in several ways to interfere with the activity of the pathogen, such as binding to and directly blocking target viruses, and binding to target pathogens and marking them for destruction by other immune cells. For B cells to achieve the heterogeneity that is required to target the diverse onslaught of pathogens that threaten the host body, they must be capable of undergoing a series of differentiation steps that introduce extreme variability into their Igs, thus expanding their targeting abilities.

B cells begin in the bone marrow as progenitors to fully matured B cells. In the bone marrow, these B cell progenitors undergo genetic rearrangement of their Ig locus, resulting in the first stages of varying their Igs, and the production of a B cell receptor that is a surface-bound Ig. A selection process targets B cells that react with host antigens, prohibiting the

generation of an autoreactive clone. Upon completion of this phase, these immature B cells leave the bone marrow and travel to secondary lymphoid tissues, such as the spleen and lymph nodes, where the antigen to which they react is presented to them by antigen-presenting cells. This contact with their cognate antigen, as well as co-stimulatory signals from T cells, results in further variability of the Ig locus by a process known as somatic hypermutation, allowing clones with stronger and weaker reactivity to be generated. The weaker responders are selected out of the population by further clonal deletion, and the optimal B cell clone is allowed to proceed with its maturation into a mature plasma cell, that produces Ig, or a memory B cell, that monitors the body in preparation for re-exposure to their cognate antigen. A more detailed account of B cell differentiation is available from Hardy and Hayakawa (Hardy and Hayakawa, 2001).

2.2 The Development of Cancer

Cancer is characterised by the uncontrolled proliferation and immortality of a clone of cells that can outgrow other cell populations, spread throughout the body and destroy the patient's immune system and organs. While the root cause of cancer can be due to a combination of hereditary and acquired factors, DNA plays a crucial role in facilitating the transformation of healthy cells into malignant. Genetic changes can include the loss of genes that slow cell cycle or facilitate cell death, or the over-expression of genes the promote cell division and survival. Most nucleated cells can develop into malignant cells, forming solid cancers, such as skin cancer, liver cancer and breast cancer, or haematological malignancies, such as leukaemia or lymphoma, where a clone of the patient's white blood cells outgrows their non-transformed counterparts and spreads throughout the body. While huge progress has been made in the last century for the treatment of cancer, increasing incidence of these diseases and the emergence of cases that resist current therapies elevates the need for research into novel areas of therapeutic intervention.

One such process that is frequently manipulated in cancer is programmed cell death or apoptosis, whereby a cell, in response to infection, stress or irreparable damage, will undergo a form of highly-coordinated suicide (Elmore, 2007). Apoptosis prevents pathogens from exploiting living cells and spreading, and prevents damaged cells from growing and dividing, reducing the chances of transforming into cancerous cells. Cancer, however, can arise when mutations occur in pathways and proteins that control

apoptosis, such as the deletion of a pro-apoptotic genes, such as Bcl-2-like protein 11 (BIM) and p53 upregulated modulator of apoptosis (PUMA), which can be downregulated in Burkitt's Lymphoma (Fitzsimmons et al., 2017), or the amplification of anti-apoptotic ones, such as members of the B-cell lymphoma 2 (BCL-2) family of proteins which as overexpressed in a variety of solid and haematological malignancies, such as leukaemias and lymphomas (Reed, J.C., 2017). This results in a cell clone that is more resistant to pro-apoptotic signals and more difficult to kill. Recent cancer therapy research has involved a focus on treatments that overcome the anti-apoptotic state in cancer cells, such as BH3 mimetics like Obatoclax that blocks BCL-2 and renders the cancer cells more sensitive to apoptotic cell death (Baig et al., 2016).

2.3 Non-Hodgkin's Lymphoma

2.3.1 Background

Non-Hodgkin Lymphoma (NHL) is a diverse group of predominantly B cell cancers of the lymphatic system that affected over 13,000 people in the UK in 2015, accounting for 4% of the total number of cancer cases (CRUK, 2018). NHLs range from indolent or "slow-growing", such as follicular lymphoma (FL) and small lymphocytic lymphoma, to aggressive or "fast-growing", such as Burkitt's lymphoma (BL), Diffuse Large B Cell Lymphoma-Germinal Centre B cell (DLBCL-GCB) subset and Diffuse Large B Cell Lymphoma-Activated B cell (DLBCL-ABC) subset. However, this binary system of classification is not definitive as some individual cases of indolent NHL can be highly aggressive or can transform from an indolent to a more aggressive form (Correia et al., 2015). Likewise, some cases of otherwise aggressive subsets may present with a slower rate of progression and a more favourable survival (Menon et al., 2012), demonstrating the heterogeneity of this class of diseases. The factors associated with disease progression depend on the specific NHL subset and the tumour characteristics. These can include the presence of chromosomal aberrations, such as the t(14:18)(q32:q21) translocation in FL which conveys constitutive expression of the anti-apoptotic protein BCL-2, or the 3q27 rearrangement in DLBCL which causes the over-expression of BCL-6 (Ong and Le Beau, 1998). BCL-6 is a transcriptional repressor that prevents premature activation and differentiation of germinal centre (GC) B cells during their development, and suppresses p53 expression, allowing the cells

to tolerate DNA breaks during chromosomal rearrangements (Basso and Dalla-Favera, 2012).

Other factors, such as expression of the CD20 antigen (Bellesso et al., 2011) bone marrow (BM) infiltration (Beider et al., 2013), and expression of the anti-apoptotic protein, Mantle Cell Lymphoma 1 (MCL-1), are commonly associated with poor prognosis in DLBCL-ABC (Wenzel et al., 2013). Mutations in the RAS–RAF–MEK–ERK–MAP kinase pathway, which are associated with enhancing the proliferation of cancer types such as pancreatic cancer, lung cancer and leukaemia (Bos, 1989), are also present in some cases of DLBCL (Lee, J.W. et al., 2003).

NHLs are predominantly B cell in nature; however, some rare cases are composed of malignant T cells or Natural Killer (NK) cells such as anaplastic large cell lymphoma and blastic NK cell lymphoma. These forms of NHL are rare and together comprise only 10-15% of NHL cases in the Western world (American Cancer Society, 2017). To demonstrate the variety of subtypes of NHL, a pie chart showing the proportions of NHL subtypes is shown in Figure 2-1.

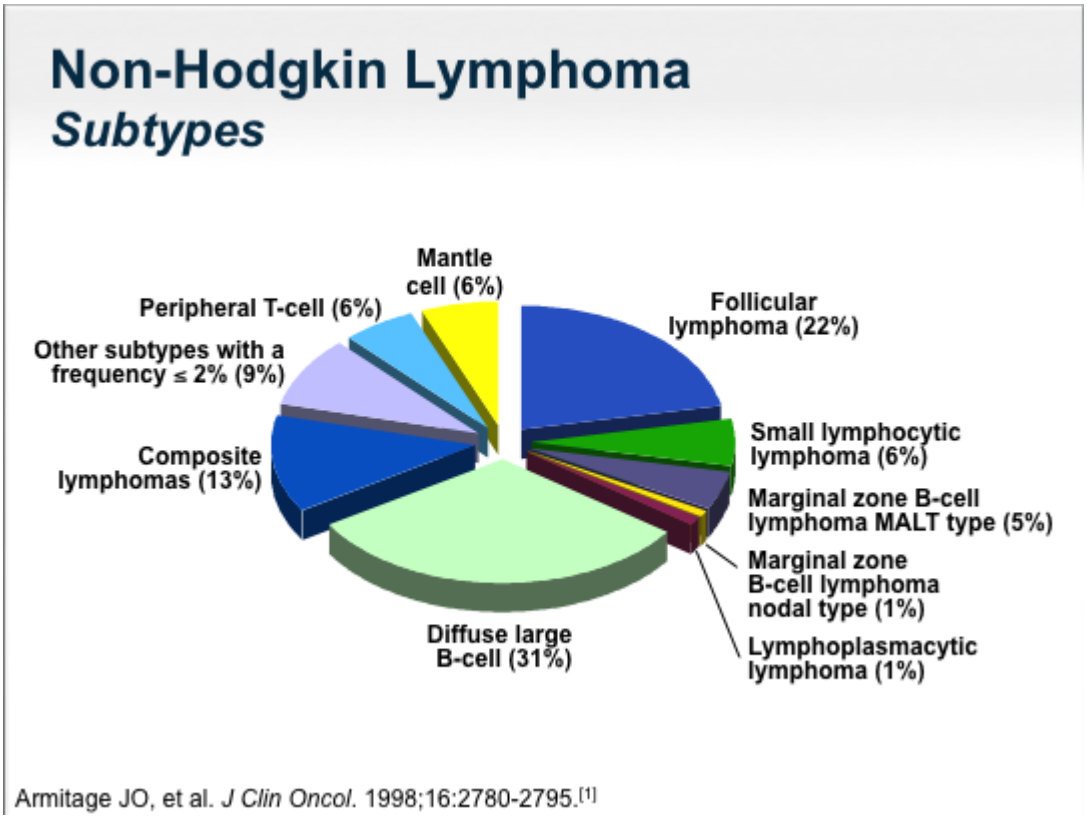

Figure 2-1: Prevalence of NHL subtypes.

DLBCL and FL represent large groups of NHL cases (31% and 22%, respectively), and a variety of other subtypes are present at lower frequencies, such as MCL (6%) and Marginal Zone B cell lymphoma nodal type (1%). Although not all subsets are represented on this chart, it demonstrates the heterogeneity of this group of diseases (Armitage and Weisenburger, 1998).

NHL is typically classified at diagnosis as being at one of four stages, depending on the degree to which malignant cells have spread throughout the body. This staging system is termed the Cotswold system (formerly the Ann Arbor Staging System) and is described in **Table 2-1**.

Stage	Characteristics
I	Lymphomas that are restricted to one lymph node (LN)
II	Lymphomas that have spread to other LN on the same side (above or below) the diaphragm
III	Lymphomas that have spread to other LN on both sides of the diaphragm
IV	Lymphomas that have spread outside of the lymphatic system to an organ that is not immediately associated with a malignant LN

Table 2-1 Description of NHL staging criteria.

The stage denoted to a patient with NHL typically reflects the location(s) in the body to which the malignant cells have spread (Izumi and Ozawa, 2000).

Stage IV lymphomas can also include disease that has spread to the BM or the central nervous system (CNS). CNS involvement is more common in aggressive NHL, such as BL, and is associated with poor patient survival (Hollender et al., 2002). Most diagnoses occur at Stages III and IV (Ansell, 2015) which can be detrimental to the patient's prognosis due to the advanced spread of the disease. Detection at earlier stages is associated with better prognosis (Fields and Wrench, 2015), allowing monitoring of disease progression and early treatment.

Historically, the emergence of NHL as a class of diseases arose from a study of Hodgkin's Lymphoma (HL) patients where some patients did not present with the typical characteristics of HL, such as Reed-Sternberg cells, huge infiltration of immune cells and an ordered lymph node – by – lymph node progression. These diseases were first acknowledged by Henry Rappaport in 1956 who aimed to classify lymphomas other than Hodgkin's (Lukes and Collins, 1975). Since then, several methods of classifying NHL have been developed, resulting in the World Health Organisation classifying NHLs as B cell or T/NK cell in origin, and the diagnosis of specific subtypes being derived from a variety of genetic and immunophenotypic findings (Good and Gascoyne, 2008), as well as the maturation stage of the cell of origin. The classification of NHLs, based on their stage in B cell differentiation, will be discussed in more detail in section 2.3.6.

2.3.2 Burkitt's Lymphoma

BL is a highly aggressive subset of B cell NHL that can be classified as endemic (eBL), which is associated with Epstein-Barr Virus (EBV) infection and malaria in Africa, or sporadic (sBL) which only has a 1-2% association with EBV. Human Immunodeficiency Virus (HIV)-associated BL is another classification and is associated with the loss of a functioning immune system due to HIV infection in Acquired Immunodeficiency Syndrome (AIDS) patients (Brady et al., 2007). The development of eBL requires the complementary activity of the malaria parasite, *Plasmodium falciparum*, and the EBV virus and, as a result, accounts for very few cases in the UK. *Plasmodium falciparum* induces the production of Activation-induced Cytidine Deaminase (AID) in GC B cells, which promotes genetic rearrangement, translocations and DNA damage. This process is complemented by EBV's ability to prevent DNA repair by blocking p53 activity. Taken together, this suggests a complex relationship between a pathogen that promotes DNA damage in GC B cells and a pathogen that prevents DNA repair, giving rise to DNA mutation-prone B cells and a

greater risk of developing BL (Thorley-Lawson et al., 2016). Most BL cases in the UK and Western world are sBL and are treated with rituximab-based (αCD20 monoclonal antibody (mAb)) chemotherapy regimens with promising survival rates reported (Hoelzer et al., 2012), (Barnes et al., 2011). BL can develop resistance, leading to relapse (Pineda et al., 2015), emphasising the need for new therapies.

2.3.3 Diffuse Large B Cell Lymphoma

DLBCL is the most commonly diagnosed form of NHL in the Western world, accounting for 30-40% of all NHL diagnoses (De Paepe and De Wolf-Peeters, 2007). DLBCL is characterised by the presence of malignant B cells and may present as the GCB subtype, comprised of malignant centroblasts (Sehn and Gascoyne, 2015), or the more aggressive ABC subtype, comprised of B cells that have arrested during their differentiation into plasma cells and transformed (Perry et al., 2012). DLBCL-ABC is less responsive to current standard of care (Alizadeh et al., 2000), warranting research into novel mechanisms of therapeutic intervention.

In the majority of cases, the cause of NHL is unknown, however, >30% of DLBCL-GCB cases present with a translocation between chromosomes 14 and 18 (t(14:18)), which induces overexpression of BCL-2 (Iqbal et al., 2004). Interestingly, despite the fact that there are no recorded cases of DLBCL-ABC that present with the t(14:18) translocation, BCL-2 is upregulated by enhanced activation of the Nuclear Factor Kappa-Light-Chain-Enhancer of Activated B Cells (NFkB) pathway that is characteristic of this disease (Davis et al., 2001). Upregulation of NFkB is associated with mutations in multiple genes, including the NFkB negative-regulator, *A20,* which is mutated or deleted in ~30% of DLBCL-ABC cells (Compagno et al., 2009). Overexpression of the anti-apoptotic protein, MCL-1, is also commonly associated with aggressive DLBCL-ABC (Wenzel et al., 2013). Elevated expression of anti-apoptotic proteins, such as BCL-2 and MCL-1, induce resistance to chemotherapy and, as such, are detrimental to the success of NHL treatments (Mounier et al., 2003), (Phillips et al., 2015).

2.3.4 Follicular Lymphoma

FL, the second most common NHL in the Western world, is classically indolent and accounts for 20-30% of all NHL (Ciobanu et al., 2013). FL is characterised by malignant B cells in the follicles of the LN. BM involvement is prevalent in 50-60% of FL cases (Salles, 2007) and is associated with a reduced response to standard therapy. The indolent nature of some FL

cases permits a “watch and wait” strategy, whereby therapy is withheld pending the progression of the disease (Berget et al., 2014). In advanced FL (stages III or IV), rituximab is used either alone or in combination with other chemotherapeutic agents, such as cyclophosphamide, Doxorubicin, vincristine and prednisolone. FL patients on rituximab-based chemotherapy have a response rate of >90% and a complete remission rate of 20-60% (Hiddemann and Cheson, 2014). FL has a propensity to relapse and/or transform, years after therapy, into a more aggressive and resistant disease (Solal-Celigny et al., 2004). This further demonstrates the urgent need for novel treatment strategies to target drug-resistant malignant cells.

2.3.5 Current Therapy

The vast range of NHL subtypes is met by an equally diverse array of therapies that can be used in isolation or in combination with each other. The most prominent treatment regimens are chemotherapy, radiotherapy or monoclonal antibody (mAb) therapy.

2.3.5.1 The R-CHOP Regimen

The current standard of care therapy for patients with NHL is the R-CHOP regimen comprised of **R**ituximab, **C**yclophosphamide, Doxorubicin (**H**ydroxydaunomycin), Vincristine (**O**ncovin) and **P**rednisolone.

Rituximab is a chimeric αCD20 mAb that selectively binds to CD20 on B cells of all stages of development, except plasma cells, which do not express CD20. Rituximab’s cytotoxicity is mediated by mechanisms such as Antibody-Dependent Cellular Cytotoxicity (ADCC), Antibody-Dependent Cellular Phagocytosis (ADCP), Complement-Dependent Cytotoxicity (CDC) and activation of caspase 3, which makes the cell sensitive to apoptotic cell death (Weiner, 2010). ADCC is the best characterised mechanism of cell death with data implicating a role for NK cells, whereby the FcγRIIIa on the NK cell binds to the Fc (fragment crystallisable) region on the CD20-bound mAb, inducing perforin/granzyme-mediated lysis of rituximab-opsonised cells (Rudnicka et al., 2013). FcγRI engagement by monocytes and macrophages (Uchida et al., 2004), and neutrophils (Hernandez-Ilizaliturri et al., 2003) can also eliminate rituximab-opsonised cells by ADCP. Rituximab is a first generation αCD20 antibody, and is proceeded by second generation mAbs, such as ocrelizumab, veltuzumab and ofatumumab, which are humanised to reduce immunogenicity, and third generation, such as GA101/obinutuzumab which is fully humanised and has a modified Fc region (Lim et al., 2010); obinutuzumab’s Fc region lacks a fucose molecule, increasing its affinity for

FcyRIII on NK cells and promoting enhanced ADCC (Gagez and Cartron, 2014).

Cyclophosphamide adds an alkyl group to the guanine base of DNA and inhibits DNA replication (El-Serafi et al., 2014). Doxorubicin intercalates with DNA and inhibits DNA synthesis. It also inhibits the actions of topoisomerase II and causes DNA breaks, which increases the ratio of pro- (for example Bax) vs. anti-apoptotic (for example BCL-2) proteins to promote apoptosis (Tacar et al., 2013). Vincristine acts by binding to tubulin, inhibiting the separation of chromosomes during mitosis and forcing the cell to undergo apoptosis (Rai and Wolff, 1996).

Lastly, prednisolone irreversibly binds to glucocorticoid receptors α and β causing them to dimerize, traffic to the nucleus and interact with cellular DNA to regulate gene transcription. This involves the regulation of several immunoregulatory genes, such as the suppression of IL-2 (Walker et al., 1987); inhibition of the immune response eases discomfort for the patient (Dorff and Crawford, 2013).

While some lymphomas show promising survival rates with R-CHOP therapy (FL; 76% 5-year survival with (Press et al., 2013)), others have a much poorer prognosis (DLBLC-ABC; 25% 5-year survival (Sehn and Gascoyne, 2015)). NHL cases can also relapse following R-CHOP treatment or develop resistance to the therapy (Chao, 2013). The aggressive nature of these lymphomas warrants further research into more effective novel areas of therapeutic intervention with the hope of improving patient survival.

2.3.5.2 Radiotherapy

Radiotherapy involves using cytotoxic radiation exposure, locally applied to malignant LNs, to ablate cancer cells. It is more commonly used to treat indolent subtypes, such as FL, and can be used in conjunction with chemotherapy for aggressive subtypes, such as DLBCL (Zimmermann et al., 2016). Radiotherapy for NHL patients is tailored to suit the individual with most regimens involving daily exposure of 30-35Gy for 2-4 weeks (Tsang, R.W. and Gospodarowicz, 2005). Whole body radiotherapy can also be used to deplete the patient's immune system in preparation for a stem cell transplant (Kahn et al., 2005). Despite the fact that radiotherapy is not the primary method of treating NHL, it remains a useful tool in the clinic for supplementing the efficacy of other therapies or preparing the patient for a stem cell transplant.

2.3.5.3 Surgery

Surgery plays a diminished role in treating NHL due to the advancement of more specific chemical, biological and radioactive therapies in recent decades. Surgery remains an option to retrieve malignant tissue for biopsies, to remove small, localised disease that is affecting non-lymphatic organs such as the stomach or small bowel, and a splenectomy to remove a malignant spleen (Weledji and Orock, 2015). Splenectomies are largely reserved for patients with enlarged spleens due to Splenic Marginal Zone Lymphoma or lymphoma that has invaded, and enlarged, the spleen (Kennedy et al., 2018).

2.3.6 The Lymph Node Environment

While the primary focus of cancer research is on the cancer cells, the tumour microenvironment (TME) is a vital factor when investigating candidate treatments for efficacy. The TME comprises the cancer cells, their surrounding immune and stromal cells, including blood supply and nutrients. These neighbouring cells, while non-transformed, can inadvertently provide support to cancer cells, making them more difficult to treat. While this is very true for solid malignancies, haematological malignancies, which may comprise blood cells that circulate in the peripheral blood, can also home to locations in the body that provide a comparable support system, such as leukaemias which reside in the bone marrow, making them more difficult to treat. Research by Ilkow, *et al*., has highlighted the role of the TME when considering OV as a treatment option for solid malignancies and shown that the TME can actually assist the OV by diminishing the ability of the cancer cells to destroy the virus (Ilkow et al., 2015). this data highlights the importance of considering the TME when examining novel therapies for efficacy against cancer, such as NHL, which predominantly resides in the patient's lymph nodes.

The human body contains ~450 LNs that are interconnected by the lymphatic system, a complex network of vasculature, closely associated with the circulatory system. LNs provide densely packed, tightly regulated environments for migrating immune cells to interact, present their cognate antigen, mature and induce an immune reaction to foreign antigens. They also provide a microbe filter for the blood, allowing immune cells, such as dendritic cells, that have identified and ingested foreign microbes to migrate out of the blood and into the LN where they present their antigen to immune effector cells and stimulate an immune response. A schematic of a human LN is shown in **Figure 2-2**.

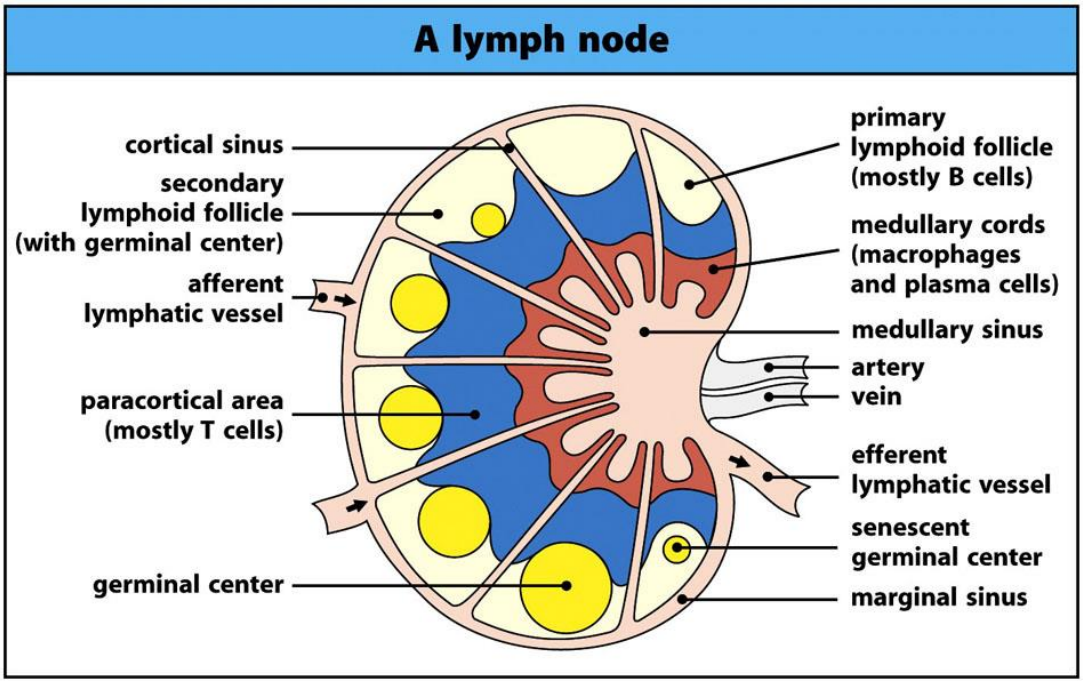

Figure 2-2: The structure of the human LN.

The LN is comprised of segments known as lobules, of which there may be one or several per LN. Within each lobule, lies a B cell-rich follicle (white) which contains a densely-packed area of proliferating B cells known as the germinal centre (yellow). B cells migrate to this area upon entering the LN where they interact with follicular dendritic cells and other antigen presenting cells (APCs) and activate to become mature B cells during infection. The germinal centre and follicle are closely associated with the T cell-rich paracortex (blue) which allows T cells to interact with B cells, promoting their maturation and function. The paracortex itself, much like the follicle, is encapsulated in a layer of extracellular matrix and provides a location for migrating T cells to interact with APCs, which present antigens to T cells, to promote their activation and clonal expansion to combat foreign antigens. Beyond the paracortex are the macrophage- and plasma cell-rich medullary cords (red). It is to here that the maturing B cells will migrate from the follicles and complete their maturation into plasma cells before they release antibodies into the lymph to fight infection. The nodules are separated from each other by sinuses that are composed of extracellular matrix and follicular dendritic cells (Andrews, 2008), (Willard-Mack, 2006).

As previously mentioned (section 2.3.1), the classification of NHL is partially based on cellular characteristics, their stage in B cell development and location within the LN, such as the follicle for FL and BL, the dark zone of the germinal centre for DLBCL-GCB and light zone for DLBCL-ABC (Pasqualucci and Dalla-Favera, 2014). **Figure 2-3** demonstrates the different B cell malignancies and where they arise during B cell development.

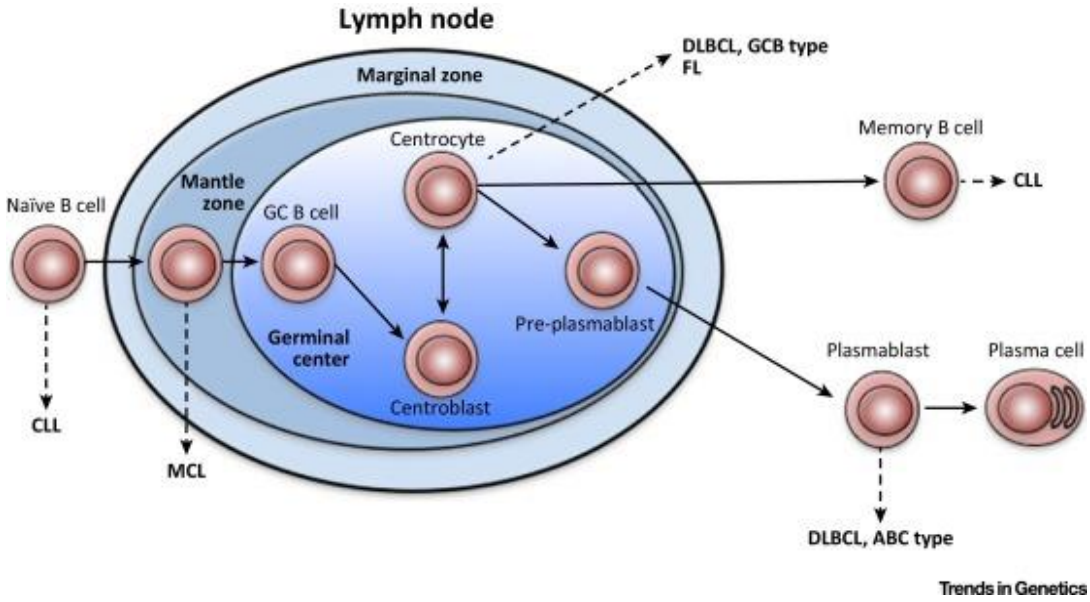

Figure 2-3: The emergence of malignancies during B cell development.

This diagram shows the progression of a naïve B cell through the LN where it will undergo somatic hypermutation and class switching to form a B cell clone that targets a specific antigen. During these processes, errors in genetic rearrangement can result in the emergence of a malignant B cell clone. This can occur before the B cell enters the LN, such as with Chronic Lymphocytic Leukaemia (CLL), in the GC as a centrocyte, such as DLBCL-GCB, or as a plasmablast, such as DLBCL-ABC. (Koues et al., 2015)

The LN plays a critical role in controlling the development and activation of immune cells and generating an immune response. Interactions between cells residing in the LN facilitate these events and can be hijacked by tumorigenesis. B cell: T cell interactions in the LN are important for B cell selection, maturation and proliferation (Janeway CA Jr, 2001). In particular, the CD40:CD40L interaction gives a strong pro-survival signal to developing B cells (Elgueta et al., 2009), allowing B cells to survive the maturation process. B cell: T cell interactions within the LN have been described previously to confer drug resistance to malignant B cells through manipulation of pro- and anti-apoptotic protein ratios (Romano et al., 1998), (Kater et al., 2004), (Kitada et al., 1999), (Romano et al., 1998). To simulate the B cell: T cell reaction in the LN, NHL cell lines can be co-cultured on $CD40L^+$ fibroblasts (L929 murine fibroblasts transfected with human CD40L), which has previously been shown to induce resistance to Doxorubicin in Daudi, Raji, BJAB, BL36 and BL70 NHL cell lines (Voorzanger-Rousselot et al., 1998). The emergence of drug-resistant NHL poses a challenge to the efficacy of current treatments, warranting the need for alternate methods to eliminate drug resistant cells.

2.4 Oncolytic Virotherapy

Oncolytic (“cancer bursting”) viruses (OV) preferentially infect and kill malignant cells and/or manipulate the patient immune system to mount an anti-cancer immune response. The concept of harnessing the cytotoxic and immunogenic properties of viruses for selective use against malignant cells dates to the early 20th century when it was first observed that patients with solid tumours or leukaemia developed a brief or sustained remission following viral infection (Dock et al., 1904). The mechanisms behind this phenomenon were researched during the decades that followed. This research, alongside the characterisation of viral human pathogens and cancer and the advent of genetic manipulation, lead to the development of oncolytic virotherapy as a novel and promising therapy for several cancers (Kelly and Russell, 2007).

Some OVs have been genetically modified to enhance their selectivity for malignant cells and their immunomodulatory effects. Talimogene Laherparepvec (T-Vec), an oncolytic Herpes Simplex Virus 1 (HSV-1) which was approved by the FDA for clinical use in 2015, has been genetically modified to lack the *Infected cell protein 34.5* (*ICP 34.5)* gene and express granulocyte-macrophage colony-stimulating factor (GM-CSF), thus

prohibiting its replication in normal cells, such as neuronal cells, and activating the immune system, respectively (Randazzo et al., 1997). Other OVs such as Reolysin® (reovirus Type 3 Dearing) and CAVATAK™ (Coxsackievirus Type A21, CVA21) are naturally occurring human pathogens. These OV have not been genetically manipulated but have been selected due to their innate preferential targeting of malignant cells. Most of the healthy population has already been exposed to reovirus (Douville et al., 2008) and less than 10% has been exposed to CVA21 (Israelsson et al., 2011). Pre-exposure to either virus could result in neutralising antibodies or immune memory against them, potentially resulting in eradication by the patient's immune system (Ferguson et al., 2012). However, replication-competent reovirus has previously been retrieved from the blood and liver metastasis of colorectal cancer patients that received intravenous virus before surgery, despite the presence of pre-existing anti-reovirus antibodies (Adair et al., 2012). Moreover, a phase I clinical trial that examined the safety and tolerability of reovirus in patients with advanced cancers demonstrated viral localisation and replication in 3 out of 33 patient tumours, despite the presence of neutralising antibodies (Vidal et al., 2008). These findings demonstrate a potential use for reovirus, despite the presence of pre-existing immunity.

2.4.1 Mechanism of action

The primary mechanism of action of OVs was initially believed to be direct lysis of tumour cells which would result in the release of progeny viruses, thus perpetuating the oncolytic effect (Bauzon and Hermiston, 2014). Recent research has shown that this is not their sole mechanism of action, and OVs also target the tumour stroma and vasculature, and activate the innate and adaptive immune system to destroy malignant cells, thus providing a multi-armed effect against the tumour (Lichty et al., 2014). The potential for immune modulation by OV therapy will be discussed further in section.

2.4.1.1 Oncolysis

A range of molecular and cellular factors will determine whether a malignant cell will be susceptible to OV infection, some of these are summarised in Table 2-2 and discussed below.

Virus	Modifications	Preferential infectivity
NDV	Strain 73T-R-198; Altered fusion protein	Preferential targeting of mammalian over avian cells, reducing risk of environmental damage if released (Cheng et al., 2016)
HSV-1	Strain R5111; glycoprotein replaced with human IL-13	Targets cancer cells that express elevated levels of IL-13Rα2 receptor on their surface (Zhou et al., 2002)
	Strain T-vec; viral ICP 34.5 deleted, human GM-CSF inserted	Resulting virus is unable to infect healthy cells with normal antiviral response, preferentially targets malignant cells with a defective response (Randazzo et al., 1997)
Poliovirus	Strain PVS-RIPO; coding region replaced with type 1 live attenuated vaccine strain	Preferentially targets cancer cells that express elevated levels of CD155 (Ochiai, H. et al., 2006)
CVA21	n/a	Over-expression of entry receptor ICAM-1 on tumour cells (Au et al., 2005)
Reovirus	n/a	Deregulation of ras family proteins in tumour cells, resulting in defective antiviral signalling (Marcato et al., 2007)
VSV	n/a	Unable to replicate in cells with functioning IFN response, instead infect IFN-deficient tumour cells (Hastie and Grdzelishvili, 2012)
Vaccinia virus	n/a	Targets tumour cell antiviral response pathways (Colamonici et al., 1995)
	Insert human epidermal growth factor receptor 2 (HER2)	Targets $HER2^{+}$ breast cancer tumour (Sharp and Lattime, 2016)

	transgene	

Table 2-2: List of Oncolytic viruses being investigated at clinical and pre-clinical levels in various malignancies.

This list provides an overview of the diverse range of oncolytic viruses that are being investigated in cancer research

2.4.1.1.1 Overexpression of Viral Entry Receptors

OV often rely on overexpression of surface receptors on malignant cells for viral entry (Jhawar et al., 2017). These receptors are often highly expressed on cancer cells, making them more susceptible to OV infection than their non-transformed counterparts. T-Vec, as with the parental HSV-1 strain, utilises Herpesvirus Entry Mediator (HVEM) and nectin-1 and -2, which are overexpressed on a variety of cancer types (Kohlhapp et al., 2015), for viral entry. CVA21, a human enterovirus that targets cells in the upper airways, preferentially infects cancer cells that express enhanced levels of its attachment (Decay Accelerating Factor, DAF) and entry receptors (Intercellular Adhesion Molecule-1, ICAM-1) (Au et al., 2005). Echovirus 1, another enterovirus, targets ovarian cancer cells that display enhanced levels of integrin α2β1 on their cell surface (Shafren, D.R. et al., 2005). Similarly, an oncolytic recombinant poliovirus strain, that preferentially targets malignant glioblastoma multiforme (GBM) cells that express high levels of CD155 has been developed (Ochiai, H. et al., 2006). Importantly, as discussed in a review by Singh, *et al.*, overexpression of a viral entry receptor, a receptor that may also be present on the surface of many healthy cells, is unlikely to be sufficient for preferential infection of malignant cells (Singh et al., 2012). Other mechanisms of OV tumour specificity are discussed below.

2.4.1.1.2 Genetic Manipulation of Viruses

The advent of the genetic manipulation of organisms has allowed viruses to be modified to alter their host tropism and pathogenicity. This can result in diminishing the cell tropism of a potentially dangerous virus, such as HSV-1, so that it only targets cancer cells. HSV-1 is one of the most studied viruses in this regard as numerous oncolytic strains of the virus, with various genetic modifications, have been developed (Sokolowski et al., 2015). HSV's large, stable DNA genome is an ideal candidate for genetic modification, allowing genes to be deleted and added. HSV-1 also possesses an outer envelope that can be manipulated to enhance targeting of cancer cells. For example, a HSV-1 strain, which has had its glycoprotein gD replaced with human IL-13, targets cancer cells that express elevated levels of IL-13Rα2 receptor on their surface (Zhou et al., 2002).

Newcastle Disease Virus (NDV), an avian paramyxovirus, is currently being investigated as an oncolytic agent in many tumours such as advanced renal and breast carcinoma (Omar et al., 2003). Due to its ability to target avian

species, the use of NDV carries some environmental risks, leading to the development of a genetically modified strain of NDV, with an altered fusion protein, which preferentially infects mammalian cells (Cheng et al., 2016).

2.4.1.1.3 Defective Antiviral Response

The antiviral response is a broad term that includes all aspects of the immune system's ability to prevent viral infection. This response can be innate and fast-acting, such as the interferon (IFN) response (depicted in Figure 2-4) and NK cells which can detect and target virally-infected malignant cells through loss of MHC-I, or acquired and slower to develop, such as priming of virus-specific T cells that target virally-infected malignant cells or generating a humoral immune response where B cells produce neutralising antibodies against a virus. The IFN response is a common obstacle to viral infection and may prevent the application of IFN-sensitive OV to cancer cells with functional IFN signalling (Singh et al., 2012).

The IFN response allows infected and neighbouring cells to communicate and prevent further viral replication. Infected cells detect Pathogen Associated Molecular Patterns (PAMPs), such as viral genetic material or bacterial components, by Pattern Recognition Receptors (PRRs), such as Toll-Like Receptors (TLRs) or other sensors of virus material (Takeuchi and Akira, 2010). TLRs, such as TLR7 and 8, recognise viral single-stranded RNA (ssRNA) in endosomes upon viral entry (Wang, J.P. et al., 2007), (Triantafilou et al., 2005) and TLR3 recognises double-stranded RNA (dsRNA), and has been implicated in detecting the genome of reovirus (Maitra et al., 2017). Coxsackieviruses can be detected by a variety of intracellular proteins such as Melanoma Differentiation-Associated protein 5 (MDA5), which senses viral dsRNA during replication in the cytoplasm (Valaperti et al., 2013), and TLR7 and 8.

Pathogen detection triggers signalling pathways that induce the expression of pro-inflammatory cytokines and the production of type 1 IFNs (Zhu and Mohan, 2010). Upon IFN release, IFN binds receptors on neighbouring cells, triggering a signalling cascade through Signal transducer and activator of transcription (STAT) molecules, such as STAT1, which induces the expression of Interferon-Stimulated Genes (ISGs) to inhibit propagation of viruses and other pathogens (Schneider et al., 2014). ISGs include Tripartite Motif-containing protein 5-α (TRIM5α), which binds to, and disrupts, retroviral capsids (Black and Aiken, 2010), tetherin, which sequesters new enveloped virus particles to the cell surface (Mahauad-Fernandez and

Okeoma, 2016), MHC-I and –II, which are involved in antigenic presentation, Protein Kinase R (PKR), which senses viral dsRNA and shuts down host cell protein translation (Sadler and Williams, 2007), and Oligoadenylate synthetase 1 (OAS1), which detects viral dsRNA and activates RNase L to degrade it. The IFN response in neighbouring non-infected cells results in a highly defensive, antiviral state preventing replication in these cells and limiting infection.

Many cancers have defective IFN response pathways, due to the accumulation of mutations that render the pathway ineffective (Critchley-Thorne et al., 2009). This provides an opportunity for OV to replicate freely without the constraints of host natural defences. Some OVs, such as Vesicular Stomatitis Virus (VSV), are sensitive to IFN, which protects healthy tissues that have retained the pathway, while the virus can replicate in and destroy IFN-defective malignant cells (Hastie and Grdzelishvili, 2012).

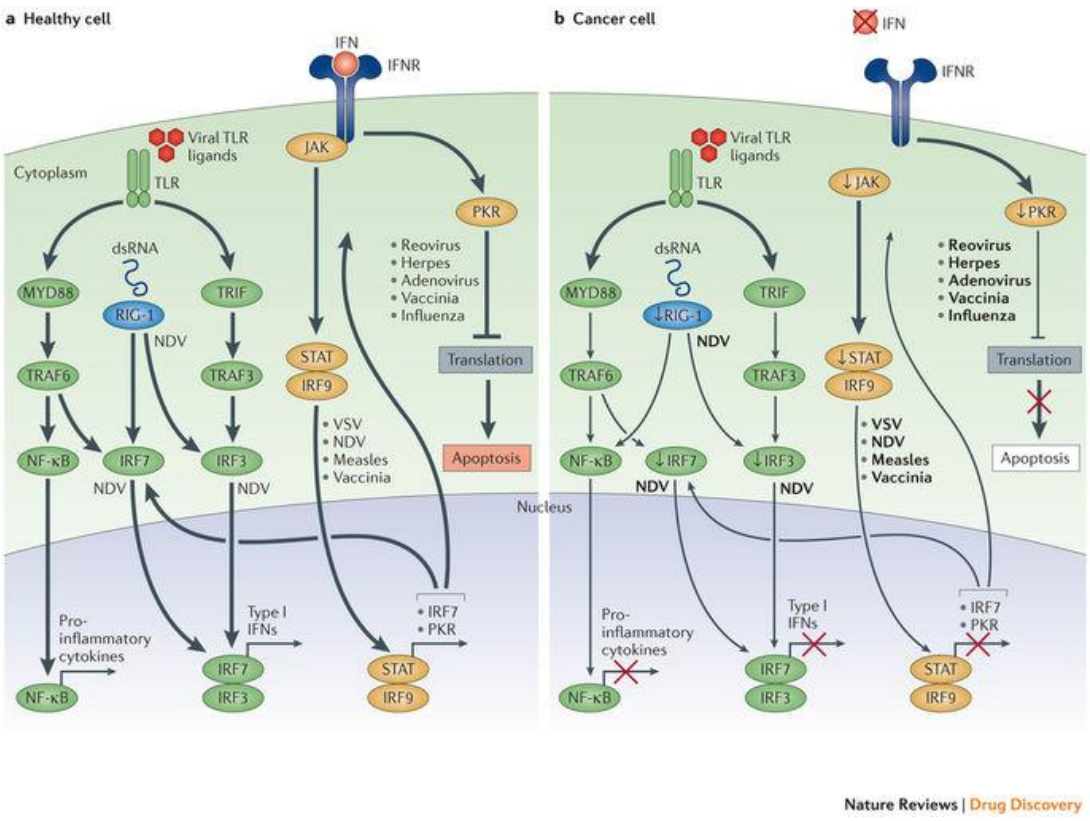

Figure 2-4: **Defective IFN response facilitates OV replication in malignant cells.**

In healthy cells, a functioning IFN response will block viral replication and dissemination, as described. Dysfunction of these pathways have been reported in many cancers, providing OV with a vulnerability that can be exploited to target malignant cells while sparing healthy cells (Kaufman et al., 2015).

Some viruses have also evolved mechanisms to overcome functional IFN responses to allow viral replication. For example, the V protein encoded by the avian paramyxovirus NDV can target the antiviral response by degradation of STAT1 molecules in avian cells, but not in human cells (Park et al., 2003), suggesting that cancer cells with deficient IFN signalling may be more susceptible to NDV-induced cell death (Fiola et al., 2006). Furthermore, the B18R protein encoded by Vaccinia virus is able to bind to IFN-α, thus blocking its ability to signal neighbouring cells (Colamonici et al., 1995). A summary of how viruses can subvert the antiviral IFN response pathway is shown in **Figure 2-5**.

(a)

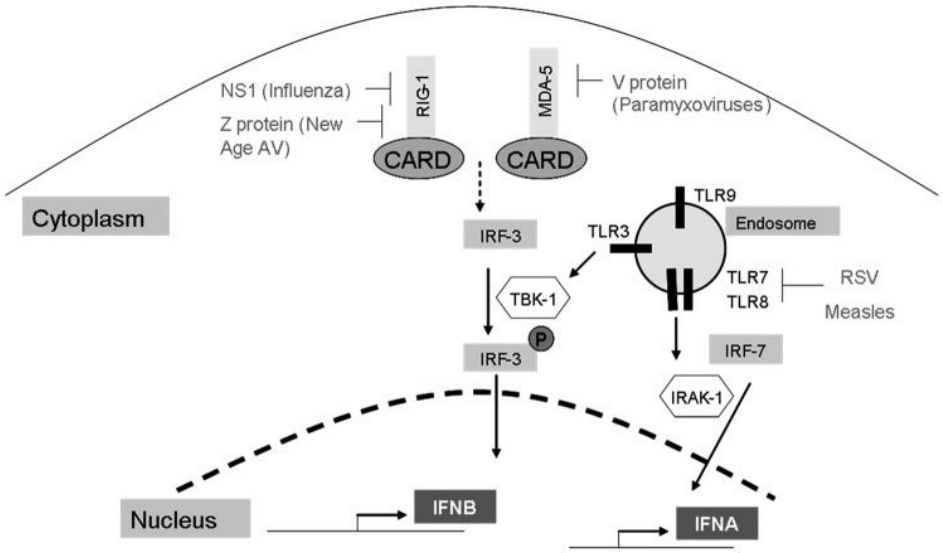

(b)

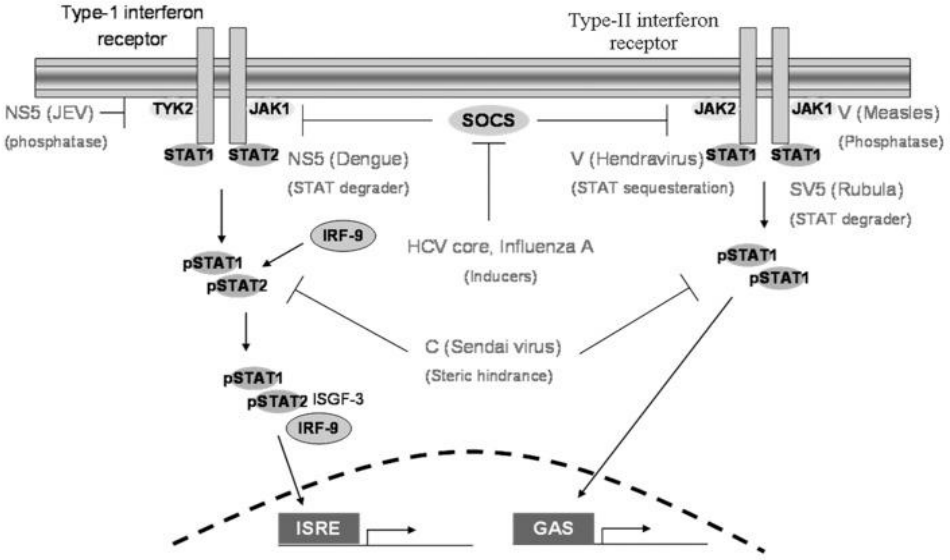

Figure 2-5: Viral mechanisms for evading the antiviral IFN response.

(a) Proteins expressed by Influenza, Arenaviruses and paramyxoviruses can block virus-detecting PRRs, such as RIG-1 and MDA5, while RSV and Measles viruses inhibit TLR7 and 8 signalling. This results in defective viral detection and inhibits the induction of IFN proteins. (b) Japanese Encephalitis Virus, Dengue virus, Inluenza A, Hepatitis C Virus, Sendai Virus, Measles, Rubula virus and Hendraviruses inhibit downstream signalling of IFN receptors, resulting in a diminished antiviral response. (Devasthanam, 2014)

2.4.1.1.4 Mechanistic Target of Rapamycin (mTOR)

Dysregulation of the Ras pathway confers sensitivity of malignant cells to oncolytic reovirus (Strong et al., 1998) and dysfunctional IFN signalling prevents the production of antiviral proteins, contributing to a favourable intracellular environment for OV replication (Wollmann et al., 2007). Another example of a pathway that is altered in cancer cells is the Mechanistic Target of Rapamycin (mTOR) pathway, which contributes to cell proliferation, nutrient sensing, transcription, translation, and cytoskeletal remodelling. MTOR's reported hyperactivity in a variety of cancers (Saxton and Sabatini, 2017), its importance for NHL cell survival (Bhatt et al., 2010), and its frequent hijacking by viruses to control the stress response of cells (Le Sage et al., 2016), make it a possible determinant of OV susceptibility.

2.4.1.1.4.1 Role of mTOR in Cellular Biology

MTOR is a serine/threonine protein kinase that plays a major role in cell metabolism, growth and survival (Tan and Miyamoto, 2016) and is a key regulator of autophagy; the process by which cells degrade and recycle intracellular proteins during times of stress. MTOR is active in either of two functionally distinct protein complexes; mTOR Complex 1 or 2 (mTORC1 or mTORC2), as shown in Figure 2-6.

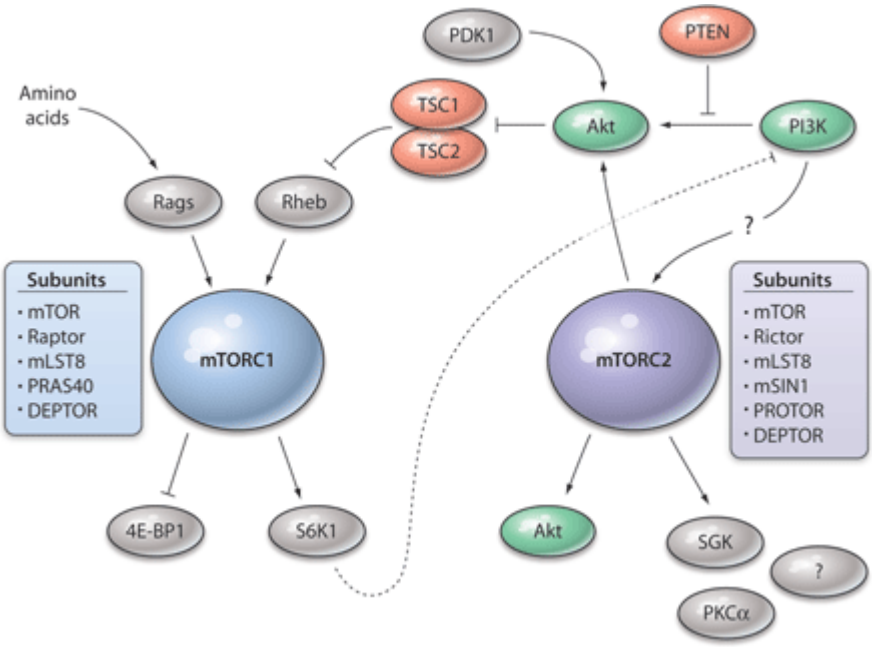

Figure 2-6: Components of mTORC1 and 2.

MTORC1 consists of mTOR, Regulatory-associated protein of mTOR (Raptor), mammalian lethal with SEC13 protein 8 (mLST8), proline-rich Akt substrate of 40 kDa (PRAS40) and DEP domain-containing mTOR-interacting protein (DEPTOR) (Ding et al., 2018). MTORC2 is composed of mTOR, mLST8, mammalian stress-activated protein kinase interacting protein 1 (mSIN1), DEPTOR, Rapamycin-insensitive companion of mammalian target of rapamycin (RICTOR) and Protein observed with Rictor (PROTOR), and regulates cell survival and cytoskeleton remodelling by downstream effectors such as Akt and members of the Protein Kinase C (PKC) family, respectively (Saxton and Sabatini, 2017). (Figure obtained from (Guertin and Sabatini, 2009).

MTORC1 is a nutrient sensor that controls transcription and cap-dependent translation by phosphorylating downstream pathway components, such as S6 Kinase (S6K) or Eukaryotic translation initiation factor 4E-binding protein 1 (4EBP1) (Showkat et al., 2014), under nutrient-rich conditions. Before activation by mTORC1, 4EBP1 is bound to Eukaryotic translation initiation factor 4E (eIF4E), preventing it from initiating translation; mTORC1 phosphorylates 4EBP1, releasing eIF4E to initiate translation (Faller et al., 2015). The second pathway downstream of mTORC1 signals through S6K which regulates ribosomal translation by phosphorylating S6 on ribosomes and initiating translation (Magnuson et al., 2012). MTORC2 has been identified as a prominent influencer of amino acid metabolism in cancer, allowing malignant cells to adapt to new conditions (Gu, Y. et al., 2017), and contributes to tumourigenesis by promoting lipid synthesis (Guri et al., 2017).

2.4.1.1.4.2 Role of mTOR in viral replication

Viruses rely heavily on cellular processes, such as transcription and translation, for replication (Walsh et al., 2013). MTOR's control over pathways that affect these processes make it, and its downstream effector molecules, targets for viral manipulation. EBV's Latent Membrane Protein 2A (LMP2A) activates upstream regulators of mTOR, such as phosphatidylinositol 3-kinase (PI3K)/Akt, resulting in enhanced translation of viral proteins (Moody et al., 2005). Adenoviruses express two proteins, E4-ORF1 and E4-ORF4, which mimic growth factors and glucose, respectively, to activate mTOR, even in low-nutrient conditions (O'Shea et al., 2005). Viruses also mimic the downstream effectors of mTOR, for example, HSV-1 expresses Infected Cell Protein 6 (ICP 6) which overrides 4EBP1's control of RNA translation by acting as a chaperone for Eukaryotic initiation factor 4F (eIF4F) (Walsh and Mohr, 2006) to initiate translation. Other viruses, such as Respiratory syncytial virus (RSV), abrogate memory $CD8^+$ T cell differentiation by phosphorylating and activating mTOR, thus impairing the ability of $CD8^+$ T cells to develop immunological memory to RSV (de Souza et al., 2016).

Autophagy, which is controlled by mTOR, can be essential or detrimental to viral replication, as the process is required by some viruses to replicate, such as Influenza A (Yeganeh et al., 2018), while also posing a risk to other viruses by degrading viral proteins (Levine, 2005). In the latter case, which is termed xenophagy, autophagy can be used as an antiviral response mechanism. Some viruses, such as CVA16 and other picornaviruses, have developed mechanisms to control autophagy, so that autophagic bodies are

produced within the cell to allow viral replication (Shi et al., 2015), (Klein and Jackson, 2011).

2.4.1.2 OV anti-tumour immunity

An alternate mechanism of action of OV therapy is the activation of the patient immune system to mount a response against malignant or virally-infected cells. This effect is summarised in **Figure 2-7**.

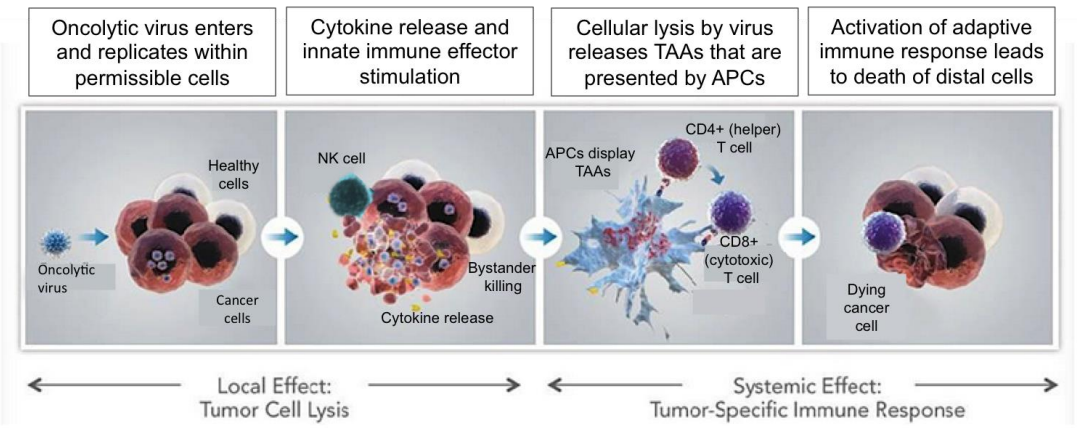

Figure 2-7: OV-induced immune response against malignant or virally-infected cells.

While the primary mechanism of action of OVs was believed to be direct cytotoxicity (1st panel), alternate mechanisms have been discovered. The presence of OV can activate NK cells to target malignant or virally-infected cells, or induce the secretion of cytotoxic cytokines to kill malignant cells (2nd panel). The rupture of malignant cells can result in the presentation of Tumour-Associated Antigens (TAAs) and OV antigens to T cells by APCs to stimulate an adaptive response (3rd panel). The benefits of this response include a systemic effect of memory circulating tumour- or OV-specific T cells, and their ability to target distant metastases (4th panel) (Labiotech.eu, 2015).

Immunogenic cell death, as distinct from apoptosis, arises from the rupture of a dying cell, resulting in the release of its intracellular components. Upon release, these components may be detected by the immune system as a “danger signal”, resulting in the stimulation of an immune response to mop up and clear the debris from the dead cell. Immunogenic cell death can also arise during the late stages of a lytic viral infection, whereby the newly-synthesised virions within an infected cell burst out, killing the cell and releasing themselves and the cellular components. This can result in an immune response to these viruses (Donnelly et al., 2013). This form of cell death can be instrumental in OV therapy, as it can result in an immune response against the virus and the cancer cells, contributing to the anti-cancer effect. Such a response can be evaluated in vitro by examining the cells for non-apoptotic cell death by flow cytometry, release of nuclear proteins such as High mobility group box 1 (HMGB1) and release of Adenosine Triphosphate (ATP) (Kepp et al., 2014).

Despite the co-existence of malignant B cells with normal immune cells, such as NK cells, T cells and dendritic cells (DCs), within the highly immunological environment of the LN, the patient immune system fails to obliterate the aberrant cells. The presence of these immune cells provides an arsenal for priming an immune response against NHL, however, the effects of immunosuppressive cells in the LN prevents recognition and destruction of the NHL cells. This will be discussed in more detail in section 2.4.1.2.2. The duration of an OV-induced anti-cancer immune response can vary from short term innate responses, such as NK cell-mediated responses, to long term adaptive responses comprising immunological memory, such as T cell-mediated responses (Filley and Dey, 2017). This will be discussed in more detail in section 2.4.1.2.2.

2.4.1.2.1 Innate immune responses

The innate immune response is a broad range of cellular responses to antigenic assault, ranging from the IFN response, as described in 2.4.1.1.3, to NK cell-mediated responses. IFNs, in addition to stimulating the enhanced expression of ISGs, such as Tetherin and MHC-I, exert a range of effects on their target cells that aid their antiviral effects. These effects can include inducing cell cycle arrest to hamper viral replication (Sangfelt et al., 2000), inducing apoptosis in infected and malignant cells (Chawla-Sarkar et al., 2003), and cell metabolism (Wu et al., 2016). IFNs also play a critical role in immune regulation, such as promoting class switching during B cell development and the production of a humoural immune response (van den

Broek et al., 1995), activating monocytes (Buchmeier and Schreiber, 1985) and elevating MHC expression to facilitate antigen presentation and promote T cell responses (Bernard Mach et al., 1996).

An NK cell-mediated response can be achieved following OV treatment, whereby an infected cancer cell could be manipulated by the virus to decrease MHC I expression and subsequently block antigen presentation to T cells (Bhat et al., 2011). Inadvertently, this would result in the NK cell detecting the lack of MHC I expression ("lack of self"), resulting in NK-mediated killing of malignant, virus-infected, cells (Woller et al., 2014). Moreover, OV, such as reovirus, can also activate NK cells, through stimulating monocytes to produce IFN-α, to target non-infected malignant cells, as has been demonstrated in HMs, such as CLL (Parrish et al., 2015) and AML (Hall et al., 2012). Research by Miyamoto, *et al.,* also demonstrated enhanced NK cell and granulocyte infiltration into established lung cancer tumours following intratumoral treatment with Coxsackievirus B3 (CVB3) in female BALB/c nude mice (Miyamoto et al., 2012). The decision by an NK cell to kill results in the trafficking of intracellular granules to the cell surface where the contents are released (known as degranulation) into the extracellular space to attack the target cell. Cytolytic granules contain perforin, a glycoprotein that inserts itself into the target cell membrane and oligomerises to form a pore (Osinska et al., 2014), and multiple proteases, such as Granzyme B, a serine protease that enters the cell via the perforin pore and initiates a proteolytic cascade resulting in apoptosis of the target cell (Lord et al., 2003). Interestingly, perforin alone can kill the target cells by causing it to lyse (Waterhouse et al., 2006). Alternatively, NK cells can deliver death signals to target cells via interactions between Fas (First apoptosis signal) Ligand and TRAIL (TNF-related apoptosis-inducing ligand) on the NK cell surface, or secreted tumour necrosis factor-α (TNF-α), with their cognate receptors on the target cell. These interactions result in the activation of the caspase cascade and directly trigger apoptosis (Zamai et al., 1998).

Virus infection can also result in infected and neighbouring cells secreting cytokines, for example, the alphavirus M1 stimulates the secretion of IL-8, IL-1A, and TRAIL, which induced cell death in hepatocellular carcinoma and colorectal cancer cell line models (Cai et al., 2017). This indirect cytotoxicity towards malignant cells is known as bystander killing.

Reovirus has displayed immunogenic properties, including activation of innate immunity, such as enhancing NK cell-mediated targeting of anti-

epidermal growth factor receptor (αEGFR) antibody (cetuximab)-coated colorectal cancer cell lines (Zhao, X. et al., 2015), inducing the IFN response against AML cells (Hall et al., 2012) and inducing $CD8^+$ antigen-specific T cells to target melanoma LN metastases in a C57BL/6 mouse model (Prestwich, R. J. et al., 2008). Innate immune responses are potent tools in targeting malignant cells, however, an adaptive T cell-mediated response can provide a more durable anti-cancer effect.

2.4.1.2.2 Adaptive Immune responses

Oncolysis results in the release of antigens of viral or cellular origin which can be ingested and presented by professional APCs, such as DCs, to developing T cells. This can lead to an antigen-specific T cell response that can recognise and target malignant cells (Howells et al., 2017). This has been demonstrated in multiple animal models including: a FVB/N mouse model of breast cancer that used a GM-CSF- and human epidermal growth factor receptor 2 (HER2)-expressing vaccinia virus to induce cytotoxic $CD8^+$ T cell targeting of a $HER2^+$ breast cancer tumour (Sharp and Lattime, 2016); and a Syrian (golden) hamster model of pancreas ductal adenocarcinoma that demonstrated $CD8^+$ T cell-dependent antitumour response in wild-type adenovirus type 5-treated animals (Li, X. et al., 2017). Healthy $CD4^+$ and $CD8^+$ T cells are functional and capable of destroying NHL cells, lending hope to the possibility that the patient's immune cell arsenal could be utilised to fight the malignancy (Yang, Z.Z. et al., 2006a), (Yang, Z.Z. et al., 2006b).

$CD8^+$ cytotoxic T cells fail to destroy NHL cells due to the presence of immunosuppressive regulatory T cells (Tregs) (Yang, Z.Z. et al., 2006b). Treg populations in NHL result in an inhibited adaptive T cell-mediated immune response and the persistence of the malignant cells (Wang, Jing and Ke, 2011). Recent research has shown that OV can alleviate the immunosuppressive effects of Tregs; examples include oncolytic adenovirus that decreases tumour-infiltrating Tregs in a syngeneic glioblastoma multiforme (GBM) mouse model (Qiao et al., 2015), oncolytic HSV-1, which reduced Treg populations in melanoma patient tumours following intratumoural injection (Kaufman et al., 2010), and reovirus, which decreased numbers of tumour-residing Tregs in a C57BL/6 ovarian cancer model (Gujar, S. et al., 2013). Taken together, these findings implicate a role for OV in priming an adaptive anti-cancer immune response by alleviating the immunosuppressive effects of Tregs and promoting T cell-mediated targeting of malignant or virally-infected cells.

2.4.1.2.3 Combinations with Immunomodulatory Drugs

The ability of OV to promote anti-cancer immune responses is being investigated in combination with immunomodulatory drugs, such as mAbs. MAbs specifically bind to their target antigen, resulting in blocking of an interaction between malignant cells and immune cells, such as PD-L1 (Programmed death-ligand 1) on malignant cells signalling to PD-1 (Programmed cell death protein 1) on immune cells to inhibit immune cell targeting of malignant cells. MAbs have shown efficacy against a range of solid and haematological malignancies, for example, the αPD-1 antibody, pembrolizumab, lead to a progression-free survival rate in 38% of melanoma patients vs 16% in those that received chemotherapy (carboplatin and/or paclitaxel) (Ribas et al., 2015). MAbs can also mark the mAb-coated malignant cells for immune destruction, as previously discussed with rituximab (section 2.3.5.1).

Rituximab binds to CD20 on malignant B cells and, coupled with its direct effects, such as downregulating the B Cell Receptor (BCR) (Kheirallah et al., 2010) and inducing apoptosis (Pedersen et al., 2002), stimulates anti-tumour immunity against them by ADCC, CDC and possibly ADCP (Oflazoglu and Audoly, 2010). Given that rituximab achieves its efficacy by activation and utilisation of the immune system, and OVs can activate the immune system (Aurelian, 2016), combinations of OV and mAbs to treat a variety of cancers are being investigated. Previous work by Parrish, *et al.*, showed that *in vitro* reovirus treatment enhanced rituximab-mediated NK cell ADCC against *ex vivo* CLL (Parrish et al., 2015). The enhanced effects of this combination could be investigated in other B cell malignancies such as NHL where rituximab is already part of the current standard of therapy. Despite low NK cell numbers in the LN (Bajenoff et al., 2006), it may be possible to induce the trafficking of NK cells to LN during OV therapy, as has been demonstrated in mouse models in which virus infection, for example, influenza (Duan et al., 2017) and ectromelia virus (ECTV) (Parker et al., 2007), can stimulate NK cell trafficking to the LN.

Current immunotherapy strategies, including rituximab, are successful against NHL, providing scope for further harnessing of the immune system with OV therapy. The possibility for the immune system to eradicate malignant cells in the LN suggests that OV therapy, alone or in conjunction with immunomodulatory drugs, may harness the potential of anti-tumour immunity.

2.4.1.3 OV in B Cell Malignancies

Previous work on OV therapy in the context of NHL has shown that some NHL cell lines in isolation are sensitive to reovirus oncolysis, while others are resistant (Alain et al., 2002). This could present a challenge for treating NHL with reovirus as some patients may remain resistant to OV direct oncolysis, however this does not preclude a role for reovirus-induced immunotherapy. Other OVs have been investigated in pre-clinical research for efficacy against B cell malignancies. **Table 2-3** summarises these findings (Angelova et al., 2017).

B cell Malignancy	OV	Outcome	References
Multiple Myeloma	Reovirus	Reovirus induced autophagy-dependent apoptosis in a myeloma cell line (RPMI 8226)	(Thirukkumaran, C. M. et al., 2013)
	VSV	VSV induced cell death in myeloma cell lines and primary patient cells, but not PBMCs.	(Lichty et al., 2004)
	Myxoma	Intravenous myxoma virus reduced myeloma burden in female Balb/C mice by 70-90% through direct oncolysis and priming of a $CD8^+$ T cell-mediated response.	(Bartee et al., 2016)
	Vaccinia	Vaccinia virus induced replicative cell death in myeloma cell lines	(Deng et al., 2008)
	Adenovirus	Ad 5 induced cell death in most myeloma cell lines and primary patient cells	(Senac et al., 2010)
	CVA21	CVA21 induced replicative cell death in myeloma cell lines and purged patient BM biopsies of up to 98·7% of $CD138^+$ plasma cells.	(Au et al., 2007)
NHL	HSV-1	HSV-1 replicated in 1/3 NHL lines	(Esfandyari et al., 2009)
	Reovirus	Reovirus exhibited significant purging of NHL cells from patient blood, but not healthy PBMCs.	(Thirukkumaran, Chandini M. et al., 2003)
		Reovirus induced cell death in 6/9 NHL cell lines and 21/27 primary patient samples, but not PBMCs.	(Alain et al., 2002)
	Adenovirus	Adenovirus induced cell death in all primary MCL samples.	(Medina et al., 2005)
	Measles	Replication-competent measles virus induced tumour regression in established human lymphoma xenografts in Balb/C mice	(Grote et al., 2001)
CLL	VSV	BCL-2 inhibitors sensitised primary CLL cells, but not PBMCs, to VSV oncolysis.	(Tumilasci et al., 2008)
	Reovirus	Reovirus promotes rituximab-mediated ADCC of CLL targets	(Parrish et al., 2015)
B-lineage-ALL	Measles	Measles virus-loaded BM-derived mesenchymal stromal cells deliver virus to ALL cell targets in a SCID mouse model	(Castleton et al., 2014)
B-lymphoblastic leukaemia	Adenovirus	IL-24-expressing Adenovirus5 induced cell death in human B-lymphoblastic leukaemia and lymphoma cell lines and patient cells	(Qian et al., 2008)

Table 2-3: List of B cell malignancies that have been investigated as potential targets for OV therapy.

The data shows a wide range of OVs have been investigated against a variety of B cell malignancies, with promising results against cell lines, primary patient material and *in vivo* models.

Table 2-3 demonstrates the interest in the use of OV to treat a variety of B cell malignancies. While these studies have yielded promising data into the efficacy of OV against HMs, most studies have only examined these cells in isolation, and have not investigated roles for the immune response, or the TME. These data have demonstrated reovirus susceptibility in some BL cell lines, however, more research is needed to characterise the susceptibility of DLBCL cell lines to reovirus infection, the role of the (TME) in reovirus oncolysis of NHL cells, and reovirus' ability to potentiate an anti-NHL immune response. Other than investigating the susceptibility of multiple myeloma cells, no other data on the efficacy of CVA21 in the context of B cell malignancies have been reported.

2.4.2 REOLYSIN®/Reovirus

2.4.2.1 Origins and Discovery

Reolysin® is the proprietary formulation of the Type 3 Dearing (T3D) strain of reovirus (Respiratory Enteric Orphan virus) and is produced by Oncolytics Biotech Inc. It is a non-manipulated member of the Reoviridae family and has a small dsRNA genome and an icosahedral capsid. The reovirus genome is comprised of 10 segments that encode for structural and non-structural proteins that are necessary for its infection and replication (Shatkin et al., 1968). Reovirus was first identified as a novel oncolytic agent by Hashiro, *et al.*, who described how the virus preferentially infected and killed malignant cells but not non-transformed cells (Hashiro et al., 1977), leading to further research into its potential as an oncolytic agent. Historically, the proprietary strain of Reolysin was propagated in murine L cells to provide a bioselected strain of the virus, i.e., one that has been passaged multiple times through one homogeneous cell line to create a more consistent formulation of the virus than what would be isolated from patients (Duncan et al., 1978).

2.4.2.2 Pathogenic Significance and Virulence

Reovirus is a common human pathogen that causes a mild enteric or respiratory illness in young children (Rosen et al., 1960). Exposure to the T3D strain of reovirus is widespread, with some studies reporting up to 90% seropositivity for neutralising antibodies against the virus (Minuk et al., 1985). The primary receptor for reovirus is Junctional Adhesion Molecule A (JAM-A) that is ubiquitously expressed in endothelial and haematological cells throughout the body (Sugano et al., 2008). The role of JAM-A in reovirus infection has previously been investigated by the transfection of

Chinese Hamster Ovary (CHO) cells with JAM-A, -B and –C. These experiments demonstrated that only cells expressing JAM-A were permissive to reovirus infection (Campbell et al., 2005). JAM-A plays a vital role in several cellular processes such as tight junction formation and leukocyte migration, and its dysregulation in cancer is advantageous for tumour progression (Zhao, C. et al., 2014). Elevated JAM-A expression is not implicated in enhancing reovirus' preferential infection of malignant cells, however, reovirus is thought to preferentially target malignant cells with activated Ras signalling (Marcato et al., 2007), elevated in many cancers (Downward, 2003). Another factor that contributes to reovirus susceptibility is enhanced levels of cathepsin B and L, which aid virus uncoating to allow replication, as reported in an *in vivo* glioma model (Alain et al., 2007). Enhanced cathepsins B and L expression were reported when tumour cells were grown *in vivo* and not *in vitro*, illustrating the importance of considering the TME in OV therapy. Although activation of the Ras pathway is infrequent in NHL cells (Ahuja et al., 1990), activating mutations in factors downstream of this pathway, such as ERK and p38, have been reported in NHL (Kurland et al., 2003), (Kawauchi et al., 2002), (Jazirehi et al., 2004), suggesting NHL cells as a good target for reovirus oncolysis. The presence of the JAM-A receptor on B cells (Xu et al., 2017) and the previously mentioned immunogenic potential of reovirus (section 2.4.1.2.1) make it a worthwhile candidate OV for NHL treatment.

2.4.2.3 Progress in Clinical Trials

Reolysin® is a promising candidate for oncolytic virotherapy due to its preference for transformed cells and high tolerability, only inducing low grade adverse effects in patients (Comins, C. et al., 2010), (Lolkema et al., 2011), (Karapanagiotou et al., 2012). Reovirus has also been reported to induce an increase in $CD4^+$ T cells, $CD8^+$ T cells, NK cells and cytokine production in heavily pre-treated patients with advanced cancers, who had received surgery, radiotherapy or chemotherapy, prior to reovirus treatment (White et al., 2008). A table showing some examples of reovirus clinical trials is shown below (**Table 2-4**).

Disease	Combinations	Phase	Trial numbers	Results
Gliomas	N/A	I	NCT00528684	No dose-limiting toxicity, 1/12 patients remained disease free for >6 years (yrs) (Forsyth et al., 2008)
Pancreatic Cancer	Carboplatin/ Paclitaxel	II	NCT01280058	No significant enhancement of progression-free survival with reovirus vs drugs alone (4.9 vs 5.2 months) (Noonan et al., 2016)
Head and Neck Cancers	Carboplatin/ Paclitaxel	II	NCT00753038	4/13 patients had partial response, 2/13 had stable disease for >12 weeks (Karnad et al., 2011)
	Carboplatin/ Paclitaxel/ Placebo	III	NCT01166542	Not reported
Melanoma	N/A	II	NCT00651157	Virus was well-tolerated, viral replication was detected in 2/15 patients (Galanis et al., 2012)
	Carboplatin/ Paclitaxel	II	NCT00984464	Partial response in 3/14 patients (Oncozine, 2013)
Myeloma	N/A	I	NCT01533194	Virus was well-tolerated (Sborov et

				al., 2014)
Lung Cancer	Carboplatin/ Paclitaxel	II	NCT00861627	11/37 partial responses, 20/37 stable diseases (Villalona-Calero et al., 2016)
		II	NCT00998192	12/25 partial responses, 10/25 stable diseases (Mita et al., 2013)
	Pemetrexed/ Docetaxel	II	NCT01708993	Virus was well-tolerated, no enhancement of progression-free survival with reovirus vs drugs alone (2.96 vs 2.83 months) (Morris et al., 2016)
Prostate Cancer	Docetaxel and Prednisone	II	NCT01619813	Poorer overall survival in virus and drug combination arm, vs drug alone (Eigl et al., 2017)
Breast Cancer	Paclitaxel	II	NCT01656538	Combination arm showed improved overall survival vs drug alone arm (17.4 vs 10.4 months) (Erum Naqvi, 2013)

Table 2-4: Clinical trials investigating reovirus alone or in combination with other therapies for the treatment of various cancers.

Reovirus has been investigated alone and in combination with other therapies as a potential treatment for a wide range of malignancies, with some promising results.

Table 2-4 demonstrates the diverse applicability of reovirus in treating a variety of cancers. Most of these trials are in solid malignancies, however, reovirus was well-tolerated by patients with multiple myeloma (Sborov et al., 2014), but reported minimal effects on disease stability (4-8 months stable disease in 3/12 treated patients). Ongoing clinical trials are currently investigating reovirus in combination with Bortezomib and Dexamethasone for relapsed or refractory myeloma (ClinicalTrials.gov, 2015c) and in combination with lenalidomide or pomalidomide against relapsing myeloma (ClinicalTrials.gov, 2017c).

2.4.3 CAVATAK™/Coxsackievirus Type A21

2.4.3.1 Origins and Discovery

Coxsackievirus Type A21 (CVA21) is a non-enveloped member of the Enterovirus C species of the picornavirus family. It has a linear single-strand positive-sense RNA genome that is 7.4kb long (Bruu, 2013) . CVA21 is one of 23 Coxsackievirus Type A viruses (1-22 and 24).

CAVATAK™ is a non-manipulated clinical-grade formulation of CVA21. It is one of several aetiological agents of the common cold (Xiao et al., 2001). Similarly to Reolysin, CAVATAK was purified by routine passage in human ICAM-1-transfected rhabdomyosarcoma (ICAM-1-RD) cells to obtain a formulation of the virus that would be more homogenous than clinically-isolated virus samples (Shafren, D.R. et al., 2004). ICAM-1, the CVA21 entry receptor, is a member of the immunoglobulin superfamily with roles in cell signalling (Hubbard and Rothlein, 2000), endothelial transmigration (Rahman and Fazal, 2009) and endocytosis (Muro et al., 2003) and is widely expressed on both endothelial and immune cells, including B cells (Yashiro, 2008). DAF, the CVA21 attachment receptor, is a negative regulator of the complement system and acts by blocking the formation of the membrane attack complex (MAC) by inhibition of the C3 and C5 convertases (Kinoshita, 1998). ICAM-1 is expressed at high levels on lymphoma B cells in comparison to healthy B cells (The Human Protein Atlas, 2017) and DAF is highly expressed on a number of tumour types as a mechanism of complement resistance (Jurianz et al., 1999), including NHL (Terui et al., 2006), suggesting a strong rationale for using CVA21 to target NHL B cells. It is important to note that, while some clinical isolates of CVA21 do not always rely on both receptors to infect cells, the Kuykendall strain, which is the subject of these experiments, requires both receptors for successful infection (Newcombe et al., 2004).

Preclinical work has shown that CVA21 kills prostate cancer cell lines that expressed ICAM-1 (Berry et al., 2008), reduces tumour burden in human breast cancer xenografts (Skelding et al., 2009) and can reduce tumour burden and increase survival in a syngeneic mouse model of melanoma where B16 murine myeloma cells had been transfected with human ICAM-1 (Shafren, D. et al., 2014). Although research into the use of CVA21 to target HMs is at an early stage, CVA21 has efficacy as an oncolytic agent against myeloma cell lines that express both ICAM-1 and DAF, can target BM-derived primary patient MM cells and has no cytotoxicity against healthy lymphocytes (Au et al., 2007). Taken together, these data implicate CVA21 as a highly toxic agent against myeloma cells, and as a potential *ex vivo* purging agent.

2.4.3.2 Pathogenic Significance and Virulence

CVA21 is one of hundreds of aetiological agents of the common cold and primarily infects upper respiratory tract epithelial cells (Shafren, D.R. et al., 2004). Initially found to cause mild upper respiratory tract infections (URTIs) (Lennette et al., 1958), it is not expected to pose a significant risk as a pathogen to the public and has received a biosafety level of 2 from the ATCC (ATCC, 2017). This rating is designated to agents that pose a mild risk to the public and environment.

2.4.3.3 Progress in Clinical Trials

CAVATAK™ has been tested in several trials for various solid malignancies. It has successfully progressed through 5 phase one trials for bladder cancer in combination with Mitomycin C, non-small cell lung cancer in combination with pembrolizumab (anti-PD1 antibody), advanced melanoma in combination with pembrolizumab, melanoma in combination with ipilimumab and as a single agent for prostate cancer. CAVATAK™ has also completed a phase II trial for late stage melanoma where 63 patients with stage IIIc or IV melanoma received 10 intratumoural (IT) injections of CAVATAK™ across 18 weeks. This study showed 6-month progression-free survival in 22.5% of patients, surpassing (Andtbacka et al., 2015). This progress through a phase II trial shows promise for CAVATAK™'s possible acceptance as an approved therapy for melanoma. A summary of trials that examine the safety and efficacy of CAVATAK is shown in **Table 2-5**.

Disease	Combinations	Phase	Trial Numbers	Results
Melanoma	Pembrolizumab	I	NCT02565992	Recruiting, 18/23 disease control rate (Ann W. Silk, 2017)
	Ipilimumab	I	NCT02307149	Recruiting, combination well-tolerated, 14/18 disease control rate (Viralyitics, 2016)
		I	NCT03408587	Recruiting
	N/A	II	NCT01227551	22/57 Immune-related Progression-Free Survival (Andtbacka et al., 2015)
		I	NCT02316171	Virus well-tolerated, evidence of replication, apoptosis and inflammation in TME. (Nicola E Annels, 2015)
		I	NCT02043665	Virus was well-tolerated (ClinicalTrials.gov, 2016)
Bladder Cancer	Mitomycin C	I	NCT02043665	Virus was well-tolerated (ClinicalTrials.gov, 2016)
	Pembrolizumab	I	NCT02824965	Recruiting
Lung Cancer	Pembrolizumab	I	NCT00636558	Virus was well-tolerated, some evidence of replication (Pandha et al., 2015b)

Table 2-5: Clinical trials investigating CVA21 alone or in combination with other therapies for the treatment of various cancers.

CVA21 has been investigated alone and in combination with other therapies as a potential treatment for a wide range of malignancies, with some promising results.

As previously mentioned, no published research has demonstrated CVA21-induced cell death of NHL cell lines or primary patient material, however, CVA21 has induced cell death in other cancer types such as multiple myeloma (Au et al., 2007), melanoma (Au et al., 2005), breast cancer (Skelding et al., 2009), and prostate cancer (Berry et al., 2008), but no cell death in healthy donor PBMCs (Au et al., 2007). CVA21 and closely-related viruses have also demonstrated immunogenic properties in cancer models. Examples include, immunogenic cell death in CVA21-treated bladder cancer cells, and a role for $CD4^+$ T cells in targeting a murine C57/BL6 bladder cancer model (Annels et al., 2018), and CVB3-mediated NK cell infiltration and elimination of human non-small-cell lung carcinoma (NSCLC) in a nude BALB/c xenograft model (Miyamoto et al., 2012). CVA21's ability to preferentially target malignant cells, coupled with its demonstrated immunomodulatory potential, make it an exciting candidate for the treatment of NHL.

2.5 Aims of the study

This study aimed to investigate, by use of cell lines and primary patient material in isolation and in an NHL TME model, and an animal model for reovirus-mediated NK cell trafficking to the LN, the potential to use oncolytic virotherapy for the treatment of NHL, focusing on the efficacy of CVA21 and reovirus for the treatment of Burkitt's lymphoma, Diffuse Large B Cell Lymphoma-Germinal Centre B Cell Subset and Diffuse Large B Cell Lymphoma-Activated B Cell Subset. These NHLs were chosen due to their aggressive nature and high prevalence in patients. These studies will be undertaken to investigate novel and exciting avenues of therapeutic intervention to target resistant and aggressive NHL cells. More specifically, this study aimed to:

1. Compare two candidate OVs (reovirus and CVA21) for their ability to directly kill NHL cells by oncolysis and examine their efficacy against drug resistant malignant cells co-cultured with TME support. Reovirus and CVA21 were selected due to their impressive performance in clinical and pre-clinical trials to date, the elevated expression of ICAM-1 on NHL cells and the immunogenic potential of both viruses.
2. Investigate the specificity of CVA21 for malignant cells and characterise the cellular determinants responsible for CVA21 sensitivity.

3. Investigate the potential to use OVs, CVA21 and reovirus, to stimulate an anti-NHL immune response.
4. Validate the efficacy of CVA21 and reovirus against NHL using primary NHL samples.

Chapter 3:
Materials and Methods

Chapter 3

3.1 Cell Culture

3.1.1 Cell lines

Ramos, Raji, SU-DHL-4 and OCI-LY19 cells were kindly supplied by Dr. Reuben Tooze and Dr. Gina Doody from Experimental Haematology (Leeds Institute of Cancer and Pathology - LICAP). U2932, OCI-LY3, L929, MEL-624 and SK-MEL-28 cells were purchased from American Type Culture Collection (ATCC). Genotypic validation of Ramos, Raji, OCI-LY19, SU-DHL4, OCI-LY3 and OCI-LY10 was conducted in-house by Short Tandem Repeat (STR) profiling and compared with the Deutsche Sammlung von Mikroorganismen und Zellkulturen (DSMZ) database by Dr. Claire Taylor. The results from the STR profiling are shown in Figure 9-1 to Figure 9-6 (Chapter 9).

All cell lines were maintained at 37^{o}C in a humidified atmosphere containing 5% CO_2 (Sanyo). Ramos, Raji, OCI-LY19, SU-DHL4, U2932, CD40L^{+} L929 cell lines and parental L929 cells were maintained in sterile Roswell Parks Memorial Institute 1640 medium (RPMI 1640 – Sigma Aldrich) supplemented with 10% volume/volume (*v/v)* heat-inactivated (56^{o}C for 30minutes (mins)) Foetal Calf Serum (FCS – Life Technologies). OCI-LY3 cells were maintained in RPMI 1640 supplemented with 20% *v/v* FCS. SK-MEL-28 and MEL-624 cells were maintained in Dulbecco's Modified Eagle's Medium (DMEM – Sigma Aldrich) supplemented with 10% *v/v* FCS. For routine maintenance, once the cells had reached 80-90% confluence, the adherent cell lines (SK-MEL-28, MEL-624, CD40L^{+} L929 and parental L929) were washed in sterile Phosphate Buffered Saline (PBS – Oxoid) before being incubated with 1X Trypsin (Sigma Aldrich; 10X Trypsin was diluted 1 in 10 with HBSS and stored at -20^{o}C) to detach the adherent cells. Cells were then resuspended in fresh medium and a proportion transferred to a new tissue culture flask with fresh medium added as required. All tissue culture flasks were purchased from Corning unless stated otherwise. All cell lines were checked daily and split between 1:10-1:20 ratio once they had reached >80% confluence. Cell lines were maintained for ~20 passages to minimise variability and genetic drift. Viable cells were enumerated using Trypan blue (Beckman Coulter) exclusion, followed by cell counting on a

haemocytometer (Hawksley), for calculating seeding densities for subsequent assays.

3.1.2 Cryopreservation

Cell lines or primary patient cells were centrifuged at 400g for 5mins and resuspended in freezing medium (90% RPMI-1640 and 10% Dimethyl sulphoxide (DMSO, Sigma) for cell lines, and 50% human serum (Sigma), 40% RPMI-1640 and 10% DMSO for human primary patient cells). Cell suspensions were aliquoted at $5x10^6$/mL for cell lines and $10x10^6$/mL for primary patient material, in 1mL in a 1.2mL cryovial (Nunc, Sigma-Aldrich), and transferred to polystyrene boxes which were then placed at -80^{o}C overnight before being transferred to liquid nitrogen (LN_2). All centrifugation was carried out using an Eppendorf Centrifuge 5810R, unless otherwise stated.

Frozen cell stocks were retrieved from LN_2 storage and thawed in a 37^{o}C water bath and added dropwise, using a 3mL Pasteur Pipette (Fisher), to 10mL of their respective media (pre-warmed to 37^{o}C). Cell suspensions were pelleted by centrifugation at 400g for 5mins and the supernatant discarded, Cells were resuspended in 7mL of media, before being transferred to T25 flasks and allowed to rest overnight. Cells were monitored the following day by light microscopy, and a sample analysed by Trypan blue exclusion to give an estimate of cell viability. U2932s and OCI-LY3s were cultured in RPMI 1640 containing FCS at 20% and 30%, respectively, for the first week to aid their recovery. Once the cultures had been established, cells were harvested by centrifugation and place in RPMI 1640 containing 10% and 20% FCS, respectively, for routine culture.

3.1.3 Isolation of Human Mononuclear Cells from Peripheral Blood and Lymph Nodes

Lymph Node Mononuclear Cells (LNMCs) were isolated from LN biopsies of suspected cases of lymphoma which were supplied by the Haematological Malignancy Diagnostic Service (HMDS, Level 3, Bexley Wing, St. James' University Hospital (SJUH), Leeds). Ethical approval for the use of human LN samples was received from the NHS/HSC Research and Development offices / Research Ethics Committee (reference number: 14/WS/0098). Due to the non-sterile techniques used to harvest patient NHL LN biopsies, LN sample medium (RPMI 1640 and 10% (v/v) FCS) was further supplemented with Penicillin (50units/mL)/Streptomycin (50µg/mL) (Life Technologies). LNMCs were isolated from fresh samples by density centrifugation over

Lymphoprep™ (Axis Shield) (800g for 20mins, acceleration 6, brake 0). A 3mL Pasteur Pipette was used to aspirate the cell layer from the top of the Lymphoprep™ and isolated cells were washed in Hank's Balanced Salt Solution (HBSS – Sigma Aldrich) three times (600g for 10mins, acceleration 6, brake 6) before being assessed for cell viability using Trypan blue exclusion. Cells were resuspended at $2x10^6$ cells/mL in RPMI-1640 supplemented with 10% *v/v* FCS and Penicillin (50units/mL)/Streptomycin (50µg/mL). Cell numbers varied and not all samples yielded enough cells for immunophenotyping or viability assays. Cells that were not used immediately were frozen in LN_2 for longer term storage.

Peripheral blood mononuclear cells (PBMCs) were isolated from the whole blood of healthy donors with informed verbal consent by density centrifugation over Lymphoprep™ and prepared as described above for LNMCs. Cells were cultured at $2x10^6$ cells/mL in RPMI-1640 supplemented with 10% *v/v* FCS.

3.1.4 Cell culture decontamination and disposal

1% Virkon (DuPont UK Ltd.) was used to disinfect cell lines and LN sample waste, and 10% Distel (Tristel Solutions Ltd.) was used for whole blood waste products. Materials were decontaminated for a minimum of 60mins in their respective decontaminant.

3.1.5 NHL Co-cultures

Murine L929 cell lines, stably transfected to express human CD40L, were used to simulate the B cell (CD40) – T cell (CD40L) interaction thought to occur in the LNs (Clodi et al., 1998a). Parental, non-transfected L929 cells were used as a CD40L-negative control for these experiments. Both cell lines were trypsinised, harvested into 50mL Falcon tubes which were placed on ice, and irradiated with 50 Gray (Gy), 50mins at 1Gy/min Metrix NDT X-ray Irradiator. The cells were then retrieved from the irradiator, returned to culture and left overnight to allow them to adhere to the flask/well.

On day 2, NHL cells lines, healthy donor PBMCs or NHL LNMCs were added to L929 feeder layers at fixed ratios ($3x10^5$ NHL cell lines: $2x10^5$ L929 cells per $2cm^2$ or $2x10^6$ primary cells: $2x10^5$ L929 cells per $2cm^2$) in fresh media and returned to the incubator overnight. Controls were cultured in identical volumes and cell densities, in adjacent wells with no feeder layer. Cells were routinely cultured on the feeder layers for 24hrs before being used in experiments.

3.1.6 Cell Treatments

3.1.6.1 Oncolytic Viruses

3.1.6.1.1 Coxsackievirus Type A21 (CVA21)

CAVATAK™, the clinical-grade formulation of CVA21, was provided by Viralytics ltd. Clinical vials were stored at -80^{o}C for long term storage. For use, vials were thawed and aliquoted before being re-frozen at -80^{o}C. In-use vials were kept at 4^{o}C for no more than 24hrs due to the instability of the virus resulting in a loss of potency over time. CVA21 was also propagated in-house using the identical Kuykendall strain of CVA21, purchased from ATCC (#VR-850). CVA21 was added directly to cell culture medium at the required plaque-forming unit (pfu) per cell (pfu/cell) following quantification of viral titres using plaque assay (Section 3.1.6.1.1.2).

3.1.6.1.1.1 CVA21 Propagation and Purification

CVA21 Kuykendall Strain was propagated using MEL-624 cells and purified by density ultra-centrifugation; MEL-624 cells were used to propagate CVA21 due to their susceptibility at low doses.

On day 1, 12.5x10^{6} MEL-624 cells were seeded in T150 tissue culture flasks in 20mL DMEM supplemented with 10% *v/v* FCS, and Penicillin (50units/mL)/Streptomycin (50µg/mL). The cells were placed at 37^{o}C overnight. On day 2, the MEL-624 flasks were checked for 90% confluence and inoculated with CVA21 at 0.0005 pfu/cell and returned to the incubator for 72hrs.

On day 4, solutions were prepared for density centrifugation using Optiprep (Sigma). 0.1M EDTA (Sigma), 1M Tris (Sigma) and 1M NaCl (Sigma) were prepared, filtered using a 0.22µm filter and stored at 4^{o}C.

Subsequently, Solution B (100mL) was prepared using 50mL ddH_2O, 30mL 1M Tris stock solution and 3mL 0.1M EDTA. The pH was adjusted to pH7.4 using 5M Hydrochloric acid (HCl, Sigma) and the volume made up to 100mL with ddH_2O prior to filtration and storage at 4^{o}C.

Solution C (100mL) was then prepared using 50 mL ddH_2O, 10mL 1M NaCl, 5mL 1M Tris and 0.5mL 0.1M EDTA. The pH was adjusted to 7.4 with 5M HCl and the volume was made up to 100mL with ddH_2O prior to filtration and storage at 4^{o}C.

To prepare Solution D, 20mL of 60% Optiprep was added to 5mL of Solution B and used to prepare different concentrations of Optiprep as outlined below:

• 15% Optiprep: 3mL Solution D + 7mL Solution C

• 23% Optiprep: 4mL Solution D + 6mL Solution C

• 28% Optiprep: 6mL Solution D + 4mL Solution C

• 35% Optiprep: 7mL Solution D + 3mL Solution C

2.5mL of each concentration was then gently layered on top of one another, beginning with the highest percentage of Optiprep at the bottom and the lowest at the top, in two ultracentrifuge tubes (Beckman Coulter 344059; Tube, Thinwall, Ultra-Clear™, 13.2 mL, 14 x 89 mm). The gradients were then wrapped in parafilm, gently laid on their sides and kept at 4^{o}C overnight.

On day 5, the MEL-624 cells were examined under light microscope for cytopathic effect (CPE), with typically 50-80% of cells detaching from the flask upon agitation. The media was removed from the flasks, transferred to 50mL Falcon tubes (Corning) and centrifuged at 400g for 10mins. The supernatants were harvested from each falcon tube and amalgamated while the cell pellets were discarded. The amalgamated supernatant was filtered through a 0.22µm filter unit (Corning). The filtrate was distributed equally among an even number of 94mL Beckman Coulter heat-seal tubes (Tube, Thinwall, Polypropylene, 94 mL, 38 x 102 mm). The tubes were filled to maximum capacity and heat-sealed using Beckman Tube Topper (Beckman Coulter). The tubes were weighed to assure an equal distribution of weight (to within 0.1g difference) and placed in a Ti45 rotor (Beckman Coulter) for ultracentrifugation using a Beckman Optima L-80 Ultracentrifuge (Beckman Coulter) (150,000g, 2hrs, 4^{o}C). The tubes were subsequently removed from the ultracentrifuge, the sealed nib was removed with a scalpel (Swann-Morton) and 20mL media was aspirated and discarded. Following this, the tops of the tubes were cut off using a scalpel and the media discarded. The virus pellets were resuspended in PBS and amalgamated in less than 1mL. The virus formulation was then equally distributed onto Optiprep gradient tubes and approximately 1mL of solution C added, leaving a 3mm gap at the top of each tube. The Optiprep tubes were loaded into a SW41Ti swing rotor (Beckman Coulter) for ultracentrifugation (160,000g, 1hr 30min, 4^{o}C). After centrifugation, the virus was extracted from the gradients by removal of approximately 1mL of supernatant, ~8cm from the bottom of the tube, and

CVA21 stocks were aliquoted in 25µL volumes and stored at -80ºC. A representative diagram of the virus-loaded Optiprep gradients is shown in **Figure 3-1**.

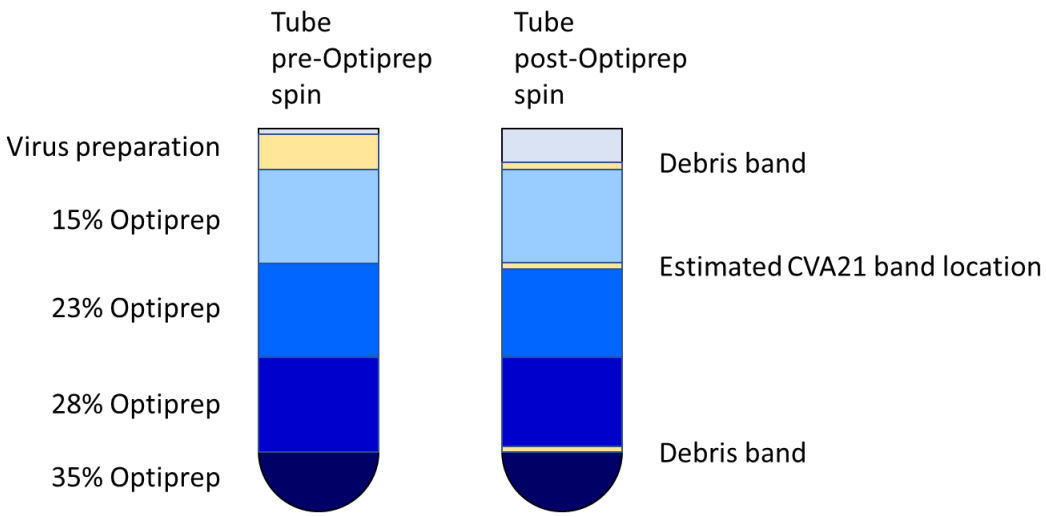

Figure 3-1 Representative Optiprep gradients before and after ultracentrifugation.

Virus was loaded onto optiprep gradients. Following ultracentrifugation, the virus preparation loaded on top of the gradient separates into a low debris band (above the 35% gradient), a high debris band (above the 15% gradient) and the CVA21 band estimated to be between the 15 and 23%.

3.1.6.1.1.2 CVA21 Plaque Assay

CVA21 infectious particles were enumerated by plaque assay on MEL-624 cells. On day 1, $9x10^5$ MEL-624 cells were seeded in 2mL media per well of a 6-well plate (Corning) and left to adhere overnight. On day 2, MEL-624 cells were examined under light microscope for 95% confluence. Stock samples of CVA21 were serially diluted by a factor of 10 from 10^{-3} to 10^{-10} (25µL of each dilution into 225µL of media). The media was aspirated from the MEL-624 wells and 100µL of each virus dilution was then added with 500µL serum-free DMEM to duplicate wells of 95% confluent MEL-624 monolayers and incubated at 37°C for 2hrs. After 2hrs, the virus dilution samples were aspirated and 2mL overlay media was gently added to each well. Overlay medium comprised of a 1:1 ratio of 3% Carboxymethylcellulose (CMC, in sterile ddH20, Sigma) and 2xDMEM (pH7.6 adjusted with sodium bicarbonate, Sigma) supplemented with 20% FCS, creating a 1.5% CMC: 1xDMEM-10% FCS solution. Following addition of the CMC overlay media, the plates were returned to the incubator for a further 72hrs. On day 5, the CMC overlay was gently aspirated, and the wells were washed in 1mL PBS. The PBS was subsequently aspirated, and the cells were fixed in 1mL 1% Paraformaldehyde (PFA; Sigma) in PBS for 20mins. The PFA was removed and the monolayers were stained with 300µL 1% methylene blue in PBS (Sigma) for 10mins before the methylene blue was discarded and the plates were rinsed gently with water. Plates were left to dry and plaques were counted in wells where 10-90 plaques were present. To calculate pfu/mL, the plaque count was averaged from duplicate wells and this figure was multiplied by the appropriate dilution factor, and then multiplied by 10 to give the plaque count per millilitre, because 100µL of the virus dilution was used.

3.1.6.1.1.3 CVA21 50% Tissue culture Infective Dose ($TCID_{50}$)

$TCID_{50}$ assays were used to measure virus replication in NHL, PBMC and LNMC samples. On day 1, $6x10^3$ SK-MEL-28 cells were seeded in 100µL DMEM supplemented with 10% FCS into flat-bottomed 96-well plates and left overnight. On day 2, virus samples were serially diluted 10-fold (100µL of each dilution in 900µL of media) from 10^{-1} to 10^{-10} and 100µL of each dilution was added to octuplicate wells of the SK-MEL-28 cells. The plates were returned to the incubator for 5 days. On day 7, media was aspirated, and the wells were washed with 200µL PBS. Cells were then fixed (100µL 4% PFA) for 10mins at room temperature before staining in 1% methylene blue solution (30µL/well, 5mins, room temperature). Excess methylene blue was removed using running water and the plates were left to dry. Wells that

stained blue were deemed to contain viable cells and therefore no infectious virus, while wells that did not stain were deemed to be devoid of cells due to lytic replication of the virus causing CPE. The number of wells where CPE had occurred was counted for each dilution and this data was analysed using the Reed-Muench method (Reed, L.J. and Muench, 1938) which calculated the $TCID_{50}$ for that sample. $TCID_{50}$ values were used to calculate the fold increase in viral replication at appropriate time points after CVA21 treatment.

3.1.6.1.1.4 Ultraviolet irradiation of CVA21

Stock virus was diluted in 100µL PBS in 1 well of a 48-well plate (Corning). The virus was subjected to 3mins of UV exposure (Stratalinker® UV Crosslinker). Virus inactivation at this time point was validated by plaque assay. Control, non-UV-exposed CVA21 was transported and stored identically to the UV-inactivated CVA21.

3.1.6.1.2 Reovirus

Clinical grade Reolysin was provided by Oncolytics Biotech Inc. and stored at -80ºC. Bottles were thawed and aliquoted into 1.2mL cryovials and re-frozen at -80ºC. These vials were thawed as required and the virus concentration (pfu/mL) was quantified by plaque assay on L929 cells in an identical protocol to the CVA21 plaque assay. Reolysin aliquots were stored at 4ºC for up to 4 weeks due to the stability of reovirus particles.

3.1.6.1.3 Rapamycin

Rapamycin (Selleckchem), a potent mTORC1 inhibitor, was used alongside DMSO-treated and untreated controls to measure the effects of mTORC1 blockade on CVA21 cytotoxicity, proliferation and cell cycling in NHL cell lines. A stock solution of 100µM was prepared by reconstituting in DMSO. This was aliquoted and stored at -20ºC.

3.1.6.1.4 ICAM-1 Blockade

A human anti-ICAM-1 (αICAM-1, Biolegend) antibody was used to block ICAM-1 on NHL cell lines. NHL cell lines were seeded at $3x10^5$ cells/mL in multi-well plates (Corning) and αICAM-1 antibody or IgG1 isotype control antibody was added in escalating concentrations ranging from 1µg/mL to 20µg/mL. The cells were returned to the incubator for 30mins prior to treatment with CVA21.

3.1.7 Flow Cytometry – Fluorescence activated cell sorter (FACS)

Flow cytometry assays were performed using an Attune® Acoustic Focusing Cytometer (Applied Biosystems).

3.1.7.1 LIVE/DEAD™ Cell Viability

Cells were harvested into FACS tubes (Falcon), washed in 2mL PBS and pelleted by centrifugation (400g, 5mins, room temperature). The supernatant was discarded, and the cell pellet was resuspended in the residual volume and stained with LIVE/DEAD™ Fixable Yellow Dead Stain (Life Technologies); 0.5µL of LIVE/DEAD™ stain diluted in 0.5mL PBS, was added to each tube or 0.5mL PBS (without LIVE/DEAD™ stain) as a negative control. Samples were incubated at 4^{o}C, in the dark for 30mins, washed in 2mL PBS and pelleted by centrifugation (400g, 5mins). The supernatant was discarded, and the cell pellet was resuspended in 300µL 1% PFA (4^{o}C), prior to data acquisition and analysis by Flow Cytometry.

3.1.7.2 Extracellular Marker Staining

All extracellular staining and analysis was conducted using a similar protocol. Cells (cell lines, LNMCs, PBMCs) were harvested into FACS tubes and washed in 2mL FACS buffer (0.1% Sodium Azide (Sigma Aldrich), 1% FCS in PBS) and cells were pelleted by centrifugation (400g, 5mins). The supernatant was discarded, and cell pellets were resuspended in residual volumes. Fluorescently-conjugated antibodies were added (5 or 10µl per 1x10^{6} cells) and cells were left at 4^{o}C, in the dark for 30mins. Samples were subsequently washed in 2mL FACS buffer, pelleted by centrifugation (400g, 5mins), and the cells were fixed in 300µL 1% PFA. Cells were then analysed by Flow Cytometer at a constant flow rate. Forward Scatter/Side Scatter (FSC/SSC) plots were used to identify cell populations of interest prior to analysis. Marker expression was quantified using histogram plots along with mean fluorescence intensity (MFI), as appropriate. FACS antibodies used are detailed in **Table 3-1**.

3.1.7.3 Intracellular Phosflow™ Staining

Phosflow™ staining was performed as per the manufacturer's recommendations. Treated cells were harvested into FACS tubes and washed in 2mL FACS buffer prior to centrifugation (600g, 10mins). Extracellular staining to identify specific cell populations (e.g. CD20 on B

cells) was performed at this point, if required (detailed in section 3.1.7.2). Samples were washed in 2mL FACS buffer, centrifuged (600g, 10mins) and resuspended in 1mL warmed media and 1mL Cytofix™ (BD Biosciences). The tubes were incubated at 37^{o}C for 12mins in the dark to fix the cells. The cells were then centrifuged (600g, 8mins) and the supernatant was discarded. Tubes were vortexed to resuspend the cell pellets and 1mL chilled Perm Buffer III (BD Biosciences) was added to each tube; cells were vortexed again and placed at 4^{o}C, in darkness for 30mins. Cells were then washed twice in 2mL FACS buffer (centrifugation at 600g for 8mins), and cell pellets were resuspended in residual volumes. Antibodies αp-S6, αp-4EBP1, αp-STAT1 and isotype controls were diluted 1 in 10 with FACS Buffer (10µL Antibody: 90µL FACS buffer per 1x10^{6} cells) and 100µL was added to the respective FACS tubes. The cells were incubated in darkness for 60mins at room temperature before being washed in 2mL FACS buffer and pelleted by centrifugation (600g, 10mins). After the supernatant was discarded the cell pellet was resuspended in 500μL FACS buffer and data acquired by flow cytometer. FACS antibodies and volumes used are detailed in **Table 3-1**.

Target	Species	Fluorophore	Clone	Volume µL /1x10^6cells	Provider
IgG1	Mouse BALB/c	PE	EMR8-5	5µL	BD
IgG2B	Mouse C57BL/6	PE	2H7	5µL	BD
MHC I	Mouse BALB/c	PE	EMR8-5	5µL	BD
CD3	Mouse BALB/c	PE	SP34-2	10µL	BD
CD3	Mouse BALB/c	FITC	UCHT1	5µL	BD
CD19	Mouse	FITC	HIB19	5µL	BD
CD19	Mouse	PE	HIB19	5µL	BD
CD20	Mouse C57BL/6	PE	2H7	5µL	BD
CD20	Mouse	VioBlue	LT20	5µL	Miltenyi Biotec
IFN-α/β receptor	Mouse	APC	85228	5µL	R & D Systems
ICAM-1 (CD54)	Mouse BALB/c	PE	HA58	5µL	BD
DAF (CD55)	Mouse	PE	IA10	5µL	BD
p-STAT1	Mouse	PE	4a	10µL	BD
p-S6	Mouse BALB/c	PE	N7-548	10µL	BD
p-4EBP1	Mouse BALB/c	PE	M34-273	10µL	BD
CD56	Mouse	PE	p282 (H19)	5µL	BD

CD56	Mouse	FITC	B159	5µL	BD
CD69	Mouse BALB/c	FITC	L78	5µL	BD
CD107a	Mouse BALB/c	FITC	H4A3	10µL	BD
CD107b	Mouse	FITC	H4B4	5µL	BD
Nectin-2	Mouse	PE	R2.525	5µL	BD
CD40L (CD154)	Mouse BALB/c	PE	89-76	5µL	BD
JAM-A	Mouse BALB/c	PE	M.Ab.F11	5µL	BD
Tetherin	Rat	PE	eBio927	10µL	eBiosciences

Table 3-1 List of Anti-Human Antibodies

Table lists the anti-human antibodies that were used for flow cytometry-based analysis, their animal of origin, fluorophore, clone, volume per test and manufacturer.

3.1.7.4 Cell Proliferation Assays

CFSE (Carboxyfluorescein succinimidyl ester, Thermofisher Scientific) fluorescent dye was used to measure the proliferation of NHL cell lines, whereby maximal fluorescence was recorded upon cell staining on day 0 and subsequent cell divisions resulted in diminishing CFSE fluorescence on daughter cells (as shown in **Figure 3-2**).

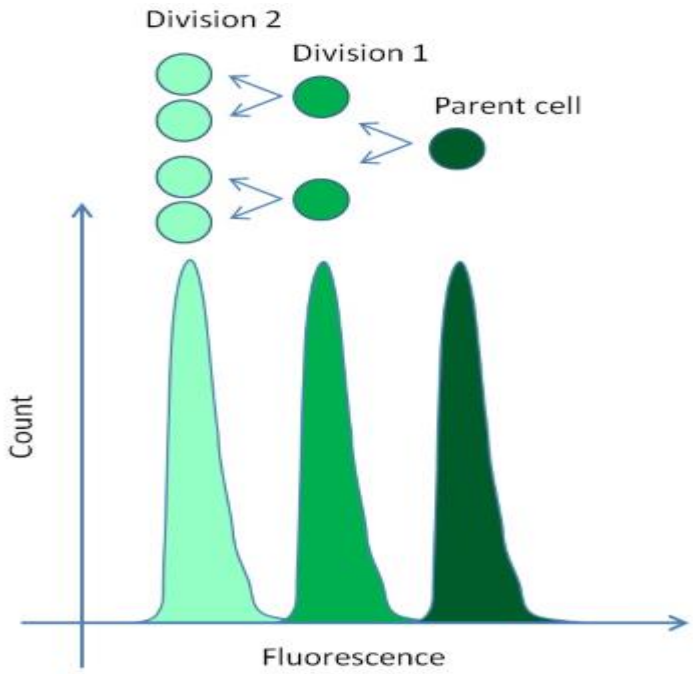

Figure 3-2 Representative diagram of the principles of CFSE staining.

Parent cells are stained with CFSE on day 0 (maximal fluorescence). Subsequent cell divisions result in the halving of CFSE staining, and fluorescence, between daughter cells. Cell proliferation can be inferred from diminishing CFSE fluorescence by flow cytometry.

On day 0, $2x10^6$ cells were washed in 2mL PBS and pelleted by centrifugation (400g, 5mins). CFSE was reconstituted in DMSO and used at a concentration of 500nM to stain the cells. For comparison, unstained controls were also prepared. The cells were then incubated at 37^{o}C for 20mins, washed in 10mL medium at room temperature for 5mins before being centrifuged (400g, 5mins), resuspended at $3x10^5$ cells/mL and seeded at 0.5mL per well in 48-well plates. After 3hrs in culture, prior to treatment, unstained and stained samples were analysed for CFSE fluorescence to quantify maximal CFSE fluorescence prior to cell proliferation. Treated and untreated CFSE-labelled and CFSE-unlabelled cells were harvested at 24hr intervals and CFSE intensity was quantified by flow cytometry.

3.1.7.5 Cell Cycle Analysis

NHL cells were harvested and fixed in ice cold 70% ethanol (Sigma) and incubated at 4°C for a minimum of 30mins. The cells were then stained with propidium iodide (PI, Sigma, 1mg/mL) at 50µg/mL in PBS in the presence of 100ng/mL RNAse (Sigma), to remove contaminating RNA, for 30mins. The samples were then washed twice in PBS and cells pelleted by centrifugation (400g, 5mins) and immediately analysed by Attune® Accoustic flow cytometer using the BL-2 fluorescence channel set to a linear scale. For assessment of cell cycle phase, cells that are 4n (tetraploid, G2/M) have double the fluorescence of cells that are 2n (diploid, G1), as depicted in **Figure 3-3**.

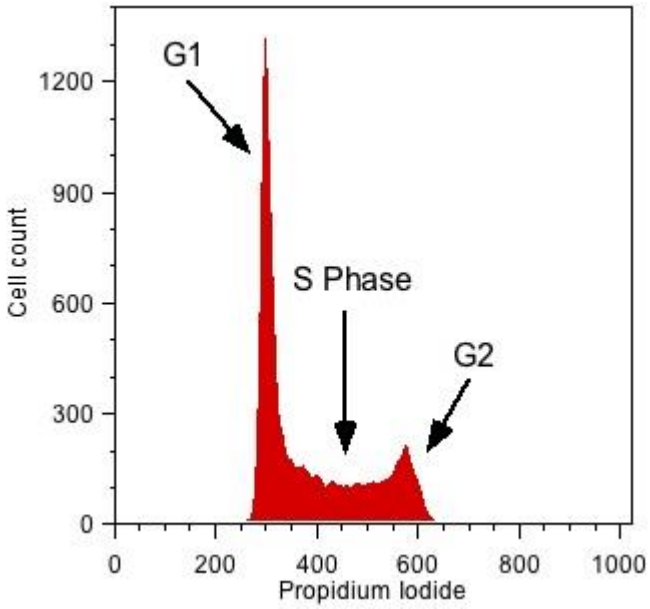

Figure 3-3 Representative histogram of Propidium Iodide Analysis.

PI-stained cells were analysed by flow cytometry on a linear scale. Cells in G1, S and G2M phase of the cell cycle are labelled according to the PI intensity and correlating DNA content.

3.1.7.6 NK cell Degranulation Assay

HDPBMCs (untreated or OV-treated; CVA21 or reovirus) were resuspended at $2.5x10^6$ per mL and cell line targets (unlabelled, isotype-labelled or mAb-labelled.) at $2.5x10^5$ per mL. HDPBMCs and cell lines were co-cultured at a fixed effector to target ratio of 10:1 ($5x10^5$:$5x10^4$) in 400µL of media in FACS tubes at 37^{o}C for 1hr. During this time a master mix was prepared containing αCD3 and αCD56 antibodies for identification of NK cells ($CD3^-CD56^+$), and CD107a and CD107b, for assessment of NK degranulation. Brefeldin A (Sigma; 1mg/mL stock) was also included at 50µg/mL to prevent CD107a/b recycling into the cell. The master mix recipe per tube is shown in **Table 3-2**.

Item	Per tube (µL)
CD3 VioBlue (Miltenyi)	2
CD56 PE (BD)	2
CD107a FITC BD)	4
CD107b FITC (BD)	4
Brefeldin A (Sigma)	0.5
RPMI-10% FCS	87.5
Total	100

Table 3-2 Master mix recipe per tube for NK cell degranulation assay.

Table shows the relative volumes of antibodies, Brefeldin A and media per tube used to detect NK cell degranulation.

After 1hr co-culture, 100µL of the master mix was added to each tube and the FACS tubes were returned to the incubator for a further 4hrs. After 4hrs, the cells were washed in 2mL FACS Buffer, pelleted by centrifugation (400g, 10mins) and fixed in 300µL 1% PFA. The samples were stored at 4^{o}C and protected from light until acquisition and analysis by flow cytometer; degranulating NK cells were identified as $CD3^{-}CD56^{+}CD107a/b^{+}$.

3.1.8 Enzyme-linked Immunosorbent Assay (ELISA)

ELISAs were used to measure the production of interferon-α (IFN-α) in cell-free supernatants in response to OV treatment.

On day 1, NUNC 96 well MAXISORP flat-bottomed plates (Thermo Scientific) were coated with 100µL per well anti-human IFN-α capture antibody (stock concentration of 1mg/mL, Mabtech, MT1/3/5), diluted 1 in 250 in coating buffer; 10x coating buffer (1M $NaHCO_3$ (BD Laboratory Supplies, Poole, UK) pH8.2) was diluted 1 in 10 (1x coating buffer, 0.1M NaHCO3, pH8.2) using dd$H_2$0 prior to use. The plates were wrapped and left at 4^{o}C overnight.

On day 2, the plates were washed 3 times with 300µL 0.05% Tween (Sigma) in PBS (PBS-Tween) with a SkanWash 300 (Gemini BV Laboratory) and blocked using 200µL of blocking solution (10% *v/v* FCS in PBS) per well for 2hrs at room temperature. The plates were then washed 3 more times with 300µL PBS-Tween. IFN-α standards (Biolegend) were prepared by diluting the stock in RPMI to give a top standard of 5000pg/ml with halving dilutions used to give a standard range down to 78.125pg/ml. Samples were then added to the wells in triplicate at 100µL per well. The plates were wrapped and left at 4^{o}C overnight.

On day 3, the plates were washed 6 times in 300µL PBS-Tween with a SkanWash 300 and the anti-h IFN-α detection antibody (1mg/mL, Mabtech, MT2,4,6) was prepared as a 1 in 1000 dilution in blocking solution, added at 100µL per well and left at room temperature for 2hrs. The plates were then washed a further 6 times in 300µL PBS-Tween/well and 100µL Extravidin (Sigma; stock concentration of 5mg/mL) was added to each well after a 1:5000 (in PBS-Tween) dilution. Plates were left for 1hr at room temperature, during which time the substrate solution (p-nitrophenyl phosphate (pNpp) in Tris-buffered saline (TBS) (Sigma) at 1mg/ml in 20mL ddH_2O) was prepared and protected from light. Following the Extravidin incubation, the plates were washed 3 times again in PBS-Tween, and 3 times with H_2O, and 100µL of substrate solution was added to each well.

The wells were incubated in darkness at room temperature for 20mins and optical density was then determined using a plate reader (Multiskan Ex, Thermo Scientific) and 405nm filter. The Optical Density (OD) values of the wells were calculated as the mean of the triplicate wells, minus the media only control. The IFN-α standards were used to generate a standard curve, using Microsoft Excel, and the resulting equation was subsequently used to calculate the concentration of IFN-α in each of the samples tested, using their observed OD values.

3.1.9 *In vivo* experiments

In vivo animal experiments were performed at the St. James' Biomedical Service (SBS). All experiments were approved by Home Office and standards of care were based on UKCCCR Guidelines for the welfare and use of animals in cancer research (Workman et al., 2010). Experiments were carried out on non-tumour-bearing male C57BL/6 mice.

6 male C57BL/6 mice aged 6-8 weeks were inoculated with 100 µL PBS or 10^8 pfu reovirus in 100µL PBS (3 mice/group) via tail vein injection. Inguinal, axillary, and brachial LN were dissected from the C57BL/6 mice 24hrs post-infection. The LN were then transferred to a mixture of Liberase™ (Sigma), HBSS and DNAse (Sigma) to allow digestion of the LN and release of the LNMCs.

Murine LNMCs were enumerated by Trypan Blue exclusion and $1x10^6$ viable cells were transferred to FACS tubes. Cells were stained with CD3e and NK1.1 antibodies (**Table 3-3**) as described previously (section 3.1.7.2) and NK cells were enumerated by flow cytometry. NK cells were defined as $CD3e^-NK1.1^+$ and expressed as a percentage of the total LN cell population.

Target	Species	Fluorophore	Clone	Volume µL /1x10^6cells	Provider
CD3e	Hamster	PE	BM10-37	2	BD
NK1.1	Mouse	FITC	PK136	2	Biolegend

Table 3-3: Anti-Mouse Antibodies

Table shows antibodies used to identify murine NK cell from C57/BL6 mice.

3.2 Statistics

GraphPad Prism (version 7.04) software was used to analyse data and perform paired, two-tailed student's t-test, one-way and two-way Analyses of Variance (ANOVAs), and Pearson's tests as required. If the resulting p-value was less than 0.05 then the difference was deemed statistically significant. Microsoft Excel was used to generate standard curves for ELISAs.

Chapter 4:

Efficacy of CVA21 and reovirus against Non-Hodgkin Lymphoma

Chapter 4

4.1 Introduction

OVs can target cells by direct oncolysis, whereby they replicate in malignant cells and release their progeny virions by rupturing the cell membrane (Zeyaullah et al., 2012). This chapter details the comparison of two candidate OV, reovirus and CVA21, in terms of the expression of their entry receptors, due to the reliance of both OV on the availability of their receptors for cell entry and infection, and their ability to induce cell death of NHL B cell lines while sparing healthy B cells.

Previous work by Kim, *et al*., has shown that reovirus is a poor lytic agent against the Burkitt's lymphoma (BL) cell lines, Ramos and Raji (Kim et al., 2010). The work described in this chapter expands upon this study to test the susceptibility of other NHL cell lines to reovirus, namely the DLBCL cell lines, SU-DHL-4 and OCI-LY19 of the GCB subset, and U2932 and OCI-LY3 of the ABC subset. Currently there are no studies investigating the efficacy of CVA21 against NHL.

Importantly, CD40:CD40L engagement is associated with activation of germinal centre B cells under normal production of a humoral immune response and provides a strong pro-survival signal to B cells (Elgueta et al., 2009), and has also been associated with drug resistance in NHL models (Voorzanger-Rousselot et al., 1998). Moreover, given the reported increase in ICAM-1 expression on CD40L-stimulated B cells (Shinde et al., 1996), the effects of the CD40:CD40L interaction on OV receptor expression and susceptibility in NHL cell lines and healthy B cells, and sensitivity of NHL cell lines to vincristine-induced cell death were also investigated. Under the medical name Oncovin®; vincristine inhibits microtubule formation and affects cell division (prophase), causing intracellular cell stress and apoptosis (Jordan and Wilson, 2004). Vincristine was investigated due to its prominent role as a component of the R-CHOP regimen and its potency at inducing apoptosis (Groninger et al., 2002), a process that is reportedly diminished by stimulation of CD40 (Lee, S.W. et al., 2012), potentially resulting in reduced efficacy of the drug.

Overall, the results reported in this chapter investigate the direct oncolytic potential of CVA21 and reovirus against NHL.

4.2 Results

4.2.1 Oncolytic Virus Receptor Expression on NHL cell lines.

Infection of a target cell by a virus involves a carefully orchestrated interaction between the virus and the host cell surface to facilitate entry into the intracellular compartment. This process requires expression of viral entry receptors on the surface of the target cell to enable virus binding and entry (Marsh and Helenius, 2006). CVA21 requires DAF and ICAM-1 (Shafren, D.R. et al., 1997b) to enter target cells, while reovirus uses JAM-A, therefore, the expression of these proteins was examined on a panel of 6 NHL cell lines (**Figure 4-1**, **Figure 4-2**).

Figure 4-1 shows representative histogram plots for αICAM-1 (a-f), αDAF (g-l) and αJAM-A (m-r) (all light grey) antibody staining on NHL cell lines overlaid with isotype antibody-stained controls (dark grey). This data shows that the OV receptors ICAM-1, DAF and JAM-A are widely expressed on most NHL cell lines tested. To quantify this expression, the MFI of antibody-stained cells was expressed as a fold change above isotype-stained cells, **Figure 4-2**. ICAM-1 (a) is highly expressed on Ramos, Raji, SU-DHL-4, U2932 and OCI-LY3 cell lines, with a range of 10- to 120-fold increase in MFI, but very low on OCI-LY19 cells, with only a 2-fold increase. DAF (b) is expressed on all cell lines, ranging from 10- to 30-fold increased MFI. JAM-A (c) expression on NHL cell lines ranges from 27- and 20-fold increase in MFI on U2932 and Ramos cells, respectively, to a 5-fold increase on Raji and OCI-LY19 cells, and only a 2-fold increase on SU-DHL-4 and OCI-LY3.

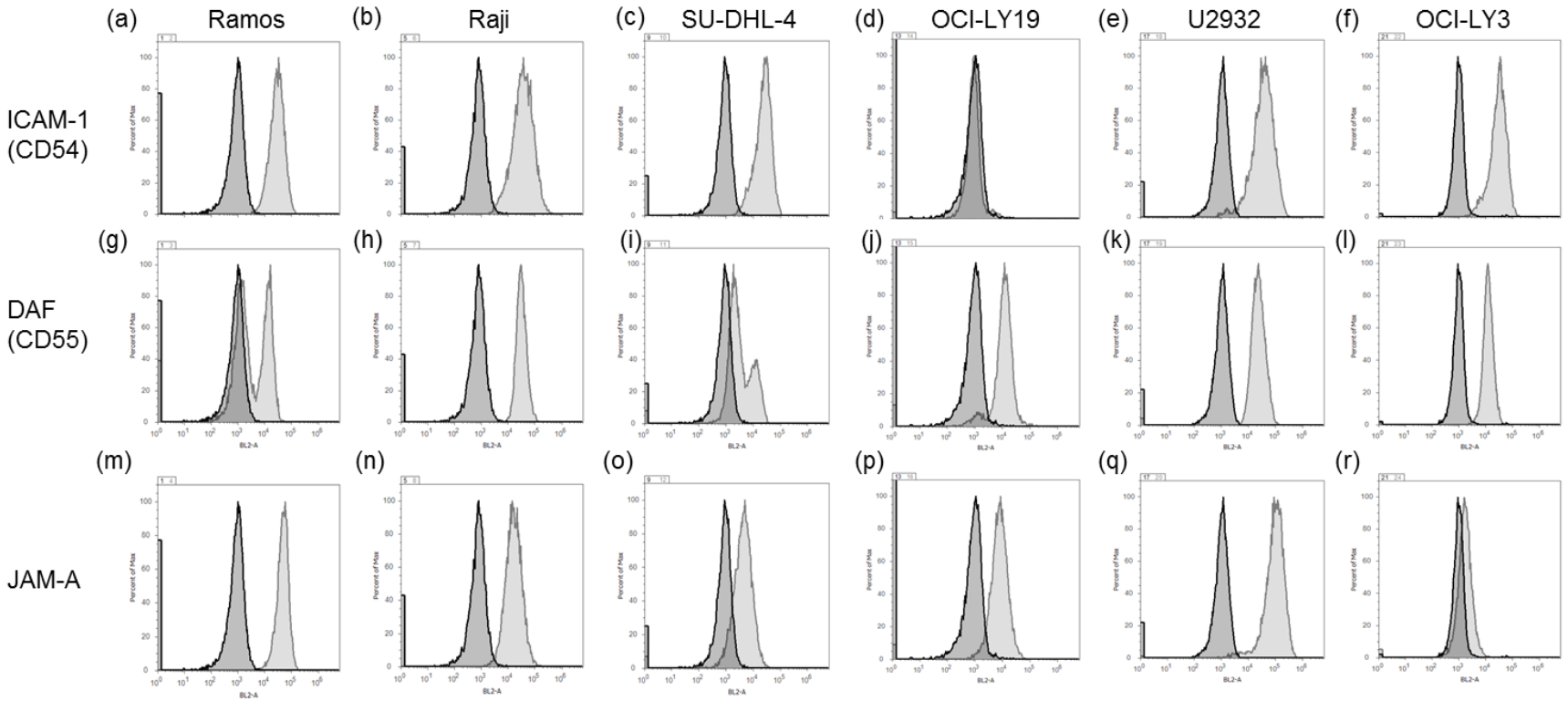

Figure 4-1 Histogram plots showing OV Receptor expression on NHL cell lines.

Ramos, Raji, SU-DHL-4, OCI-LY19, U2932 and OCI-LY3 NHL cell lines were harvested and analysed for surface expression of the CVA21 entry receptor, ICAM-1 (a-f), co-receptor, DAF (g-l), and reovirus receptor, JAM-A (m-r), by flow cytometry. Receptor expression is illustrated by representative histogram plots overlaying isotype (negative control) in dark grey and receptor staining in lighter grey. Results shown are representative of n=3 independent experiments

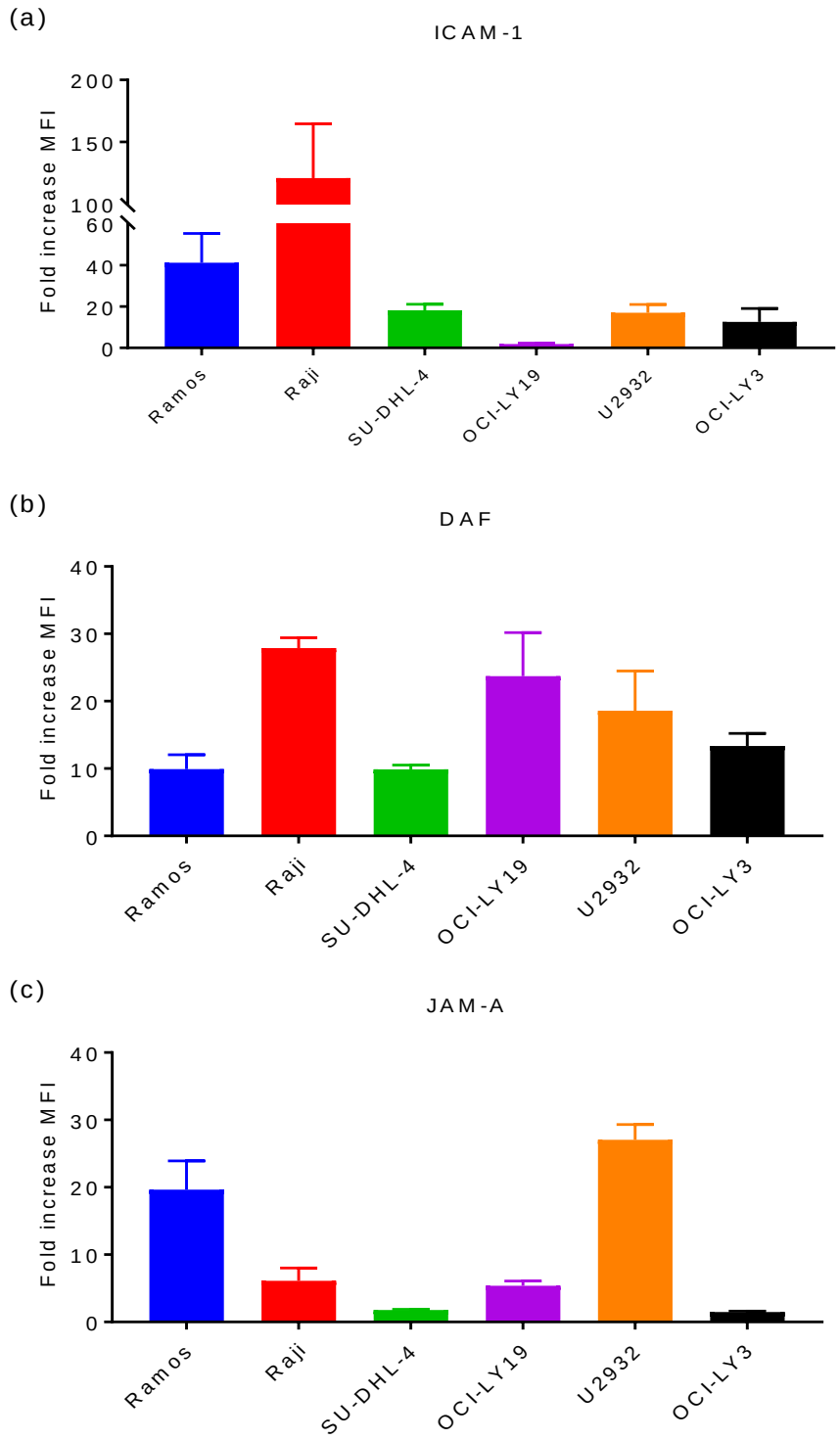

Figure 4-2 Quantification of OV Receptor Expression on NHL cell lines.

Ramos, Raji, SU-DHL-4, OCI-LY19, U2932 and OCI-LY3 NHL cell lines were harvested 24hrs post-passage and analysed for surface expression of OV receptors by flow cytometry. ICAM-1 (a), DAF (b) and JAM-A (c) expression was measured as the fold increase in MFI of receptor antibody-stained cells above isotype antibody-stained controls. Data shows the mean of n=3 independent experiments + SEM.

4.2.2 Efficacy of reovirus against NHL

Reovirus has previously demonstrated potent lytic abilities against a range of solid malignancies, as well as an ability to target HMs, such as myeloma (Thirukkumaran, C. M. et al., 2012), and NHL (Alain et al., 2002), where it induced cell death in some myeloma and NHL cell lines, and primary myeloma, NHL and CLL samples, while others were resistant. To examine the efficacy of reovirus in targeting a wider variety of NHL cell lines, including DLBCL lines, Ramos (a), Raji (b), SU-DHL-4 (c), OCI-LY19 (d), U2932 (e) and OCI-LY3 (f) cell lines were treated with increasing doses of reovirus for up to 72hrs and analysed for viability every 24hrs by LIVE/DEAD™ staining and flow cytometry. **Figure 4-3** shows that reovirus cytotoxicity is limited in all cell lines tested, with Raji and U2932 cells exhibiting 20 and 30% cell death after treatment with 10pfu/cell at 72hrs, respectively. SU-DHL-4 and OCI-LY19 cells demonstrated a small (10% above background cell death), yet significant increase in cell death after treatment with reovirus at 10pfu/cell by 72hrs, while Ramos and OCI-LY3 cells remained resistant. This data shows that, despite JAM-A expression, not all cells were susceptible to reovirus oncolysis, suggesting alternate determinants of reovirus susceptibility.

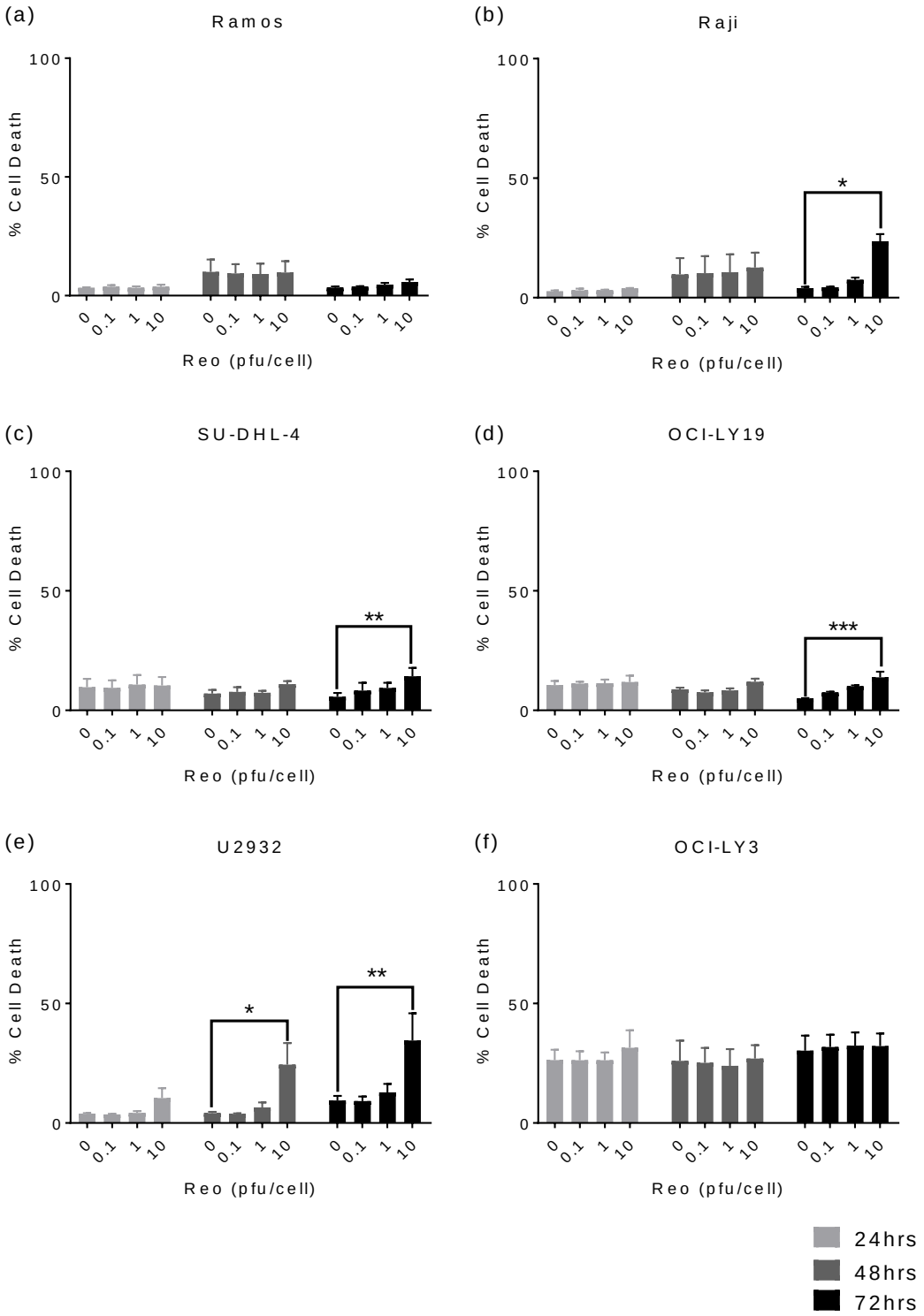

Figure 4-3 Cytotoxicity of reovirus against NHL cell lines.

Ramos (a), Raji (b), SU-DHL-4 (c), OCI-LY19 (d), U2932 (e) and OCI-LY3 (f) cell lines were treated with 0.1, 1 and 10 pfu/cell reovirus for 24, 48 and 72hrs. At each time point, cells were analysed for viability by flow cytometry using LIVE/DEAD™ staining. Data shows the means of n=3 independent experiments + SEM. Significance was determined by two-way ANOVA.

4.2.3 Efficacy of CVA21 against NHL

Using LIVE/DEAD™ staining and analysing cells by flow cytometry, the cytotoxic effects of CVA21 on NHL B cell lines was determined. **Figure 4-4** shows that CVA21 induced cell death in Ramos (a), Raji (b), SU-DHL-4 (c), U2932 (e) and OCI-LY3 (f) cell lines in a dose- and time-dependent manner. The cell lines displayed varying degrees of susceptibility to CVA21, with Raji, SU-DHL-4 and OCI-LY3 cells showing significant death by 48 and 72hrs at as little as 0.01pfu/cell, while cell death of Ramos and U2932 increased up to 72hrs with maximal death at 1 pfu/cell. By contrast, OCI-LY19 (d) cells remained completely resistant to the virus, even at 96hrs (data not shown), in keeping with the low expression of ICAM-1 on the surface of this cell line.

The lowest dose of CVA21 represents a ratio of 0.01 CVA21 particles per NHL cell (or 100 cells per infectious CVA21 particle). This suggests that CVA21 is replicating and releasing progeny viruses to infect and kill neighbouring cells. To test this, cell-free supernatants were harvested from 0.01 and 0.1pfu/cell-treated samples and analysed for viral titre by $TCID_{50}$ assay (**Figure 4-5**). **Figure 4-5** shows increased viral titre above input levels in Ramos, Raji, SU-DHL-4, U2932 and OCI-LY3 cell lines confirming viral replication within these cells.

To confirm that viral replication was required for CVA21-induced cell death of NHL cell lines, UV-inactivated (replication-deficient) CVA21 was used. **Figure 4-6** (a) shows representative plaque assays of non-UV and UV-inactivated CVA21, demonstrating that 3mins of UV exposure is sufficient to completely abrogate CVA21-induced plaque formation on MEL-624 cells. NHL cell lines Ramos (b), Raji (c), SU-DHL-4 (d), U2932 (e) and OCI-LY3 (f) were then treated with non-UV and UV-inactivated CVA21 for up to 48hrs and analysed for viability. This data demonstrates that UV-inactivated CVA21 was unable to induce cell death, highlighting the importance of viral replication for CVA21-induced cell death.

As previously discussed, CVA21 relies on DAF as its binding receptor and ICAM-1 as its entry receptor (Shafren, D.R. et al., 1997b). Previous research has outlined how both receptors are required for cell entry by the Kuykendall strain of CVA21 (Newcombe et al., 2004), highlighting that, although clinical isolates can vary in their receptor requirements, the Kuykendall strain is dependent on the availability of both receptors. To examine whether CVA21 relies on ICAM-1 to infect and kill NHL B cell lines, an αICAM-1 antibody was used to block ICAM-1 on NHL cell lines and cell death was measured

following CVA21 treatment. **Figure 4-7** shows the efficacy of CVA21 against Ramos (a), Raji (b), SU-DHL-4 (c), U2932 (d) and OCI-LY3 (e) cells that have not been treated with antibody (white bars), treated with the isotype control antibody (grey bars), or the αICAM-1antibody (black bars). αICAM-1-treated Ramos, SU-DHL-4 and U2932 cells showed complete abrogation of CVA21-induced cell death, while αICAM-1-treatment of Raji and OCI-LY3 cells showed a significant reduction in CVA21-induced cell death at lower viral doses only. It is possible that the Raji and OCI-LY3 cells were not completely protected by the αICAM-1 antibody as these cells grow as aggregates in culture, hindering antibody binding. However, it is also possible that infection is not solely dependent on ICAM-1 in these cell lines. These data demonstrate that, as with other cancer models, ICAM-1 is essential for CVA21-induced oncolysis.

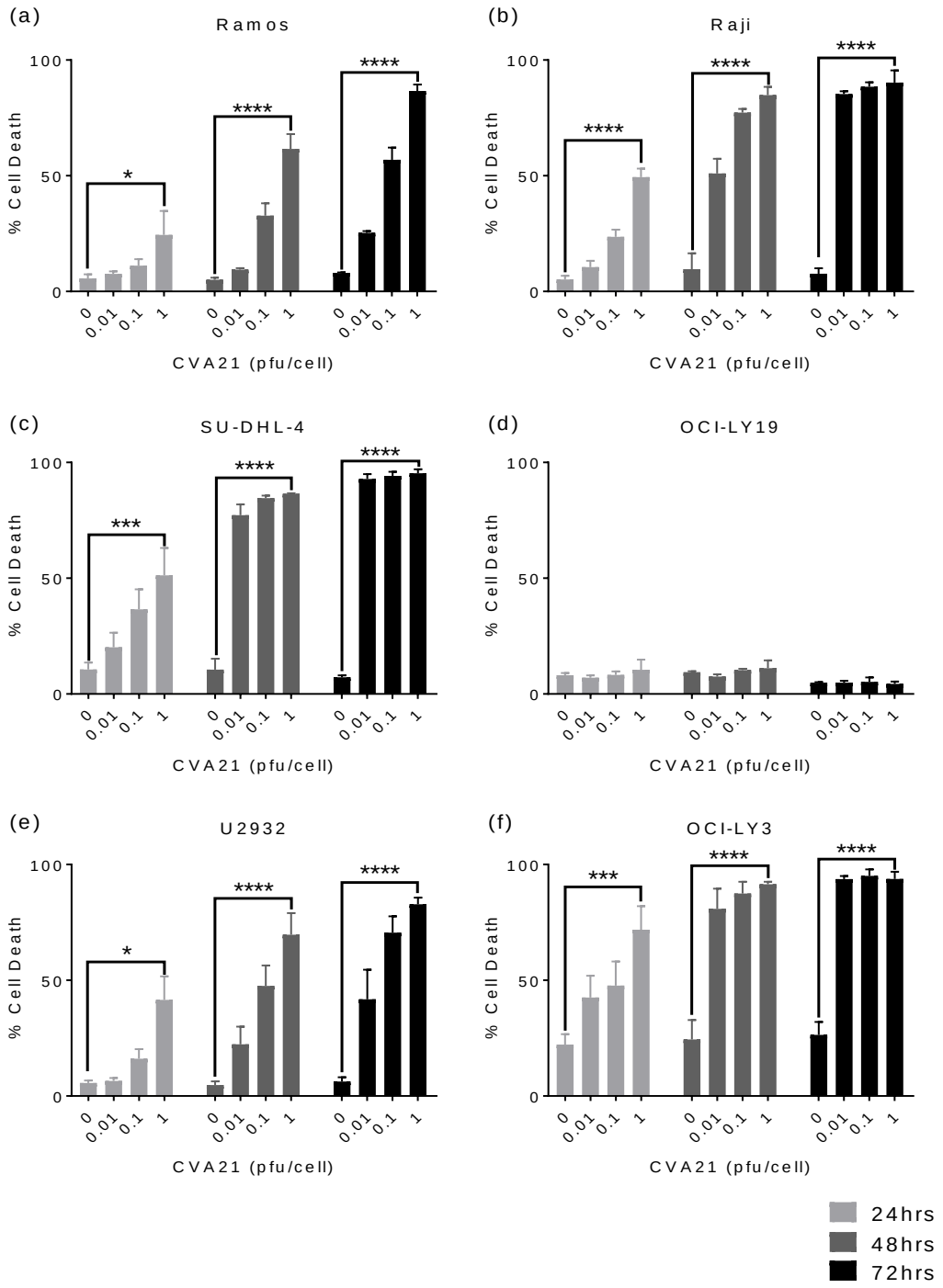

Figure 4-4 Cytotoxic effects of CVA21 against NHL cell lines.

Ramos (a), Raji (b), SU-DHL-4 (c), OCI-LY19 (d), U2932 (e) and OCI-LY3 (f) cell lines were treated with 0.01, 0.1 and 1 pfu/cell CVA21 for 24, 48 and 72hrs. At each time point, cells were analysed for viability by flow cytometry using LIVE/DEAD™ staining. Data shows the mean of n=3 independent experiments+ SEM. Statistical significance was determined by two-way ANOVA.

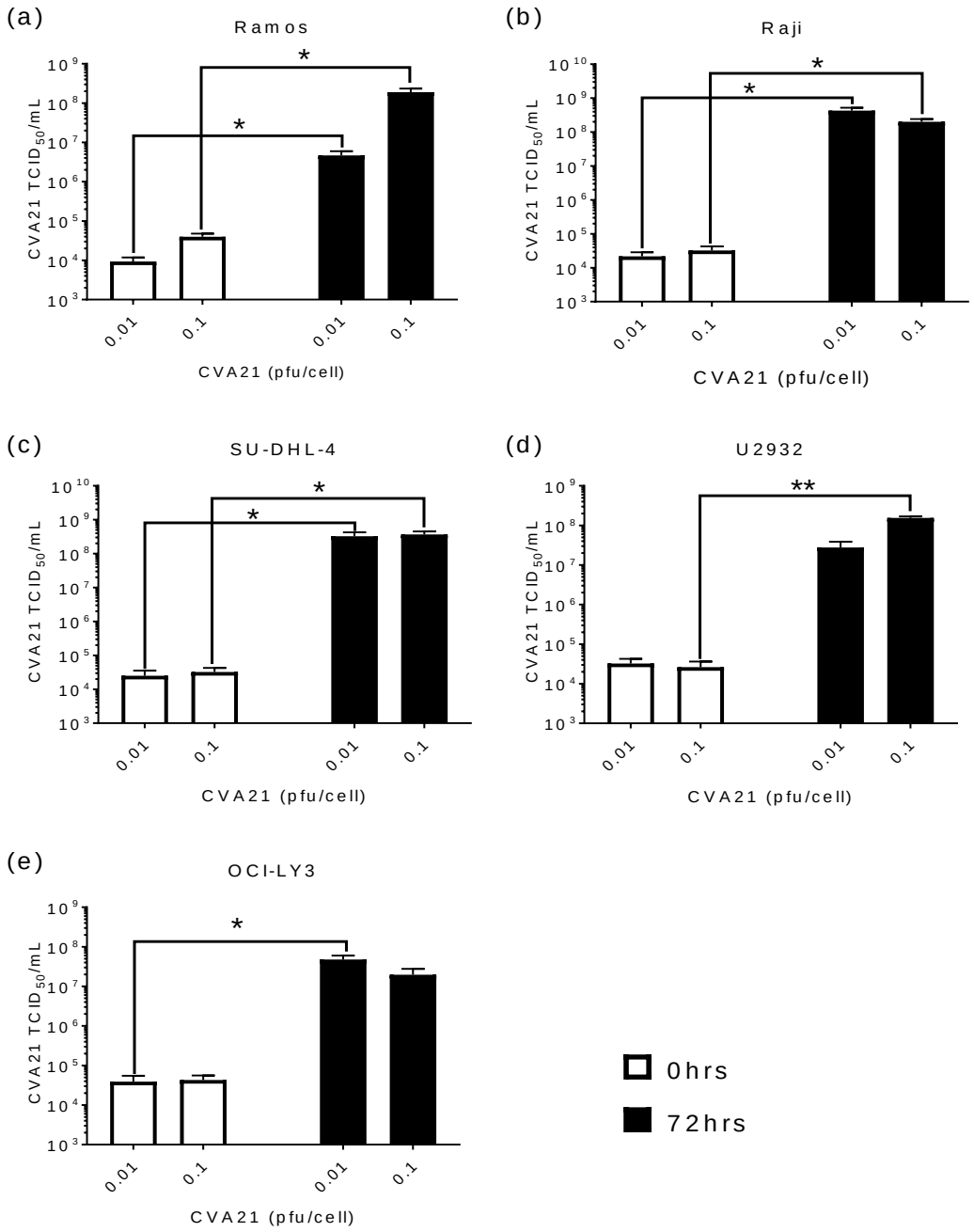

Figure 4-5 CVA21 replication in NHL cell lines.

Ramos (a), Raji (b), SU-DHL-4 (c), U2932 (d) and OCI-LY3 (e) cells were treated with CVA21 for 72hrs. Cell free supernatants were taken at 0hrs as input (white bars) and again at 72hrs (black bars). Supernatants were then analysed for virus titre by $TCID_{50}$ assay. Results show the mean from n=4 independent experiments + SEM. Statistical significance was determined by paired, two-tailed student's t test.

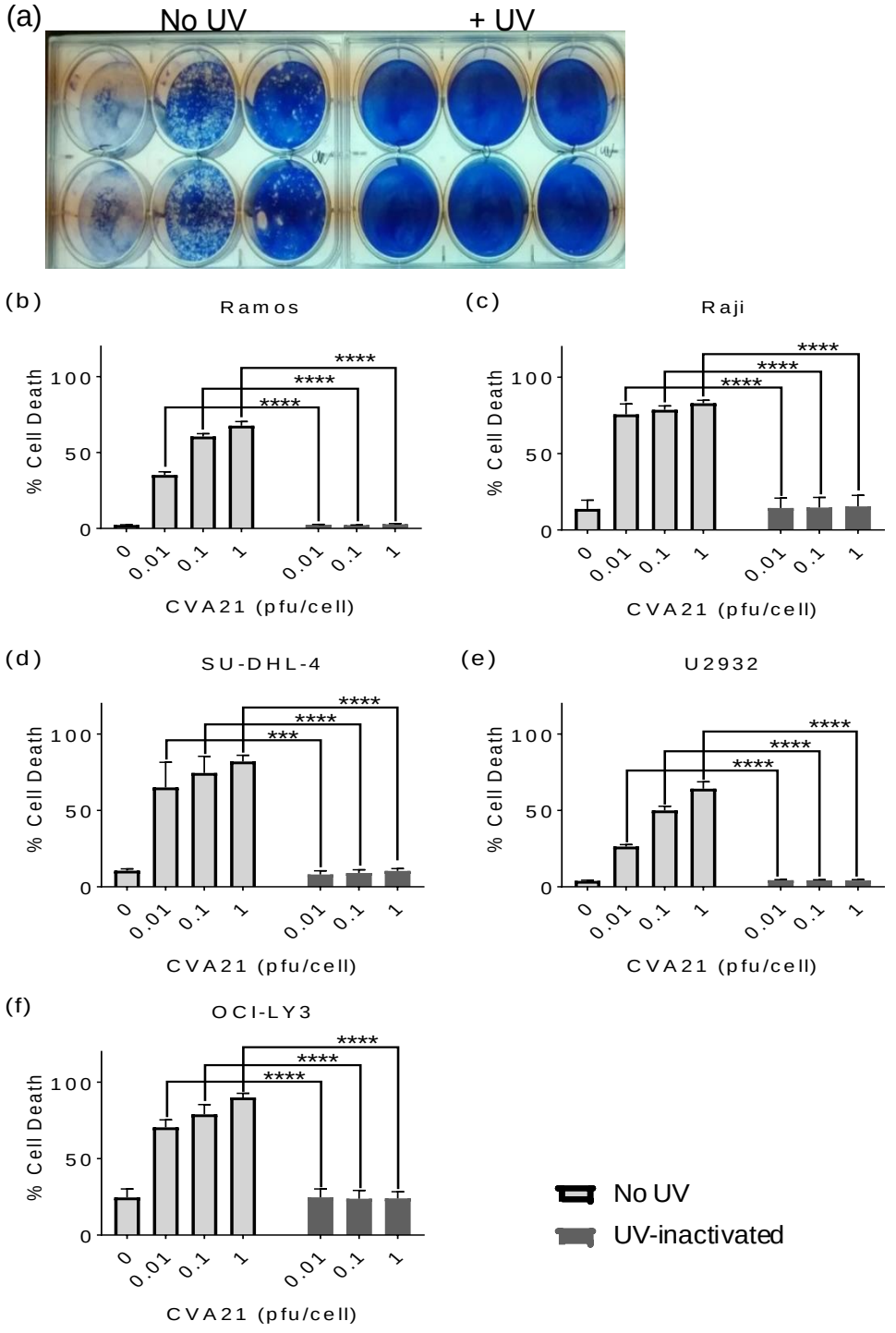

Figure 4-6 Viral replication is required for CVA21-induced death of NHL lines.

(a) Representative plaque assay result from live (Non-UV) and UV-inactivated CVA21 (3 min UV exposure) on MEL-624 cells. Ramos (b), Raji (c), SU-DHL-4 (d), U2932 (e) and OCI-LY3 (f) cells were treated with non-UV and UV-inactivated CVA21 in increasing doses for up to 48hrs. Cell viability was assessed by flow cytometry using LIVE/DEAD™ viability dye. Data shows the mean of n=3 independent experiments + SEM. Statistical significance was determined by two-way ANOVA.

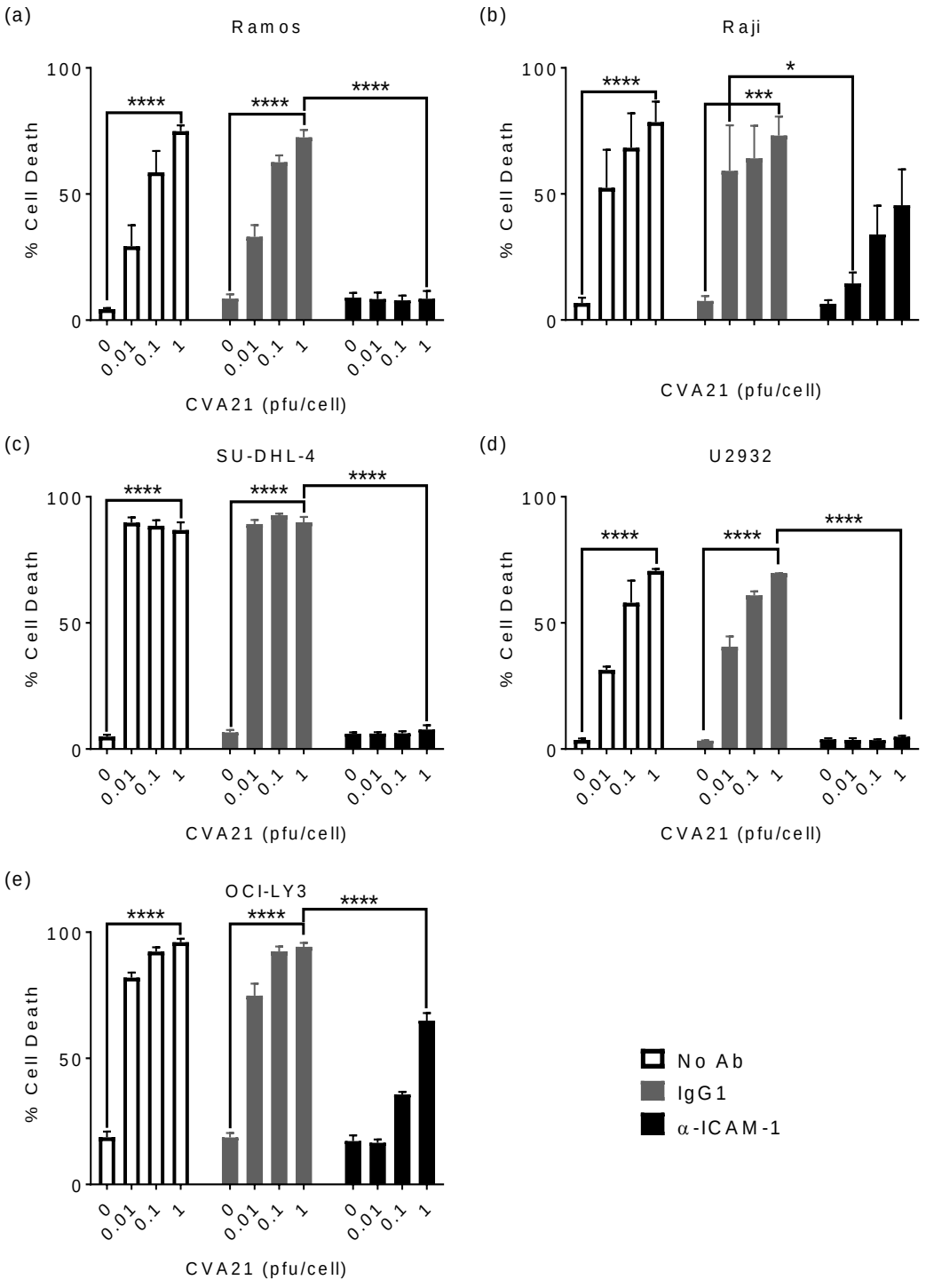

Figure 4-7 ICAM-1 blockade abrogates CVA21-induced cell death of most NHL cell lines.

Ramos (a), Raji (b), SU-DHL-4 (c), U2932 (d) and OCI-LY3 (e) cells were cultured alone (white bars) or with an isotype control (grey bars) or αICAM-1 (black bars) antibody. The cells were then treated with increasing doses of CVA21 and analysed for virus-induced cell death after 48hrs using LIVE/DEAD™ viability dye by flow cytometry. Data shows the mean of n=3 independent experiments+ SEM. Statistical significance was determined by two-way ANOVA.

4.2.4 Correlating OV receptor expression with susceptibility to infection

The NHL cell lines used in these investigations differentially expressed the OV receptors and varied in their susceptibility to either virus. Therefore, an important question is whether susceptibility to either virus correlated with viral receptor expression. This would serve as the simplest explanation for the differing susceptibility between the cell lines tested. To examine this, the mean fold increase in MFI of OV receptor expression, above the isotype control, was plotted against the mean percentage cell death, after subtraction of background cell death, for each NHL cell line. For CVA21, the mean percentage cell death observed at 0.1pfu/cell at 48hrs was chosen to best illustrate the variation between the cell lines. For reovirus, cell death induced by 10pfu/cell at 72hrs was selected, as reovirus-induced cell death occurred in some cell lines at this time point. **Figure 4-8** shows OV receptor expression plotted against susceptibility, as well as significance values (p) and a measure of how well the data fits the regression line (r^2).

In **Figure 4-8** (a), ICAM-1 expression on OCI-LY19, Ramos and Raji cells showed that low, medium and high expression appeared to correlate with virus-induced cell death, however, this pattern was only observed in these three cell lines and SU-DHL-4, U2932 and OCI-LY3 cell lines displayed high cell death at this time point and comparatively low ICAM-1 expression. Taken together, these data yielded an r^2 value of 0.1596 and showed no correlation between CVA21-induced cell death and ICAM-1 expression of NHL cell lines, as shown by Pearson's Test.

DAF expression (**Figure 4-8** (b)) yielded an r^2 value of 0.00277, suggesting no correlation between DAF expression and CVA21-induced cell death. Similarly, in **Figure 4-8** (c), an r^2 value of only 0.3685 demonstrates no correlation between JAM-A expression and reovirus sensitivity. Taken together, this data demonstrates that susceptibility to either virus does not correlate with the expression levels of their respective entry receptors in these 6 NHL cell lines.

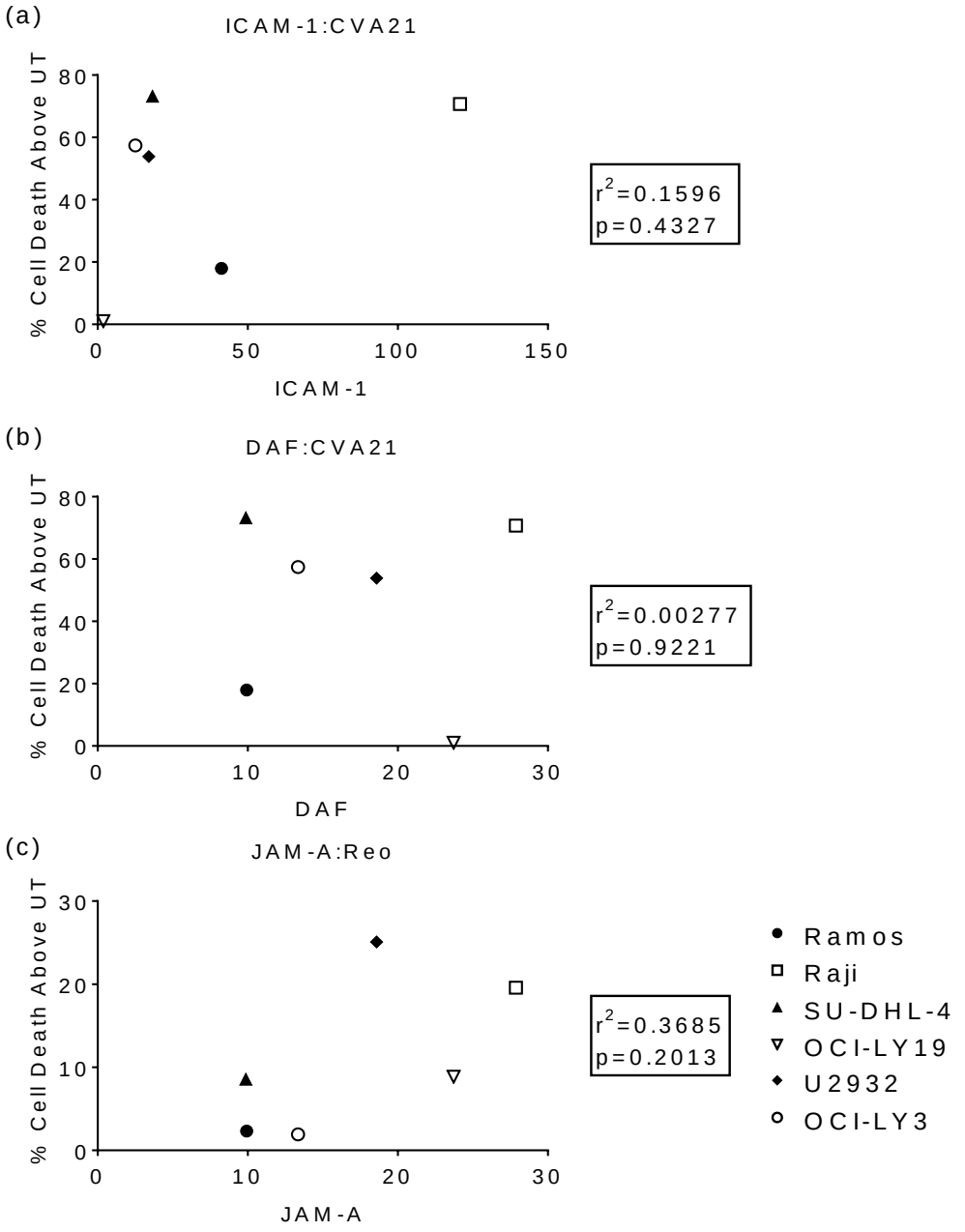

Figure 4-8 Correlation of OV receptor expression with virus-induced cell death:

Baseline OV receptor expression, as determined by mean MFI over isotype control MFI, was plotted against susceptibility to OV, as determined by the percentage cell death above untreated controls for Ramos, Raji, SU-DHL-4, OCI-LY19, U2932 and OCI-LY3 cells. For CVA21, data for 0.1pfu/cell after 48hrs was used, whilst for reovirus, 10pfu/cell for 72hrs was used. Data shows the mean percentage cell death and receptor expression from n=3 independent experiments. Statistical analysis was determined by Pearson's test with resulting r^2 values deemed to show a correlation if they were close to 1 and p values showing statistical significance of the trend, where $p<0.05$ denotes significance.

4.2.5 Validating the CD40L$^+$ L929 co-culture as a model of Chemo-Resistance

As discussed previously, tumours cannot be accurately modelled by two-dimensional cell culture systems whereby cancer cells are grown in isolation in nutrient-rich media and stable, optimised conditions. Due to the high complexity of the NHL LN, it is not yet sustainable to control for every possible contributing factor within the TME *in vitro*. However, careful selection of highly influential signals allows elements of cell: cell cross talk, and their effects on the efficacy of novel therapies, to be measured. For these studies, CD40L was chosen because it provides support and survival signals to malignant B cells and can induce resistance to classical chemotherapy agents (Korniluk et al., 2014). CD40L stimulation of NHL B cells has also been associated with increased anti-apoptotic signals and resistance to chemotherapy *in vitro* (Voorzanger-Rousselot et al., 2006), suggesting a potential problem for current therapies.

Firstly, to validate the expression of CD40L on the CD40L$^+$L929 cell lines, CD40L$^+$ and parental L929 cells were analysed for CD40L expression by flow cytometry. The parental cells lacked CD40L expression while the CD40L-transfected cells expressed CD40L, demonstrated by enhanced αCD40L antibody staining above the isotype control (**Figure 4-9**). CD40 expression on the NHL cell lines was also confirmed by flow cytometry (n=2, data not shown).

Next, to confirm that CD40:CD40L interactions induced a drug-resistant phenotype, the effect of CD40L stimulation on the sensitivity of NHL cells to chemotherapy was investigated. Ramos (a), SU-DHL-4 (b) and U2932 (c) cells were cultured alone, or on the CD40L$^+$L929 and parental L929 feeder layers for 24hrs and treated with vincristine, a key component of the R-CHOP chemotherapeutic regimen for the treatment of NHL. **Figure 4-10** demonstrated that vincristine-treated NHL cell lines, in isolation, undergo cell death by 48hrs (blue bars). Importantly, co-culture of Ramos, SU-DHL-4 and U2932 cells on the CD40L$^+$L929 cells significantly inhibited vincristine-induced cell death. Moreover, NHL cells cultured on the parental L929 cells were not protected from vincristine-induced cell death, although this was not significant for U2932 cells. This data demonstrates that CD40L stimulation induced drug resistance to conventional NHL therapies.

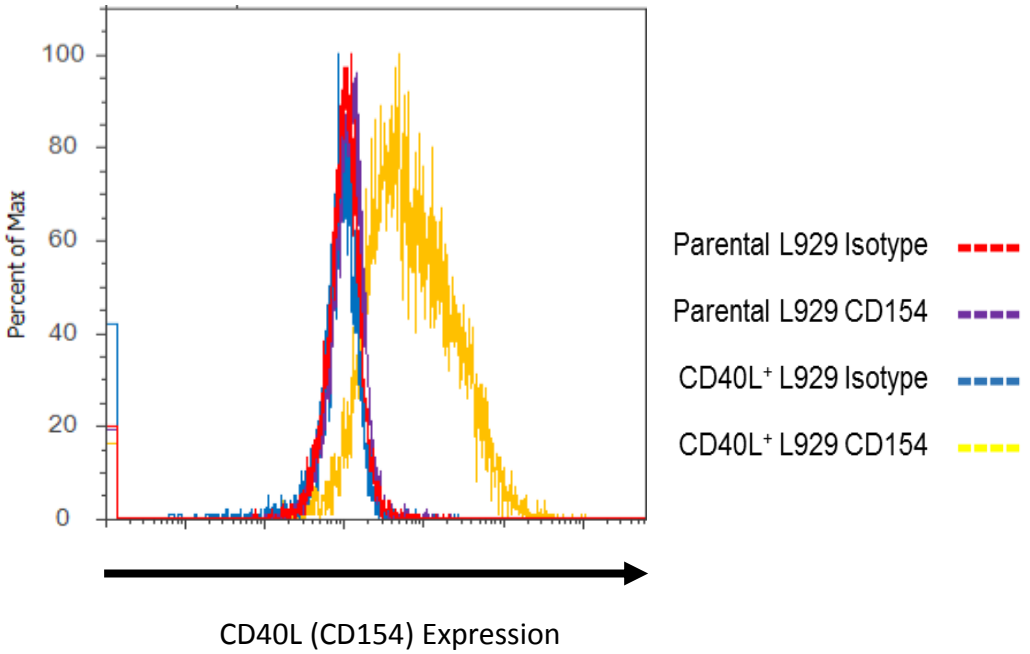

Figure 4-9 Validating CD40L (CD154) Expression on CD40L$^+$L929 cell lines.

Parental and CD40L$^+$ L929 cells were stained with an isotype control or αCD40L (CD154) antibody. CD40L expression was subsequently determined by flow cytometry. Data shows a representative overlay histogram of parental L929 isotype control (red), parental L929 αCD154 antibody-stained (purple), CD40L$^+$L929 isotype control (blue), CD40L$^+$L929 αCD154 antibody-stained (yellow). Data is representative of n=2 experiments.

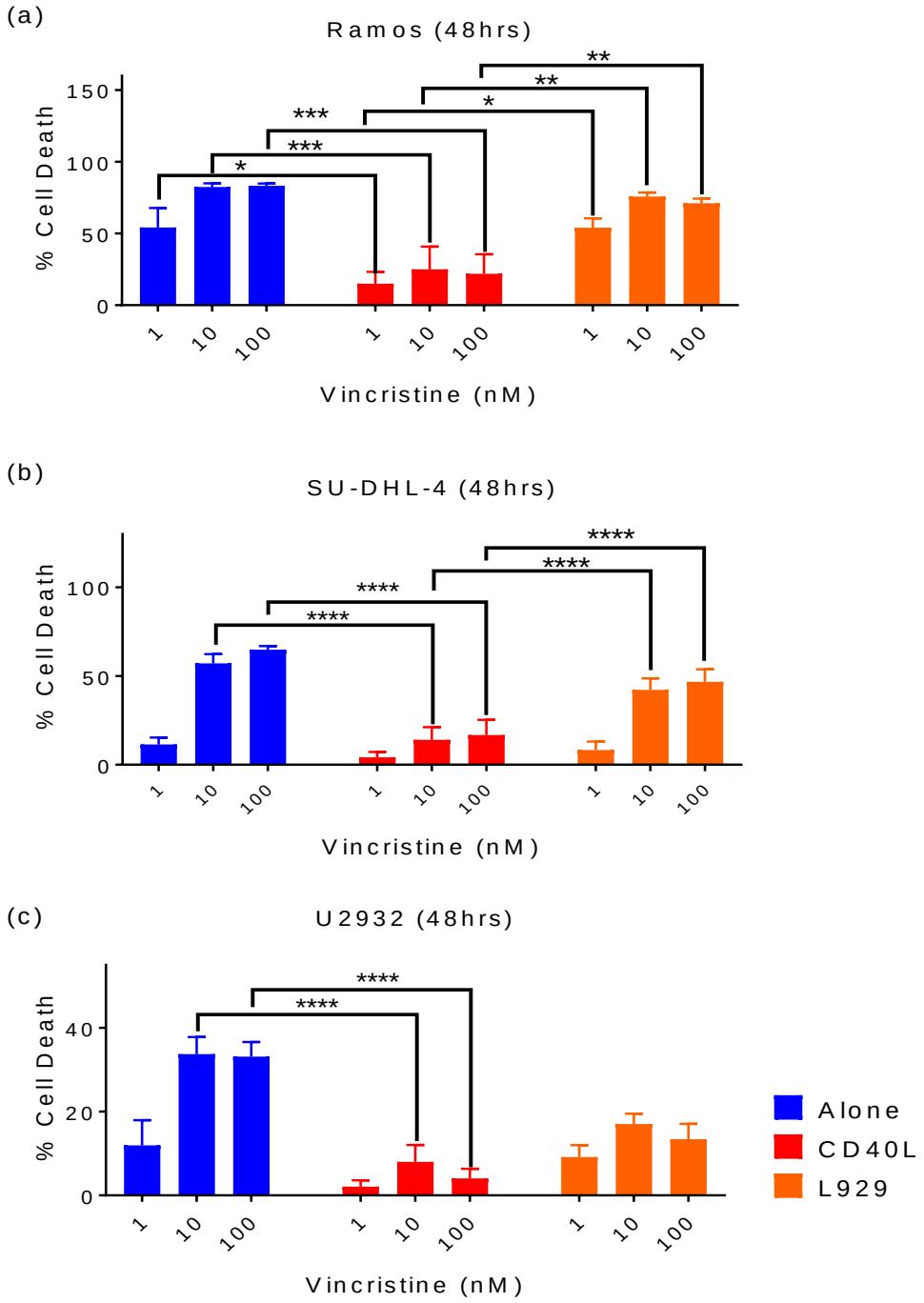

Figure 4-10 Resistance to Vincristine in NHL B cell lines.

NHL B cell lines, Ramos (a), SU-DHL-4 (b) and U2932 (c) were cultured alone, or on the CD40L^{+}L929 or parental L929 cells for 24hrs before being treated with increasing concentrations of vincristine for 48hrs and analysed for viability using LIVE/DEAD™ staining and Flow Cytometry. Data shows mean cell death of n=3 independent experiments + SEM, following subtraction of untreated control values. Statistical significance was determined by two-way ANOVA.

4.2.6 The effects of CD40L stimulation on OV receptor expression

Initial experiments examining OV receptor expression were repeated following CD40L stimulation to determine if CD40L stimulation alters OV receptor expression. Previous research by Shinde, *et al.*, has demonstrated that ICAM-1 expression is upregulated on B cells upon CD40L expression (Shinde et al., 1996). The effect of CD40L stimulation on ICAM-1 expression, and subsequent changes in susceptibility to CVA21, was investigated after promising research showed enhanced ICAM-1 expression in CD40L-stimulated CLL cells which correlated with enhanced susceptibility to CVA21 (Gina Scott – personal communication). NHL B cell lines were cultured in isolation or co-cultured on $CD40L^{+}$L929s, or parental L929s, for 24hrs before being harvested and analysed for the expression of OV receptors by flow cytometry. **Figure 4-11** shows that CD40L stimulation significantly enhanced ICAM-1 expression on Ramos (a), SU-DHL-4 (c), OCI-LY19 (d) and U2932 (e) cells. However, although ICAM-1 expression was increased by CD40L stimulation in Raji (b) and OCI-LY3 (f) cells, this increase was not statistically significant. Co-culture with the parental L929 cells did not significantly affect the expression of ICAM-1 on any NHL cell line. Furthermore, CD40L stimulation did not induce any significant changes in DAF expression (**Figure 4-12**) or in JAM-A expression (**Figure 4-13**).

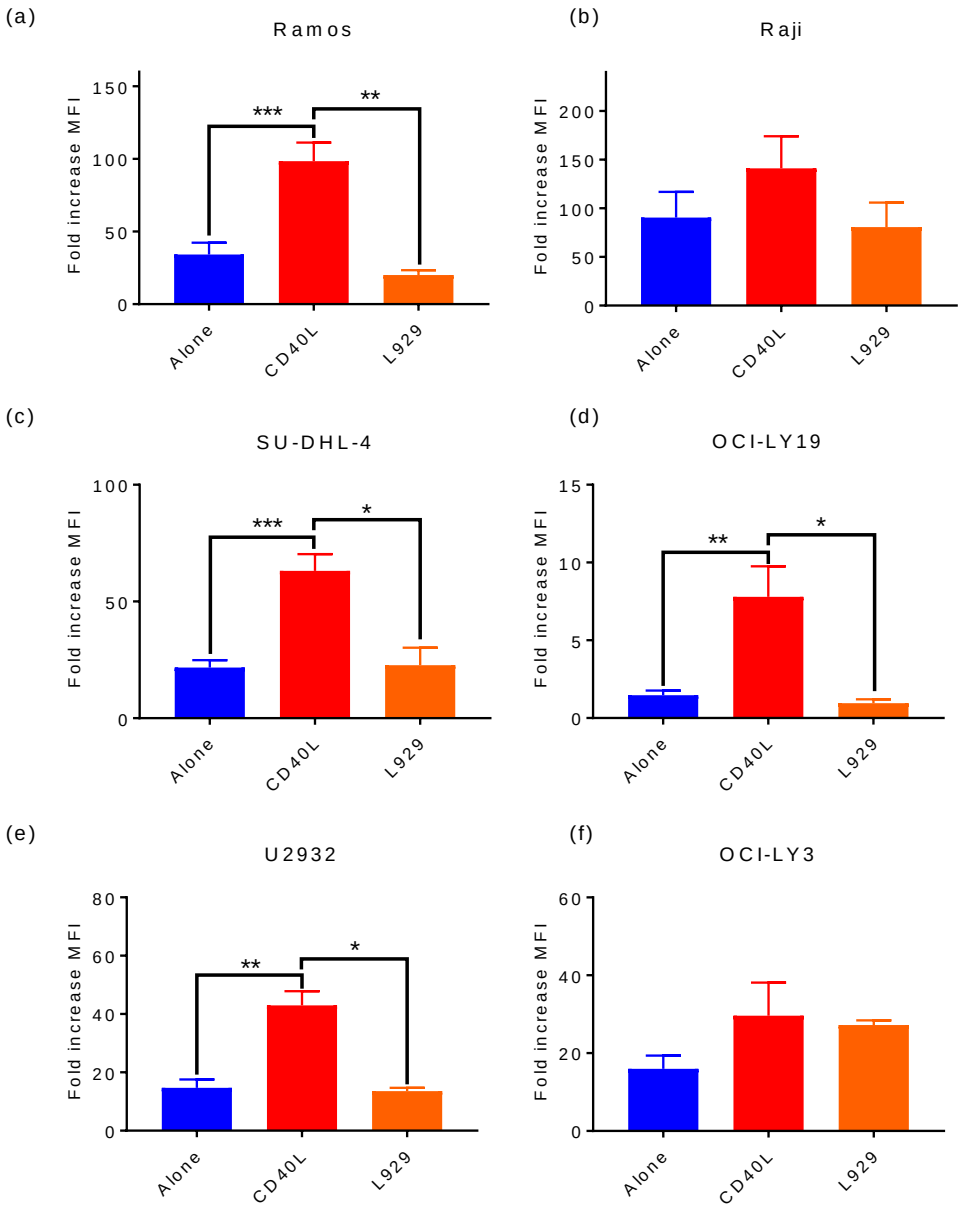

Figure 4-11 Effect of CD40L stimulation on ICAM-1 expression on NHL cell lines

Ramos (a), Raji (b), SU-DHL-4 (c), OCI-LY19 (d), U2932 (e) and OCI-LY3 (f) were cultured alone or on CD40L^{+}L929 or parental L929 cells for 24hrs before being harvested and stained with an isotype control or an αICAM-1 antibody. Surface ICAM-1 expression was measured by flow cytometry and expressed as fold increase in MFI above isotype antibody-stained control levels. Data shows the mean of n=4 independent experiments + SEM, significance was determined by unpaired, two-tailed student's t test.

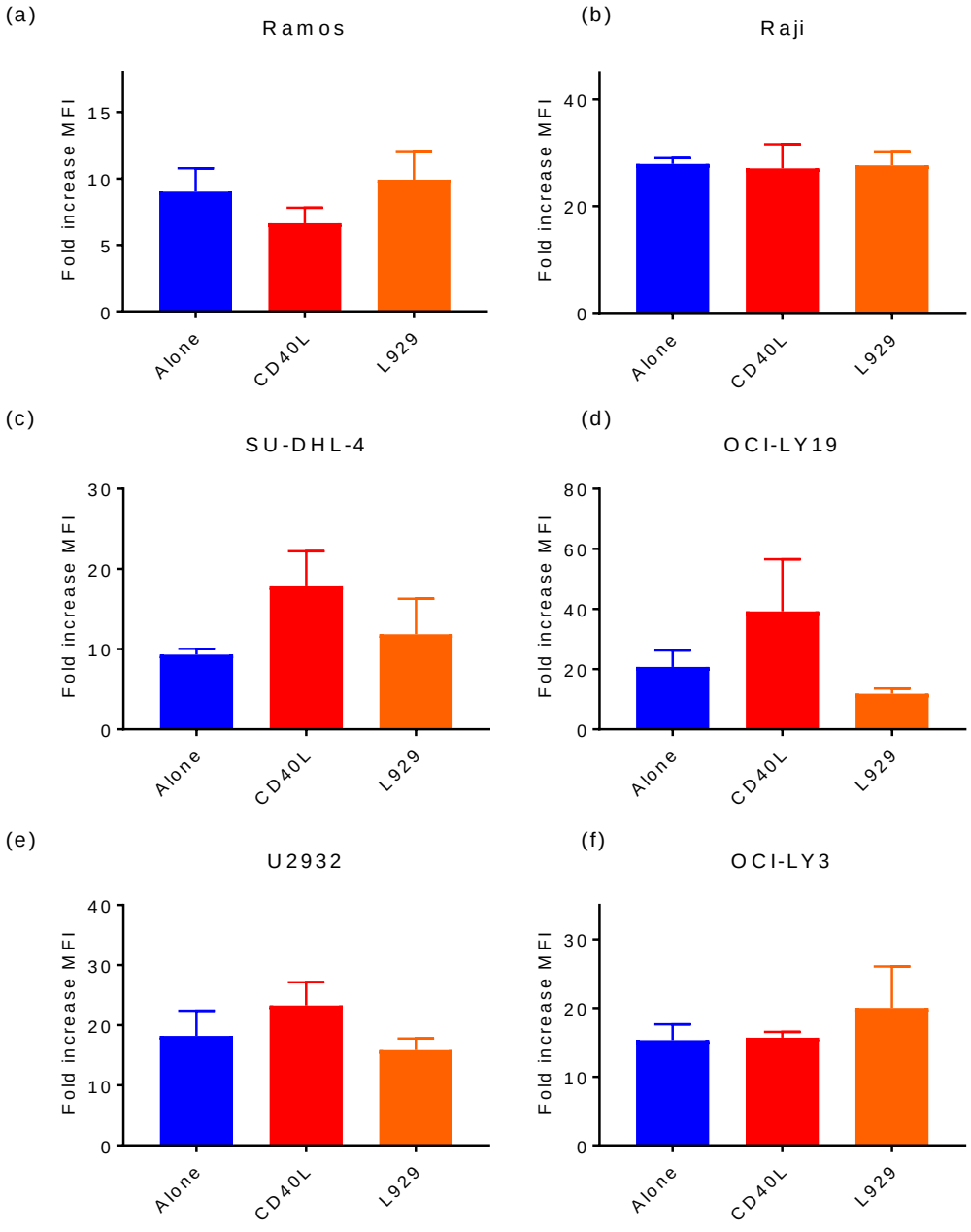

Figure 4-12 Effects of CD40L stimulation on DAF expression on NHL B cell lines:

Ramos (a), Raji (b), SU-DHL-4 (c), OCI-LY19 (d), U2932 (e) and OCI-LY3 (f) were cultured alone or on CD40L^{+}L929 or parental L929 cells for 24hrs before being harvested and stained with an isotype control or αDAF antibody. Surface DAF expression was measured by flow cytometry and expressed as fold increase in MFI above isotype control levels. Data shows the mean of n=4 independent experiments + SEM. Significance was investigated by unpaired, two-tailed student's t test, but no significance was detected.

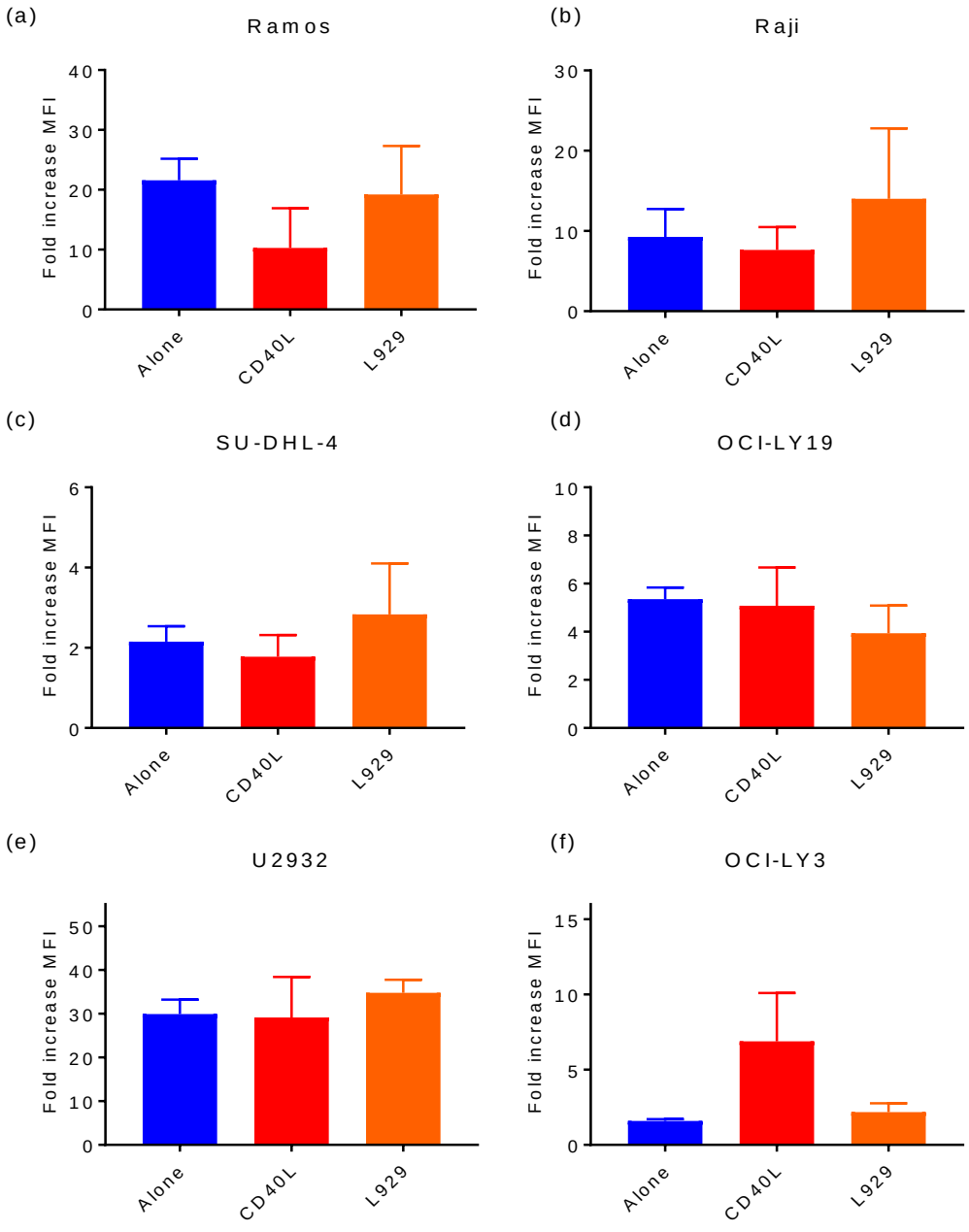

Figure 4-13 Effects of CD40L stimulation on JAM-A expression on NHL B cell lines:

Ramos (a), Raji (b), SU-DHL-4 (c), OCI-LY19 (d), U2932 (e) and OCI-LY3 (f) were cultured alone or on CD40L^{+}L929 or parental L929 cells for 24hrs before being harvested and stained with an isotype control or αJAM-A antibody. Surface JAM-A expression was measured by flow cytometry and expressed as fold increase in MFI above isotype control levels. Data shows the mean of n=4 independent experiments + SEM, significance was investigated by unpaired, two-tailed student's t test, but no significance was detected.

4.2.7 Effect of CD40L stimulation on CVA21-induced cell death

ICAM-1 expression is required for CVA21 infection (Newcombe et al., 2004) and is increased by CD40L stimulation of NHL cell lines (**Figure 4-11**), therefore, the effects of CD40L stimulation, and subsequent ICAM-1 upregulation, on CVA21-induced cell death were determined. NHL cell lines were cultured in isolation or in co-culture with $CD40L^{+}$L929 and parental L929 cells for 24hrs before being treated with CVA21 for 24hrs.

Figure 4-14 shows that CVA21 treatment induced cell death in a dose-dependent manner, in the 4 candidate NHL cell lines tested (Ramos, Raji, SU-DHL-4 and U2932; (a)-(l)), when cultured alone (blue bars); comparable with the data shown in **Figure 4-4**. CVA21-induced cell death was increased significantly after CD40L stimulation in Ramos at 1pfu/cell (c) and U2932 cells at 0.1 pfu/cell (k). No change in CVA21 susceptibility was observed on the parental L929 feeder layer. This data suggests that enhanced ICAM-1 expression, due to CD40L stimulation, can increase CVA21-induced cell death in some cell lines. Further experiments could clarify the role of CD40L stimulation, and subsequent ICAM-1 upregulation, in enhancing CVA21-induced cell death by blocking ICAM-1 on CD40L-stimulated NHL cells by an αICAM-1 blocking antibody or siRNA knockdown of ICAM-1, and measuring the ability of CVA21 to kill the NHL cells.

Identical experiments were also conducted with reovirus, however, there was no increase in cell death of NHL cells that were co-cultured with CD40L (data not shown). Despite the unchanged JAM-A expression on NHL cells following CD40L stimulation, these experiments were conducted as previous research had demonstrated a role for the TME in enhancing OV-induced cell death of malignant cells (Ilkow et al., 2015). Due to the limited cell death observed in NHL cell lines, suggesting that they are only mildly susceptible, reovirus was not investigated further as a lytic agent but was investigated in the context of priming an anti-NHL immune response (Chapter 6) and targeting primary NHL cells (Chapter 7).

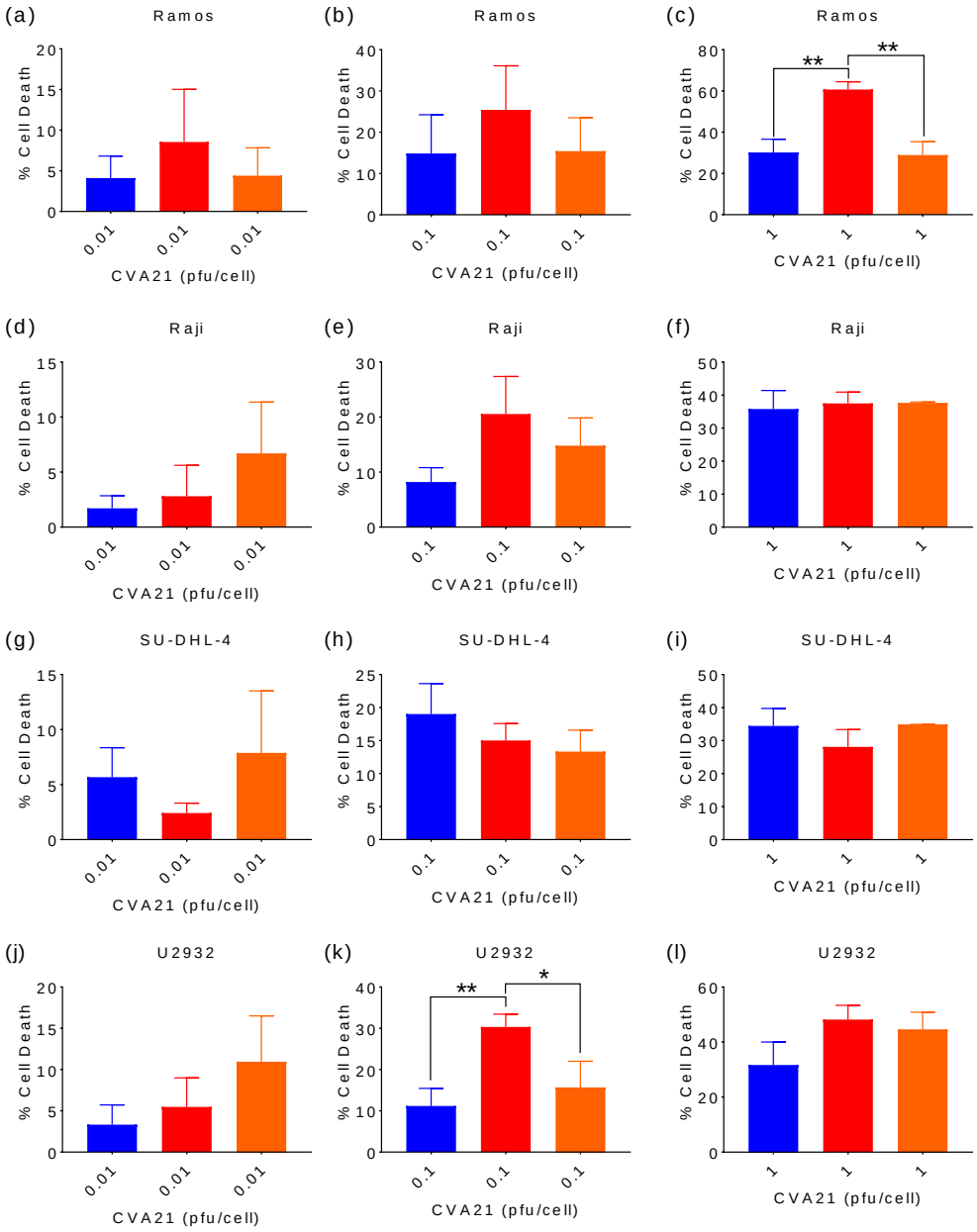

Figure 4-14 CD40L stimulation of NHL B cells enhances CVA21-induced cell death in some cell lines:

NHL cell lines Ramos (a)-(c), Raji (d)-(f), SU-DHL-4 (g)-(i) and U2932 (j)-(l) were cultured alone (blue) or on $CD40L^+$ (red) or parental L929 (orange) cell lines for 24hrs. CVA21 was added at increasing doses and cells were cultured for a further 24hrs. Cells were then harvested and analysed for viability using LIVE/DEAD™ staining and flow cytometry. Cell death is expressed as the percentage dead cells above respective untreated controls. Data shows the mean of at least n=3 independent experiments + SEM, significance was determined by two-tailed, paired student's t test.

4.2.8 Specificity of CVA21 for malignant B cells.

Previous work in this chapter has shown the ability of CVA21 to kill NHL cell lines. It is difficult to distinguish transformed B cells from non-transformed in the NHL LN by flow cytometry; therefore, healthy peripheral blood B cells were used to determine the effects of CVA21 on non-malignant B cells, and the effects of CD40L stimulation on their susceptibility.

Healthy donor B cells (in the context of PBMCs) express a significantly lower level of ICAM-1 than the NHL cell lines Ramos, Raji, SU-DHL-4, U2932 and OCI-LY3, **Figure 4-15**. However, the level of expression was comparable to the CVA21-resistant OCI LY19 (**Figure 4-1**, **Figure 4-2**). CD40L stimulation of healthy donor B cells significantly increased ICAM-1 expression on these cells, but this remained significantly lower than levels observed on the Ramos, Raji and SU-DHL-4 cell lines (**Figure 4-15**).

In order to investigate whether enhanced ICAM-1 expression on healthy B cells made them susceptible to CVA21, and whether CVA21 can kill healthy donor B cells in the context of a mixed cell population, PBMCs were cultured alone, on $CD40L^{+}L929$ or on parental L929 cells and treated with CVA21 for up to 120hrs. **Figure 4-16** demonstrates that CVA21 did not induce significant cell death under any growth condition tested. The majority of samples (4 of 7) remained completely resistant to CVA21-induced cell death, even after CD40L stimulation and enhanced ICAM-1 expression, and minimal cell death was detected in the remaining samples.

Cell-free supernatants from CVA21-treated healthy donor PBMC samples were subject to $TCID_{50}$ assays to examine whether viral replication was supported in non-malignant cells. **Figure 4-17** indicates that the high viral titres at the start of the experiment (input), diminished by the 120hr time point (a). The input titres for both doses were normalised to 100% in (b) and the 120hr results expressed as a percentage of this. This data shows a significant decrease in CVA21 titre in healthy PBMC samples, suggesting that virus replication was not taking place.

Lastly, replication was measured in healthy donor samples that had been cultured alone, on $CD40L^{+}L929$ or on parental L929 feeder layers, **Figure 4-18**. Viral titre appeared to be higher in healthy B cells cultured on both feeder layers at 120hrs, however, this was not significantly higher than observed in the B cells cultured alone. Taken together, these data suggest that CVA21 is unable to replicate in, or kill, healthy donor B cells, even when ICAM-1 expression is enhanced by CD40L stimulation.

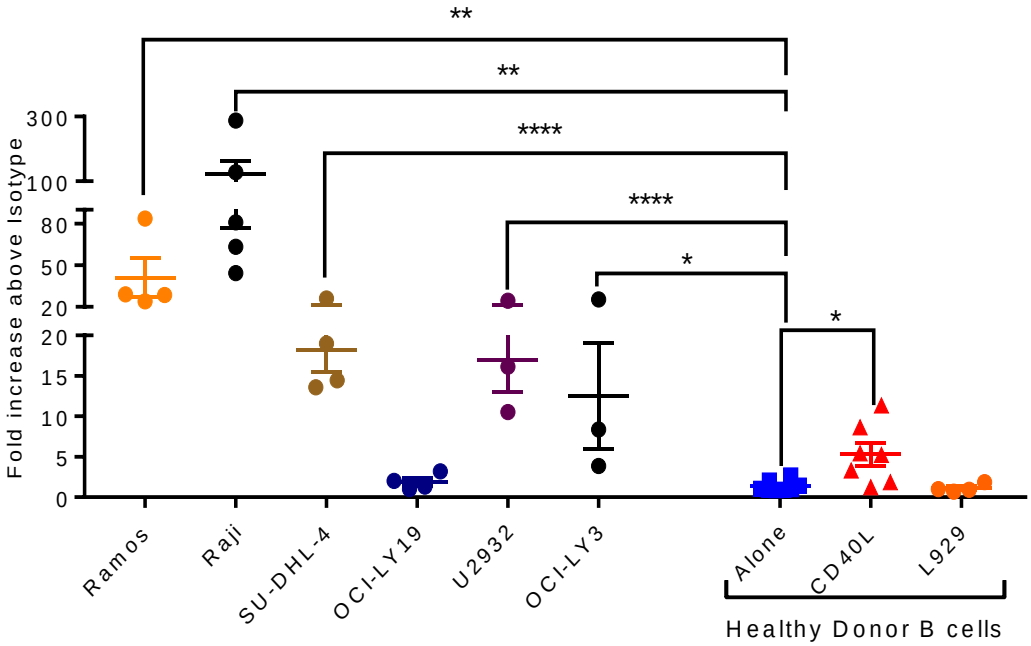

Figure 4-15 ICAM-1 Expression on NHL B cells vs Healthy B cells

Healthy donor PBMCs were cultured alone and on $CD40L^+$ and parental L929 feeder layer for 24hrs. ICAM-1 expression was then measured on the surface of $CD19^+$ or $CD20^+$ B cells in each culture by flow cytometry. This result was then expressed as the fold increase in MFI over the isotype MFI. For comparison, data is plotted with the ICAM-1 expression data of the NHL cell lines Ramos, Raji, SU-DHL-4, OCI-LY19, U2932 and OCI-LY3 from 0. Data shows the mean from n≥3 independent experiments ± SEM. Statistical significance was determined by paired, two-tailed student's t test.

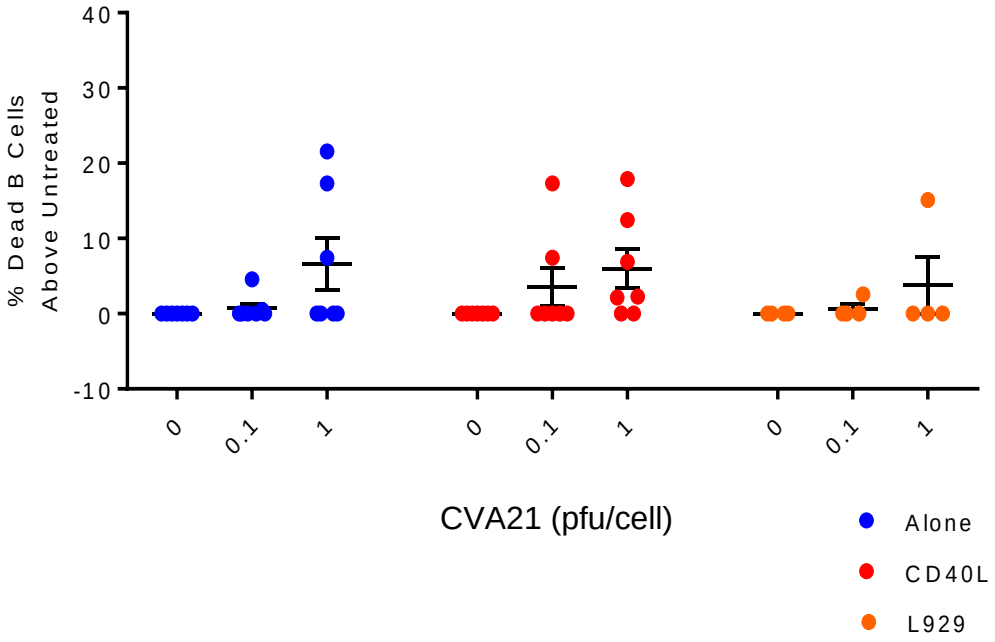

Figure 4-16 CVA21 induced cell death of healthy donor B cells.

Healthy donor PBMCs were cultured alone or on the CD40L^{+}L929 or parental L929 feeder layers. The cells were then treated with CVA21 and returned to culture for 120hrs. The cells were stained with αCD20 or αCD19 antibodies for identification of B cells and analysed for viability using LIVE/DEAD™ exclusion by flow cytometry. Cell death is represented as the percentage of LIVE/DEAD™-positive B cells minus the untreated control. Results show the mean of n≥4 independent experiments ± SEM. Statistical significance was analysed by two-way ANOVA, but no significance was detected.

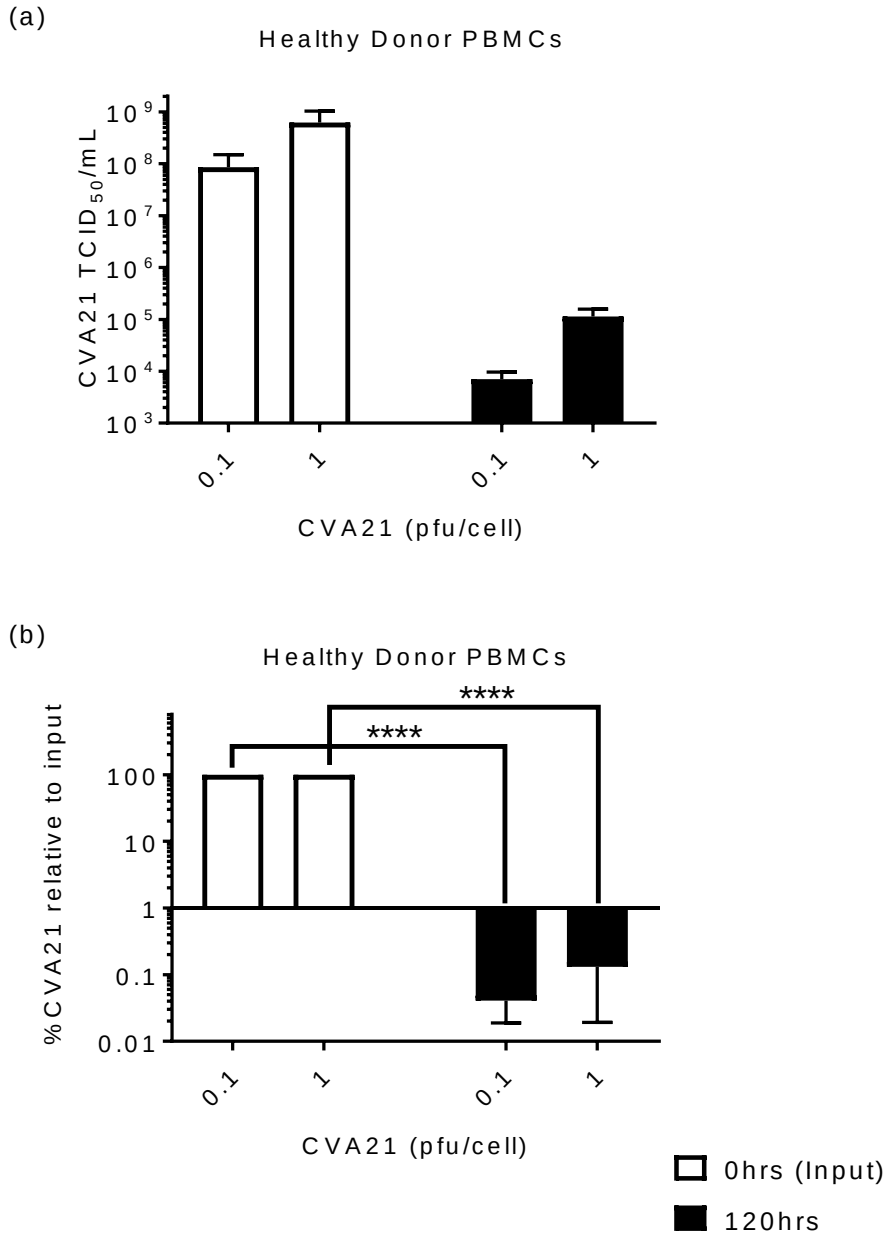

Figure 4-17 Replication of CVA21 in healthy PBMCs:

Healthy donor PBMCs were treated with CVA21 for up to 120hrs. Cell-free supernatants were taken at 0hrs as input (white bars) and again at 120hrs (black bars) when cell death was analysed. Virus titre of the supernatants was then determined by $TCID_{50}$ assay. (a) Shows virus titre at input and 120hrs, and (b) shows this data after both input doses were normalised to 100% and the 120hr data was expresses as a ratio of this. Results show the mean from n=4 independent samples + SEM. Statistical significance was determined by paired, two-tailed student's t test.

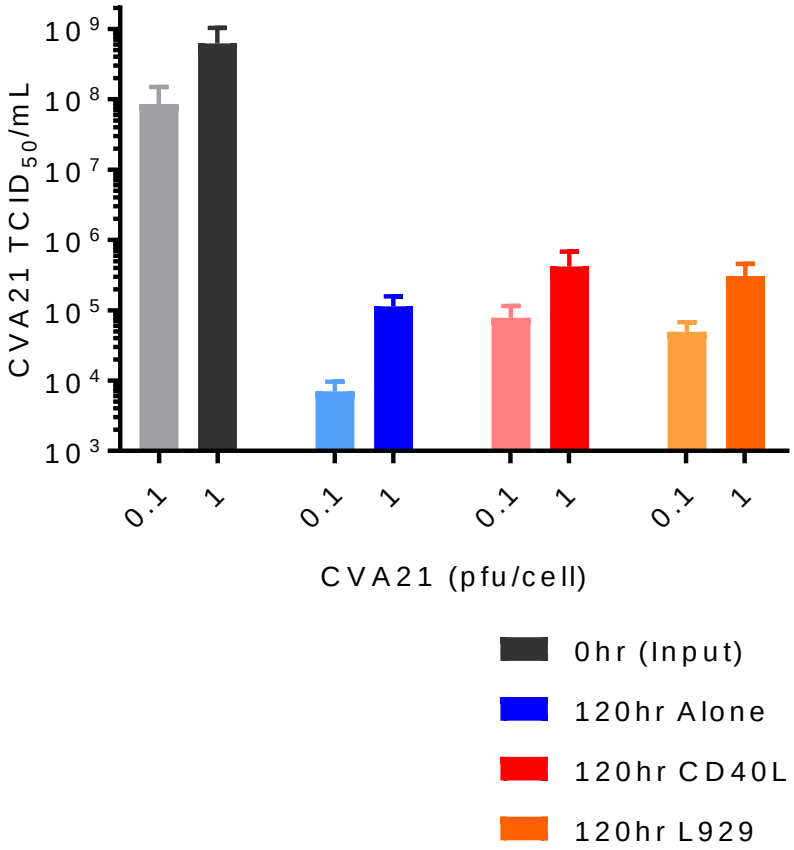

Figure 4-18 Replication of CVA21 in healthy CD40L-stimulated and non-stimulated PBMCs:

Healthy PBMCs were isolated from fresh blood and cultured on the CD40L^{+}L929 or parental L929 feeder layers for 24hrs. CVA21 was then added to the co-culture for 120hrs. Sample supernatants were taken at 0hrs, for virus input, and again at 120hrs when cell death was being measured. Supernatants were analysed for virus titre by $TCID_{50}$ assay. Data shows the means of n=4 healthy donors, significance was analysed by two-way ANOVA, but no significance was detected.

4.3 Discussion

The aim of this research was to examine whether CVA21 and reovirus can kill NHL cell lines. Previous research on the ability of reovirus to target HMs has demonstrated its potential as both a lytic and immunogenic agent by 1) enhancing NK cell targeting of rituximab-coated CLL cell lines (Parrish et al., 2015), 2) stimulating NK cell targeting of, and causing direct killing of, AML cells (Hall et al., 2012) and CLL cells (Parrish et al., 2015), and 3) inducing direct lysis of cell lines and tumour destruction by immune activation in a multiple myeloma model (Thirukkumaran, C. M. et al., 2012). Reovirus is also being investigated in clinical trials for the treatment of relapsed or refractory myeloma in combination with the proteasome inhibitor, Bortezomib, and the corticosteroid, Dexamethasone (ClinicalTrials.gov, 2015c), and with immunomodulatory drugs, Lenalidomide or Pomalidomide (ClinicalTrials.gov, 2017c). Conversely, the efficacy of CVA21 against HMs is less characterised, but some research has demonstrated its ability to kill myeloma cell lines directly and purge myeloma-contaminated BMs upon exposure *ex vivo* (Au et al., 2007). These data demonstrate the potential of CVA21 as an anti-HM agent and highlight the requirement for more HM-oriented OV research. It should be acknowledged that the research shown in this chapter is derived from cell lines and primary healthy PBMCs that were cultured and treated with reovirus and CVA21 *in vitro*, making comparisons with effects in animals or patients difficult, as the OVs could be exerting their efficacy by a variety of mechanisms, such as activation of the immune response or destruction of the tumour stroma or vasculature *in vivo*, which would not be observed *in vitro*.

The CVA21 receptors, ICAM-1 and DAF, and reovirus receptor, JAM-A, have distinct roles in the development and function of normal healthy B cells. JAM-A expression on NHL B cells plays a role in cell migration and invasion and is associated with poor survival in both DLBCL patients (Xu et al., 2017), and multiple myeloma patients (Solimando et al., 2018), warranting research into the use of reovirus to target these cells. Enhanced ICAM-1 on LN-residing B cells interacts with Lymphocyte Function-associated Antigen 1 (LFA-1) on T cells to provide a co-stimulatory signal for B cell activation (Holland and Owens, 1997), and increased DAF expression has been observed on B cells during the early stages of B cell development to protect them from complement-dependent cytotoxicity (CDC) (Terstappen et al., 1992). DAF expression on NHL B cells is being targeted by other forms of therapeutic intervention, such as antibody blockade of DAF in combination

with rituximab to potentiate CDC in NHL (Federica et al., 2005). High ICAM-1 and DAF expression on NHL cells presents CVA21 with an advantage in targeting malignant B cells compared to healthy B cells. This outlines the importance of matching OV to malignancies that may be more susceptible to viral targeting. High ICAM-1 expression is also associated with other tissue types, such as the gut epithelium (Veres et al., 2001), potentially posing a risk of gastric infection in CVA21-treated patients. While no patients have presented with serious gastric symptoms in any CVA21-based clinical trials to date, tissues that express high ICAM-1 could be monitored in CVA21-treated patients to pre-empt the onset of adverse reactions to the virus.

All NHL cell lines expressed the reovirus receptor, JAM-A, making virus entry into the cell possible, however, reovirus demonstrated a poor ability to induce cell death in NHL cell lines (**Figure 4-3**). Reovirus was previously shown to selectively target NHL cell lines with deficient p53 activity, for example, Ramos cells, that have an intact p53 response, were not permissive to reovirus infection, whilst the p53-deficient Raji cells were (Kim et al., 2010). This data is congruous with results in this chapter that showed Ramos cells were resistant to reovirus while Rajis were susceptible, as were U2932 cells which also harbour mutant p53 (Amini et al., 2002). However SU-DHL-4 and OCI-LY19 cells reportedly possess wildtype p53 (Wang, F. et al., 2011), (Morin et al., 2011), (Drakos et al., 2011), but were susceptible to reovirus infection, suggesting that, while susceptibility to reovirus may be partially dependent on p53 deficiency, there are likely other, as yet undefined factors involved. The reported mutation or loss of p53 in 23% of DLBCL cases (Xu-Monette et al., 2012), (Leroy et al., 2002) suggests a potential use for reovirus in targeting primary NHL cells. Overall this data suggests that the presence of its entry receptor, JAM-A, although necessary, is not sufficient to make cells permissible to infection.

Previously, CVA21 has demonstrated potent lytic killing in a variety of cancer models such as melanoma, multiple myeloma, breast cancer, prostate cancer and lung cancer (Bradley et al., 2014). Data presented in this chapter demonstrates that CVA21 was highly toxic to Ramos, Raji, SU-DHL-4, U2932 and OCI-LY3 cell lines, but not OCI-LY19 cells, most likely due to the virus' dependence on co-expression of DAF and ICAM-1, the latter of which is expressed at very low levels on OCI-LY19 cells. Stable transfection of ICAM-1 into OCI-LY19 cells and measuring their susceptibility to CVA21 infection could be used to examine this further. This has previously been investigated using an AML cell line, KG-1, which expressed low levels of

ICAM-1; stable transfection with human ICAM-1 conferred susceptibility to CVA21 (manuscript submitted). Previous research has also shown that murine L929 cells transfected with human ICAM-1 were rendered susceptible to CVA21 infection (Shafren, D.R. et al., 1997a). Shafren *et al.*, also demonstrated that ICAM-1 blockade abrogated CVA21-induced cell death in ICAM-1^{+} L929 cells, validating the results observed in 0 which demonstrated that ICAM-1 blockade inhibited CVA21-induced cell death in NHL cell lines. This result highlights the importance of ICAM-1 in CVA21 infection. It is currently unknown whether ICAM-1 receptor density is important for CVA21 infection, however, the lack of cytotoxicity in CVA21-treated ICAM-1-low OCI-LY19 cells demonstrates that low levels of ICAM-1 prevent infection.

While the effects of DAF blockade by αDAF antibodies on CVA21-induced cell death of NHL cells was not investigated, research by Johannsen, *et al.*, demonstrated inhibition of a bioselected DAF-dependent strain of CVA21 (CVA21-DAFv, generated by multiple passaging of the Kuykendall strain of CVA21 through DAF-positive, ICAM-1-negative rhabdomyosarcoma (RD) cells) by αDAF antibodies (Johansson et al., 2004). It is also important to note that the blockade of DAF, a negative regulator of the complement cascade, could trigger complement-mediated cytotoxicity of the αDAF antibody-coated cells. This is unlikely however, due to the destruction of complement proteins during the heat-inactivation of FCS.

It is important to note that lytic cell death is not the only mechanism of action of OV. Although OCI-LY19 cells can resist CVA21 lytic cell death, and most cell lines were resistant to reovirus-induced cell death, it may be possible for either virus to target them indirectly through the induction of an anti-tumour immune response. This has been reported for multiple OV, for example, HSV-1 promoted immune cell infiltration and targeting of a HSV-1-resistant melanoma model (Miller and Fraser, 2003), reovirus enhanced NK and T cell numbers in patient tumours (White et al., 2008), Coxsackievirus B3 enhanced granulocyte and NK cell-mediated elimination of lung adenocarcinoma xenografts (Bhat and Rommelaere, 2015) and VSV enhanced IL-28 secretion in the TME, induced NK ligand expression on tumour cells and enhanced NK cell killing of these cells (Wongthida et al., 2010). Research by Prestwich, *et al*., also demonstrated reovirus-induced elimination of murine melanoma cells that was immune-mediated and independent of viral oncolysis or replication (Prestwich, Robin J. et al., 2009). Investigating the potential for these effects, that were largely

observed in *in vivo* models, is beyond the scope of *in vitro* research, however, the ability of either virus to induce immune cell targeting of the NHL cell lines will be the focus of Chapter 6.

CVA21 replicated significantly in susceptible NHL cell lines (**Figure 4-5**), suggesting that cell death was replication-dependent, as confirmed by UV-inactivation of CVA21 which inhibited cytotoxicity (0). Oncolysis would be beneficial to OV therapy as it perpetuates the virus within the TME, leading to the continual destruction of malignant cells or the induction of an immune response against the cancer (as discussed in section 2.4.1.2). While the properties of this lytic cell death were not investigated in this research, this could be analysed by the use of confocal microscopy to elucidate whether the cells have ruptured in the latter stages of viral infection. Interestingly, research into the use of VSV has shown that it remains toxic to leukaemia cell lines despite UV-inactivation (Tsang, J.J. and Atkins, 2015), the mechanism of this remains undefined, but could be due to the production of cytotoxic cytokines. Therefore, while CVA21-induced cell death of NHL cell lines is replication-dependent, other viruses do not require replication to induce cell death. Moreover, research by Batenchuk, *et al.*, demonstrated a reduction in AML blasts from the peripheral blood of two patients following treatment with UV-inactivated Rhabdoviruses (Batenchuk et al., 2013). This effect was attributed to a combination of replication-independent cytolysis and T cell-mediated apoptosis of malignant cells. Taken together, both papers demonstrate a replication-independent role for viruses in targeting cancer cells.

As previously discussed, tumours are comprised of neighbouring cells (immune cells and fibroblasts) that can provide supporting signals to malignant cells. The LN in NHL is no exception to this as it is comprised of immune cells, such as T cells and macrophages, and fibroblasts that provide a complex network of signals to malignant B cells (Scott and Gascoyne, 2014). Mimicking the TME *in vitro* is essential to understand the efficacy of OV against cancer. To this end, the CD40:CD40L interaction between B cells and T cells was investigated for its effect on the efficacy of CVA21 against LN-residing NHL cells. Although, to date, the TME has not been reported to enhance susceptibility of tumour cells to CVA21, this has been demonstrated in other OV models; VSV, which infects CAFs, induces neighbouring cancer cells to downregulate components of their antiviral response, such as RIG-I, thus increasing the susceptibility of the cancer cells to viral infection (Ilkow et al., 2015). The role of the TME can also be

detrimental to OV therapy as research by Liu, *et al.,* demonstrated an enhanced antiviral state was induced by Interferon-β-secreting $CD68^+$ macrophages residing in ovarian and breast tumours (Liu et al., 2013), resulting in diminished susceptibility of cancer cells to VSV. These findings suggest that other aspects of the NHL TME should be investigated to further characterise the impact of the TME on CVA21 efficacy against NHL; for example, interferon-secreting cells, such as plasmacytoid Dendritic Cells, can be present in the LN (Diacovo et al., 2005), and may stimulate a similar antiviral response.

The use of a $CD40L^+$L929 feeder layer co-culture to model the CD40:CD40L interaction in the LN, has previously been used to investigate the effects of this interaction on B cell activation, where it induced resistance to anti-IgM-induced apoptosis in WEHI-231 murine lymphoma cells (Leopoldo et al., 2001), and resistance to Doxorubicin in Daudi, Raji, BJAB, BL36 and BL70 NHL cell lines (Voorzanger-Rousselot et al., 1998), warranting its use as a model of drug-resistance. CD40L stimulation has also been achieved by other methods, such as $CD40L^+$3T3 cells and soluble CD40L trimers, that have induced chemotherapeutic resistance in CLL (Younes et al., 1998), (Romano et al., 1998), (Kitada et al., 1999) and MCL (Clodi et al., 1998b) models.

Results presented in this chapter showed that CD40L stimulation induced vincristine resistance in NHL cell lines, suggesting that CD40:CD40L interactions could reduce vincristine's efficacy *in vivo*, and increase the risk of patient relapse following treatment. Therefore, strategies such as OV, which may target drug-resistant cells, and thus eradicate residual disease, are important. Data presented in **Figure 4-11** illustrates that CD40L stimulation significantly enhanced ICAM-1 expression on Ramos, SU-DHL-4, OCI-LY19 and U2932 cell lines, and healthy donor B cells. This coincided with enhanced CVA21-induced cell death in Ramos and U2932 cells (**Figure 4-14**), but not in healthy B cells (**Figure 4-16**), which remained resistant. These data demonstrate the ability of CVA21 to target drug-resistant NHL cells, suggesting a potential to eradicate untreatable neoplastic cells, but not healthy LN-residing B cells. Research into the ability of CVA21 to target chemotherapy-resistant cells in other cancer types also reported CVA21-induced cell death of chemotherapy-resistant melanoma cell lines (Au et al., 2005), validating OV therapy as a potential strategy to complement current treatment methods.

Leopoldo, *et al.*, also reported enhanced ICAM-1 expression after CD40L stimulation of murine lymphoma cell line WEHI-231 (Leopoldo et al., 2001), supporting the ICAM-1 upregulation observed in NHL cell lines following CD40L stimulus. It is important to note that while comparing healthy B cells with NHL cell lines, the enhanced ICAM-1 on CD40L-stimulated healthy B cells was still significantly lower than baseline ICAM-1 on Ramos, Raji and SU-DHL-4 cells, but not the U2932 and OCI-LY3 cells, which were highly sensitive to CVA21. Cumulatively, these data show that, while ICAM-1 is essential for CVA21 infection, alternate mechanisms can determine susceptibility to the virus. These determinants will be investigated further in Chapter 5.

The inability of CVA21 to infect and kill healthy PBMCs has been previously demonstrated by Au, *et al*., who reported CVA21's ability to target myeloma cell lines, but not healthy PBMCs (Au et al., 2007). In agreement with this, CVA21 replication was not detectable in healthy B cells (**Figure 4-17**), contrary to the high levels of replication observed in the neoplastic NHL cell lines (**Figure 4-5**). Similarly, reovirus does not induce cell death in healthy lymphocytes (Alain et al., 2002). Reovirus and CVA21 have been used in a range of clinical trials (Thirukkumaran, C. M. et al., 2010), (White et al., 2008), (Gollamudi et al., 2010), (Pandha et al., 2015a), (Andtbacka et al., 2015), where they have not displayed significant adverse events, indicating tolerability in patients and a lack of off-target effects against healthy cells.

Overall this research has compared two candidate OV, reovirus and CVA21, for their ability to target NHL B cells. CVA21 was confirmed as a highly potent lytic agent against NHL B cells, while reovirus was less potent. For this reason, reovirus was no longer investigated as a lytic agent against NHL cells. CVA21-induced cell death of NHL cells was dependent on ICAM-1 and viral replication in malignant cells, and healthy B cells remained comparatively resistant. Other potential determinants of susceptibility to CVA21 will be the subject of future chapters.

Chapter 5:

Effect of antiviral IFN and mTOR signalling on CVA21 cytotoxicity

Chapter 5

5.1 Introduction

The aim of the research conducted in this chapter was to investigate (1) the role of host antiviral immunity in susceptible malignant B cell lines and resistant healthy donor B cells, and (2) the role of the mechanistic Target of Rapamycin (mTOR) protein complex, and the pathways it controls, in CVA21 sensitivity.

The innate antiviral response allows infected cells, or those neighbouring infected cells, to communicate with one another and prevent further viral replication. Viruses, however, are constantly evolving to generate new means of overcoming this antiviral response. This was investigated in the context of NHL by analysing the expression of a small number of ISGs after IFN-α and/or virus treatment to examine (1) whether the cells are responsive to IFN treatment and (2) whether CVA21 employs mechanisms which can abrogate IFN signalling. This may identify additional cellular determinants required for CVA21-induced death of malignant NHL cells.

The mTOR pathway is reportedly activated in a variety of cancers, including NHL (Schatz, 2011), (Westin, 2014), (Rahmani et al., 2014). MTOR is a serine/threonine protein kinase that works with several other proteins in one of 2 possible complexes; mTOR Complex 1 or 2 (mTORC1 or mTORC2). MTORC1 functions as a nutrient sensor that regulates transcription and translation (Showkat et al., 2014) while MTORC2 regulates cell survival and cytoskeleton remodelling (Saxton and Sabatini, 2017). As previously discussed, hijacking of mTOR activity is a hallmark of the replication cycles of many viruses (Chapter 2 section 2.4.1.1.4.2), highlighting it as a potentially important factor in determining the susceptibility of malignant cells to OVs. Because of the ability of rapamycin to inhibit mTORC1, a pathway known to be dysregulated in NHL cells, the effect of rapamycin on CVA21 cytotoxicity and NHL proliferation was investigated.

The findings of this chapter may facilitate the development of complementary combination strategies to enhance CVA21 efficacy in more resistant cancer models and help identify other cancer models which may benefit from CVA21 therapy.

5.2 Results

5.2.1 NHL cell lines are not protected by IFN-α despite functional IFN signalling

The type I IFN response is one of the first lines of antiviral defence. Therefore, it was hypothesised that NHL cell lines, which were highly susceptible to CVA21 infection, and healthy PBMCs, which were resistant, may differ in their IFN production and downstream signalling pathways, following CVA21 treatment. To test this, NHL cell lines and healthy PBMCs were treated with CVA21 for 48hrs and cell supernatants were analysed for the presence of IFN-α by ELISA. **Figure 5-1** shows that no IFN-α was detected in Ramos, Raji, SU-DHL-4, OCI-LY19, U2932 or OCI-LY3 cell lines following treatment with CVA21. However, healthy donor PBMCs (n=4) showed a significant dose-dependent increase in IFN-α production in response to CVA21, outlining an important difference between isolated NHL cell lines and mixed PBMCs following CVA21 treatment. It is important to note that PBMCs differ from NHL cell lines considerably, due to their non-transformed state, their limited growth and division in culture and the presence of a mix of cell types that will respond differently to the presence of CVA21, i.e., non-B cells in the PBMC culture could be producing antiviral factors that render the healthy B cells resistant to CVA21, an effect that would not be replicated in isolated NHL cell lines. Isolated B cells could not be used to compare with NHL cell lines due to the poor survival of isolated B cells in vitro within 72hrs (data not shown).

Although NHL cell lines did not produce IFN-α in response to CVA21 it was important to investigate if IFN-α, produced from possible neighbouring cells, could protect NHL cells against CVA21 infection. NHL cell lines were treated with recombinant human IFN-α (rhIFN-α) for 1hr before the addition of CVA21. The aim of this experiment was to use rhIFN-α treatment as a surrogate for viral detection and IFN-α secretion induced during the host (PBMC) antiviral response. This method was previously observed to induce significant protection from CVA21 using the AML cell line, KG-1 (Louise Müller, personal communication; data not shown). **Figure 5-2** illustrates that Ramos (a), Raji (b), SU-DHL-4 (c), U2932 (d) and OCI-LY3 (e) cells were not protected from CVA21-induced cell death by rhIFN-α. This finding was expanded upon in subsequent experiments which involved treating healthy donor PBMCs with CVA21, harvesting the virus-conditioned media (CM), and culturing the NHL cells with CVA21 in the presence or absence of CM.

Upon assessment of cell viability, CVA21 cytotoxicity was still observed, suggesting that the NHL cells were not protected by IFN-α, or other antiviral cytokines produced by PBMC in response to CVA21 treatment (data not shown).

RhIFN-α pre-treatment did not protect NHL cell lines from CVA21 infection and oncolysis, while it did protect the KG-1 AML cells (LM: manuscript submitted), suggesting a possible dysfunction of the IFN pathway in NHL cell lines. The first step in the investigation of IFN signalling in neoplastic B cells was assessment of IFN-α/β receptor expression and its ability to respond to IFN-α treatment. The expression of the IFN-α/β receptor on NHL cell lines and healthy B cells, as a normal control, was analysed by flow cytometry. **Figure 5-3** demonstrates that, Ramos (a), Raji (b), SU-DHL-4 (c), OCI-LY19 (d), U2932 (e) and OCI-LY3 (f) all expressed the IFN-α/β receptor (red) above isotype control levels (grey). Although the expression varied between cell lines, levels were comparable with that of healthy B cells, which also showed high expression of the IFN-α/β receptor (g-i).

Next, to investigate if engagement of IFN-α/β receptors by IFNs induced downstream signalling, intracellular Phosflow™ cytometry was used to detect STAT1 phosphorylation in response to rhIFN-α treatment. A preliminary time course of the p-STAT1 experiment showed that the signal diminishes after the first hour of IFN treatment (data not shown). **Figure 5-4** shows STAT1 phosphorylation was increased in 4 out of the five NHL cell lines tested (Ramos, Raji, SU-DHL-4 and U2932), in response to IFN-α treatment, although this was only significant in U2932 cells. No p-STAT1 was observed in OCI-LY3 cells upon rhIFN-α treatment. Moreover, STAT1 phosphorylation was not significantly different in NHL cells from those observed in the healthy donor B and T cells, as determined by student's T test. Collectively, these data suggest that most NHL cell lines express functional IFN receptors that are responsive to IFN. However, rhIFN-α treatment did not induce STAT1 phosphorylation in OCI-LY3 cells which expressed the IFN-α/β receptor, which was unexpected.

The functionality of the IFN response pathway was further investigated by treating NHL cells with rhIFN-α for 72hrs, followed by analysis for the expression of two surface-expressed ISGs; tetherin and MHC-I. MHC-I and tetherin were chosen as candidate ISGs for these pilot experiments due to their rapid detection by flow cytometry, the reported ability of CVA21 to target MHC-I during infection (UniProt, 2008), and the 72hr time point was chosen as previous research by Arellano-Garcia, *et al*., demonstrated

enhanced MHC-I at this time (Arellano-Garcia et al., 2014). **Figure 5-5** (a) shows significant induction of MHC-I in SU-DHL-4 cells only, and a small upward trend in expression in Ramos and healthy B cells. By contrast, tetherin expression was significantly increased in Ramos, SU-DHL-4 and U2932 cell lines following rhIFN-α treatment, **Figure 5-5** (b). OCI-LY3s showed no induction of either ISG above untreated levels, as expected given the lack of STAT1 phosphorylation observed in **Figure 5-4**. Interestingly, the induction of tetherin and MHC-I on NHL cell lines was not significantly different than that observed in healthy B cell controls, demonstrating no significant difference in their downstream IFN signalling. Taken together, these data suggest that, while the NHL cell lines are responsive to IFN treatment, IFN signalling does not protect them from CVA21-induced cell death and therefore does not offer a further explanation for the differential sensitivity of malignant B cells over healthy B cells. While this research focussed on MHC-I and Tetherin as candidate ISGs, further research is being conducted that will examine the effects of CVA21 and IFN-α on the expression of a wider range of ISGs.

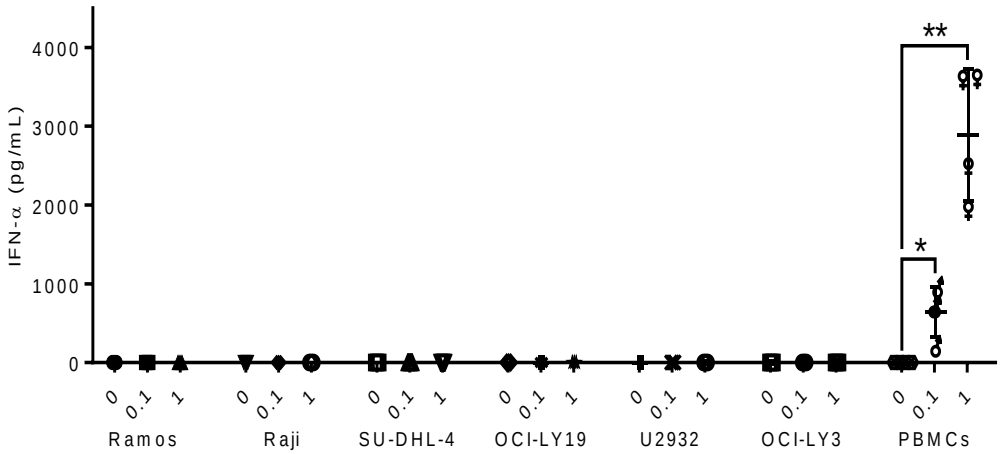

Figure 5-1 Interferon-α production by NHL cell lines and healthy PBMCs in response to CVA21 treatment.

Ramos, Raji, SU-DHL-4, OCI-LY19, U2932 and OCI-LY3 cell lines and healthy donor PBMCs were treated with CVA21 for 48hrs before analysis of supernatant for IFN-α secretion by ELISA. Data shows n=3 independent experiments for the NHL cell lines and n=4 independent healthy PBMC samples ± SEM. Significance was determined using a paired, two-tailed student's T test.

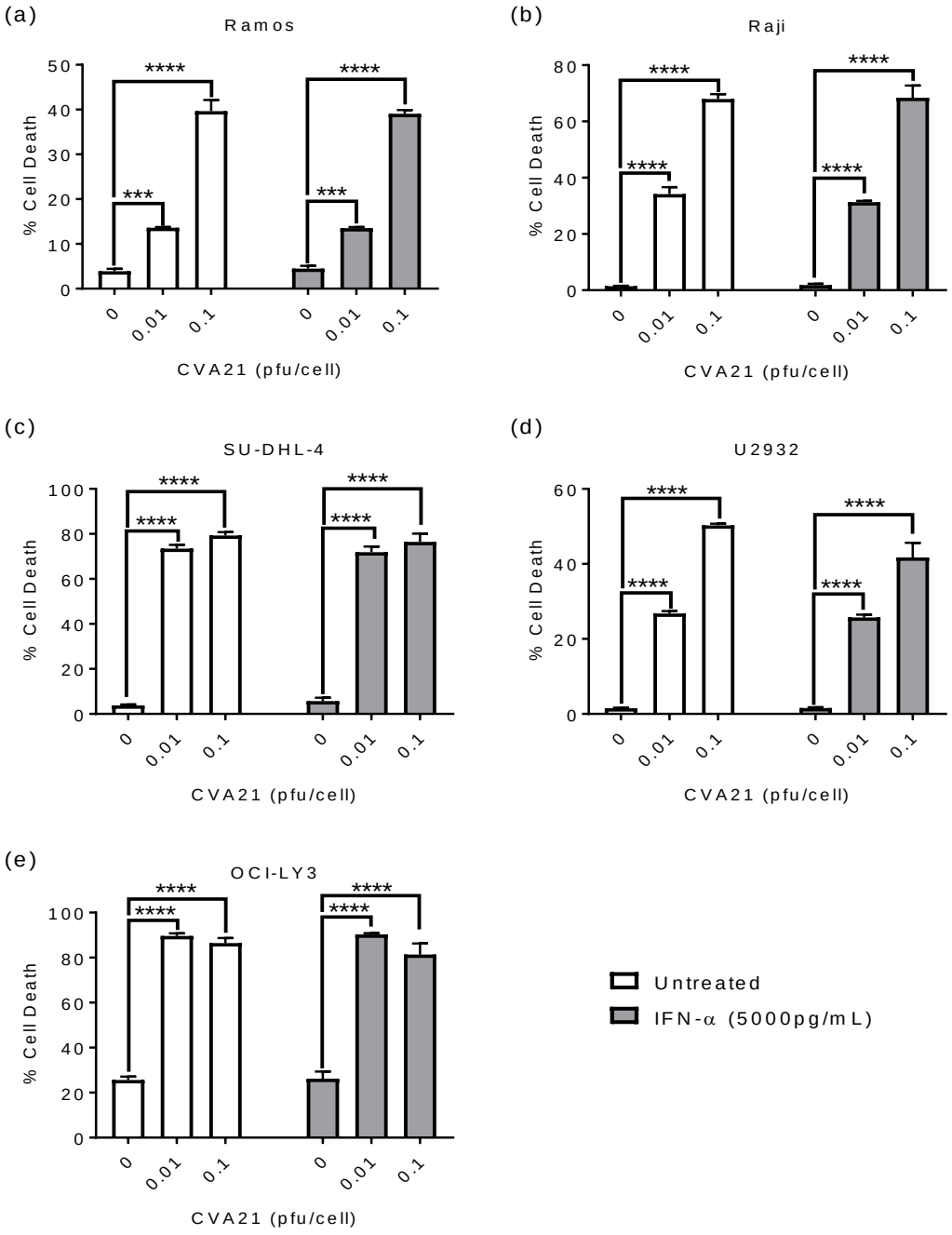

Figure 5-2 IFN-α pre-treatment of NHL cell lines does not abrogate CVA21-induced cell death.

Ramos (a), Raji (b), SU-DHL-4 (c), U2932 (d) and OCI-LY3 (e) cell lines were pre-treated with rhIFN-α (5000pg/mL) for 1hr before being treated with CVA21. Cells were cultured for 24hrs before being harvested and assayed for viability using LIVE/DEAD™ viability dye. Data shows the mean + SEM for n=3 independent experiments. Statistical analysis was determined by two-way ANOVA.

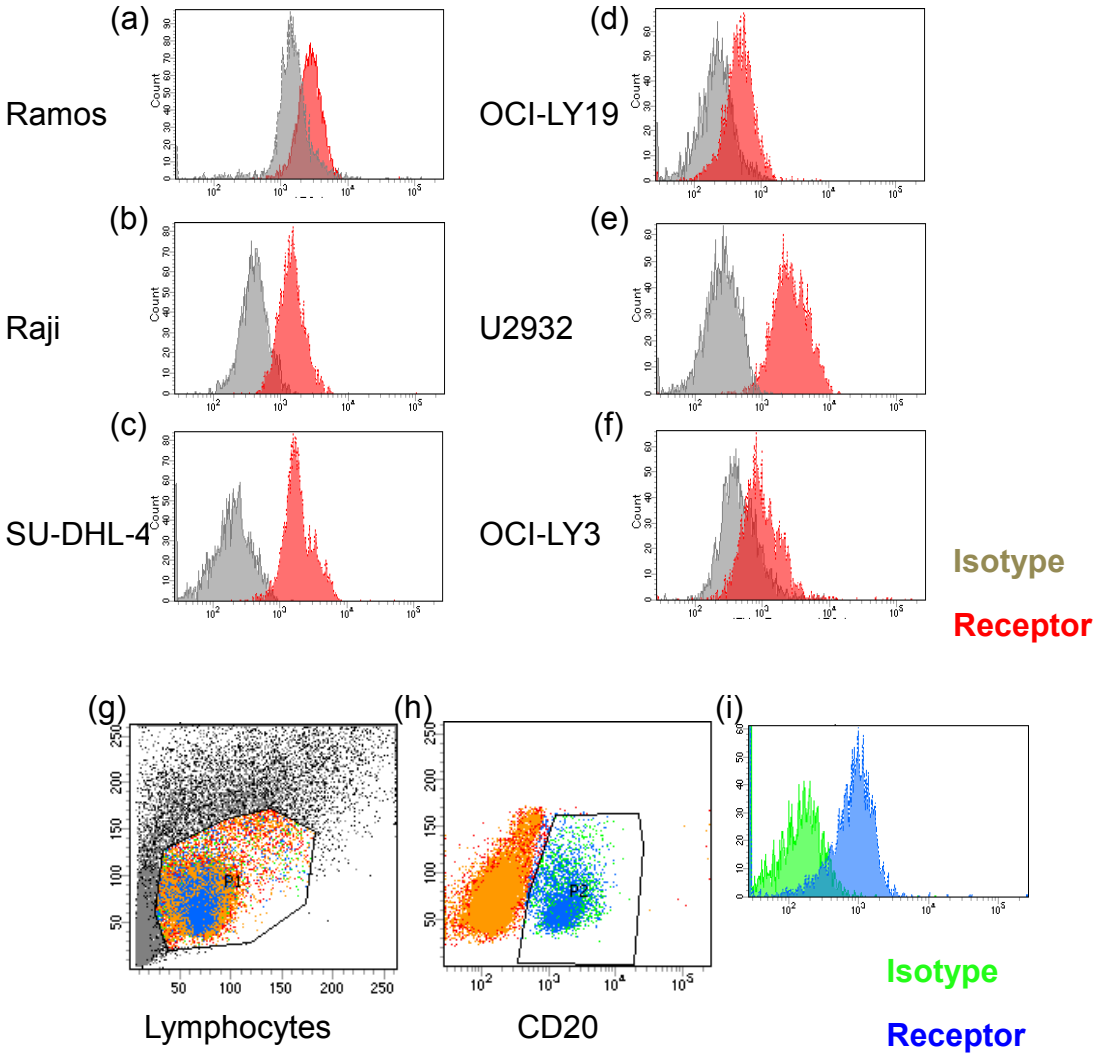

Figure 5-3 Interferon-α/β receptor expression on NHL cell lines and healthy B cells.

Ramos (a), Raji (b), SU-DHL-4 (c), OCI-LY19 (d), U2932 (e) and OCI-LY3 (f) cell lines were analysed by flow cytometry for surface expression of the IFN-α/β receptor. Receptor expression is illustrated by representative histogram plots overlaying IFN-α/β staining (red) and the matched isotype control (grey) (a-f). Lymphocytes were identified by FSC/SSC (g) and healthy donor B cells by CD20 expression (h). Healthy donor B cell IFN-α receptor expression (i) is illustrated by a representative histogram plot overlaying IFN-α/β receptor staining (blue) and isotype control (green). All data is representative of n=2 independent experiments.

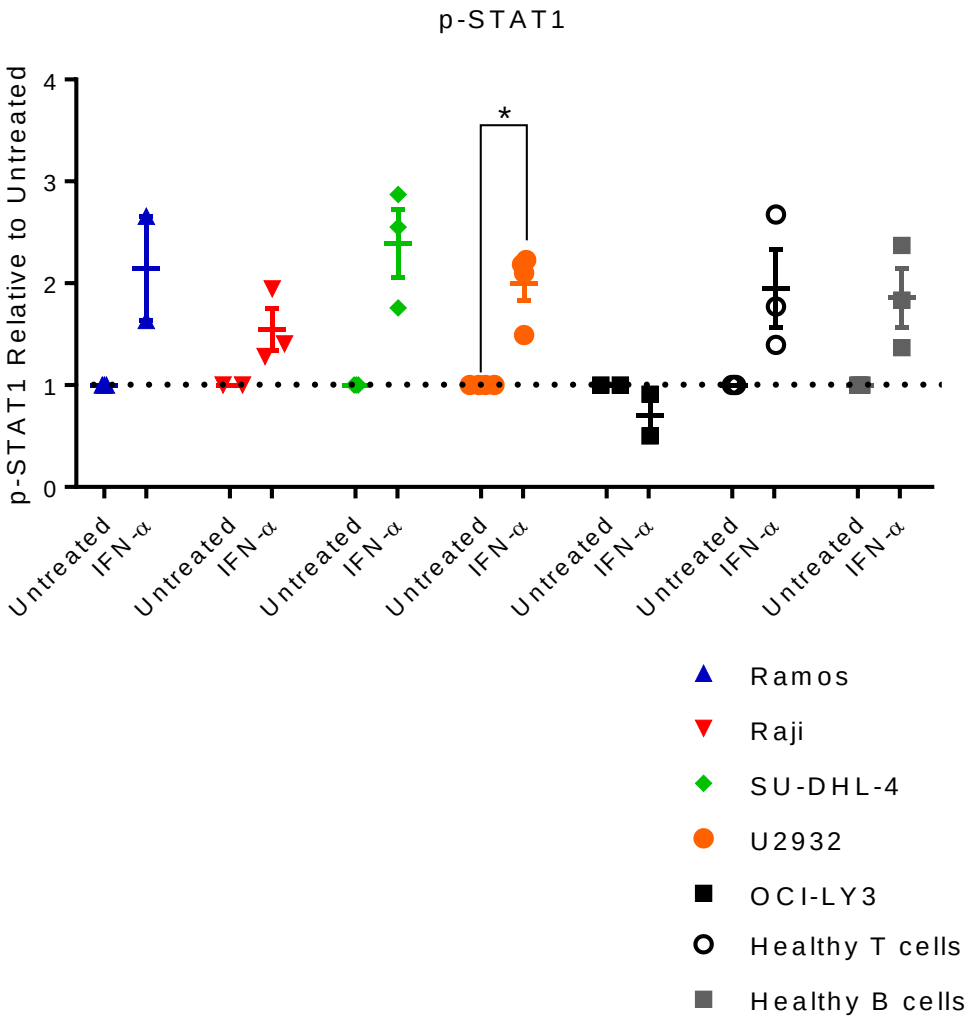

Figure 5-4 STAT-1 phosphorylation in NHL cell lines and healthy B cells in response to rhIFN-α treatment.

NHL cell lines, Ramos (blue), Raji (red), SU-DHL-4 (green), U2932 (orange) and OCI-LY3 (black), and Healthy PBMC T cells (open circles) and B cells (grey squares) were analysed for STAT1 phosphorylation 30 min after rhIFN-α treatment (5000pg/mL). STAT1 phosphorylation MFI was normalised to the MFI of treatment-matched isotype controls and the graph illustrates the ratio to untreated samples. Data from individual experiments is shown, ± SEM. Significance was determined by paired, two-tailed student's T test.

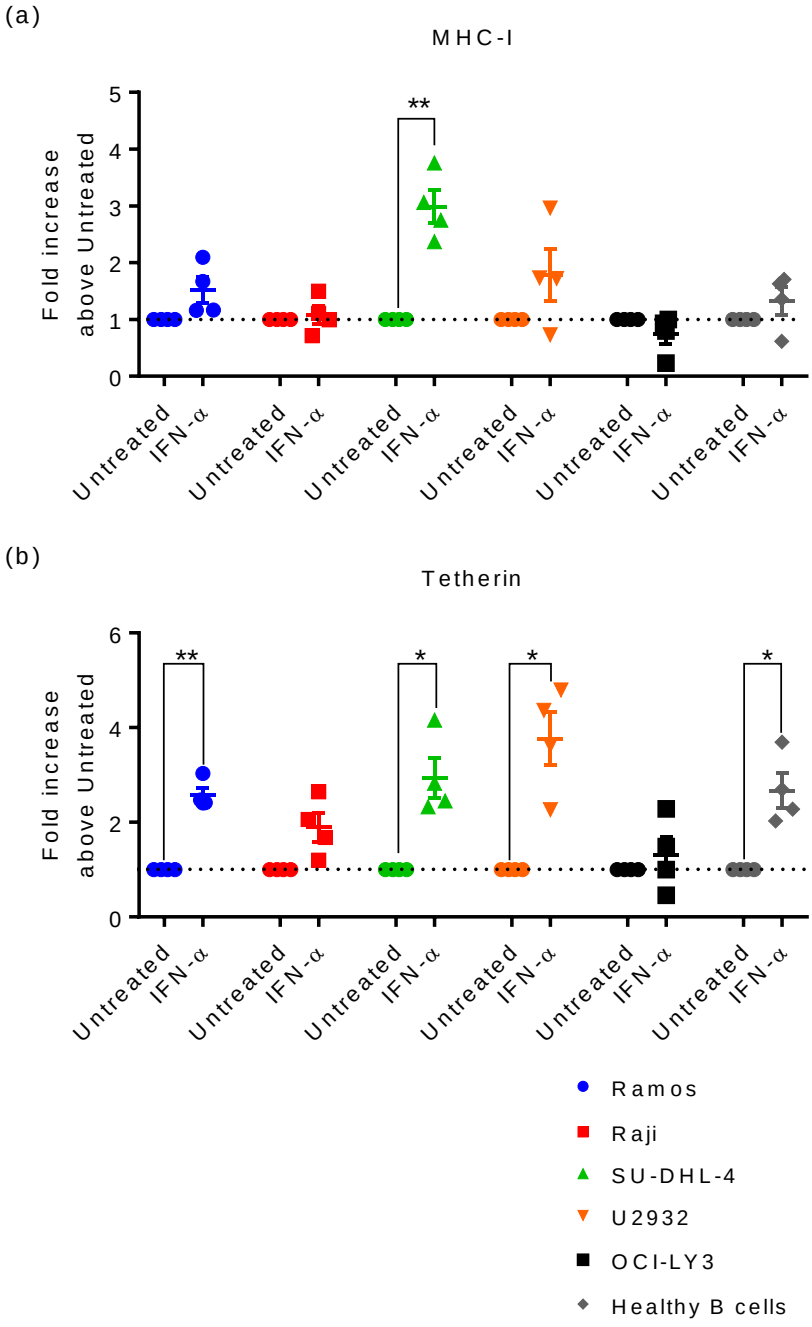

Figure 5-5 Induction of MHC-I and tetherin expression in response to rhIFN-α treatment.

Ramos (blue), Raji (red), SU-DHL-4 (green), U2932 (orange) and OCI-LY3 (black) cell lines, as well as 4 healthy donor B cells (grey; in the context of PBMCs) were treated with 5000pg/mL rhIFN-α and analysed for surface expression of MHC-I (a) and tetherin (b). Results are normalised to treatment-matched isotype controls and expressed as ratios relative to untreated samples. Data from n=4 independent experiments is shown ± SEM. Significance was determined by paired, two-tailed student's T test.

5.2.2 CVA21 inhibits the antiviral response in NHL cell lines but not healthy B cells in mixed PBMCs

The ability of NHL cell lines to respond to IFN and induce antiviral ISGs suggests that the IFN pathway is functional, yet unable to inhibit CVA21-induced cell death, as shown in **Figure 5-2**. One potential explanation for this is that CVA21 may inhibit IFN signalling in NHL cell lines, but not healthy donor B cells. To test this, NHL cell lines and healthy B cells (identified in the context of mixed PBMCs by flow cytometry) were treated with CVA21 for 16hrs before being treated with rhIFN-α for 24hrs; viable cells were then assessed for MHC I and Tetherin expression to determine whether IFN-induced ISG expression could be inhibited by CVA21. **Figure 5-6** shows increased Tetherin expression in rhIFN-α-treated Ramos (a), SU-DHL-4 (b) and U2932 (c) cells, however, this appeared to be reduced upon CVA21 treatment in all three cell lines (n=2). Contrary to earlier figures, healthy donor B cells (d) showed no significant increase in Tetherin expression upon rhIFN-α treatment, however, in contrast to NHL lines, a significant increase in Tetherin expression was observed upon CVA21 treatment. Similarly, preliminary data shown in **Figure 5-7** illustrates enhanced MHC-I expression by rhIFN-α treatment that is diminished by CVA21 infection in SU-DHL-4 cells. Collectively, these data demonstrate that NHL cell lines are susceptible to CVA21 despite having a functional antiviral response. However, decreased ISG expression following CVA21 treatment suggests that CVA21 may inhibit the antiviral response in malignant NHL cells, but not in healthy cells. It is possible that low ICAM-1 expression in healthy B cells may prevent sufficient CVA21 entry to overcome the natural host antiviral response. These data demonstrate the ability of CVA21 to manipulate the antiviral response of malignant cells and suggests this as a potential determining factor for CVA21 susceptibility.

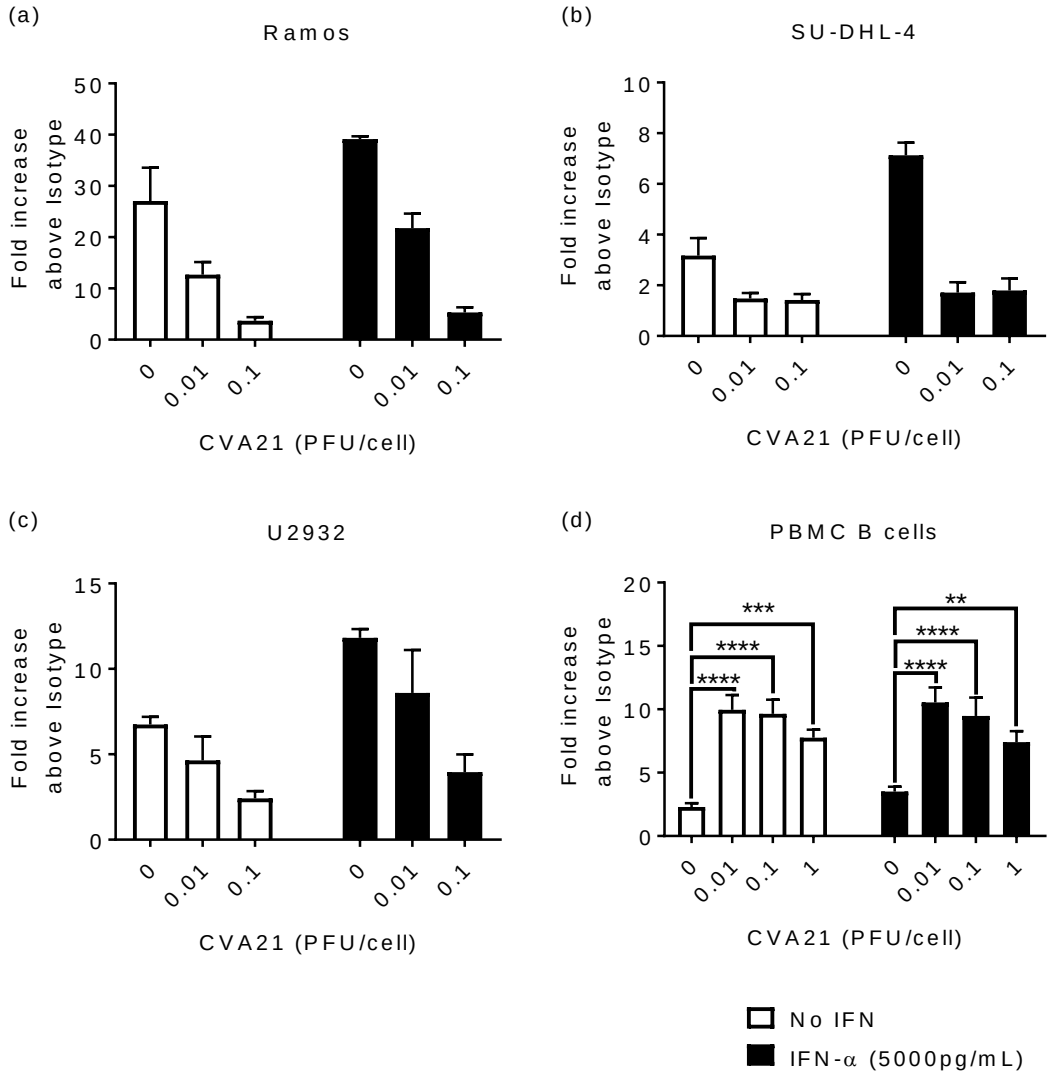

Figure 5-6 CVA21 inhibits rhIFN-α-induced expression of Tetherin in NHL cell lines.

Ramos (a), SU-DHL-4 (b), U2932 (c) cell lines and healthy donor B cells in the context of PBMCs (d) were pre-exposed to CVA21 for 16hrs before being treated with rhIFN-α for a further 24hrs. Samples were harvested and stained with an α-human Tetherin antibody prior to analysis by flow cytometry. Tetherin expression is displayed relative to isotype expression from treatment-matched samples. Results are from n=2 independent experiments for the NHL cell lines and n=3 donors for the healthy B cells. Data shows the mean + SEM, statistical significance was determined by two-way ANOVA.

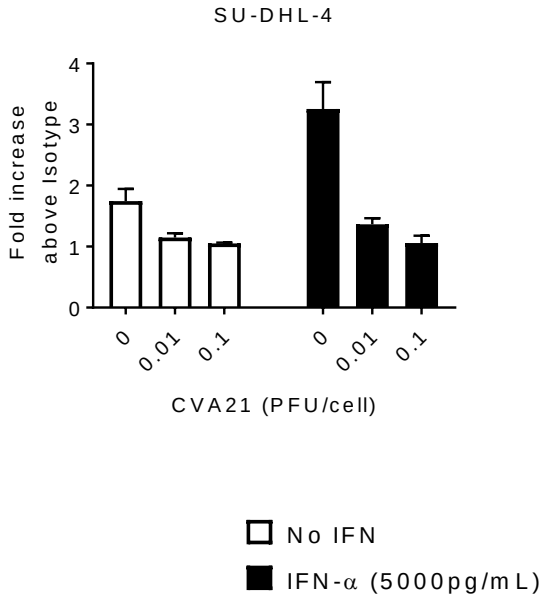

Figure 5-7 CVA21 inhibits rhIFN-α-induced expression of MHC-I in SU-DHL-4 cells.

SU-DHL-4 cells were pre-exposed to CVA21 for 16hrs before being treated with rhIFN-α for a further 24hrs. Samples were then harvested and stained with an anti-human MHC-I antibody, prior to analysis by flow cytometry. MHC-I expression is displayed relative to isotype expression from treatment-matched samples. Results are from n=2 independent experiments. Data shows the mean + SEM.

5.2.3 MTOR inhibition impairs CVA21-induced cell death in NHL cells

A literature search of the pathways that are often dysfunctional in NHL cells identified upregulated mTOR signalling as a common trait in NHL B cells (Schatz, 2011). To investigate a potential relationship between mTOR activity and susceptibility to CVA21, NHL cell lines were investigated for their mTOR activation status and the effect of mTOR inhibition on CVA21 susceptibility. NHL cell lines were analysed for basal mTORC1 activity by intracellular Phosflow™ cytometry for the phosphorylation of the downstream targets S6 and 4EBP1. These samples were analysed alongside healthy donor B cells as non-transformed controls. **Figure 5-8** (a) shows significant mTOR activity in Ramos, SU-DHL-4 and OCI-LY3 cells. This is in contrast with the healthy donor B cells (in PBMCs) which appeared to display lower mTOR activity (n=2). Similarly, for p-4EBP1 (b), mTOR activity is active in Ramos, SU-DHL-4 and U2932 cells and appears to be lower in the healthy B cells.

Having identified that mTOR signalling is active in most cell lines, but not healthy B cells, the role of mTOR in CVA21 infection and oncolysis was investigated. NHL cell lines were treated with rapamycin for 1hr prior to being treated with CVA21 for 72hrs and quantification of cell death. **Figure 5-9** demonstrates that cell death induced by CVA21 was significantly reduced in the presence of rapamycin in Ramos (a), SU-DHL-4 (c) and U2932 (d) cells, but not the Raji (b) cells. To ensure that the doses of rapamycin used were sufficient to inhibit mTOR activity, NHL cell lines were treated with rapamycin for 24hrs and analysed for S6 and 4EBP1 phosphorylation. Phosphorylation of S6 was significantly inhibited by rapamycin in all NHL cell lines, **Figure 5-10** (a), however, phosphorylation of 4EBP1 was not inhibited, **Figure 5-10** (b), suggesting an important role for mTOR-regulated S6 activity in the sensitivity of these cells to CVA21.

As previously described, CD40L stimulation increased ICAM-1 on most NHL cell lines and this coincided with enhanced susceptibility to CVA21 in two cell lines (sections 4.2.6 and 4.2.7). MTOR activity can also be increased upon CD40L stimulation (Dormond et al., 2008). NHL cell lines were cultured alone, or on $CD40L^+$ L929s or parental L929s for 24hrs, harvested and analysed for p-S6 and p-4EBP1 by Phosflow™ cytometry to test whether mTOR activity in NHL cell lines is enhanced upon CD40L stimulation. CD40L has no significant effect on S6 phosphorylation levels, **Figure 5-11** (a), and 4EBP1 phosphorylation also remained unchanged in NHL cells after CD40L

stimulation, **Figure 5-11** (b). These data showed no increase in mTOR activity upon CD40L stimulation, suggesting that enhanced mTOR signalling, in CD40L-stimulated NHL, was not responsible for the enhanced CVA21 cytotoxicity shown in section 4.2.7, **Figure 4-14**.

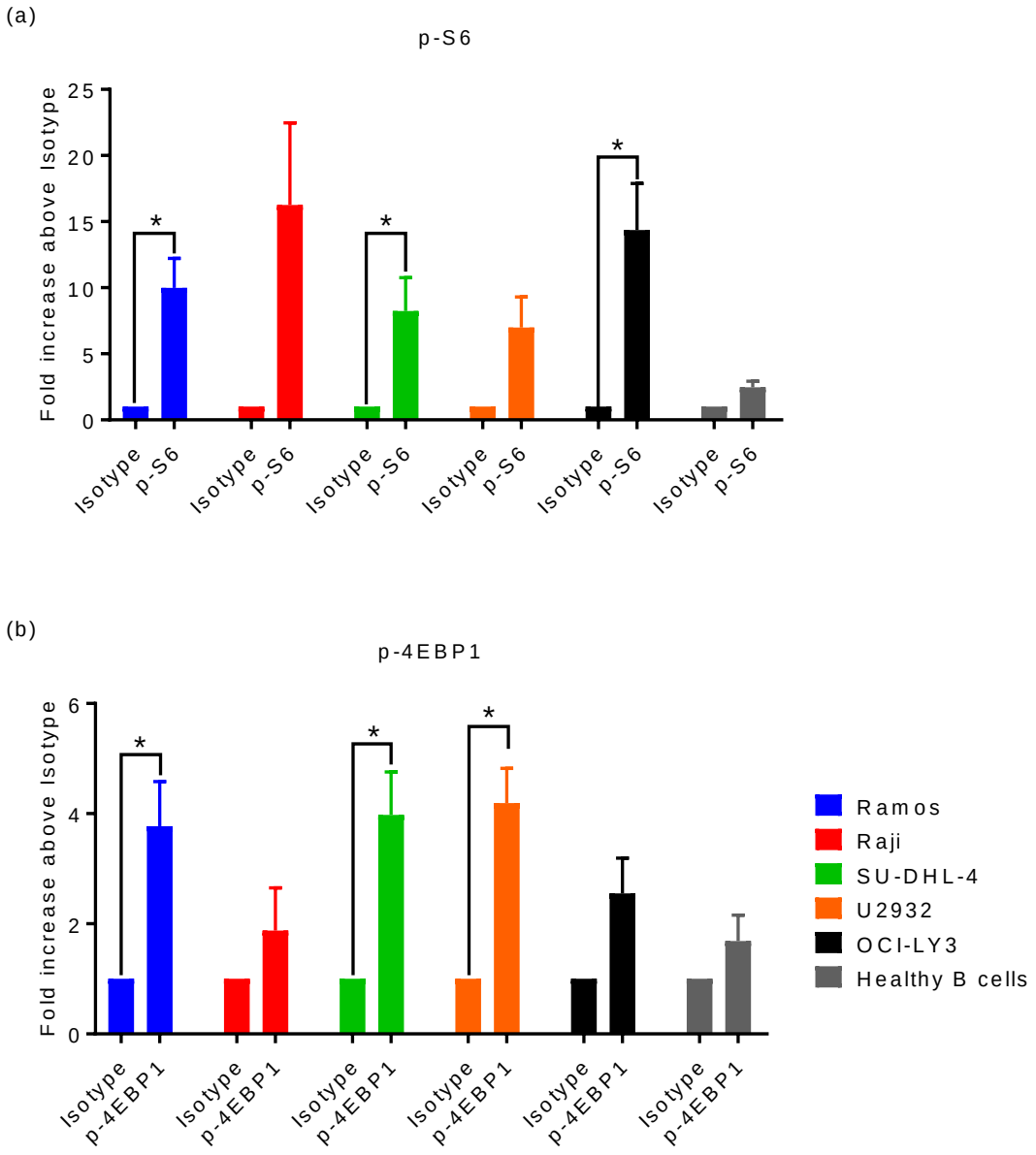

Figure 5-8 MTOR Activity in NHL cell lines and healthy B cells.

Ramos (blue), Raji (red), SU-DHL-4 (green), U2932 (orange) and OCI-LY3 (black) cell lines, and 2 healthy B cells (grey; in the context of PBMCs) were cultured for 24hrs and analysed for baseline mTOR activity by 4EBP1 and S6 phosphorylation. Isotype controls were normalised to 1 and matched p-S6 and p-4EBP1 expression was expressed as a ratio of isotype staining. Data shows the mean from n=4 independent experiments for cell lines and n=2 healthy donor samples + SEM. Significance was determined by paired, two-tailed student's t test

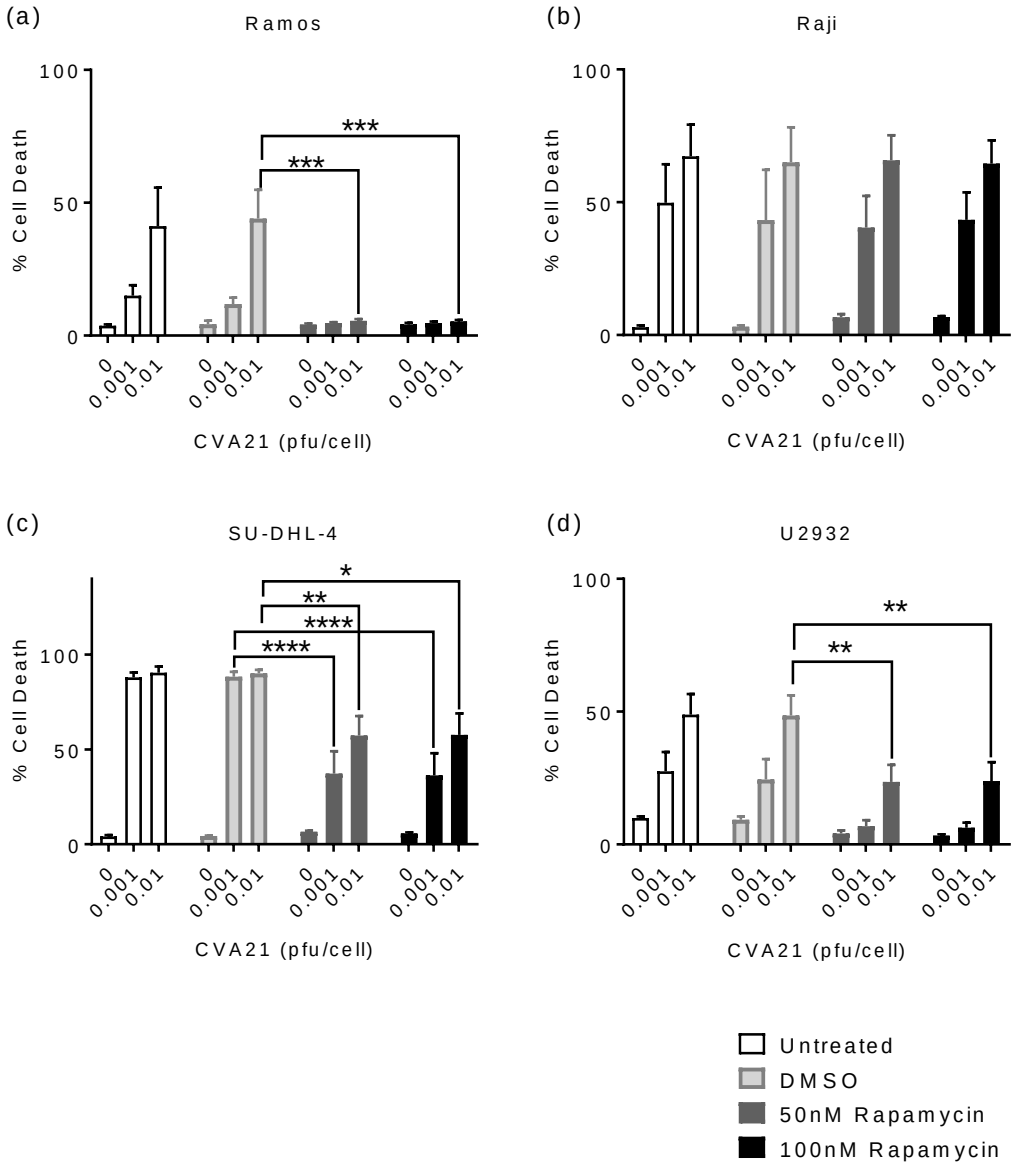

Figure 5-9 Rapamycin diminishes CVA21-induced cell death in most NHL cell lines.

NHL cell lines Ramos (a), Raji (b), SU-DHL-4 (c) and U2932 (d) were untreated (white bars) or pre-treated with DMSO (light grey), 50 or 100nM rapamycin (dark grey and black bars, respectively) for 1hr before the addition of CVA21. The cells were then cultured for 72hrs, harvested and analysed for cell death using LIVE/DEAD™ viability dye by flow cytometry. Results are expressed as the percentage dead cells from n=4 independent experiments + SEM. Statistical significance was determined by two-way ANOVA.

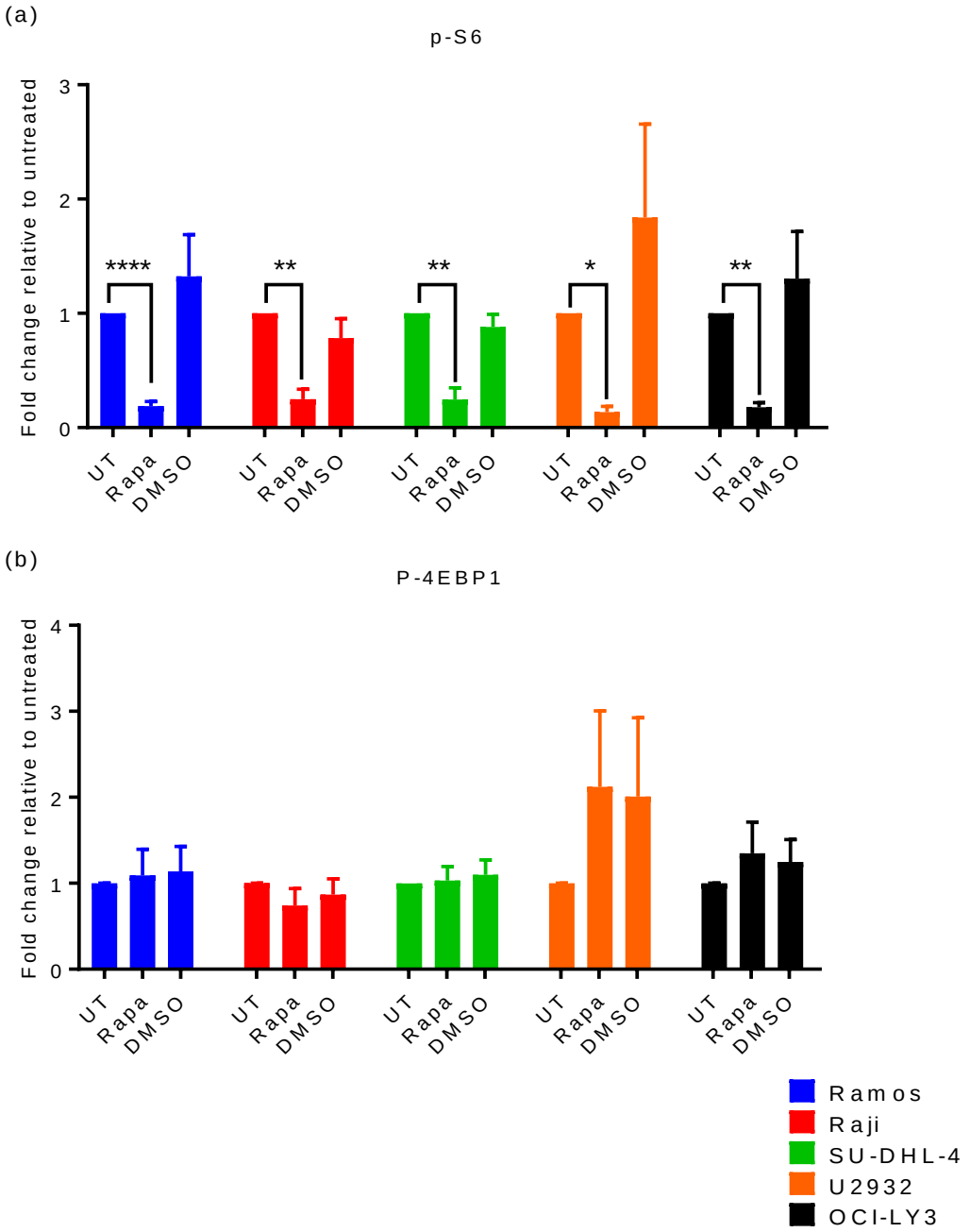

Figure 5-10 Rapamycin inhibits S6 phosphorylation, but not 4EBP1 phosphorylation.

Ramos (blue), Raji (red), SU-DHL-4 (green), U2932 (orange) and OCI-LY3 (black) cell lines were treated with rapamycin (Rapa) or DMSO for 24hrs. The cells were harvested, stained for intracellular p-S6 and p-4EBP1 and the MFI values calculated as a ratio relative to the isotype values. Data were then normalised to the untreated samples and the graphs illustrate fold change relative to untreated controls. Data shows the results from n=4 independent experiments + SEM. Statistical significance was determined by one-way ANOVA.

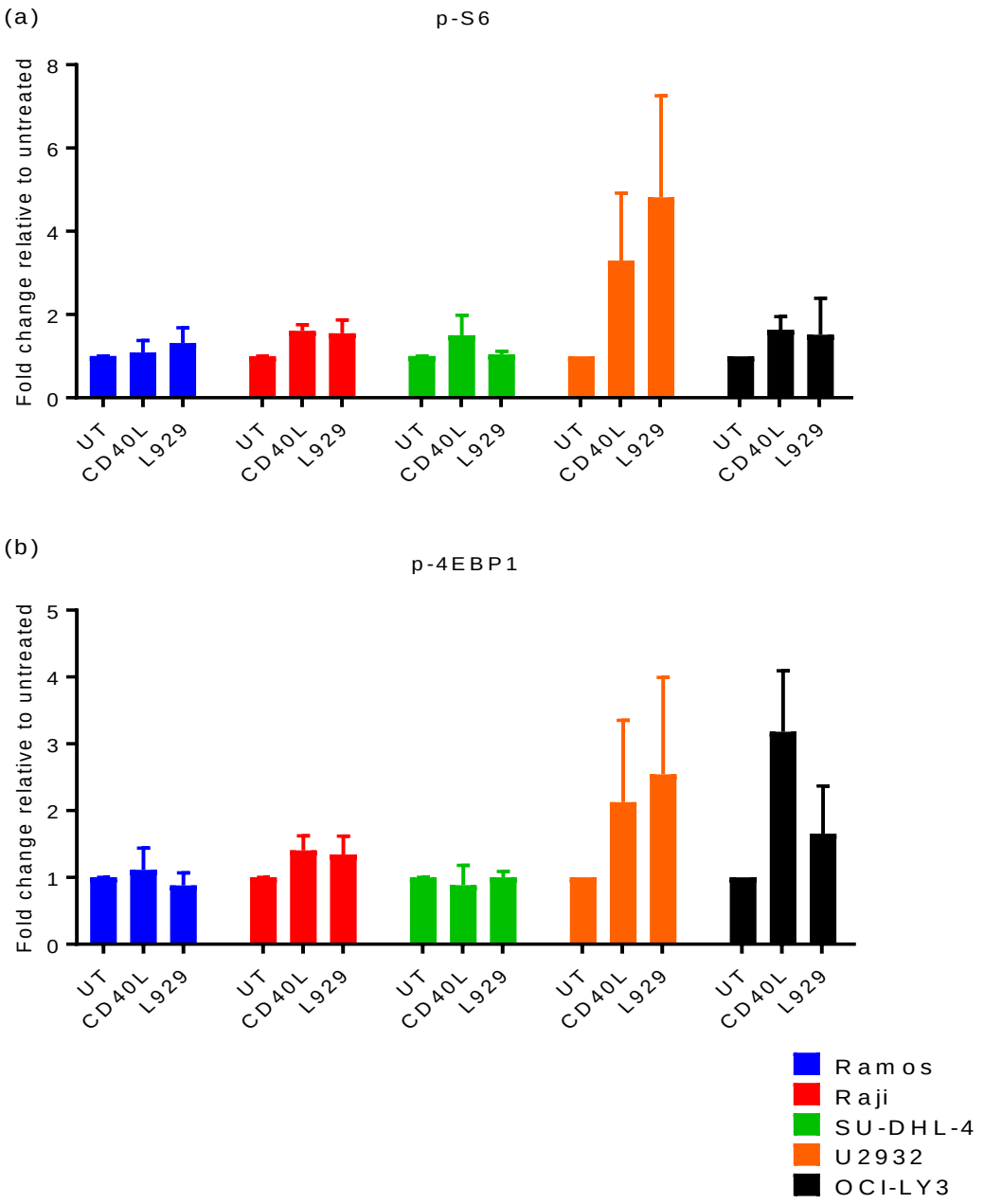

Figure 5-11 CD40L Stimulation does not enhance MTOR activity in NHL cell lines.

Ramos (blue), Raji (red), SU-DHL-4 (green), U2932 (orange) and OCI-LY3 (black) cell lines were cultured alone (UT) or on CD40L^{+}L929 (CD40L) or parental L929 (L929) cells for 24hrs. The cells were harvested, stained for intracellular p-S6 and p-4EBP1 and the MFI values calculated as a ratio relative to the isotype values. Data were then normalised to the untreated samples and the graphs illustrate fold change relative to untreated controls. Data shows the results from n=4 independent experiments + SEM. Statistical significance was determined by one-way ANOVA.

5.2.4 Rapamycin has little effect on NHL cell cycle and proliferation

Rapamycin has strong anti-proliferative effects due to its reported inhibition of translation, as shown in melanoma (Bundscherer et al., 2008) and T cell lymphoma cell lines (Zhao, Y.M. et al., 2008). As such, Rapamycin was investigated for its effects on NHL cell line proliferation using CFSE staining to determine if there is a role for mTOR inhibition in CVA21 cytotoxicity, beyond a more general block of cellular proliferation.

NHL cell lines, Ramos (a), Raji (b), SU-DHL-4 (c), U2932 (d) and OCI-LY3 (e) were stained with CFSE and incubated with and without rapamycin (**Figure 5-12**). Flow cytometry after 24hrs revealed reduced fluorescence in control untreated cells (due to cell division) that was comparable with rapamycin-(blue) and DMSO- treated (purple) cells. However, by 48hrs, the CFSE fluorescence of the rapamycin-treated cells was greater than that of untreated cells or DMSO controls. This effect was even more pronounced by 72hrs, suggesting a slowing of cell proliferation by rapamycin, rather than complete cell cycle blockade. These results are quantified in **Figure 5-13** and demonstrate a significant difference between CFSE fluorescence in untreated and rapamycin-treated cells at 72hrs (the time point shown in **Figure 5-9**) in Ramos (a), SU-DHL-4 (c), U2932 (d) and OCI-LY3 (e) cells, but not in Raji (b). By contrast, no significant delays in proliferation were observed at earlier time points (24 or 48rs) following rapamycin treatment. Importantly, rapamycin also inhibited CVA21-induced cell death to a similar extent at 48hrs in Ramos, SU-DHL-4, U2932 and OCI-LY3 cells (n=1, data not shown) when cell proliferation was not significantly inhibited suggesting that blockade of cell proliferation by rapamycin was not responsible for reduced CVA21 cytotoxicity.

To further examine the effect of rapamycin on cell cycle progression, propidium iodide (PI) staining of DNA was used to assess the cell cycle status following rapamycin treatment, **Figure 5-14**. PI analysis of rapamycin-treated NHL cell lines at 72hrs showed no significant in cell cycle between treated and untreated samples.

Collectively, these data demonstrate that rapamycin does not immediately block NHL cell proliferation or cause G1 cell cycle arrest; however, small, but significant delays in cellular proliferation were observed following rapamycin treatment after 72hrs. Given that only a small delay in cellular proliferation was observed with rapamycin in most cell lines, this suggests that the effect of rapamycin is not due to abrogation of cell proliferation but another function of

mTOR, which is important to support CVA21 replication and lysis. The significance of mTOR in CVA21-induced cell death needs to be further defined and is the subject of ongoing laboratory investigations.

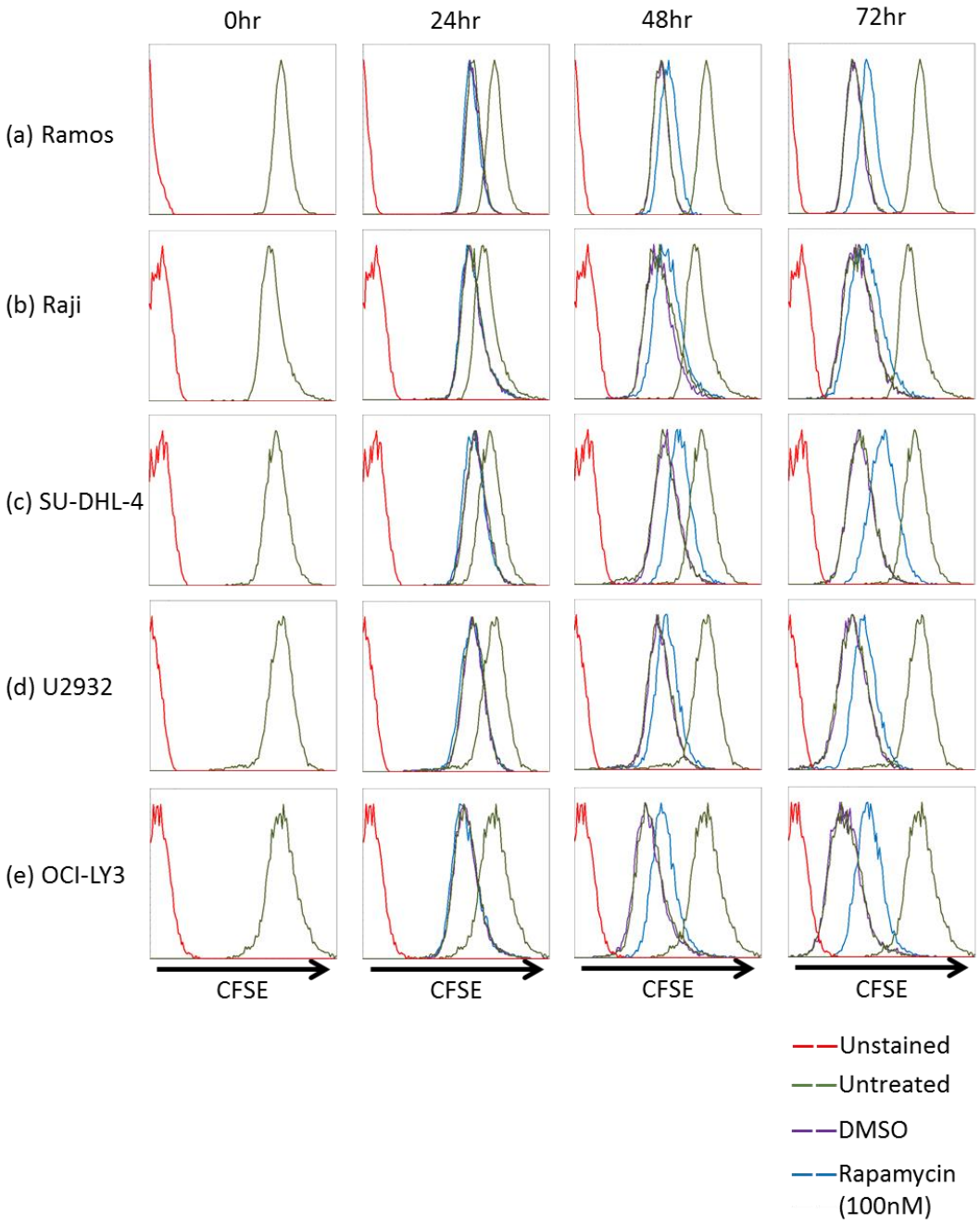

Figure 5-12 Rapamycin delays NHL cell line proliferation.

NHL cell lines were left unstained (red) or stained with CFSE before being treated with rapamycin (blue), DMSO (purple) or left untreated (green). Cells were then analysed for fluorescence immediately and every 24hrs thereafter. The 0hr untreated CFSE-stained result was included in the 24, 48 and 72hr histograms in all cell lines to demonstrate the shift in fluorescence from the start of the experiment (0hr) to the other time points. Data shows representative histogram overlays of unstained, untreated, DMSO or rapamycin treated cells from n=4 independent experiments.

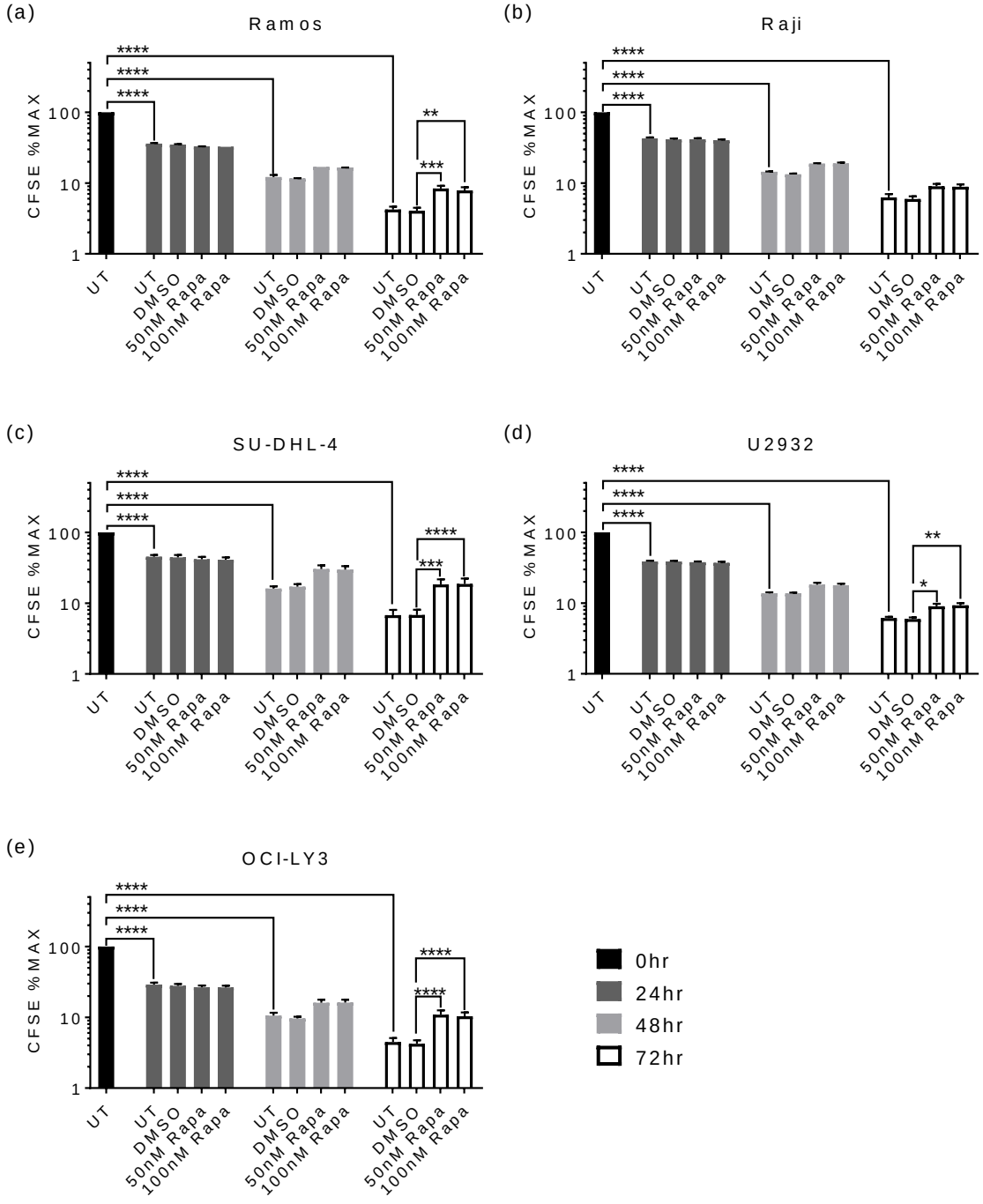

Figure 5-13 Rapamycin delays NHL cell line proliferation.

NHL cell lines were stained with CFSE before being incubated with and without DMSO or rapamycin (50 and 100nM). CFSE fluorescence was then analysed by flow cytometry immediately and every 24hrs thereafter. Data shows the mean of n=4 independent experiments +SEM, analysed for significance by one-way ANOVA.

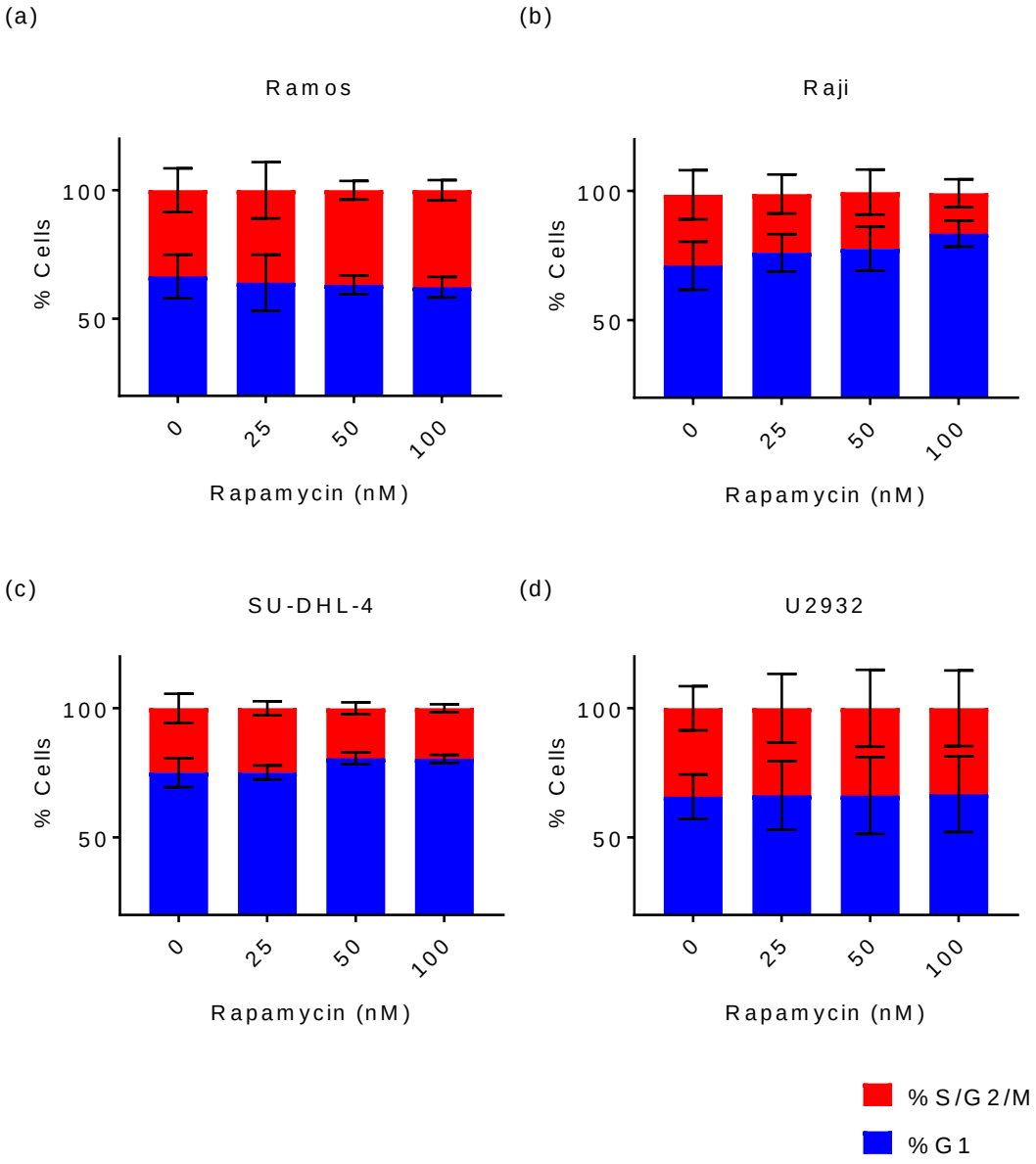

Figure 5-14 Rapamycin does not cause G1 arrest.

NHL cell lines were treated with rapamycin for 72hrs before being harvested and stained with Propidium Iodide and analysed by flow cytometry. The percentage of cells in G1 and S/G2/M phases of the cell cycle were then determined by DNA content (PI fluorescence). Data shows the results from n=3 independent experiments ± SEM. Statistical significance was determined using one-way ANOVA, no statistically significant differences were observed.

5.3 Discussion

This research aimed to investigate the role of the antiviral IFN response in preventing CVA21 infection, the ability of CVA21 to overcome this response and the role of mTOR in CVA21 infection. Vähä-Koskela, *et al*., have previously reviewed a variety of factors that impact the ability of oncolytic viruses to replicate in malignant cells, such as the role of a functional IFN response (Vaha-Koskela and Hinkkanen, 2014). Identifying cellular factors responsible for CVA21 replication and oncolysis may enable patient stratification to target susceptible disease, such as using IFN-sensitive OV to target IFN-deficient cancers.

IFN signalling can inhibit OV replication, shifting the preference of the OV towards malignant cells that lack a functional antiviral IFN response, such as NDV (Elankumaran et al., 2010), an oncolytic influenza virus (Muster et al., 2004) and VSV (Stojdl et al., 2000). In this chapter, the absence of detectable IFN-α in NHL cell line cultures, versus the high levels of IFN-α in CVA21-resistant PBMCs (**Figure 5-1**), offered a possible explanation for their sensitivity to CVA21. This result may be due to the diverse mix of cells within the PBMC samples which could produce IFN-α, while the homogenous cell line cultures could not. For example, PBMC incorporate many cell types that can produce IFN in response to a virus, such as B cells (Ward et al., 2016), T cells (Klimpel et al., 1990), NK cells (Arase et al., 1996), monocytes (Hansmann et al., 2008), and Plasmacytoid Dendritic Cells (Fitzgerald-Bocarsly, 2002). Plasmacytoid Dendritic cells (pDCs) have been implicated as the main producers of IFN-α in response to CVA21 by complimentary research conducted in the laboratory (Louise Müller: manuscript submitted). Interestingly, Ho, *et al*., reported that NHL patient lymphocytes have a diminished ability to produce IFN in response to antigenic assault (Ho et al., 1992), suggesting that a reduced IFN response in NHL patients. Moreover, it should be recognised that the production of IFN and other cytokines by OV *in vivo* can suppress tumour growth, as demonstrated by Samson, *et al.*, who showed cytokine-mediated suppression of hepatocellular carcinoma tumours in NOD/SCID mice by UV-inactivated reovirus (Samson et al., 2018).

Pre-treating NHL cell lines with rhIFN-α did not protect them from CVA21 cytotoxicity, while it did protect the AML cell line, KG-1 (Louise Müller: Manuscript submitted). Therefore, it was possible that NHL cells may be unable to respond to IFN treatment, however further investigations, measuring downstream STAT1 phosphorylation and ISG (MHC I and Tetherin)

upregulation, confirmed this was not the case. By contrast, OCI-LY3 cells, despite expressing the IFN-α/β receptor, did not respond to rhIFN-α treatment by STAT1 phosphorylation or ISG expression.

Interestingly, research conducted on other Coxsackieviruses by Lind *et al.*, and Horwitz, *et al.*, have demonstrated protective roles for IFN-λ against CVB3 (Lind et al., 2016) and IFN-γ against CVB4 (Horwitz et al., 1999), respectively, highlighting the importance of considering the IFN response when applying CVA21 to a malignancy. IFN-γ alone, and in combination with IFN-α, were investigated for their effects on CVA21 susceptibility but did not protect NHL cells from infection (data not shown). Unfortunately, due to time constraints, NHL cell lines, or healthy donor PBMCs, were not analysed for the secretion of other pro-inflammatory cytokines in response to CVA21, however, future research could test for the secretion of other IFNs, such as IFN-β, -λ or –γ, and a wider variety of secreted pro-inflammatory cytokines which have been associated with resistance to other picornaviruses (Dotzauer and Kraemer, 2012). For example, IFN-β has been implicated in resistance to CVB3 (Deonarain et al., 2004), (Runkel et al., 1998), and other Coxsackievirus and picornaviruses have displayed sensitivity to IFNs such as CVA16 (Hand, Foot and Mouth Disease Virus - HFMDV), which is abrogated in mice treated with murine IFN (Sasaki et al., 1986), and Foot and Mouth Disease Virus (FMDV), which is sensitive to IFN-α, -β and -γ in swine models (Diaz-San Segundo et al., 2010).

The fact that the IFN signalling appeared functional in the NHL cells, but was not able to inhibit CVA21, suggested that the virus may interfere with the IFN pathway. To test this, expression of MHC-I and Tetherin was examined after rhIFN-α treatment in the presence or absence of CVA21. ISG expression in the NHL cell lines appeared decreased upon CVA21 treatment, but not in healthy B cells; blockade of IFN signalling by CVA21 could provide a mechanism by which NHL cells remain susceptible despite the presence of antiviral IFN. In support of this hypothesis, Lind *et al.*, also demonstrated that CVB3 could inhibit the IFN-λ response in HeLa cells using the $2A^{pro}$ protein, which cleaved TIR-domain-containing adapter-inducing interferon-β (TRIF) and Induced by Phosphate Starvation1 (IPS1), involved in relaying signals from PRRs to the nucleus to induce IFN production. Similar blockade of downstream effectors of the antiviral interferon response has been demonstrated by the 3C protein of enteroviruses 68 and 71 cleaving TRIF (Xiang et al., 2014), (Lei et al., 2011), and the $3C^{pro}$ protein of CVB3 cleaving MAVS and TRIF (Mukherjee et al., 2011), suggesting a common mechanism of picornaviruses in blocking the antiviral IFN response.

CVA21, like other picornaviruses, has also been reported to subvert the host antiviral response by encoding proteins that interfere with host protein expression (ViralZone, 2015). CVA21 expresses proteins such as 2B, 2BC and 3A, which disrupt the trafficking of IFN receptors and MHC molecules to the surface by inhibiting the function of the Golgi apparatus (UniProt, 2008). Coxsackieviruses also manipulate transcriptional and translational machinery in the cell for their own replication (Hwang, H.Y. et al., 2007), leading to a more general shutdown of host protein expression in the infected cell. Interestingly, CVA21 ablated human myeloma in SCID mouse xenograft models (Hadac and Russell, 2006). This response was associated with systemic myositis resulting in the death of mice. However, inoculation of an adenoviral vector expressing human IFN-α, resulting in increased IFN-α concentrations (3000 pg/mL) in the blood, inhibited the adverse effects. Importantly, the presence of the IFN had no impact on tumour eradication, suggesting that CVA21 retained an ability to target malignant cells within the TME, despite the presence of IFN. Importantly, during the Phase II CALM study that investigated the efficacy of CVA21 to treat advanced melanoma, NanoString RNA analysis of 4 pre- and post-treatment samples demonstrated an induction of interferon-induced genes (Andtbacka et al., 2015). This result, coupled with the 38.6% durable response rate reported, suggests that CVA21 is effective despite the production of an antiviral IFN response.

Following the investigation of the IFN pathway's role in CVA21 infection, other factors that could influence infection, namely the mTORC1 pathway, were examined. Enhanced mTOR activity has been observed in NHL B cells (Schatz, 2011), (Kuo et al., 2011), and due to its regulation of cell growth, proliferation and metabolism, may contribute the survival and propagation of malignant cells (Rahmani et al., 2014).

Rapamycin, a macrolide compound derived from the *Streptomyces hygroscopicus* bacterium, blocks the formation of the mTORC1 complex by binding to the cytosolic protein, FKBP12 (FK506 binding protein 12), which then binds to the FKBP-rapamycin-binding (FRB) domain of mTOR and blocks its ability to function (Yang, H. et al., 2013). FKBP12 is not normally a component of mTORC1 but associates with the complex upon binding to rapamycin (Hausch et al., 2013). Rapamycin also inhibits mTORC2, but only at high doses and in certain tissue types (Schreiber et al., 2015). Importantly, rapamycin has been used in the clinic as a potent immunosuppressant for organ transplants, due to its ability to prevent B and T cell activation by inhibiting IL-2 production (Saunders et al., 2001).

Analysis of mTORC1 downstream targets, S6 and 4EBP1, allowed the selection of sub-toxic doses of rapamycin that inhibited mTOR activity. These doses completely blocked p-S6 signalling by 24hrs and significantly hampered CVA21 cytotoxicity in Ramos, SU-DHL-4 and U2932 cell lines, but not Raji cells. This result has yet to be explained but could be investigated further by testing Raji cells for downstream redundancies in this pathway, FKBP12 levels, or components of the rapamycin binding domain in the complex. It is interesting to note that, as well as having no effect on Raji cell susceptibility to CVA21, rapamycin did not affect the proliferation of Raji cells. This finding is congruous with work by Gu, *et al.*, that demonstrated the resistance of Raji cells to rapamycin (Gu, L. et al., 2015).

MTOR blockade by rapamycin coincided with diminished CVA21-induced cell death in Ramos, SU-DHL-4 and U2932 cell lines, suggesting a possible role for mTOR activity in CVA21 replication. A literature search of pathways that contribute to the replication of viruses similar to CVA21 suggested a role for mTOR in the replication of CVB3 (Chen et al., 2014). However, contrary to the observations in this chapter, this research showed that mTOR blockade by rapamycin promoted CVB3 replication in HeLa cells. The reason(s) for this remain unknown but may be due to differences in mTOR utilisation between different types of Coxsackievirus, or differences in the cell types investigated. Similar to the effects of rapamycin on CVB3 replication, research by Beretta, *et al.*, defined a role for rapamycin in enhancing the translation of viral proteins from two alternative picornaviruses, Polio and Encephalomyocarditis Virus, while blocking the translation of host proteins, in NIH 3T3 cells (Beretta et al., 1996). This effect may suggest a potential role for mTOR inhibition in enhancing viral replication in epithelial cells, but not NHL cells. This data showed inhibition of p-4EBP1 and cap-dependent translation of host proteins, following 5hrs of rapamycin treatment, while cap-independent translation of viral proteins was not inhibited. The fact that p-4EBP1 was not inhibited by rapamycin in the NHL cell lines may explain why enhanced CVA21-induced cell death was not observed in rapamycin-treated NHL cells. Rapamycin only inhibits p-4EBP1 during the first 1-3hrs of treatment (Choo et al., 2008), suggesting that p-4EBP1 returned to its phosphorylated state shortly after CVA21 treatment.

The fact that diminished CVA21-induced cell death was observed in NHL cells that responded to rapamycin with inhibited S6 phosphorylation, while neither S6 phosphorylation nor CVA21 cytotoxicity were impacted in Raji cells, strongly implicates a role for the S6-dependent side of mTORC1 activity in the susceptibility of NHL cells to CVA21. Taken together, these data suggest a

potential link between mTORC1 activity and CVA21 susceptibility. This could be examined further by assembling a panel of rapamycin-resistant cell lines, similar to Rajis, and examining whether they remain susceptible to CVA21-induced cell death after rapamycin treatment. Alternative methods of mTORC1 blockade, such as genetic or pharmacological inhibition of specific downstream effectors of mTORC1, could also be used to further elucidate the role of the mTORC1 pathway in CVA21-induced cell death and not one that is due to rapamycin.

As previously discussed, rapamycin can slow the proliferation of cells due to its impact on translation by blocking mTOR activity (Bundscherer et al., 2008). The reliance of many viruses on highly-proliferative cells made it important to investigate cell proliferation and cell cycle to ensure that rapamycin was not inhibiting CVA21 cytotoxicity solely by blocking NHL proliferation. Rapamycin induced a statistically significant slowing of proliferation after 72hrs in Ramos, SU-DHL-4 and U2932 cells, but this was minimal and thus, unlikely to be the main contributory factor for the reduced toxicity of CVA21 in these cell lines. No change in proliferation was observed in NHL cell lines at 48hrs, which, coupled with inhibition of CVA21-induced cell death at this time point, indicates an ability of rapamycin to diminish CVA21 cytotoxicity irrespective of the drug's anti-proliferative effect. The effects of mTOR inhibition on the proliferation of feline fibroblastic cells were also examined by Mortola, *et al*., who demonstrated a role for Tacrolimus, a rapamycin-analogue, in inhibiting Feline Immunodeficiency Virus (FIV) replication. This inhibition was observed alongside a decrease in cell proliferation after 3 days (Mortola et al., 1998); the exact role of Tacrolimus' antiproliferative effect on FIV replication was not elucidated, but was acknowledged as a potential factor.

It is difficult to correlate mTOR activation with CVA21 susceptibility in other tumour models. However, similar to published research on NHL, mTOR signalling is enhanced in a subset of multiple myeloma patients (Guglielmelli et al., 2015), and CVA21 displays toxicity against multiple myeloma cells (Au et al., 2007). These findings suggest a possible link, in B cell malignancies at least, between enhanced mTOR activity and CVA21 susceptibility.

Contrary to the findings in this chapter that show reduced CVA21 cytotoxicity in rapamycin-treated NHL cells, rapamycin is being investigated in combination with OV in several tumour models, and has demonstrated synergy with several OV, such as myxoma virus against glioblastoma multiforme (GBM) stem cells (Zemp et al., 2013). Rapamycin also enhanced tumour cell death and survival when used in combination with myxoma virus in an *in vivo* model of glioma (Lun

et al., 2010). Similarly, both everolimus (a rapamycin derivative) and rapamycin enhanced adenovirus targeting of, and replication in, a colon cancer model (Homicsko et al., 2005) and murine prostate cancer model (Jiang et al., 2013), respectively; these effects were attributed to a diminished antiviral response following mTOR inhibition. Research by Comin, et al., demonstrated the importance of the sequence in which rapamycin and OV is administered. In this research, a synergistic effect was observed when reovirus and then rapamycin were administered to a C57/BL6 murine melanoma model, however, pre-treatment of cells *in vitro* with rapamycin and then reovirus resulted in impaired virus replication and apoptosis (Comins, Charles et al., 2018). This research highlights the importance of the sequential administration of treatments in cancer research. It is important to acknowledge that a direct comparison between the cell line studies in this chapter and these *in vivo* results is not possible, due to the multifaceted representation of the tumour that *in vivo* models provided versus isolated cell line cultures. Since the precise role of the antiviral response in CVA21 targeting of NHL cells will be the focus of future research in the laboratory, the role of mTOR activity in this response must also be investigated. To date, no literature has reported efficacy of a combination of rapamycin and OVs to treat HMs, but inhibition of the antiviral response by rapamycin, as demonstrated in the prostate and colon cancer models, could play a role. The beneficial effect of an OV/rapamycin combination in these solid malignancies differs from the observed rapamycin-induced inhibition of CVA21 replication in NHL cell lines. This difference could reflect the different roles of mTOR for different OV, or differences between solid tumours and HMs.

Overall, the work presented in this chapter has demonstrated that CVA21 oncolysis is not inhibited by antiviral type I IFN signalling, and data suggests that CVA21 may interfere with the antiviral response pathways to enable replication. Moreover, a role for mTOR signalling in some NHL cell lines has been proved. Both factors, as well as a role for ICAM-1 expression, are important for CVA21 infection, but may not be the only relevant factors for CVA21 susceptibility. This data expands what is known about CVA21's activity in NHL cells and suggests that CVA21 may be efficacious in other cancer models that have high mTOR activity. This will develop CVA21's applicability to other cancer models, allowing researchers to target cancers that may be more responsive to CVA21 treatment.

Chapter 6:

Investigating the potential of OV to induce an anti-NHL immune response.

Chapter 6

6.1 Introduction

The aim of the research discussed in this chapter was to investigate the ability of both reovirus and CVA21 to potentiate an NK cell-mediated anti-NHL immune response, whereby OV stimulate NK cells to kill NHL cells, and whether this could be enhanced by mAbs. This alternate mechanism of killing by OV would complement direct lytic killing or replace it if the cells were resistant to oncolysis. Several clinical trials have examined the efficacy of OV in combination with immune checkpoint mAb therapy, such as reovirus and the αPD-1 antibody, pembrolizumab, to treat advanced or metastatic pancreatic adenocarcinoma (ClinicalTrials.gov, 2015b), and CVA21 and pembrolizumab to treat advanced melanoma (ClinicalTrials.gov, 2015a). Reovirus, a poor lytic agent against NHL cell lines, was included in these investigations due to its established immunogenicity (Prestwich, Robin J. et al., 2009). To date, OVs in combination with mAbs are the subject of multiple clinical trials for cancers, such as vaccinia virus and the αPD-L1 antibody, durvalumab, against colorectal carcinoma (ClinicalTrials.gov, 2017a), CVA21 and the αCTLA-4 mAb, ipilimumab, against melanoma (ClinicalTrials.gov, 2014), and vaccinia virus and the αPD-1 mAb, REGN2810 against renal cell carcinoma (ClinicalTrials.gov, 2017b). Research has shown that a combination of OV and mAbs can enhance NK cell targeting of malignant cells *in vitro*, such as combined reovirus and rituximab to kill CLL cells (Parrish et al., 2015) and combined reovirus and cetuximab against colorectal cancer (Zhao, X. et al., 2015).

The ability of CVA21 and reovirus to promote the elimination of NHL cells by NK cells was examined in this chapter. Specifically, this work looked at NK cell activation by CD69 expression, a member of the C-type lectin superfamily that is absent on resting NK cells and rapidly upregulated upon viral infection (Fogel et al., 2013) and is the earliest expressed marker on activated immune cells (Ziegler et al., 1994), as well as the ability of NK cells to degranulate against NHL cell line targets.

Due to the established role for mAbs in NK cell-mediated degranulation, and the enhanced effect when used in combination with OV, reovirus and CVA21 were combined with the αCD20 mAb, BHH2 (the laboratory-grade version of

GA101/obinutuzumab) against NHL. BHH2's effect was examined on NHL cell lines with the highest CD20 expression; Ramos, SU-DHL-4 and U2932. Moreover, as stimulation by CD40L induces drug resistance in some NHL cell lines (Section 4.2.5), potentially making current chemotherapy less effective, CD40L-stimulated NHL cells were also examined for their susceptibility to NK cell-mediated killing. Investigating the combination between OVs and an αCD20 mAb was chosen due to the previously-mentioned impressive performance of Rituximab in the treatment of NHL, the presence of the CD20 target on NHL B cells and the ability of combined rituximab and reovirus to induce enhanced NK cell targeting of CLL B cells (Parrish 2015). NK cells are significant effectors in targeting NHL cells in patients (Sarkar et al., 2017), making them appropriate effector cells to investigate. It is important to note that other signalling molecules, on both NHL cell lines and NK cells, provide activatory and inhibitory signals to NK cells, the balance of which will determine whether the NK cells target the NHL cells for cell death. With this in mind, the expression of some NK ligands was also investigated on NHL cell lines.

6.2 Results

6.2.1 OV-induced NK-mediated ADCC against NHL cells

Figure 6-1 shows CD69 expression on untreated and OV-treated NK cells after 48hrs. These data show a significant increase in CD69 expression on NK cells by both CVA21 and reovirus, demonstrating the strong immunostimulatory potential of both viruses.

To further explore the effects of CVA21 and reovirus on NK cells, and to examine whether they recognise malignant cells, untreated and OV-treated PBMCs were co-cultured with NHL cells for 4hrs. Whole PBMCs were used instead of isolated NK cells as new research has shown that CVA21-induced NK cell activation and degranulation against AML targets is dependent on IFN-α production by pDCs in the peripheral blood (Louise Muller – manuscript submitted). **Figure 6-2** shows that NK cell degranulation is significantly enhanced against Ramos (light grey), SU-DHL-4 (dark grey) and U2932 (black) cell lines when treated with reovirus. Similarly, CVA21-treated PBMCs demonstrated increased NK cell degranulation against all cell lines, however, this was not significantly higher than untreated NK cells upon co-culture with Ramos cells. CVA21 was consistently, but not significantly, less effective than reovirus at simulating degranulation of NK cells against NHL cell targets. PBMCs were also treated with either OV and cultured with no NHL targets (white). This showed a small, insignificant, increase in spontaneous degranulation in the absence of targets. The ability of both OVs to activate NK cell degranulation against NHL cell lines demonstrated their immunogenic potential against NHL, warranting further investigation in combination with the αCD20 antibody, BHH2.

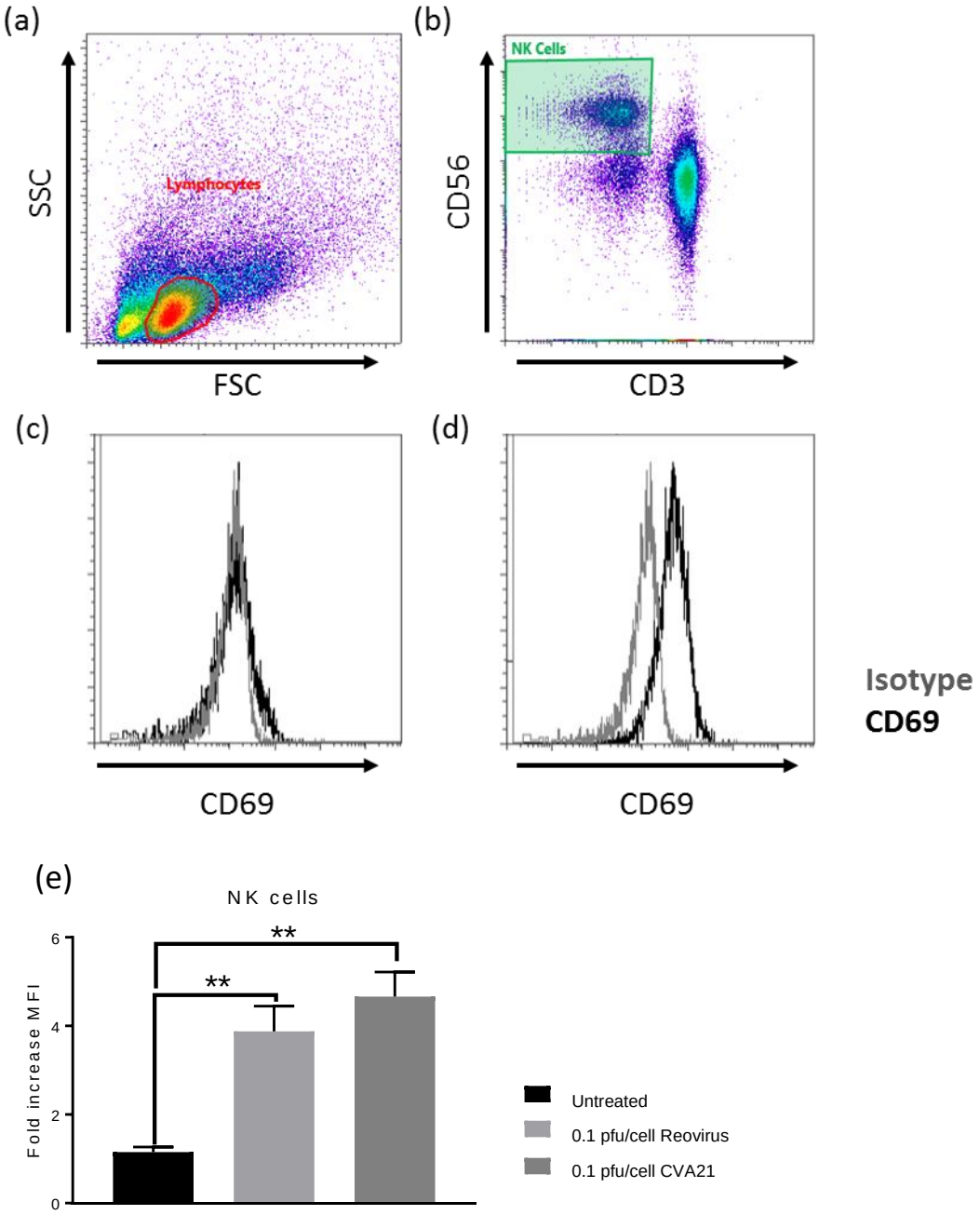

Figure 6-1 OV-induced activation of immune effector cells.

PBMCs were isolated from healthy donor blood and cultured with reovirus or CVA21 for 48hrs. PBMCs were then harvested and stained with αCD3 and αCD56 antibodies, to identify NK cell populations ($CD3^{-}CD56^{+}$), and CD69 to measure phenotypic activation. Gating strategy identifying lymphocytes by FSC/SSC (a) and NK cells within this population as $CD3^{-}CD56^{+}$ (b). (c) and (d) show overlaid histogram plots of CD69 expression (black) with isotype antibody controls (grey) on untreated and reovirus-treated samples, respectively. In (e), fold increases in CD69 MFI above dose-matched isotype controls is plotted for $CD3^{-}CD56^{+}$ NK cells. Data shows mean of n=4 PBMC donors + SEM. Significance was determined by One-way ANOVA.

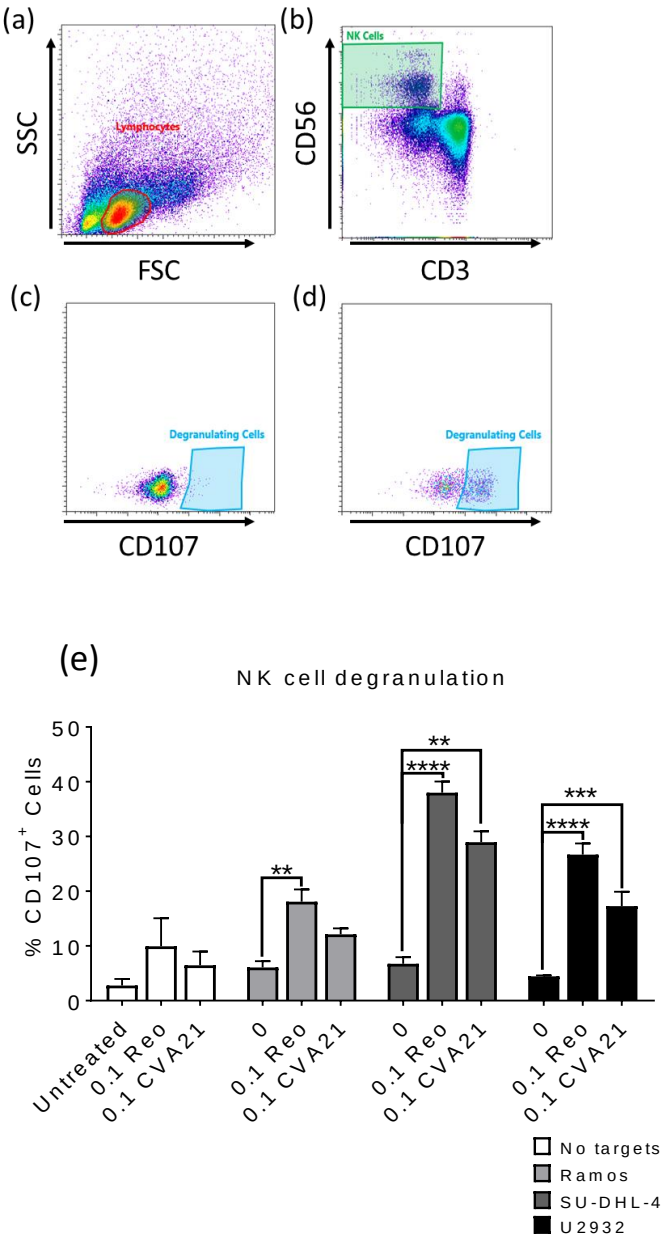

Figure 6-2 OV-induced NK cell degranulation against NHL cell lines.

Healthy donor PBMCs were cultured with reovirus or CVA21 for 48hrs before being used in a degranulation assay either alone or against NHL cell lines at a 10:1 effector: target ratio. After 1hr the co-cultures were supplemented with αCD3 and αCD56 antibodies, to identify NK cells, αCD107a/b antibodies, to identify degranulating cells, and Brefeldin A to prevent internalisation of CD107a/b, and cultured for a further 4hrs. (a) and (b) show NK cell detection. (c) and (d) show detection of degranulating ($CD107^+$) NK cells from untreated and reovirus-treated samples, respectively. NK cell degranulation was determined as $\%CD107^+$ NK cells and quantified in (e). PBMCs were cultured alone (white, spontaneous degranulation control), or co-cultured with Ramos (light grey), SU-DHL-4 (dark grey) or U2932 (black) cells. Data shows the mean of n=4 PBMC donors +SEM, significance was determined by two-way ANOVA.

6.2.2 Enhancing OV-mediated NK cell killing with an αCD20 mAb

Previous research demonstrated a possible application of combined OV and mAbs to treat cancers, such as reovirus and rituximab for enhanced ADCC against CLL (Parrish et al., 2015). The established efficacy of rituximab and more recent αCD20 mAbs in treating NHL provides ideal candidate mAbs for combination studies with OV.

NHL cell lines were screened for CD20 expression by flow cytometry in order to confirm CD20 expression. **Figure 6-3** shows that all NHL cell lines analysed expressed CD20 to varying degrees, with OCI-LY19s and OCI-LY3s expressing the lowest (2-fold increase in MFI over isotype controls) and second lowest levels (5-fold increase), respectively. Ramos and Raji expressed comparably medium levels (80- and 50-fold, respectively); while U2932's expression was 2-fold higher (~160-fold increase). In comparison, SU-DHL-4s had the highest level of CD20 expression, displaying a 700-fold increase in MFI over isotype control cells. Ramos, SU-DHL-4 and U2932 were selected as the candidate NHL targets for the combination studies as representative cell lines of BL, DLBCL-GCB and DLBCL-ABC, respectively.

PBMCs were treated with reovirus or CVA21, and NHL cell targets were opsonised with BHH2, the laboratory grade formulation of the αCD20 mAb, GA101, to examine the efficacy of combining these two treatment modalities. The cells were co-cultured at a 10:1 effector: target ratio and NK cell degranulation in the presence of NHL cell lines was analysed. The working hypothesis for this strategy is that BHH2-coating of NHL cells enhances their recognition by NK cells, and activating NK cells by pre-exposure to the OV makes them better equipped to eradicate NHL targets.

Figure 6-4 shows degranulation (CD107a and b surface expression) of NK cells following co-culture with NHL targets (a; Ramos, b; SU-DHL-4, c; U2932) without opsonisation (white), or with an isotype matched control antibody (light grey) or the BHH2 mAb (dark grey). **Figure 6-4** (a) shows NK cell degranulation against Ramos cell targets; a small increase in degranulation was observed against Ramos cells with no antibody (white) or the isotype (grey) when the PBMCs were treated with CVA21 or reovirus. By contrast, NK cell degranulation was significantly increased against BHH2-coated Ramos cells (dark grey) in the absence of virus treatment, and was significantly enhanced following OV treatment of PBMCs. **Figure 6-4** (b) demonstrates that both reovirus and CVA21 treatment of PBMCs significantly enhanced NK cell

degranulation against unlabelled (white) or isotype-labelled SU-DHL-4 targets (light grey), i.e. in the absence of BHH2. NK cell degranulation against BHH2-opsonised SU-DHL-4 cells was increased compared to unlabelled or isotype-labelled targets, demonstrating the ability of the BHH2 antibody to potentiate NK cell function; this degranulation was enhanced further by both reovirus and CVA21 treatment of PBMCs, however, this was not statistically significant. **Figure 6-4** (c) showed that reovirus, but not CVA21, treatment of PBMCs induced significant degranulation against unlabelled (white) and isotype-labelled (light grey) U2932 targets. However, NK cell degranulation was enhanced in the presence of BHH2-coated U2932 cells (in the absence of OV) and appeared to be further increased upon OV treatment. Disappointingly, the enhanced NK cell degranulation observed with OV treatment was not statistically significant. These data demonstrated that both OVs, CVA21 and reovirus, and the BHH2 antibody, can promote NK cell targeting of NHL targets. This effect can also be additive between viruses and mAb, as both OVs induced significantly higher degranulation against mAb-coated Ramos targets.

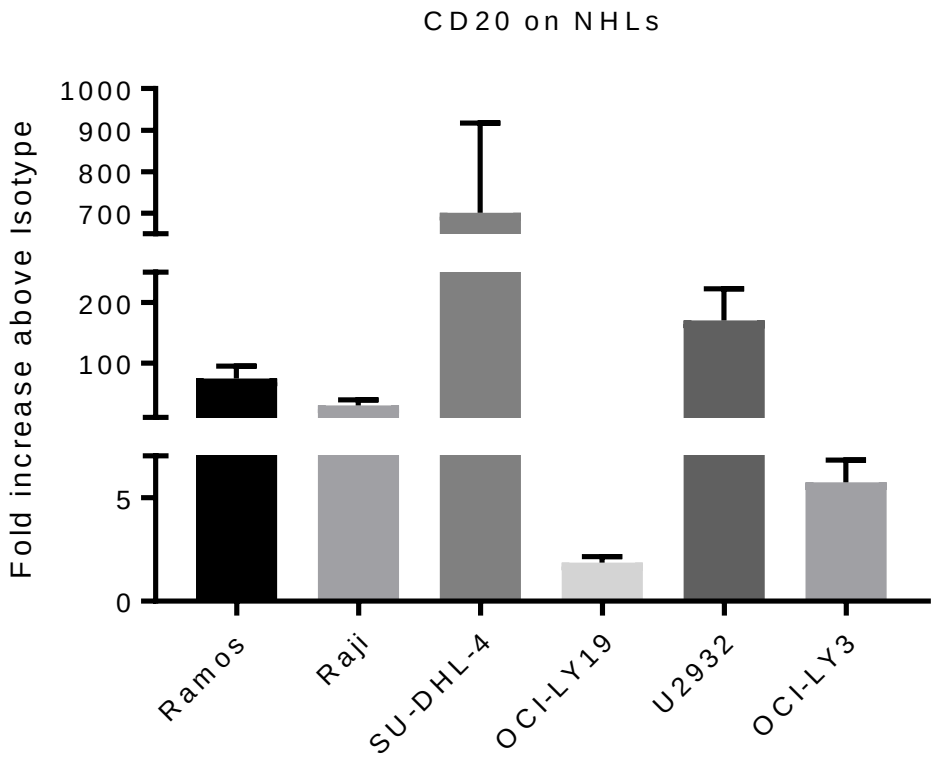

Figure 6-3 CD20 expression on NHL cell lines.

NHL cell lines Ramos, Raji, SU-DHL-4, OCI-LY19, U2932 and OCI-LY3 were stained for CD20 expression and analysed by flow cytometry. CD20 expression is displayed as the fold increase in MFI of αCD20 antibody-labelled cells over isotype control antibody-labelled cells. Results show means from n=4 independent experiments + SEM.

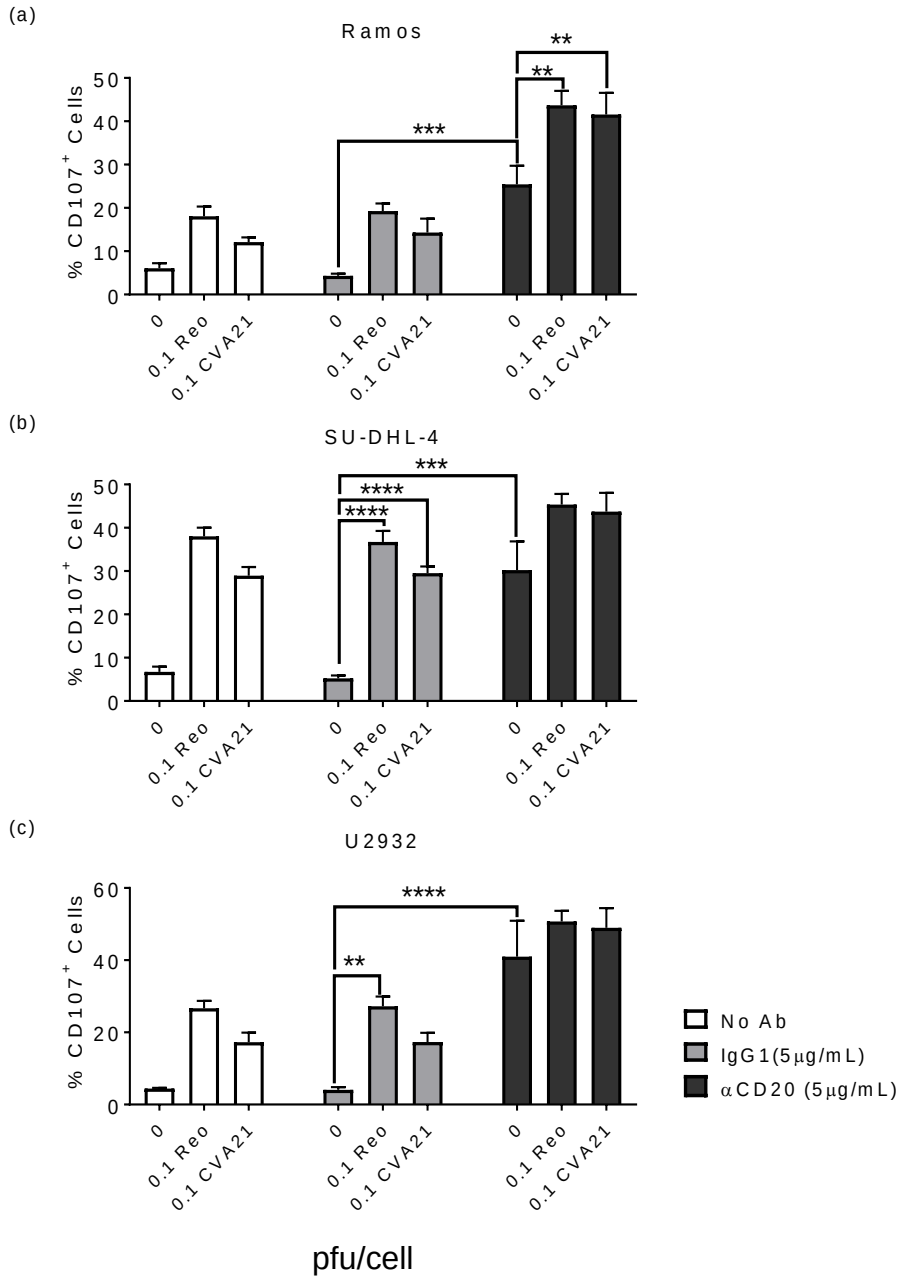

Figure 6-4 OV-mediated NK cell degranulation is enhanced by αCD20 antibodies in some NHL cell lines.

PBMCs were isolated from healthy donor blood and cultured with reovirus or CVA21 for 48hrs. NHL cell line targets Ramos (a), SU-DHL-4 (b) and U2932 (c) were untreated (white bars) or labelled with an isotype-matched control (light grey) or BHH2 (dark grey) at 5μg/mL for 30mins. PBMCs were co-cultured with cell line targets for 1hr at a 10:1 effector: target ratio. The co-cultures were then supplemented with a mix of αCD3 and αCD56 antibodies, to identify NK cells, αCD107a and b antibodies, to identify degranulating NK cells, and Brefeldin A to prevent re-internalisation of the CD107a and b and cultured for a further 4hrs. Degranulation was determined as %CD107$^+$ NK cells. Data shows the mean of n=4 PBMC donors +SEM, significance was determined by two-way ANOVA.

6.2.3 The effects of CD40L on an OV-induced anti-NHL NK cell response

Research in Chapter 4, section 4.2.5 demonstrated CD40L-dependent drug resistance in NHL cell lines, highlighting the need for alternate methods to eradicate these resistant cells. The ability of NK cells to recognise and kill target cells depends on the ratios of activatory and inhibitory NK ligands expressed. As described previously (Chapter 4, section 4.2.6), CD40L stimulation of NHL cell lines increased ICAM-1 expression. Previous research has demonstrated enhanced NK cell killing of AML targets due to increased ICAM-1 expression on the target surface (Parameswaran et al., 2016). Elevated ICAM-1 on NHL B cells in the LN could enhance NK cell: NHL interactions and potentiate NK cell killing. In addition, the interaction between a target cell and an NK cell involves signalling between multiple activatory and inhibitory ligands and their cognate receptors on the NK cell surface which determines the outcome of the target: NK cell interaction. Therefore, it was important to also investigate the effect of CD40L stimulation on the expression of NK cell activatory and inhibitory receptor ligands on NHL cell targets.

NHL cell lines were screened for several activatory NK ligands, such as ICAM-1, PVR (Poliovirus Receptor; CD155), Nectin-2 (CD112), MICA/B (MHC class I polypeptide-related sequence), ULBP-1 (UL16 binding protein 1), and ULBP-2/5/6, and inhibitory ligands, such as MHC-I. NK ligand expression profiling showed an absence of most NK ligands, with the exception of Nectin-2 (CD112, which has a role in cell adhesion and tight junctions, (Lopez et al., 1998) and MHC-I (which is involved with antigen presentation to $CD8^+$ cytotoxic T cells and recognition of self by NK cells, (Kratky et al., 2011). These ligands were taken forward for further investigation. In the context of NK cell killing, Nectin-2 on target cells interacts with DNAM-1 (DNAX Accessory Molecule-1) on the NK cell surface, triggering its cytotoxic activity (Bottino et al., 2003). MHC-I, on the other hand, inhibits NK killing by interacting with killer cell immunoglobulin-like receptors (KIRs) and C-type lectin-like receptors, such as Ly49 (Sawicki et al., 2001). Diminished MHC-I expression due to, for example, viral infection, can eliminate this inhibitory effect, thereby making virally-infected cells more susceptible to NK cell killing (Brandstadter and Yang, 2011).

Figure 6-5 shows that NHL cell lines Ramos (a), Raji (b), SU-DHL-4 (c), OCI-LY19 (d), U2932 (e) and OCI-LY3 (f) express low levels of the activatory NK ligand, Nectin-2. Upon CD40L stimulation, there was no significant change in Nectin-2 expression on any NHL cell line. Although there were small changes in

expression on Ramos and Raji cells, these effects were not significant. Co-culturing the NHL cell lines on the parental L929 feeder layer had no effect on Nectin-2 expression.

Figure 6-6 illustrates MHC-I expression on NHL cell lines; all cell lines expressed basal MHC-I in the Alone treatment (blue). Upon CD40L stimulation, MHC-I was significantly increased in Ramos and SU-DHL-4 cell lines and the expression trended towards an increase in all cell lines. MHC-I expression was not affected by co-culturing the NHL cell lines on the parental L929 feeder layer. The enhanced MHC-I expression on the Ramos and SU-DHL-4 cells could result in diminished NK cell recognition of these cells, due to the inhibitory effects of MHC-I.

Next, to examine the ability of the NK cells to target drug resistant CD40L-stimulated NHL cells, NK cells were co-cultured with unstimulated and CD40L-stimulated NHL cells. **Figure 6-7** shows a small increase in NK cell degranulation against CD40L-stimulated Ramos (a), SU-DHL-4 (b) or U2932 (c) cells, regardless of OV treatment. NK cell degranulation was enhanced when the PBMCs were treated with either OV, however, this preliminary experiment was only carried out in n=2 donors, therefore, statistical significance could not be determined. This pilot experiment suggests that CD40L stimulation, associated with changes in MHC-I (in Ramos and SU-DHL-4 cells, **Figure 6-6**) and ICAM-1 expression (in Ramos, SU-DHL-4, OCI-LY19 and U2932 cells, **Figure 4-11**), of NHL cell lines does not confer protection from NK cell-mediated death, despite inducing resistance to chemotherapy (Chapter 4, section 4.2.5). These findings suggest that MHC-I expression may not be relevant for this degranulation and that other activatory or inhibitory ligands may be having an effect. These findings are being validated by ongoing laboratory studies.

Lastly, to investigate the effects of CD40L stimulation on CD20 expression and examine the potential impact of CD40L:CD40 interactions on αCD20 therapy, CD20 expression was also analysed on unstimulated and CD40L-stimulated NHL cells, as shown in **Figure 6-8**. These data show a decrease in CD20 expression on Ramos (a), Raji (b), SU-DHL-4 (c) and U2932 (e) cells, but not on OCI-LY19 (d) or OCI-LY3 (f) cells; however, these decreases were not statistically significant. Loss of CD20 expression on NHL cells by CD40L stimulation could result in diminished efficacy of αCD20 mAb therapy. This warrants further investigations which are beyond the scope of this work.

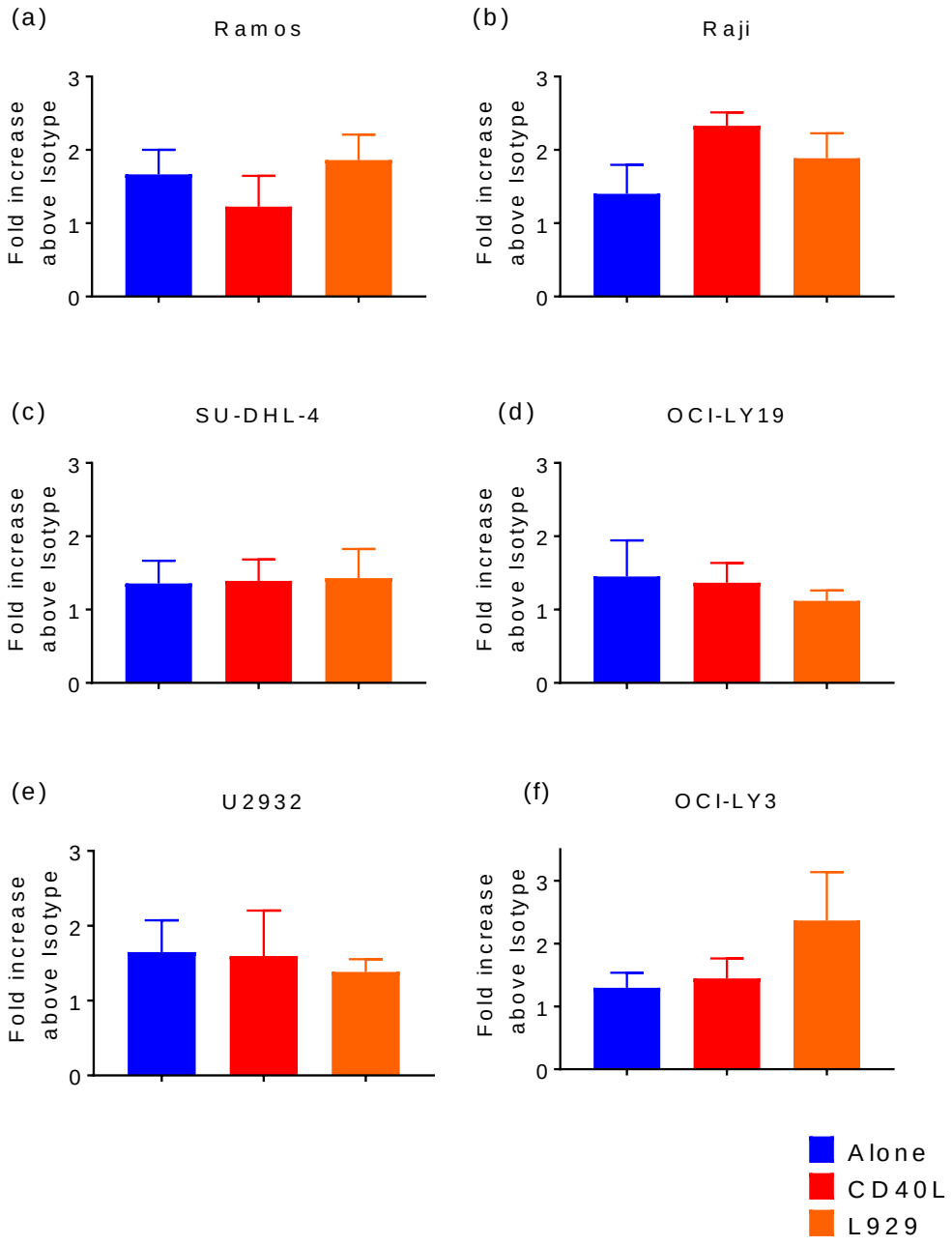

Figure 6-5 Effect of CD40L stimulation on Nectin-2 expression.

NHL cell lines were cultured alone (blue) with CD40L^{+} (red) or parental (orange) L929 feeder layers for 24hrs. NHL cells were then stained for Nectin-2 expression and analysed by flow cytometry. Expression is displayed as the fold increase in MFI of αNectin-2 antibody-labelled cells over isotype control antibody-labelled cells. Data shows mean fold increase from n=4 independent experiments + SEM. Statistical significance was determined using a One-way ANOVA, no significant differences were observed.

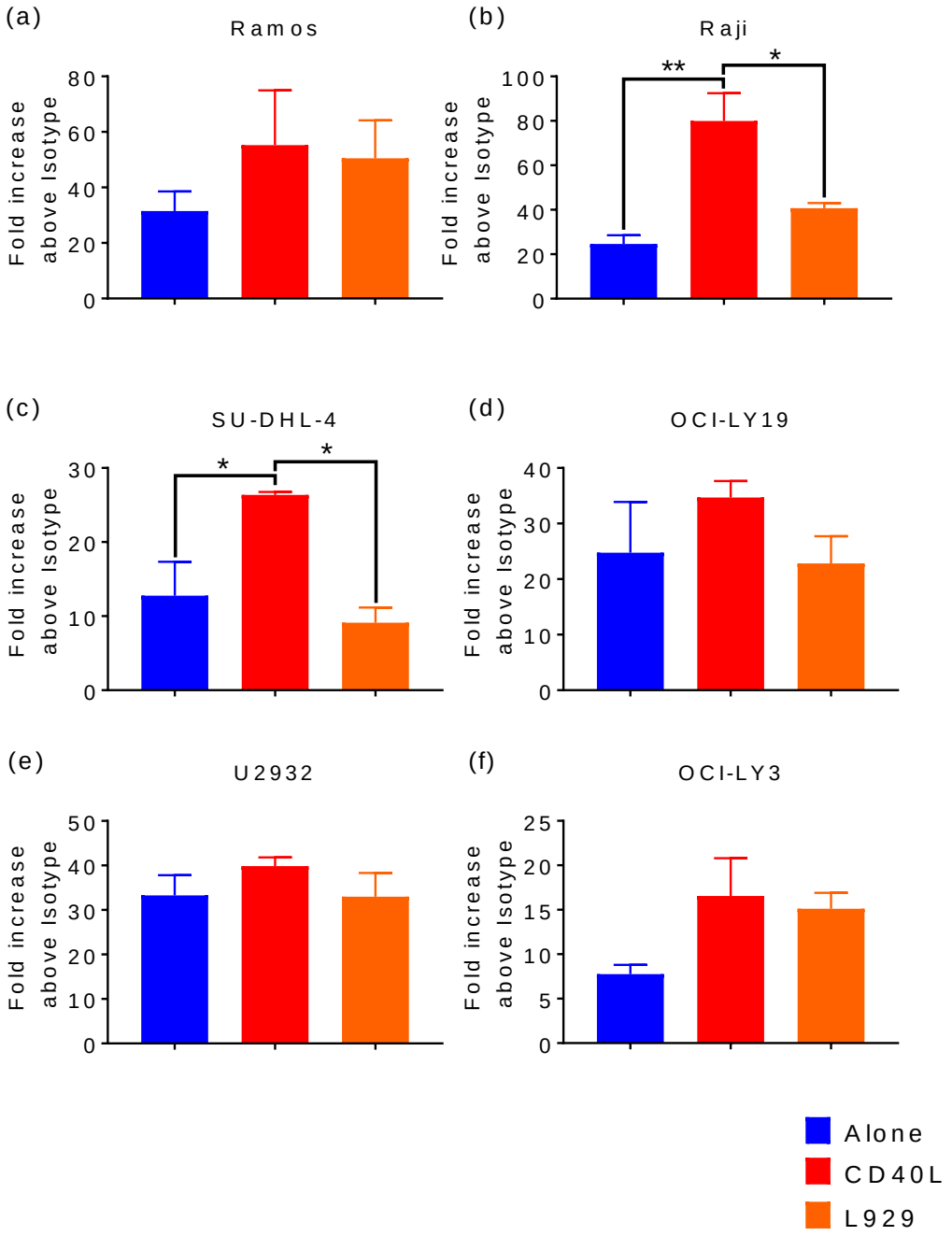

Figure 6-6 Effect of CD40L stimulation on MHC-I expression.

NHL cell lines were cultured alone (blue) or on the CD40L^{+} (red) or parental (orange) L929 feeder layers for 24hrs. NHL cells were stained for MHC-I expression and analysed by flow cytometry. Relative expression is displayed as the fold increase in MFI of αMHC-I antibody-labelled cells over isotype control antibody-labelled cells. Data shows mean fold increase from n=4 independent experiments +SEM. Statistical significance was determined using a One-way ANOVA.

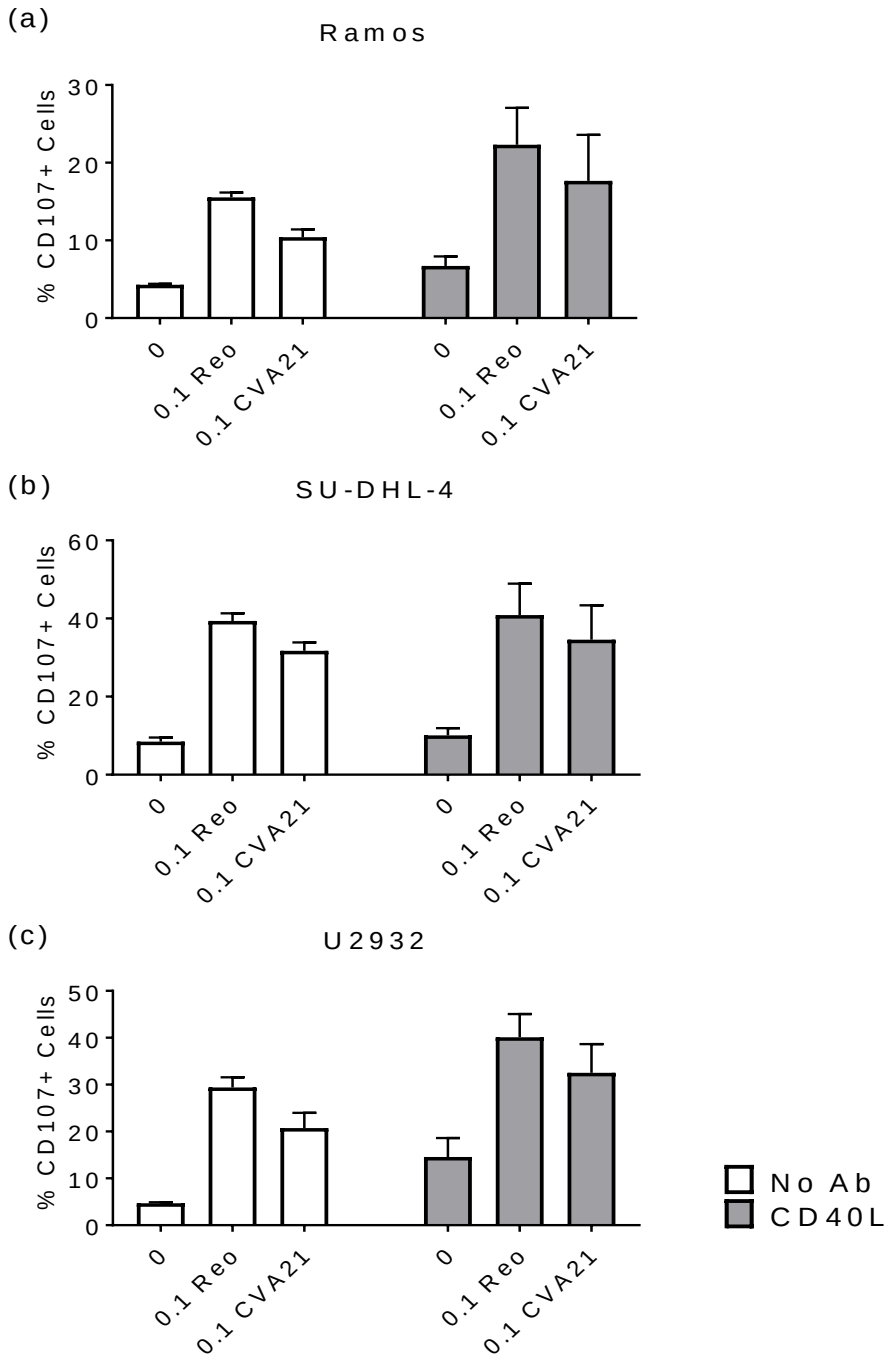

Figure 6-7 NK cells degranulate against CD40L-stimulated NHLs.

Healthy donor PBMCs were cultured with reovirus or CVA21 for 48hrs. NHL cell lines were cultured alone (white) or on $CD40L^+$ (grey) L929 feeder layers for 24hrs. Virally-activated PBMCs were then co-cultured with the targets (10:1 ratio) for 1hr before supplementation with αCD3 and αCD56, to identify NK cells, αCD107a and b antibodies, to identify degranulating cells, and Brefeldin A to prevent re-internalisation of the CD107a and b and cultured for a further 4hrs. Degranulation was determined as $\%CD107^+$ NK cells. Data shows the mean of n=2 independent experiments +SEM.

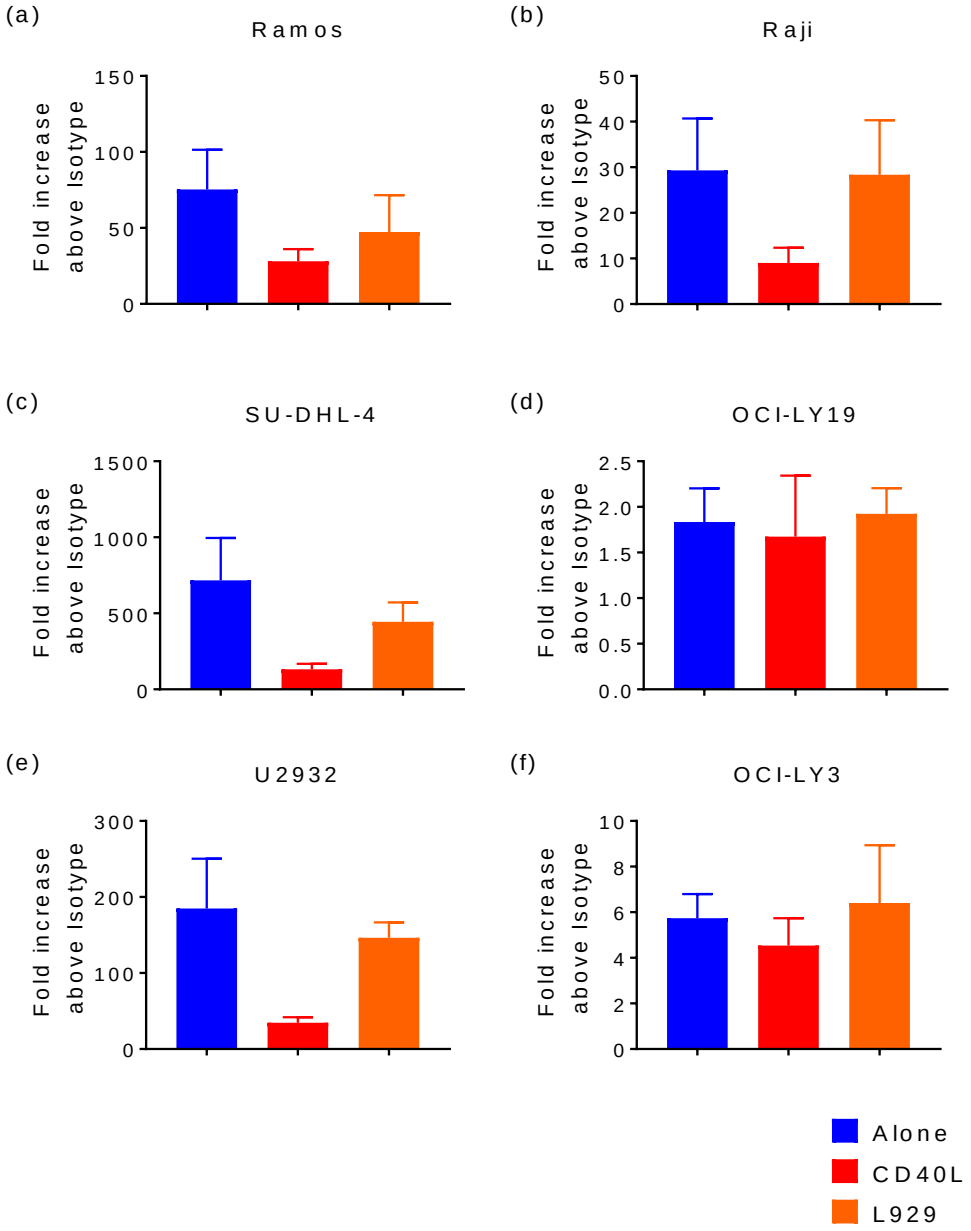

Figure 6-8 Effect of CD40L stimulation on CD20 expression.

NHL cell lines were cultured alone (Blue) with CD40L^{+} (red) or parental (orange) L929 feeder layers for 24hrs. NHL cells were stained for CD20 expression and analysed by flow cytometry. Expression was measured as fold increase above isotype staining. Data shows mean fold increase for n=4 independent experiments + SEM. Analysed by One-way ANOVA, no significant differences were detected.

6.3 Discussion

The work in this chapter examined the role of OVs, CVA21 and reovirus, in activating healthy donor NK cells and stimulating them to attack NHL cell line targets. This anti-NHL effect was also examined in combination with a candidate αCD20 mAb, BHH-2, a glycoengineered mAb that has undergone post-translational modification to remove a fucose molecule from its Fc region, giving it a higher affinity for FcγRIII (CD16) on NK cells (Kern et al., 2013). Reovirus and CVA21 both activated NK cells, as measured by CD69 expression, by 48hrs (**Figure 6-1**). This result suggested a promising role for both OVs in stimulating NK cells to attack NHL targets. Previous research by Hall, *et al.*, demonstrated similar upregulation of CD69 on healthy donor NK cells after reovirus treatment (Hall et al., 2012). To date, there is no published data showing CVA21-induced upregulation of CD69 on human healthy donor NK cells, however, research by Godeny, *et al.* (Godeny and Gauntt, 1987), and Yuan, *et al.* (Yuan et al., 2009), has shown enhanced NK cell activity, as measured by IFN-γ secretion, in CVB3-treated murine myocarditis models. This would suggest that CVA21 may be able to activate NK cells *in vivo*.

CD107 degranulation assays showed that both OVs induced significant NK cell degranulation against most NHL cell line targets (the only exception being for CVA21-activated NK cells against Ramos targets), proving the potential for these OV in stimulating an anti-NHL immune response. IFN secretion can be partially or wholly responsible for CD69 upregulation on cells such as NK cells (Benlahrech et al., 2009), neutrophils (Atzeni et al., 2002), eosinophils (Ochiai, K. et al., 2000), and T cells (Sun et al., 1998). Data in Chapter 5 (section 5.2.1) demonstrated enhanced IFN secretion in CVA21-treated PBMC samples and previous research has shown that reovirus can induce IFN secretion in healthy donor PBMCs and activation of NK cells (Parrish et al., 2015). Research by Ho, *et al.*, however, has shown that NHL PBMCs have a diminished ability to produce IFN in response to antigenic stimulation *in vitro* (Ho et al., 1988), potentially hampering OV-induced NK cell activation in NHL patients, compared with those observed in the healthy donor samples used in this study.

Interestingly, given its ability to activate NK cells and induce higher levels of degranulation than CVA21, reovirus has proven itself a worthy candidate for further research as an immunotherapy for NHL. This data, coupled with the low cytotoxicity described in Chapter 4, outlines a role for reovirus as an immunotherapeutic, rather than a lytic, agent. Heat-inactivated replication-incompetent reovirus has previously demonstrated $CD8^+$ T cell-mediated killing

in a murine B16ova melanoma model (Prestwich, Robin J. et al., 2009), highlighting the role of the immune response when considering candidate OV, even in the absence of oncolysis.

In order to expand upon the full potential of reovirus and CVA21 to target NHL, the role of T cells in an OV-mediated anti-NHL response could be investigated, as T cells, unlike NK cells, have the capacity to develop long-lasting memory responses (Aurelian, 2016), resulting in a lifelong immunity that could target relapsed NHL many years later, assuming the relapsed tumour maintains the expression of specific TAAs.

BHH2 was chosen as a candidate αCD20 mAb due to its promising performance in other research and the superiority of GA101 (its parent form) over rituximab, in driving an NK cell-mediated response (Kern et al., 2013). CD20 was highly expressed on SU-DHL-4, U2932 and Ramos cells, with CD20 expression on SU-DHL-4s being significantly higher than all other cell lines tested. The relatively low expression on Ramos cells may explain why OV-activated NK cells degranulated significantly more against BHH-2-coated Ramos cells than uncoated, but not for the other two cell lines. Degranulation of NK cells following BHH2 is due to FCR engagement, consequently, more BHH2 binding is likely to stimulate more NK cell degranulation in the absence of virus. Therefore, if Ramos cells had been coated with sub-optimal BHH2 levels, the added effect of OV-activation of NK cells may have been more apparent, i.e. the degranulation of the NK cells may be maximised by the αCD20 antibody preventing further activation by the OV. To test this, lower doses of BHH2 could be used, or the experiments could be repeated on cell lines with lower CD20 expression such as the Raji, OCI-LY19 and OCI-Y3 cells. The BHH2 dose of 5µg/mL was selected from a pilot experiment that used 5 and 10µg/mL, as this was comparable with rituximab doses reported in previously published work (Parrish et al., 2015). Cetuximab, an anti-epidermal growth factor receptor (αEGFr) mAb, was also used as a negative control for BHH2's effects in n=2 PBMC donors, as EGF was not expressed on the B cell lines and the mAb is humanised (Galizia et al., 2007), making it a better control than the isotype-matched IgG1 isotype. NK cell degranulation against cetuximab-coated cells was similar to non-humanised isotype-matched controls (data not shown). Unfortunately, due to time constraints, it was not possible to investigate the ability of the virus-stimulated NK cells to kill NHL targets using Chromium release assays. This information would serve to validate the observed increases in NK cell degranulation against NHL targets and provided detailed information

on whether NHL cell lines are susceptible to NK cell degranulation-mediated killing.

One potential issue with using αCD20 mAbs in patients is the elimination of $CD20^+$ malignant cells, driving the propagation of a $CD20^-$ clone, (Alvaro-Naranjo et al., 2003). The possibility of such clonal selection remains a good reason to use combination regimens to target the emergence of resistant cells. It would be interesting to examine the ability of both OV to induce an NK cell-mediated response against resistant cells, such as OCI-LY19, which are resistant to both CVA21 and reovirus infection/oncolysis. This would prove a role for OV in eradicating drug/virus-resistant cell populations via activation of immune effector cells, such as NK cells.

Given the ability of reovirus to also activate monocytes, as determined by IFN-α secretion in reovirus-treated isolated monocytes (Parrish et al., 2015), it would be interesting to explore the ability of OV to enhance ADCP, in the presence or absence of αCD20 antibodies. This was investigated briefly by stimulating healthy donor monocytes with either virus and measuring their ability to phagocytose FITC-labelled dextran molecules, however, no phagocytosis was detected (data not shown). Previous research has demonstrated ADCP of rituximab-coated CLL cell line targets (Borge et al., 2015) highlighting a potential role for combining OV with αCD20 mAbs to promote ADCP.

Previous research has demonstrated the ability of NK cells to target drug-resistant cancer cells, such as doxorubicin-resistant breast cancer cells (Hwang, M.H. et al., 2015). CD40L stimulation of NHL cell lines did not diminish NK degranulation against the targets. Moreover, it is possible that degranulation was enhanced slightly, suggesting a more pronounced role for NK cells in eradicating drug-resistant cells which warrants further validation. Of note, elevated MHC-I on CD40L-stimulated NHL cell lines would be expected to inhibit NK cell activity, however, it is possible that increased ICAM-1 expression (or changes in NK ligands not investigated), and sustained NHL: NK cell interactions, may overcome the inhibitory effects of enhanced MHC-1 expression.

The use of mAbs to promote NK cell killing of NK-“escaping” CLL cells has been validated in other studies (Veuillen et al., 2012). However, the downregulation of CD20 upon CD40L stimulation, although not significant in these assays, has previously been described (Jennifer et al., 2003), and may limit the effectiveness of aCD20 Abs in this setting. This may result in less binding of αCD20 mAbs that potentiated immune-mediated killing of these cells, thus

validating a role for combinations with OV therapy, as OV may enhance the efficacy of NK cell killing in cells with lower CD20 expression. The examination of NK ligand expression on NHL cell lines, with or without CD40L-stimulation, was needed to demonstrate whether these drug-resistant cells would remain as targets for an NK cell-mediated response. The relatively low levels of Nectin-2, and high levels of MHC-I, observed did not prevent them from stimulating NK cell degranulation.

Future work should also investigate the role of OV infection in manipulating NHL susceptibility to NK-mediated killing. For example, NHL cells could be treated with OV for a short time to allow infection and assayed for susceptibility to NK cells to determine whether OV infection enhances NK cell recognition and killing. On infection, viruses such as CVA21, can downregulate MHC-I, the lack of which has been associated with higher NK-mediated killing (Ljunggren and Karre, 1990). It would also be interesting to explore the generation of an immune response against primary patient NHL targets, and whether OV-resistant cell lines such as OCI-LY19 could be targeted by NK-mediated killing although this was beyond the scope of this work.

The results highlighted in this chapter demonstrate a strong rationale for the application of OVs, reovirus and CVA21, and αCD20 mAb, BHH2, as potent inducers of an anti-NHL NK cell response, both as single agent therapies and in combination. Both strategies contributed to NK cell targeting of NHL cell lines by opsonising NHL cells for NK cell killing, in the case of BHH2, and activating the NK cells, in the case of the OVs.

Chapter 7:

Assessing the efficacy of Oncolytic Viruses against Primary NHL B cells

Chapter 7

7.1 Introduction

Cell lines are a vital tool for *in vitro* research, but the availability of primary patient samples provides a better model of the cancer due to the presence of primary cancer cells, tumour fibroblasts and tumour-associated immune cells, and the fact that primary cells lack many of the mutations that cell lines can accumulate after years in culture. Despite advances in attempts to mimic this complex cell mixture *in vitro*, primary samples offer a superior representation of how the tumour may respond to treatment, not just in terms of tumour cell death, but also the activity of tumour-residing immune cells. The findings described in previous chapters were thus applied to samples derived from potential NHL patients where LNs were excised from patients and analysed to detect malignant cells.

Cell line data showed efficacy for CVA21, but not for reovirus, in targeting NHL cell lines by direct oncolysis (Chapter 4, sections 4.2.2 and 4.2.3). Primary LN samples were treated with CVA21 and reovirus to measure the efficacy of both viruses in targeting malignant B cells. Further experimentation examined the ability of CVA21 to replicate in NHL samples to determine the possibility of producing progeny virions to perpetuate oncolysis. IFN-α production in response to CVA21 was also examined to elucidate the ability of primary LN samples to mount an antiviral IFN response against CVA21, given the diminished IFN production by NHL cell lines (Chapter 5, section 5.2.1) and lymphocytes derived from NHL patients (Ho et al., 1992).

Lastly, considering the immune cell populations that reside in the LN, NHL patient samples were analysed for the presence of NK cells, and the ability of reovirus to activate those NK cells and promote an NK-mediated anti-NHL immune response. Data previously described demonstrates a role for both CVA21 and reovirus in the induction of an NK cell-mediated anti-NHL immune response (Chapter 6, section 6.2.1). This data was highly promising and showed that both viruses can enhance targeting of NHL cell lines by healthy donor peripheral blood NK cells.

7.2 Results

7.2.1 Assessing the ability of reovirus to eradicate primary patient NHL cells

Reovirus demonstrated poor cytotoxicity against NHL cell lines in isolation (Chapter 4, Section 4.2.2), however, data shown in this section set out to confirm these observations in primary samples. It is important to note that, while NHL cell lines were cultured at $3x10^5$/mL in 0.5mL per well, primary mixed LNMC samples were cultured at $2x10^6$/mL in 0.5mL per well, highlighting an important difference between isolated cell lines and primary malignant B cells in the context of mixed LNMCs. To assess the suitability of reovirus in targeting LN B cells, the expression of JAM-A on the surface of primary patient LN B cells was determined. **Figure 7-1** shows the expression of JAM-A on primary patient LN B cells from 8 samples; 2 Follicular Lymphoma (FL), 1 Anaplastic Large T Cell Lymphoma (ALTCL), 1 reactive (potentially caused by an immune reaction to an infection in the LN, resulting in B cell expansion, LN swelling and a subsequent biopsy to investigate whether malignant cells were present), 1 Marginal Zone Lymphoma (MZL) and 3 classical Hodgkin's Lymphoma (cHL). It is important to note that, while this project was aimed at NHL, the diagnosis of the samples was unknown when samples were received and, as such, were not always from patients with NHL. JAM-A expression on patient LN B cells was above isotype controls in all samples; 6 samples expressed JAM-A between 4- and 10-fold increase over the isotype, while the ALTCL sample and one cHL sample expressed JAM-A at 23- and 15-fold increase over the isotype, respectively. As previously discussed (Chapter 2, section 2.4.2), reovirus relies on JAM-A to infect cells. This data illustrates a range of JAM-A expression on primary LN B cells and confirms that that JAM-A is present to facilitate viral entry. While reactive LN can present an interesting non-malignant control for NHL LN samples, reactive nodes are not normal LN and data derived from them in direct comparison with malignant cells should be interpreted with this in mind.

In order to test the efficacy of reovirus on primary LN cells, in the context of the multi-cellular microenvironment of the LN, LN samples were cultured with increasing doses of reovirus for up to 120hrs. 120hrs was chosen as this was the earliest time point by which significant cell death was observed in virus-treated cells in pilot studies. After 120hrs, the B cells were analysed by LIVE/DEAD™ exclusion. **Figure 7-2** demonstrates that reovirus was highly effective at inducing significant cell death in some LN samples, especially the FL and DLBCL+FL. By contrast, reovirus induced little cell death in either cHL

samples and was ineffective against the MZL sample and the reactive LN sample. These results were comparable with those discussed previously in demonstrating the selective efficacy of reovirus against primary NHL samples (Alain et al., 2002). However, the lack of direct or immune-mediated cytotoxicity in other samples should not prohibit reovirus' efficacy in patients, due to its demonstrated ability to promote anti-cancer immune responses in CLL (Parrish et al., 2015), AML (Hall et al., 2012) and melanoma (Errington et al., 2008).

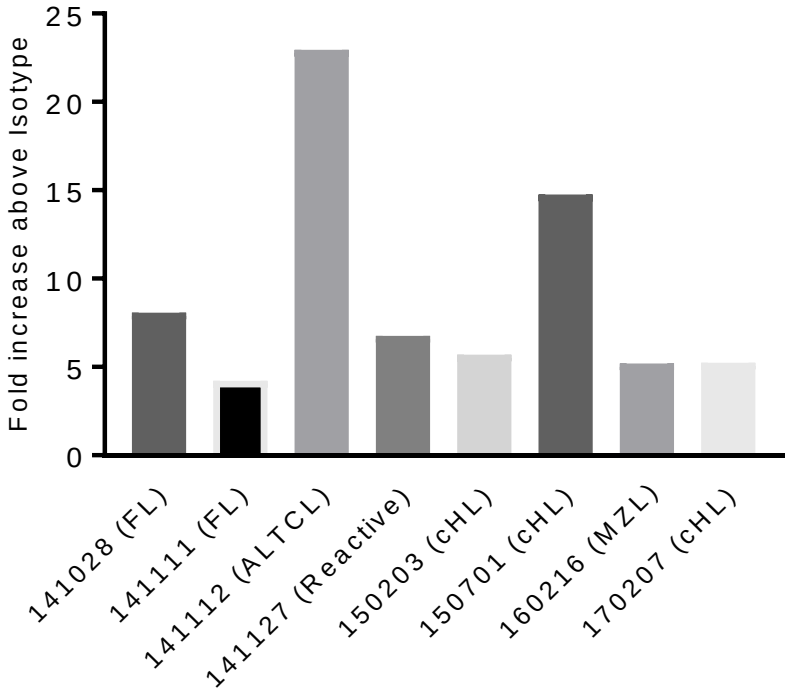

Figure 7-1 JAM-A expression on B cells from primary patient LNs:

LNMCs were isolated from LN biopsies from patients at diagnosis. The LNMCs were cultured overnight and then co-stained with either αCD19 or αCD20 antibodies to identify the B lymphocyte population, and αJAM-A or an isotype antibody as a negative control. LN samples were analysed by flow cytometry and the MFI of JAM-A expression was measured on the $CD19^+$ or $CD20^+$ B cells. JAM-A levels are expressed as the fold increase in JAM-A MFI over the isotype control MFI.

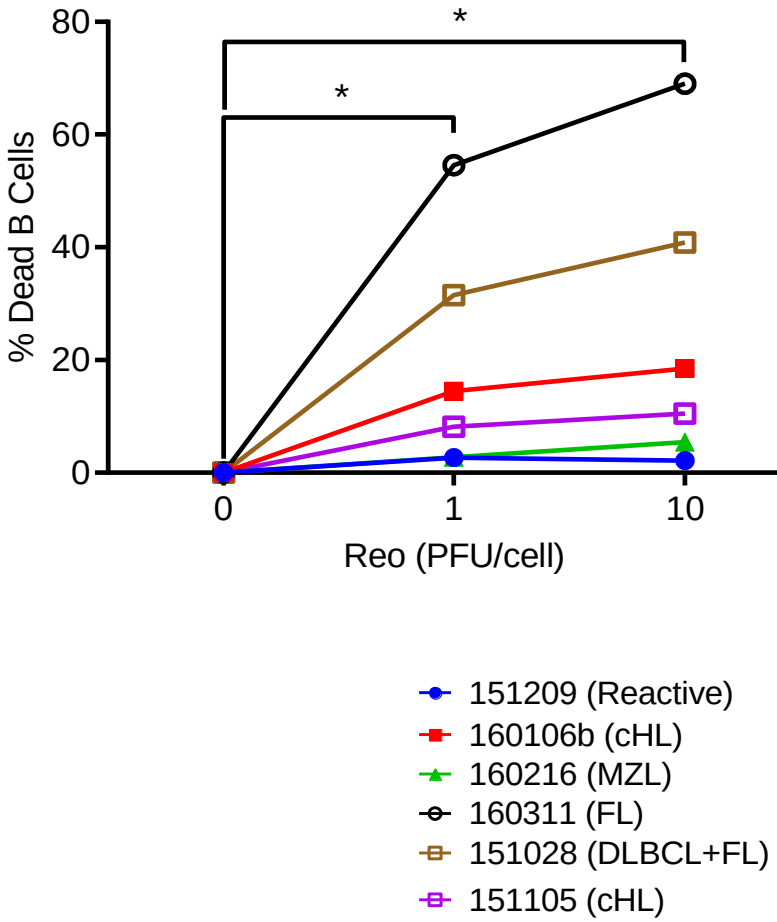

Figure 7-2 The cytotoxic effects of reovirus on B cell populations.

LNMCs were isolated from LN samples at diagnosis and cultured overnight. The cells were then treated with escalating doses of reovirus (1 and 10 pfu/cell) for 120hrs. The $CD19^+$ or $CD20^+$ B cells were then analysed for viability by LIVE/DEAD™ exclusion. The percentage of dead cells in untreated samples has been subtracted from reovirus-treated results. Significance was determined by paired student's t test.

7.2.2 Assessing the ability of CVA21 to eradicate primary patient NHL cells

Previous data showed that CVA21 induced cell death in NHL B cell lines that express ICAM-1 (Chapter 4, sections 4.2.1 and 4.2.2). Therefore, CVA21 was also investigated for its ability to target malignant B cells within primary LN samples. Firstly, ICAM-1 expression on the B cell population within LN samples was determined. **Figure 7-3** shows ICAM-1 expression on B cells from several primary patient LN samples; all samples expressed ICAM-1 with two samples, the FL (14111), and the reactive LN (141127), expressing levels with MFIs 20-fold greater than that of the isotype control. All other samples expressed ICAM-1 ranging from 5 to 17 times greater than the isotype control, demonstrating varied, but abundant, expression of ICAM-1 to facilitate CVA21 entry.

LNMCs were isolated from LN samples and treated with CVA21 for up to 120hrs; $CD19^+$ or $CD20^+$ B cells were subsequently analysed for viability by LIVE/DEAD™ staining. **Figure 7-4** shows significant CVA21-induced B cell death in most samples. This is particularly high in one FL sample (160311) while all other samples, with the exception of reactive (151209) and cHL (170504A) show a lower but consistent increase in cell death following CVA21 treatment. The cytotoxic effect of CVA21 was dose-dependent with a dose of 1pfu/cell inducing significantly more cell death than 0.1pfu/cell. While investigating a correlation between ICAM-1 expression and susceptibility to CVA21 in LN B cells might provide some insight into the relevance of ICAM-1 on susceptibility of these cells to CVA21, this analysis could not be performed due to low sample numbers.

Replication is an expected outcome in lytic cell death (Bauzon and Hermiston, 2014), therefore, to examine whether CVA21-induced cell death of primary LN B cells was indeed replication-dependent, $TCID_{50}$ assays were performed on cell-free supernatants from CVA21-treated LNMCs. In addition, viral replication within healthy donor PBMCs, which were resistant to CVA21-induced cell death (Chapter 4, section 4.2.8), was examined for comparison. In **Figure 7-5**, $TCID_{50}$ assays showed that the high viral titres at the start of the experiment (input) had diminished significantly after 120hrs in culture in the LN samples (a). However, the titre at the same time point in the healthy donor samples remains much lower (b). (c) and (d) show data when 120hr $TCID_{50}$s are expressed as a percentage of the input, to compare the sample types. This demonstrates a drastic reduction in virus copies in primary samples and may suggest that replication is either happening at a very low rate or not at all. Higher $TCID_{50}$s

were observed when a higher dose of CVA21 was used, as expected. Complementary experiments investigated the ability of UV-inactivated CVA21 to target NHL primary B cells (n=2, data not shown). Although background cell death was high in these samples, CVA21-induced cell death appeared slightly increased in normal CVA21-treated cells, but there appeared to be no detectable increase in cell death in UV-inactivated CVA21-treated cells.

As previously discussed (Chapter 2, section 2.4.1.2.1), the IFN response is one of the first lines of viral defence and may coordinate anti-tumour immune responses. In order to investigate the ability of primary LNMC samples to produce IFN-α in response to CVA21 infection, LNMCs and healthy PBMCs were treated with CVA21 for 48hrs, at which point the cell-free supernatant was analysed for IFN-α production by ELISA. **Figure 7-6** (a) shows no IFN-α was detected in 5 out of 7 primary LN samples (all of which were NHL or cHL) but was secreted in response to CVA21 in the reactive (non-malignant) LN sample. This highlights a potential interesting difference between this single reactive LN and malignant LNs that is congruent with previous data on the diminished ability of NHL PBMCs to produce IFN-α (Ho et al., 1992) and the lack of IFN-α production by the cell lines (Chapter 5, section 5.2.1). The lack of IFN-α production by NHL LN samples was markedly different from healthy PBMCs which showed significant IFN-α production in response to CVA21 from all 4 healthy PBMC donors in a dose-dependent manner, outlining an important difference between the response of NHL samples and PBMCs to CVA21. The IFN production observed from healthy PBMCs, which was absent from NHL primary samples, may reflect the different cellular composition of NHL/PBMC samples, or changes in cellular functions at different anatomical sites. However, it may also suggest compromised immune function in NHL patients, which would require further testing using PBMC from patients and/or healthy LN biopsy samples. The lack of IFN suggests an environment favourable for viral replication, although, because of the known role of type I IFN in coordinating OV anti-tumour immunity (Adair et al., 2013), may suggest that the virus may be unable to mount an anti-tumour immune response within the LN. This will be investigated further in 7.2.3.

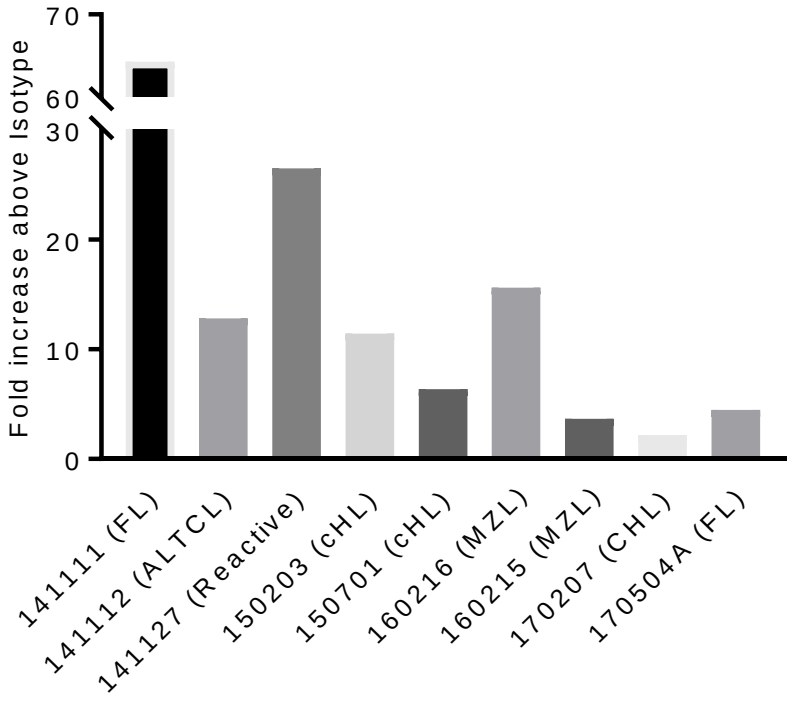

Figure 7-3 ICAM-1 expression on B cells from primary patient LNs.

PBMCs were isolated from LN biopsies from patients at diagnosis and stained with either αCD19 or αCD20 antibodies to identify the B lymphocyte population, and αICAM-1 or an isotype antibody as a negative control. The samples were analysed by flow cytometry to quantify the MFI of ICAM-1 on the $CD19^+$ or $CD20^+$ B cells. ICAM-1 levels were expressed as a fold increase of the ICAM-1 MFI over the MFI of the isotype.

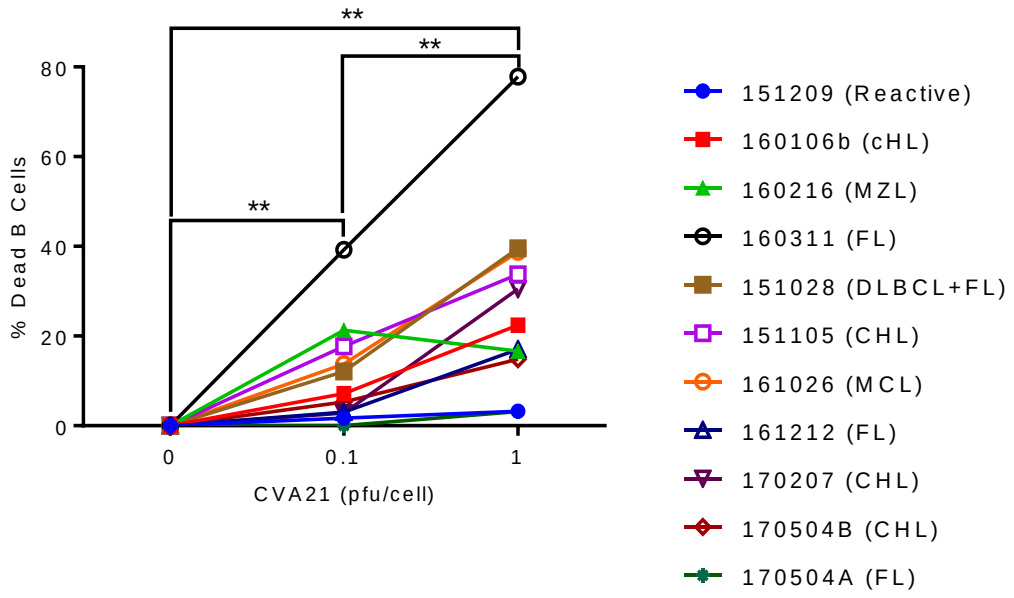

Figure 7-4 Cytotoxic effects of CVA21 on LN B cell populations.

LNMCs were isolated from patient LN samples at diagnosis and cultured overnight. The cells were treated with escalating doses of CVA21 (0.1 and 1 pfu/cell) for 120hrs and the viability of B cells assessed by LIVE/DEAD™ exclusion as previously described. The percentage of dead cells in untreated samples was subtracted from CVA21-treated results. Significance was determined by paired student's T test.

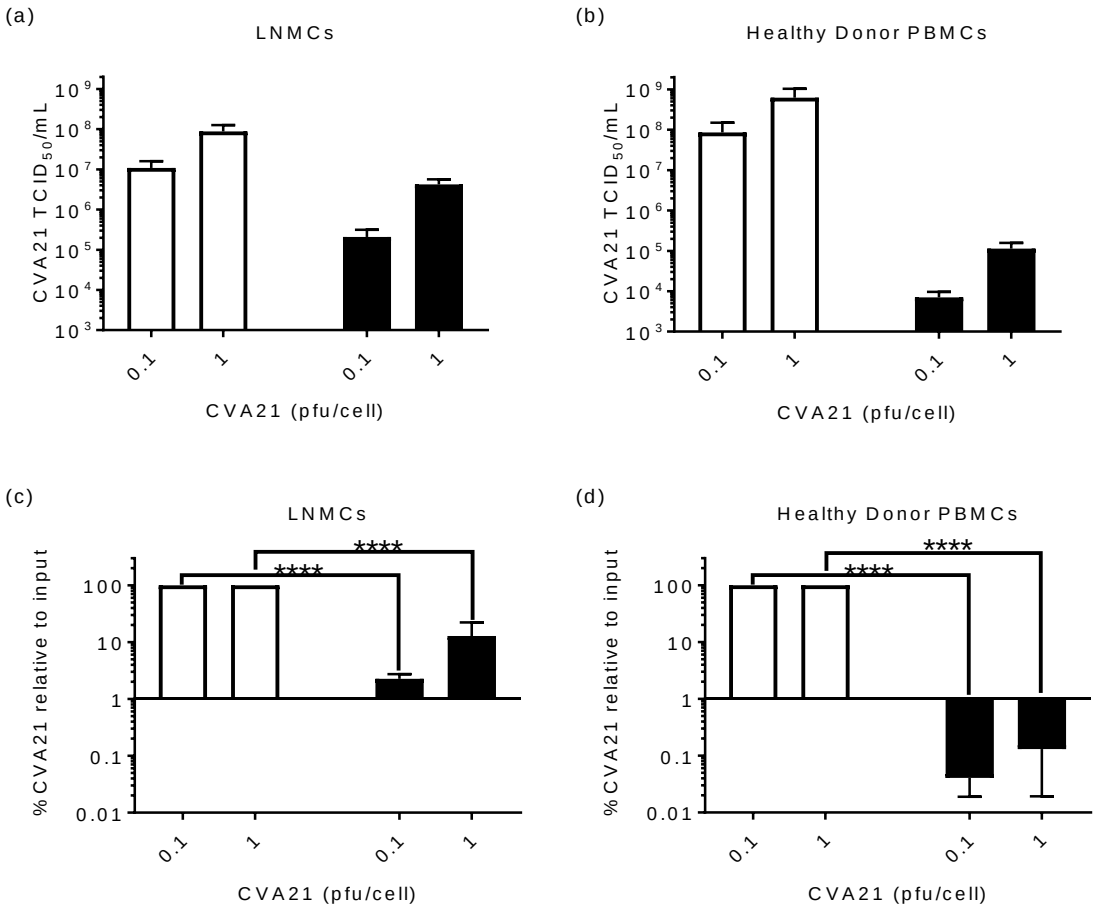

Figure 7-5 Assessment of CVA21 Replication in LN samples vs healthy PBMCs.

LN samples and healthy donor PBMCs were treated with CVA21 for 120hrs. Cell-free supernatants were taken at 0hrs as input (white bars) and again at 120hrs when cell death was observed. Supernatants were then analysed for virus titre by $TCID_{50}$ assay ((a) and (b)). To analyse this further, the titre values for both doses at 120hr are expressed as a percentage of the input (100%) viral titre ((c) and (d)). Lower titre values observed at later time points suggested diminishing viral load in sample supernatant, suggesting that little or no replication of CVA21 took place. Data shows n=3 for LNMC samples and n=4 for healthy donor samples +SEM, significance was determined by One-way ANOVA.

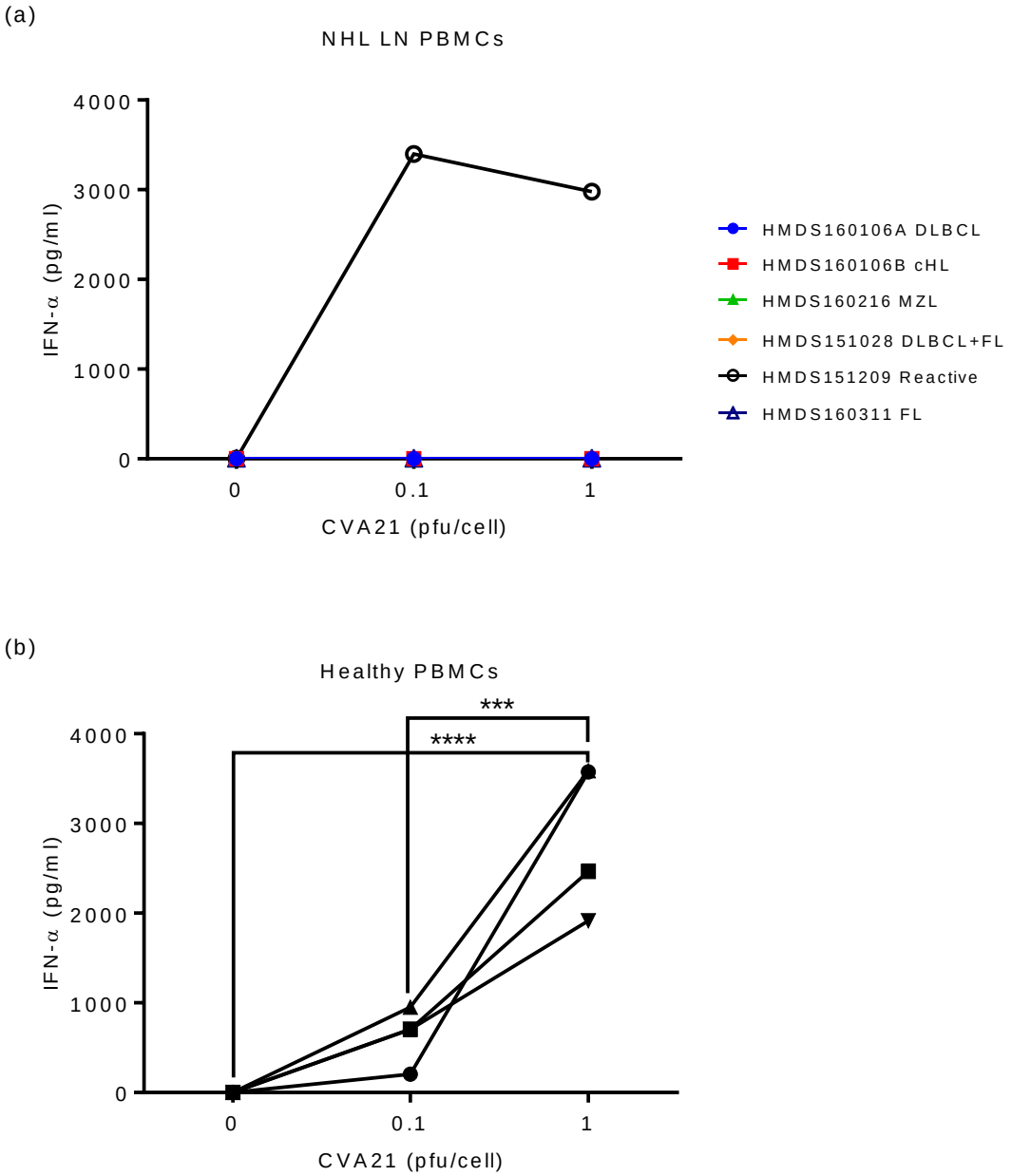

Figure 7-6 IFN-α secretion by primary LN samples and healthy PBMCs in response to CVA21 treatment.

LNMCs were isolated from patient LN biopsies (a) and healthy donors (b) and treated with CVA21 for 48hrs. Media was then collected and analysed for IFN-α secretion by ELISA. Graph shows data from n=6 independent experiments for the LN samples and n=4 independent healthy PBMC samples. Significance was determined by paired, two-tailed students T test by comparison with untreated samples.

7.2.3 Investigating the potential for an OV-induced anti-NHL immune response

Research in Chapter 6 (section 6.2.1) outlined a promising role for CVA21 and reovirus as activators of healthy peripheral blood NK cells, as determined by increased CD69 expression and NK cell degranulation upon recognition of NHL cell line targets. Using primary patient LN samples, reovirus was analysed for its ability to promote an NK cell-mediated anti-NHL immune response, in terms of NK cell phenotype activation. Unfortunately, due to a limited number of samples, it was not possible to test CVA21 for its effects on NK cell activation.

To test the effects of reovirus on primary LN NK cell activation, samples were treated with reovirus for 24hrs and analysed for CD69 expression on the NK cells ($CD3^{-}CD56^{+}$). **Figure 7-7**, shows a small increase in CD69 expression in 7 out of 9 samples, although collectively this increase was not statistically significant, these results do suggest the potential for reovirus to induce NK cell activation in some LN samples.

The NK cell population within healthy human LN typically represents 0.2-0.4% of cells in the LN (Bajenoff et al., 2006), casting doubt over whether an NK cell-mediated response would be effective with such limited numbers. In the primary LN samples analysed in this study, NK cells constituted between 0.1-2% (mean 0.81% ± 0.584%) of the lymphocyte population, as shown in **Figure 7-8**, in contrast to T cells that represented 45-75% (mean 47.56% ± 22.88%) in all but 3 samples. Low NK cell numbers may present a challenge for inducing an effective NK-mediated anti-NHL response, warranting research into methods to overcome these low numbers.

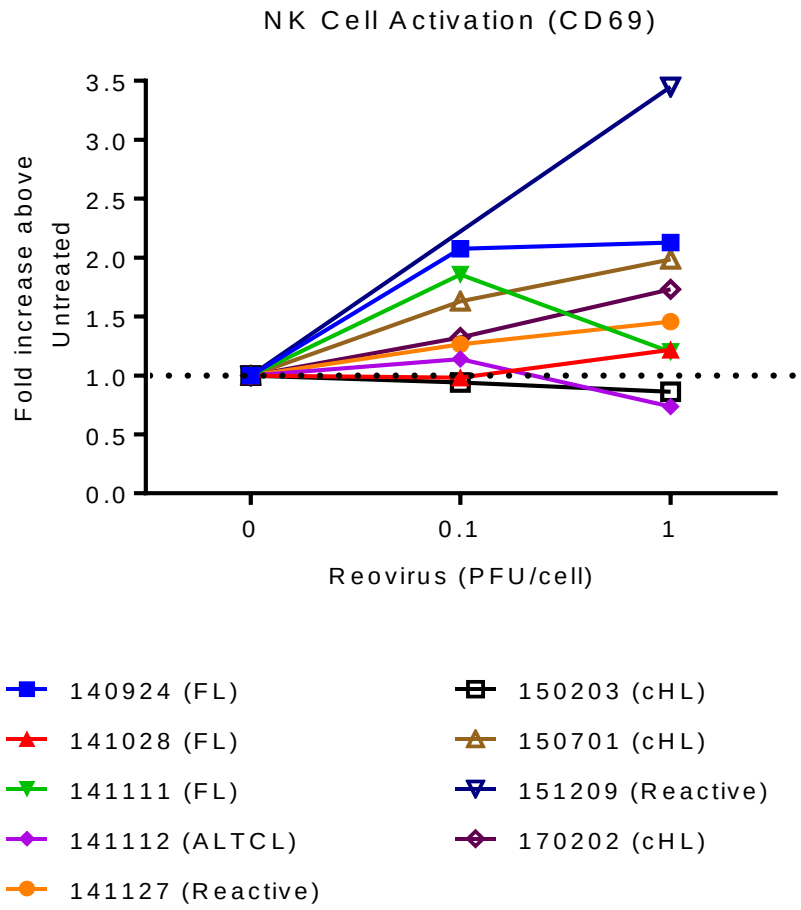

Figure 7-7 Reovirus-induced activation of LN-residing NK cells.

Primary LN samples were treated with reovirus for 24hrs before being co-stained with αCD3 and αCD56 antibodies to identify the NK cell ($CD3^{-}CD56^{+}$) population. Samples were also stained with either an αCD69 antibody, to measure activation, or an isotype antibody as a negative control. CD69 MFI levels were expressed as a fold change above isotype control MFI values. Treated values were expressed as a ratio of the untreated. Statistical analysis was performed by One-way ANOVA, but no statistical significance was observed.

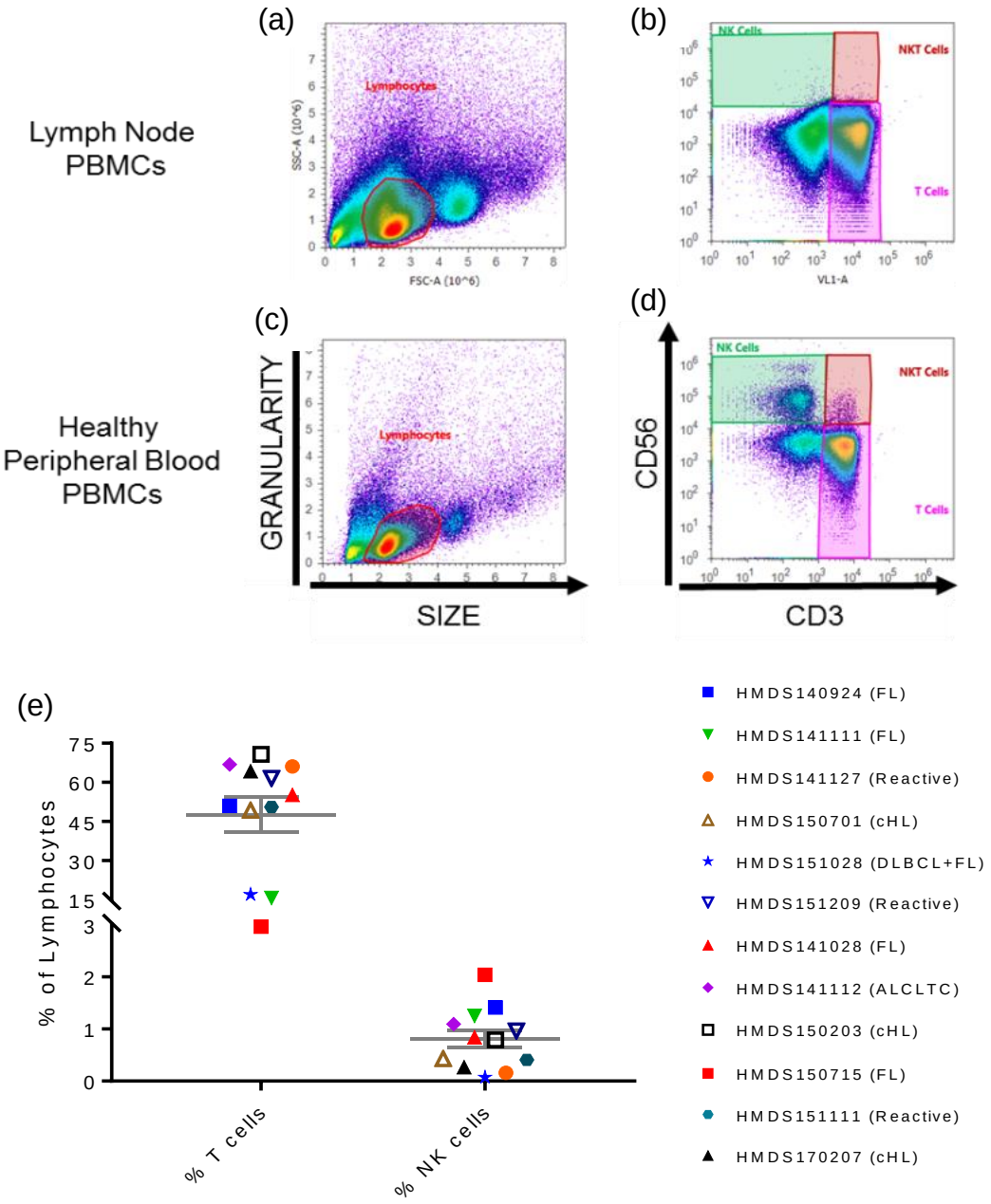

Figure 7-8 Immune effector cell populations in NHL Lymph Nodes.

Primary NHL LN samples were co-stained with αCD3 and αCD56 antibodies to identify T cell ($CD3^+CD56^-$) and NK cell ($CD3^-CD56^+$) populations. Panel (a) representative FSC/SSC dot plot from an NHL sample gated on the lymphocyte population, (b) CD3/CD56 dot plot of the lymphocyte population, depicting NK cells (green) and T cells (pink). Panels (c) and (d) show representative panels for healthy donor PBMCs for comparison. (e) NK and T cell populations from 12 patient samples as a percentage of lymphocytes. Error bars represent the mean ± SEM from n=12 independent samples.

7.2.4 Examining the potential to overcome low NK cell numbers in NHL LN.

During a systemic viral infection, enhanced lymphocyte trafficking is evident throughout the lymphatic system, including the secondary lymphoid organs (Springer, 1995). Systemic delivery of an OV could induce a similar effect in a patient, resulting in enhanced migration of lymphocytes into LNs, including NK cells (Beuneu et al., 2009). Enhanced NK cell trafficking to LN in response to a virus could be exploited by OV therapy in HMs, specifically if the systemic delivery of a virus induced such enhanced migration. To test whether reovirus could induce NK cell trafficking to lymphoid organs, a non-tumour-bearing mouse model was infected with reovirus for 24hrs and their LNs were analysed for NK cell numbers. **Figure 7-9** shows the schematic of the *in vivo* experiment; on day 0, 6-8-week-old non-tumour-bearing C57/Black 6 mice were inoculated with reovirus or PBS (control group) via tail vain injection. 24hrs later, the mice were sacrificed, and the inguinal, brachial and axillary LN were harvested, dissociated, and analysed by flow cytometry for NK cell numbers.

Figure 7-10, shows the percentage of NK cells in the LN of PBS-treated mice was consistently low, within a range of 0.1-0.3% of the lymphocyte population, however, the percentage of NK cells was significantly enhanced in reovirus-treated mice across all LN demonstrating systemic enhancement of NK cell trafficking to the LNs.

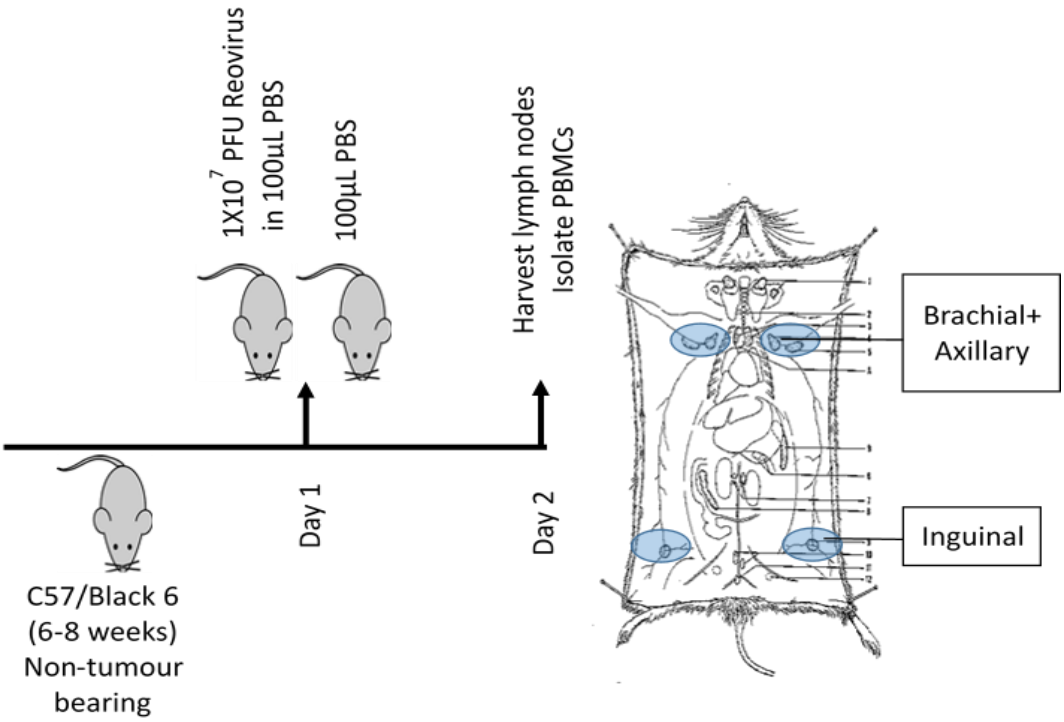

Figure 7-9 Schematic of the *in vivo* NK cell trafficking to LN experiment.

On day 0, 6-8-week-old non-tumour-bearing C57/Black 6 mice were inoculated with $1x10^7$ pfu reovirus in 100µL or 100µL PBS (control group) via tail vain injection. 24hrs later, mice were sacrificed, and the inguinal, brachial and axillary LN were harvested, dissociated, and analysed by flow cytometry for NK cell numbers. Due to projected low numbers in lymph nodes, brachial and axillary LN were combined. Image adapted from (Anatomyorgan, 2017)

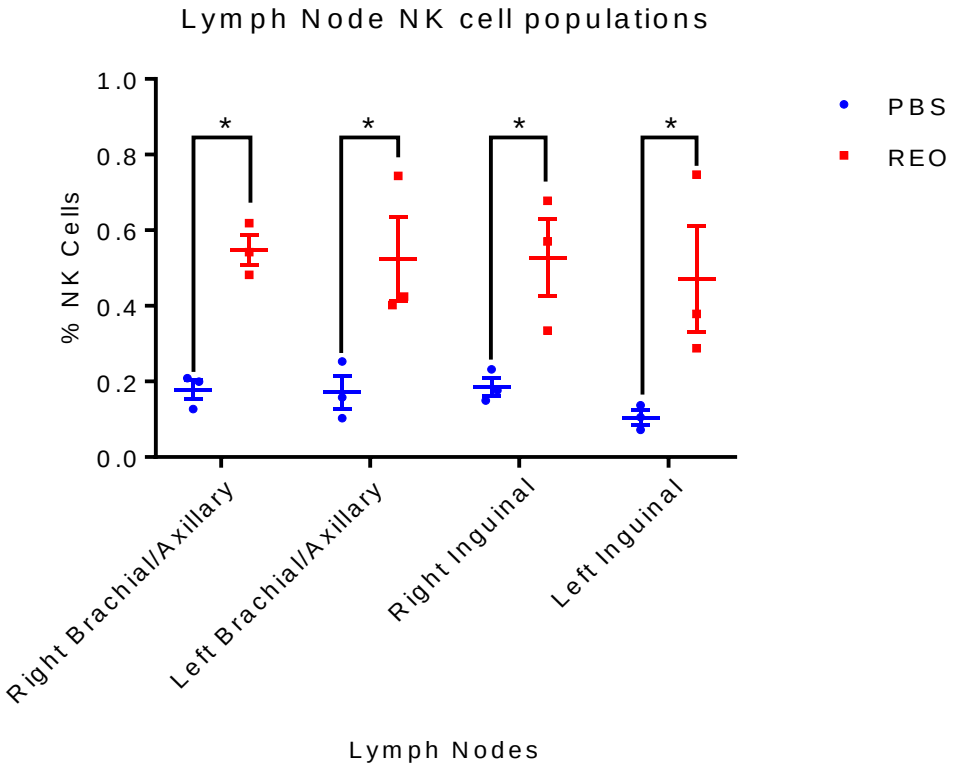

Figure 7-10 Reovirus-induced NK migration into mouse LNs

Non-tumour-bearing C57/BL6 mice were inoculated with either PBS (control) or reovirus ($1x10^7$ pfu/100µL in PBS) via tail vein injection. 24hrs later, mice were sacrificed, left and right inguinal, brachial and axillary LN were harvested, dissociated and analysed for NK cell numbers by flow cytometry. Data shows n=3 mice per condition from one experiment. Significance was determined by paired, two-tailed student's T test.

7.3 Discussion

Cell lines are a vital tool for *in vitro* research due to their immortality, infinite replicative capacity and availability. When multiple lines are used, as has been done in this project, they provide excellent insight into how cancer cells respond to treatment, when used in carefully designed and controlled experiments. Primary patient cells, on the other hand, provide a better representation of cancer, because they contain a mix of malignant and non-malignant cells, including tumour-associated immune cells and fibroblasts, and have not developed additional genetic abnormalities through long-term culture. These extra populations can provide growth support, or can mediate other effects, that will determine the outcome of treatment. Previous work by Ilkow, *et al.*, outlined a role for Cancer-Associated Fibroblasts in promoting viral replication in malignant cells, enhancing the efficacy of OV treatment (Ilkow et al., 2015), and research by Breitbach, *et al.*, showed VSV-induced tumour vasculature destruction, resulting in tumour cell death, in a 3D *in vitro* model of colon cancer (Breitbach et al., 2011). These findings emphasise the importance of considering the role of TME components when investigating the efficacy of novel OV treatments.

Contrary to the cell line data (Chapter 4, section 4.2.2), reovirus induced cell death in primary LN samples, with the exception of the MZL and reactive (non-malignant) samples (**Figure 7-2**). In support of this finding, reovirus has also demonstrated promising results as an anti-cancer agent for other models of HMs, such as myeloma (Thirukkumaran, C. M. et al., 2012), and lymphoma (Alain et al., 2002), including death of primary patient samples. It is possible that cell lines, which accrue multiple pro-survival mutations and are immortal, may be more resistant to reovirus than primary samples. However, it is also possible that malignant cells within the primary samples are being killed by bystander cytokine killing, as demonstrated by Errington, *et al.* (Errington et al., 2008); complementary research has also confirmed the ability of CVA21-induced cytokines to generate bystander killing using an AML cancer model (Louise Müller – manuscript submitted).

It would be pertinent to examine OV-induced cytotoxicity on a greater number of samples to see if it would be possible to identify “responders” and “non-responders” of OV therapy, and enable identification of determinants of OV sensitivity, including the production of cytokines (Errington et al., 2008), the presence of immune effector cells that are activated by OV, or molecular changes associated with OV oncolysis such as p53, Retinoblastoma protein

(Rb) and Ataxia telangiectasia mutated (ATM), which have all been implicated in the sensitivity of lymphoma cell lines to reovirus infection and oncolysis (Kim et al., 2010). To test whether reovirus-induced cell death is due to cytokine release or viral replication, plaque assays or $TCID_{50}$ assays could be used to measure replication in primary NHL samples. Moreover, media from treated cells could be analysed for cytokine production and cytopathic effects, as performed on a single FL sample that was treated with reovirus and CVA21 and analysed for the secretion of cytokines using a Luminex assay (preliminary data not shown). This data confirmed the secretion of cytokines following reovirus and CVA21 treatment, for example, TNF-α was secreted suggesting a potential role for cytokine-induced cell death in NHL LN samples.

ICAM-1 expression was significantly higher on LN B cells than healthy donor peripheral B cells (Chapter 4, section 4.2.8). This data is in keeping with previous data that demonstrated increased ICAM-1 expression on lymphomas, particularly DLBCL (The Human Protein Atlas, 2017). As expected, CVA21 induced significant cell death in primary LN samples, but not the reactive LN sample, as expected.

The low level or lack of CVA21 replication in susceptible NHL LN samples was unexpected, due to the significant viral replication and oncolysis observed on NHL cell lines (Chapter 4 Figure 4-5). This may mean that CVA21-induced cell death was not dependent on viral replication and was perhaps immune mediated. However, in two patient samples, the ability of UV-inactivated CVA21 to induce cell death was evaluated; no cell death was observed in UV-inactivated CVA21-treated cells (n=2 observation, data not shown), suggesting a role for viral replication in CVA21-induced cell death. Of interest, supernatants from CVA21-treated NHL LN samples did not contain detectable levels of IFN-α or IFN-γ (Figure 7-6 and IFN-γ data not shown), which would suggest limited immune cell activation by CVA21 and that CVA21-induced cell death may be dependent on viral replication and oncolysis.

Reovirus has previously been described as a highly immunogenic virus ((Prestwich, R. J. et al., 2008), (Hall et al., 2012), (White et al., 2008), (Errington et al., 2008)), and its ability to activate peripheral blood NK cells (Chapter 6, section 6.2.1) was comparable with the enhanced CD69 expression observed on NK cells from several primary malignant LN samples (Figure **7-7**). Although the enhanced CD69 on primary NHL LN NK cells was not statistically significant, 4 NHL samples showed responses ranging from 1.5 to 4-fold increase over background levels, 3 samples showed weaker responses

between 1.1 and 1.5-fold increases, and 2 samples did not respond to reovirus treatment. These data are comparable with increased CD69 expression on healthy donor NK cell which was increased 4-5-fold above the untreated control by both OV (chapter 6, section 6.2.1). **Figure 7-6** suggests that CVA21 is unable to induce IFN-α production in diseased LN, furthermore, the multiplex Luminex assay that was used to assess cytokine production from one OV-treated FL sample showed detectable IFN-α following reovirus, but not CVA21 treatment (data not shown. This suggests that reovirus may be more immunogenic than CVA21 in NHL LN samples. Complimentary research being carried out in the laboratory has shown that CVA21-induced IFN-α production is derived from pDCs (Louise Müller – Manuscript submitted), while reovirus induces IFN-α production in monocytes (Parrish et al., 2015). The fact that pDCs are only present in small numbers in the LN (~ 0.45% of LNMC population (Lehmann et al., 2010)), may account for the inability of CVA21-treated LN samples to produce IFN-α. Fiore, et al., have also shown that pDC populations in NHL LN are significantly lower than in reactive LN controls, potentially accounting for the lack of IFN-α production in NHL LN samples (Fiore et al., 2006).

In humans, NK cells comprise ~10% of the peripheral blood lymphocyte population (Li, Z.S. et al., 2011), however, the proportion of LN lymphocytes that are NK cells is much lower (0.2-0.4%, (Bajenoff et al., 2006)). Data presented in Figure 7-10 demonstrated reovirus' ability to promote significant NK cell trafficking to the LN within 24hrs of systemic virus delivery. The C57/BL6 immunocompetent mouse strain used for this study was chosen as it has been used for OV therapy in a variety of cancer models (Robinson et al., 2009), (Cheema et al., 2013), (Kober et al., 2015). While elucidating the mechanisms by which reovirus induces NK cell trafficking to the LN was beyond the scope of this work, future research could investigate this by examining the production of chemoattractant cytokines, such as CXCL10, which has been implicated in recruiting NK cells to tumour sites (Wendel et al., 2008). These experiments could measure CXCL10 production by reovirus-exposed LN and investigate the effects of CXCL10 blockade (by antibody or siRNA knockdown) on NK cell recruitment to murine LN.

OVs have previously been investigated for their ability to manipulate NK cell trafficking in murine models, such as enhanced NK cell trafficking to reovirus-treated prostate cancer tumours (Gujar, S.A. et al., 2011), an IL-12-expressing Maraba virus that elevated NK cell trafficking to colorectal cancer tumours (Alkayyal et al., 2017), and increased NK cell trafficking to glioma tumours in

measles virus-treated mice (Bhat and Rommelaere, 2015). This demonstrates a role for OV therapy in enhancing the anti-cancer immune repertoire, both in terms of immune cell activation and infiltration.

Homing of NK cells to draining LN is a common feature of many viruses, such as influenza (Duan et al., 2017), and ECTV (ectromelia virus), in C57/BL6 mice 48hrs post-infection (Parker et al., 2007). This could suggest that CVA21, as well as reovirus, may also promote NK cell trafficking to LN in an NHL context. To elaborate on the findings in this chapter, and to investigate whether the NK cells that traffic to the LN are activated by OV, future work could examine activation markers on NK cells, such as CD69 which has been used to measure murine NK cell activation in response to viruses (Wang, J. et al., 2012). LN could also be analysed for the presence of OV, to examine whether they can be delivered to the LN. Reovirus has been detected in the LN of mice in a melanoma model using C57/Bl6 mice (Ilett et al., 2009), and a role for dendritic cells and T cells as carriers of reovirus to LN metastases was reported.

The research presented in this chapter outlines a potential for both CVA21 and reovirus to target primary LN B cells as both reovirus and CVA21 induced cell death in some malignant LN samples, but not the reactive sample, demonstrating specificity of OVs for malignant B cells. Reovirus demonstrated promise as an immunomodulatory agent by enhancing CD69 expression on NHL LN NK cells and by enhancing NK cell trafficking to LN in a non-tumour-bearing C57/BL6 mouse model. The application of some of the findings from the previous chapters to primary patient material validates a potential role for reovirus and CVA21 in eradicating malignant cells in patients and represents the next step to the application of these OV for the treatment of NHL. However, future research is required to ascertain the mechanisms of efficacy of both reovirus and CVA21 against NHL within LN biopsies.

Chapter 8:
Conclusions and future studies

Chapter 8

8.1 Conclusions

The results presented within this study demonstrate that CVA21, unlike reovirus, is a potent cytolytic agent against NHL cell lines. CVA21 induced cell death in all but one cell line; OCI-LY19 cells were impervious to CVA21-induced cell death, probably due to the lack of the viral entry receptor, ICAM-1. CVA21-induced cell death required replication-competent virus as UV-inactivation completely abrogated cell death. Reovirus, on the other hand, induced only minimal cell death in 3 out of six cell lines, even at doses 10 times higher than CVA21. CD40L stimulation of NHL B cells resulted in a vincristine-resistant phenotype, suggesting reduced efficacy of vincristine in LN-residing NHL B cells. CD40L stimulation also up-regulated ICAM-1 expression on most NHL cell lines, which correlated with enhanced susceptibility to CVA21 in Ramos and U2932 cell lines. This finding potentially outlines a role for CVA21 in targeting drug-resistant NHL cells.

Further investigation into the determinants of susceptibility to CVA21, focused on the role of the antiviral IFN response to the virus. This investigation demonstrated that, although the susceptible NHL cell lines retain a functional IFN-α response (responsive to the addition of exogenous IFN), pre-treatment does not protect NHL cell lines from CVA21-induced cell death. This effect could be attributed to disruption of the IFN response pathway by CVA21 in homogenous NHL cell lines, but not primary healthy B cells in the context of PBMC.

Further study also demonstrated a role for mTOR in CVA21 cytotoxicity as treating NHL cell lines with rapamycin resulted in diminished CVA21-induced cell death in most cell lines with the exception of Raji cells, which remained susceptible to CVA21-induced cell death; rapamycin blocked S6 phosphorylation in these cells. This finding illustrates a role for S6 kinase in CVA21-induced cell death. Proliferation analysis of rapamycin-treated NHL cell lines showed minimal inhibition of cellular proliferation at 72hrs, suggesting that the anti-proliferative effects of rapamycin are not responsible for diminished CVA21-induced cell death.

The ability of an OV to induce an immune response to malignant, or virus-infected, target cells provides an alternate mechanism by which an otherwise poor lytic agent, such as reovirus, can promote the destruction of cancer cells. Both OV, CVA21 and reovirus, induced NK cell activation after 48hrs of treatment, as measured by enhanced CD69 expression. This activation translated to virus-induced NK cell degranulation against NHL cell line targets, outlining a role for both OV in promoting immune-mediated destruction of NHL cells. Investigating the effects of reovirus and CVA21 in combination with BHH2, an αCD20 mAb, also showed that, while CVA21, reovirus and BHH2 promoted NHL cell targeting as single agents, this effect was enhanced when either OV was combined with BHH2 against Ramos cells. This illustrates a possible role for a combined OV-mAb therapy for the treatment of NHL. Moreover, despite inducing vincristine-resistance and enhancing MHC-I expression, CD40L stimulation of NHL cell lines did not protect them from recognition by OV-activated NK cells, suggesting a role for OV therapy in targeting drug-resistant cells either as lytic, or immunotherapeutic, agents.

Importantly, primary NHL cells, which offer a better representation of clinical disease than immortalised NHL cell lines, were susceptible to reovirus- and CVA21-induced cell death. This validates CVA21 as a potent cytotoxic agent against NHL cells, and establishes a role for reovirus in inducing cell death in primary cells, as opposed to isolated cell lines.

Low NK cell numbers in human LN, as demonstrated by immunophenotypic studies of NHL LN samples, suggested a problem for OV in stimulating an NK cell-mediated immune response. Fortunately, systemic treatment of C57/BL6 mice with reovirus induced NK cell trafficking to the LN, overcoming the poor NK cell population numbers and highlighting an additional role for OV in promoting an anti-NHL immune response, a finding that warrants further *in vivo* validation.

NHL is a highly heterogeneous class of diseases with varied treatment response rates and poor survival in aggressive and relapsed cases, warranting research into alternative avenues of therapeutic intervention. The data presented in this thesis demonstrates the efficacy of two candidate OV, reovirus and CVA21, as potent inducers of NHL cell death through direct lytic killing for CVA21 and immune-mediated killing for both CVA21 and reovirus. These viruses also demonstrated efficacy against drug-resistant cells, emphasising their validity as promising anti-NHL therapies.

8.2 Future studies

In order to develop the application of either reovirus or CVA21 for the treatment of NHL in the clinic, further validation will be required to enhance our knowledge of the efficacy of the OVs. These studies should examine the efficacy of both viruses in a wider array of patient NHL samples in terms of cytotoxicity and immune-mediated killing of malignant cells. This work could also be compared with more reactive nodes, to fully delineate a role for either virus in targeting cells in malignant nodes, specifically. Further immunophenotypic studies could investigate the effects of both viruses on the activation status of immune effector and immunosuppressive cells, to elaborate on their ability to manipulate the LN immune microenvironment. This research could be supplemented by access to peripheral blood from NHL patients, providing insights into the effects of CVA21 and reovirus on peripheral immune cells in terms of immune activation and NHL cell targeting. These studies could include, but would not be restricted to, examination of immune checkpoint markers, such as PD-1 on LN-residing or peripheral blood immune effector cells, and PD-L1 on malignant cells, to allow the selection of appropriate immune checkpoint antibodies to enhance the efficacy of the OV. αPD-1 antibodies, such as nivolumab, have demonstrated successful outcomes in clinical trials for NHL, with 40% and 36% response rates in FL and DLBCL patients, respectively (Lesokhin et al., 2016).

Further research could confirm the ability of both OV to target drug-resistant cells through direct cytotoxicity or immune-mediated killing. This work could include the utilisation for alternative pro-survival signals (other than CD40L) that play a role in drug resistance and relapse within the LN, such as BCR engagement and addition of exogenous cytokines.

Importantly, *in vivo* models could develop these findings further to 1) investigate the effect of tumour burden in LN of treated mice, 2) test OV delivery, and replication within the NHL TME, 3) examine NK cell trafficking to LN and 4) characterise immune cell populations, activation by OV and the role for immune-mediated killing. Taken together, these studies would further validate the findings of this thesis and prove the applicability of CVA21 and reovirus as potential treatments for NHL.

The work outlined in this thesis demonstrates a potential application for CVA21 and reovirus in the treatment of NHL. This could be investigated further by combining either virus with drugs that are already being used to treat NHL, such as components of the R-CHOP regimen. While the ability of CVA21 to reduce melanoma tumour burden in immunodeficient mouse models has already been

investigated (Au 2005, shafren 2004), future combination strategies could be investigated in immunocompetent *in vivo* models, such as an immunocompetent NHL model using Female BALB/c mice (Touitou et al., 2007). The reported inability of CVA21 to infect cells expressing murine ICAM-1 could be overcome by transfecting murine NHL cells with human ICAM-1 and growing these cells in an immunocompetent mouse model, as has been demonstrated with human ICAM-1 on murine lungs in an immunocompetent BALB/c model (Traub et al., 2013). This research could provide greater insight into the ability of CVA21 to target NHL cells in vivo and the role of the host immune system in targeting the disease.

Chapter 9:
Appendix

Chapter 9

9.1 STR Profiling results

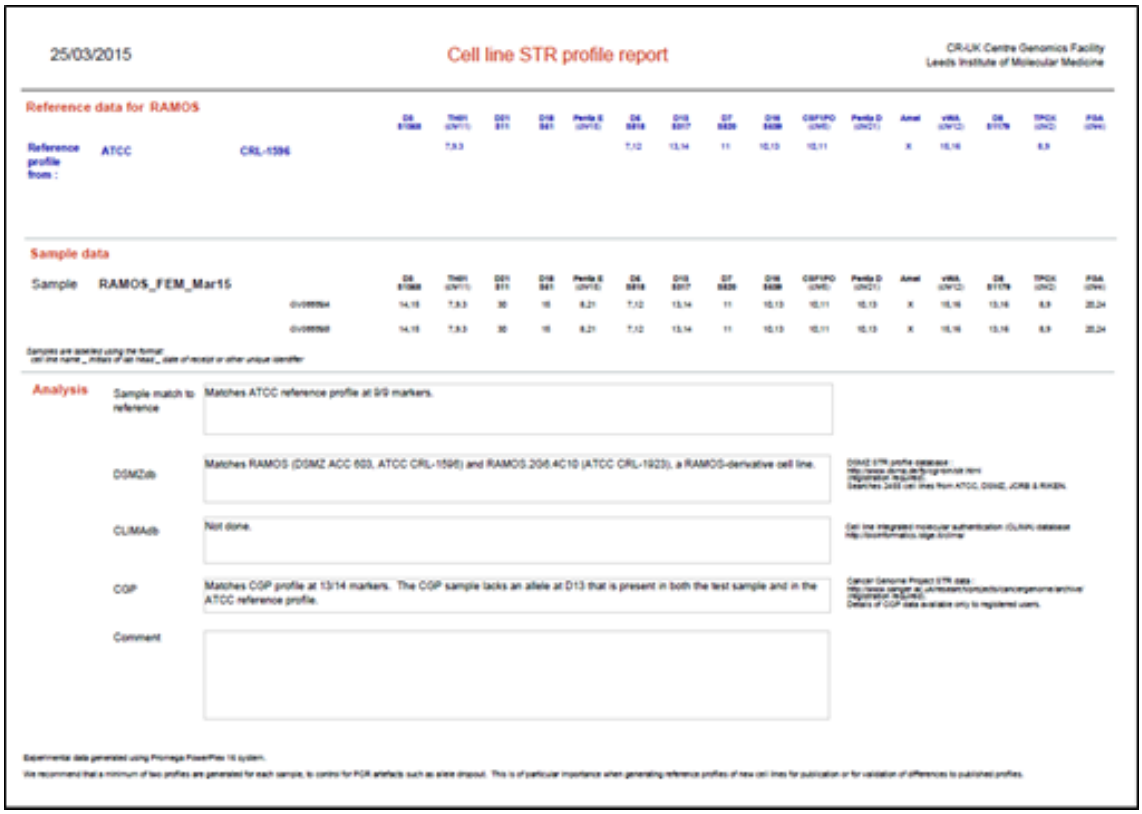

25/03/2015

Cell line STR profile report

CR-UK Centre Genomics Facility
Leeds Institute of Molecular Medicine

Reference data for RAMOS

			D8 S1360	TH01 (DN11)	D21 S11	D18 S51	Penta E (DN15)	D5 S818	D13 S317	D7 S820	D16 S539	CSF1PO (DN10)	Penta D (DN21)	Amel	vWA (DN12)	D8 S1179	TPOX (DN2)	FGA (DN4)
Reference profile from :	ATCC	CRL-1596		7,9.3				7,12	13,14	11	10,13	10,11		X	15,16		8,9	

Sample data

Sample	RAMOS_FEM_Mar15	D8 S1360	TH01 (DN11)	D21 S11	D18 S51	Penta E (DN15)	D5 S818	D13 S317	D7 S820	D16 S539	CSF1PO (DN10)	Penta D (DN21)	Amel	vWA (DN12)	D8 S1179	TPOX (DN2)	FGA (DN4)
	DV000564	14,15	7,9.3	30	15	8,21	7,12	13,14	11	10,13	10,11	10,13	X	15,16	13,16	8,9	20,24
	DV000568	14,15	7,9.3	30	15	8,21	7,12	13,14	11	10,13	10,11	10,13	X	15,16	13,16	8,9	20,24

Samples are labelled using the format:
cell line name _ initials of lab head _ date of receipt or other unique identifier

Analysis

Sample match to reference	Matches ATCC reference profile at 9/9 markers.
DSMZdb	Matches RAMOS (DSMZ ACC 603, ATCC CRL-1596) and RAMOS.2G6.4C10 (ATCC CRL-1923), a RAMOS-derivative cell line.
CLIMAdb	Not done.
CGP	Matches CGP profile at 13/14 markers. The CGP sample lacks an allele at D13 that is present in both the test sample and in the ATCC reference profile.
Comment	

DSMZ STR profile database :
Searches 2468 cell lines from ATCC, DSMZ, JCRB & RIKEN.

Cell line integrated molecular authentication (CLIMA) database

Cancer Genome Project STR data :
Details of CGP data available only to registered users.

Experimental data generated using Promega PowerPlex 16 system.

We recommend that a minimum of two profiles are generated for each sample, to control for PCR artefacts such as allele dropout. This is of particular importance when generating reference profiles of new cell lines for publication or for validation of differences to published profiles.

Figure 9-1: STR Profile results for Ramos cells

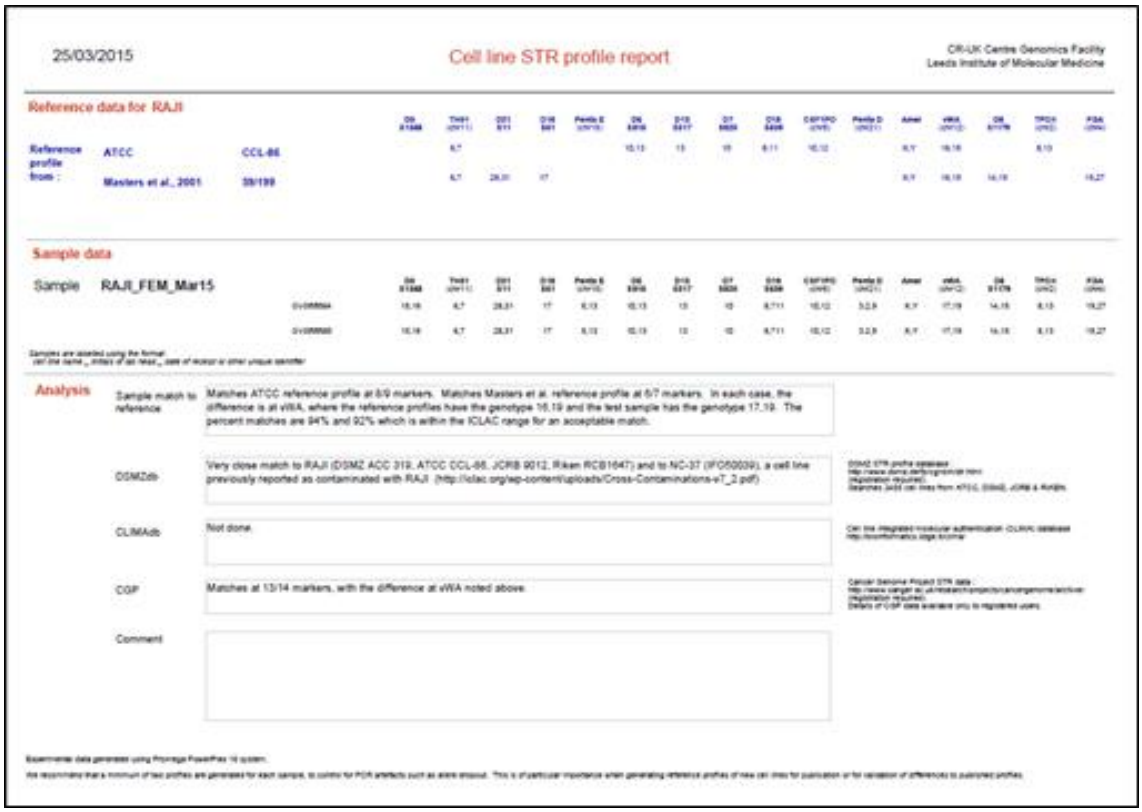

25/03/2015

Cell line STR profile report

CR-UK Centre Genomics Facility
Leeds Institute of Molecular Medicine

Reference data for RAJI

			D5 S818	TH01	D21 S11	D18 S51	Penta E	D6 S1043	D13 S317	D7 S820	D16 S539	CSF1PO	Penta D	Amel	vWA	D8 S1179	TPOX	FGA
Reference profile from :	ATCC	CCL-86		8,7				10,13	13	10	8,11	10,12		X,Y	16,19		8,13	
	Masters et al., 2001	59/199		8,7	28,31	17								X,Y	16,19	14,15		19,27

Sample data

Sample		D5 S818	TH01	D21 S11	D18 S51	Penta E	D6 S1043	D13 S317	D7 S820	D16 S539	CSF1PO	Penta D	Amel	vWA	D8 S1179	TPOX	FGA
RAJI_FEM_Mar15	DV09564	10,19	8,7	28,31	17	8,13	10,13	13	10	8,711	10,12	3,2,9	X,Y	17,19	14,15	8,13	19,27
	DV09565	10,19	8,7	28,31	17	8,13	10,13	13	10	8,711	10,12	3,2,9	X,Y	17,19	14,15	8,13	19,27

Samples are labelled using the format:
<cell line name>_<initials of lab head>_<date of receipt or other unique identifier>

Analysis

Sample match to reference	Matches ATCC reference profile at 8/9 markers. Matches Masters et al. reference profile at 5/7 markers. In each case, the difference is at vWA, where the reference profiles have the genotype 16,19 and the test sample has the genotype 17,19. The percent matches are 94% and 92% which is within the ICLAC range for an acceptable match.
DSMZdb	Very close match to RAJI (DSMZ ACC 319, ATCC CCL-86, JCRB 9012, Riken RCB1647) and to NC-37 (IFO50039), a cell line previously reported as contaminated with RAJI (http://iclac.org/wp-content/uploads/Cross-Contaminations-v7_2.pdf)
CLIMAdb	Not done.
CGP	Matches at 13/14 markers, with the difference at vWA noted above.
Comment	

DSMZ STR profile database
http://www.dsmz.de/fp/cgi/str.pl.html
(registration required)
Searches 3453 cell lines from ATCC, DSMZ, JCRB & RIKEN.

CRI: the Integrated molecular authentication: CLIMAdb database
http://bioinformatics.istge.it/climaf

Cancer Genome Project STR data
http://www.sanger.ac.uk/research/projects/cancergenome/archive/
(registration required)
Details of CGP data available only to registered users.

Experimental data generated using Promega PowerPrep 16 system.
We recommend that a minimum of two profiles are generated for each sample, to control for PCR artefacts such as allele dropout. This is of particular importance when generating reference profiles of new cell lines for publication or for validation of differences to published profiles.

Figure 9-2: STR Profile results for Raji cells

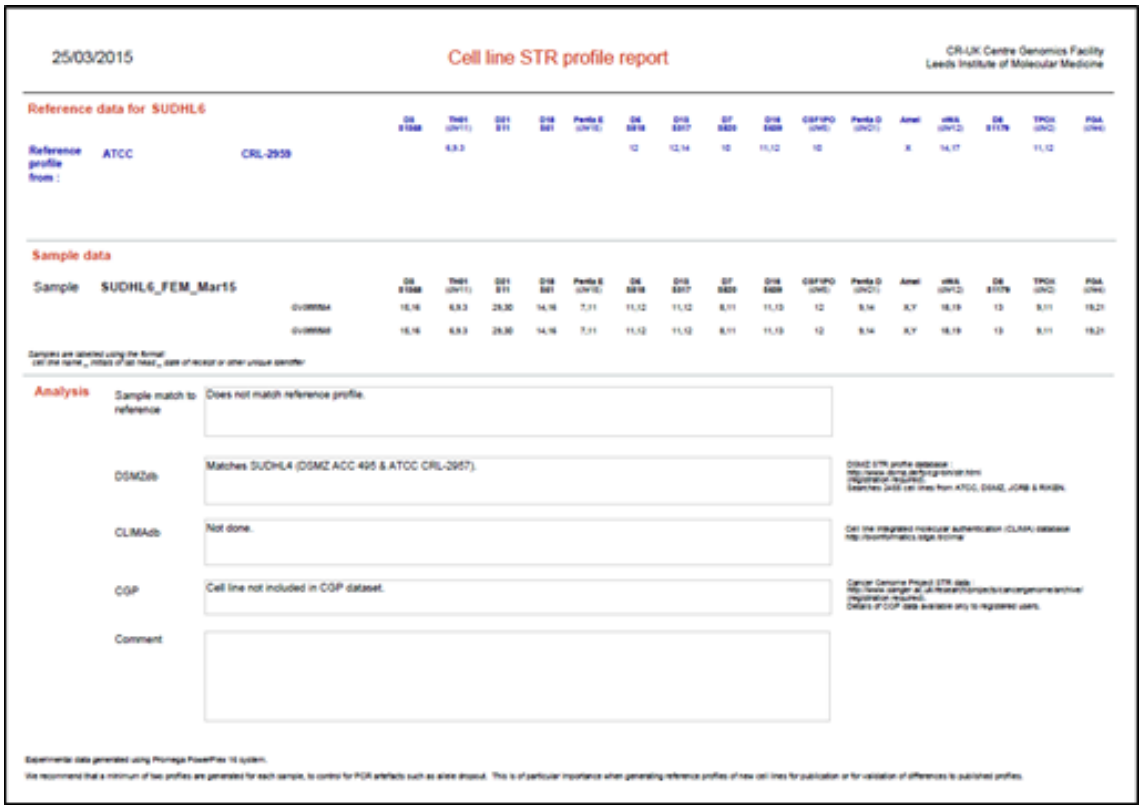

25/03/2015

Cell line STR profile report

CR-UK Centre Genomics Facility
Leeds Institute of Molecular Medicine

Reference data for SUDHL6

Reference profile from : ATCC CRL-2958

Sample data

Sample SUDHL6_FEM_Mar15

Analysis

Sample match to reference: Does not match reference profile.

DSMZdb: Matches SUDHL4 (DSMZ ACC 495 & ATCC CRL-2957).

CLIMAdb: Not done.

CGP: Cell line not included in CGP dataset.

Comment:

Figure 9-3: STR Profile results for SU-DHL-4 cells

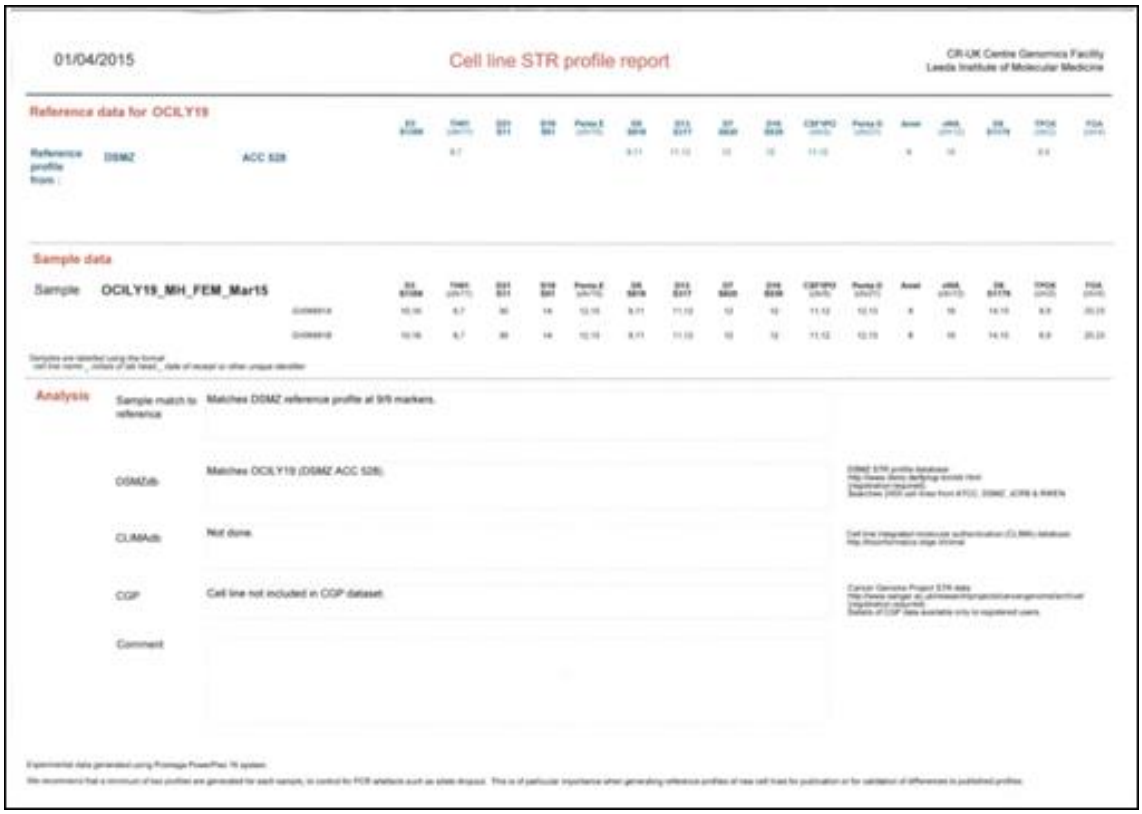

01/04/2015

Cell line STR profile report

CR-UK Centre Genomics Facility
Leeds Institute of Molecular Medicine

Reference data for OCILY19

Reference profile from : DSMZ ACC 528

Sample data

Sample OCILY19_MH_FEM_Mar15

Analysis

Sample match to reference: Matches DSMZ reference profile at 9/9 markers.

DSMZdb: Matches OCILY19 (DSMZ ACC 528).

CLIMAdb: Not done.

CGP: Cell line not included in CGP dataset.

Comment:

Figure 9-4: STR Profile results for OCI-LY19 cells

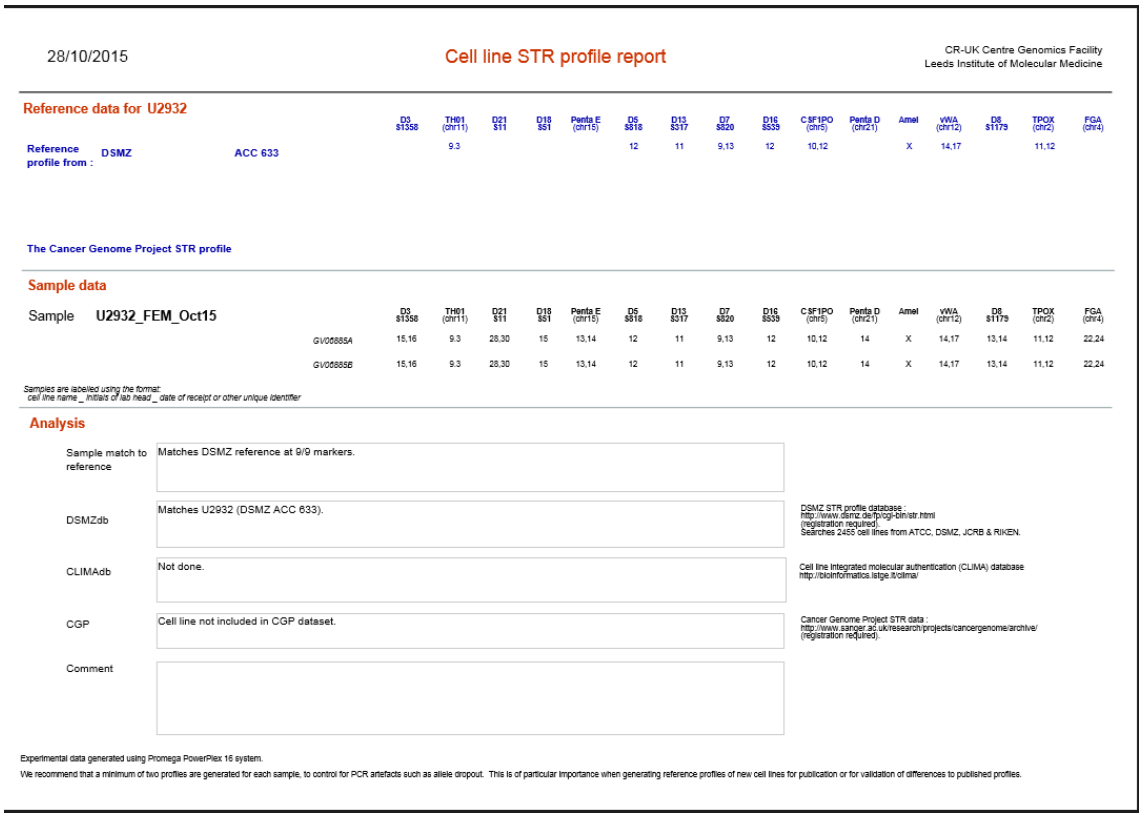

28/10/2015

Cell line STR profile report

CR-UK Centre Genomics Facility
Leeds Institute of Molecular Medicine

Reference data for U2932

			D3 S1358	TH01 (chr11)	D21 S11	D18 S51	Penta E (chr15)	D5 S818	D13 S317	D7 S820	D16 S539	CSF1PO (chr5)	Penta D (chr21)	Amel	vWA (chr12)	D8 S1179	TPOX (chr2)	FGA (chr4)
Reference profile from :	DSMZ	ACC 633		9.3				12	11	9,13	12	10,12		X	14,17		11,12	

The Cancer Genome Project STR profile

Sample data

Sample		D3 S1358	TH01 (chr11)	D21 S11	D18 S51	Penta E (chr15)	D5 S818	D13 S317	D7 S820	D16 S539	CSF1PO (chr5)	Penta D (chr21)	Amel	vWA (chr12)	D8 S1179	TPOX (chr2)	FGA (chr4)
U2932_FEM_Oct15	GV06885A	15,16	9.3	28,30	15	13,14	12	11	9,13	12	10,12	14	X	14,17	13,14	11,12	22,24
	GV06885B	15,16	9.3	28,30	15	13,14	12	11	9,13	12	10,12	14	X	14,17	13,14	11,12	22,24

Samples are labelled using the format:
cell line name _ initials of lab head _ date of receipt or other unique identifier

Analysis

Sample match to reference	Matches DSMZ reference at 9/9 markers.	
DSMZdb	Matches U2932 (DSMZ ACC 633).	DSMZ STR profile database : http://www.dsmz.de/fp/cgi-bin/str.html (registration required). Searches 2455 cell lines from ATCC, DSMZ, JCRB & RIKEN.
CLIMAdb	Not done.	Cell line Integrated molecular authentication (CLIMA) database http://bioinformatics.istge.it/clima/
CGP	Cell line not included in CGP dataset.	Cancer Genome Project STR data : http://www.sanger.ac.uk/research/projects/cancergenome/archive/ (registration required).
Comment		

Experimental data generated using Promega PowerPlex 16 system.

We recommend that a minimum of two profiles are generated for each sample, to control for PCR artefacts such as allele dropout. This is of particular importance when generating reference profiles of new cell lines for publication or for validation of differences to published profiles.

Figure 9-5: STR Profile results for U2932 cells

28/10/2015

Cell line STR profile report

CR-UK Centre Genomics Facility
Leeds Institute of Molecular Medicine

Reference data for OCILY3

			D3 S1358	TH01 (chr11)	D21 S11	D18 S51	Penta E (chr15)	D5 S818	D13 S317	D7 S820	D16 S539	CSF1PO (chr5)	Penta D (chr21)	Amel	vWA (chr12)	D8 S1179	TPOX (chr2)	FGA (chr4)
Reference profile from :	DSMZ	ACC 761		7,9.3				12	11	11,12	11,12	10,12		X,Y	17		8,12	

Sample data

Sample	OCILY3_FEM_Oct15	D3 S1358	TH01 (chr11)	D21 S11	D18 S51	Penta E (chr15)	D5 S818	D13 S317	D7 S820	D16 S539	CSF1PO (chr5)	Penta D (chr21)	Amel	vWA (chr12)	D8 S1179	TPOX (chr2)	FGA (chr4)
	GV05885A	14	7,9.3	28	17	7,11	12	11	11,12	11,12	10,12	9	X,Y	17	12,13	8,12	21,23
	GV05885B	14	7,9.3	28	17	7,11	12	11	11,12	11,12	10,12	9	X,Y	17	12,13	8,12	21,23

Samples are labelled using the format:
cell line name _ initials of lab head _ date of receipt or other unique identifier

Analysis

Sample match to reference	Matches DSMZ reference profile at 9/9 markers.	
DSMZdb	Matches OCILY3 (DSMZ ACC 761).	DSMZ STR profile database : http://www.dsmz.de/fp/cgi-bin/str.html (registration required). Searches 2455 cell lines from ATCC, DSMZ, JCRB & RIKEN.
CLIMAdb	Not done.	Cell line integrated molecular authentication (CLIMA) database http://bioinformatics.istge.it/clima/
CGP	Cell line not included in CGP dataset.	Cancer Genome Project STR data : http://www.sanger.ac.uk/research/projects/cancergenome/archive/ (registration required). Details of CGP data available only to registered users.
Comment		

Experimental data generated using Promega PowerPlex 16 system.

We recommend that a minimum of two profiles are generated for each sample, to control for PCR artefacts such as allele dropout. This is of particular importance when generating reference profiles of new cell lines for publication or for validation of differences to published profiles.

Figure 9-6: STR Profile results for OCI-LY3 cells

9.2 List of Suppliers

Applied Biosystems	Supplied by Fisher Scientific UK Ltd.
ATCC	American Type Culture Collection (ATCC), 10801 University Boulevard, Manassas, VA 20110 USA
Axis Shields	Axis Shield Diagnostics Ltd, Luna Place, The Technology Park, Dundee DD2 1XA, SCOTLAND
BD Biosciences	1030 Eskdale Road, Winnersh Triangle, Wokingham, Berkshire RG41 5TS
Beckman Coulter	Beckman Coulter (UK) Ltd, Oakley Court, Kingsmead Business Park, London Road, High Wycombe United Kingdom HP11 1JU
Biolegend	4B Highgate Business Centre, 33 Greenwood Place, London NW5 1LB, United Kingdom
Corning Costar	Distributed by Sigma Aldrich Ltd.
DSMZ	Inhoffenstraße 7B, 38124 Braunschweig, GERMANY
DuPont UK Ltd.	Du Pont (U.K.) Limited, Crop Protection Products, 4th Floor, Kings Court, London Road, Stevenage, Hertfordshire, SG1 2NG
eBioscience Ltd	2nd Floor, Titan Court, 3 Bishop Square, Hatfield, AL10 9NA,UK
Eppendorf	Supplied by Fisher Scientific UK Ltd.
Falcon	See BD Biosciences

Fisher Scientific UK Ltd.	Bishop Meadow Road, Loughborough, Leicestershire, LE11 5RG, UK
Gemini BV Laboratory	Prinses Beatrixlaan 301, 7312 DG Apeldoorn, Nederland
Hawksley	Hawksley, Marlborough Road, Lancing Business Park, Lancing, Sussex, BN15 8TN
Life technologies Ltd.	3 Fountain Drive, Inchinnan Business Park, Paisley, PA4 9RF, UK
Mabtech	Box 1233, SE-131 28 Nacka Strand, Sweden
Millipore (UK) Ltd.	Suite 3 & 5. Building 6. Croxley Green Business Park, Watford, WD18 8YH, UK
Miltenyi Biotec Ltd.	Almac House, Church Lane, Bisley, Surrey, GU24 9DR, UK
National Health Service Blood and Transplant	Bridle Path, Leeds, LS15 7TW, UK
NHS Supplies	Valley Point Valley Drive, Rugby , Warwickshire CV21 1TN, UK
NuAire Inc.	2100 Fernbrook Lane N Plymouth, MN 55447, USA
Nunc®	Distributed by Fisher Scientific

Olympus	KeyMed House, Stock Road, Southend-on-Sea, Essex, SS2 5QH, UK
Oncolytics Biotech Inc.	1167 Kensington Crescent NW Calgary, AB, Canada
Oxoid	Oxoid Ltd., Wade Road, Basingstoke, Hampshire, RG24 8PW, UK
Pharmingen	See BD Biosciences
Qiagen Ltd.	Boundary Court, Gatwick Road, Crawley, West Sussex, RH10 2AX,
R & D Systems Europe Ltd.	19 Barton Lane, Abingdon Science Park, Abingdon,OX14 3NB, UK
Santa Cruz Biotechnology Inc.	Supplied by Insight Biotechnology
Sanyo	Sanyo Gallenkamp Plc., Monarch Way, Belton Park, Loughborough, LE11 5XG, UK
Scientific Laboratory Supplies	Wilford Industrial Estate, Ruddington Lane, Wilford, Nottingham, NG11
Selleckchem	Cambridge House, St Thomas' Place Cambridgeshire Business Park, Ely CB7 4EX, UK
Sigma-Aldrich Ltd.	Sigma Chemical Company, Fancy Road, Poole, Dorset, BH17 7NH, UK
Swann-Morton	Supplied by NHS Supplies

Thermo Fisher Scientific	Unit 5, The Ringway Centre, Edison Rd., Basingstoke, Hampshire, RG21 6YH, UK
Tristel Solutions Ltd	1B, Lynx Business Park, Fordham Road, Snailwell, Fordham, Newmarket CB8 7NY
VWR International Ltd.	Hunter Boulevard, Magna Park, Lutterworth, Leicestershire, LE17 4XN, UK

Chapter 10:
References

Chapter 10

Adair, R.A., Roulstone, V., Scott, K.J., Morgan, R., Nuovo, G.J., Fuller, M., Beirne, D., West, E.J., Jennings, V.A., Rose, A., Kyula, J., Fraser, S., Dave, R., Anthoney, D.A., Merrick, A., Prestwich, R., Aldouri, A., Donnelly, O., Pandha, H., Coffey, M., Selby, P., Vile, R., Toogood, G., Harrington, K. and Melcher, A.A. 2012. Cell carriage, delivery, and selective replication of an oncolytic virus in tumor in patients. *Sci Transl Med.* **4**(138), p138ra177.
Adair, R.A., Scott, K.J., Fraser, S., Errington-Mais, F., Pandha, H., Coffey, M., Selby, P., Cook, G.P., Vile, R., Harrington, K.J., Toogood, G. and Melcher, A.A. 2013. Cytotoxic and immune-mediated killing of human colorectal cancer by reovirus-loaded blood and liver mononuclear cells. *Int J Cancer.* **132**(10), pp.2327-2338.
Ahuja, H., Foti, A., Bar-Eli, M. and Cline, M. 1990. The pattern of mutational involvement of RAS genes in human hematologic malignancies determined by DNA amplification and direct sequencing. *Blood.* **75**(8), pp.1684-1690.
Alain, T., Hirasawa, K., Pon, K.J., Nishikawa, S.G., Urbanski, S.J., Auer, Y., Luider, J., Martin, A., Johnston, R.N., Janowska-Wieczorek, A., Lee, P.W. and Kossakowska, A.E. 2002. Reovirus therapy of lymphoid malignancies. *Blood.* **100**(12), pp.4146-4153.
Alain, T., Kim, T.S., Lun, X., Liacini, A., Schiff, L.A., Senger, D.L. and Forsyth, P.A. 2007. Proteolytic disassembly is a critical determinant for reovirus oncolysis. *Mol Ther.* **15**(8), pp.1512-1521.
Alizadeh, A.A., Eisen, M.B., Davis, R.E., Ma, C., Lossos, I.S., Rosenwald, A., Boldrick, J.C., Sabet, H., Tran, T., Yu, X., Powell, J.I., Yang, L., Marti, G.E., Moore, T., Hudson, J., Jr., Lu, L., Lewis, D.B., Tibshirani, R., Sherlock, G., Chan, W.C., Greiner, T.C., Weisenburger, D.D., Armitage, J.O., Warnke, R., Levy, R., Wilson, W., Grever, M.R., Byrd, J.C., Botstein, D., Brown, P.O. and Staudt, L.M. 2000. Distinct types of diffuse large B-cell lymphoma identified by gene expression profiling. *Nature.* **403**(6769), pp.503-511.
Alkayyal, A.A., Tai, L.-H., Kennedy, M.A., de Souza, C.T., Zhang, J., Lefebvre, C., Sahi, S., Ananth, A.A., Mahmoud, A.B., Makrigiannis, A.P., Cron, G.O., Macdonald, B., Marginean, E.C., Stojdl, D.F., Bell, J.C. and Auer, R.C. 2017. NK-Cell Recruitment Is Necessary for Eradication of Peritoneal Carcinomatosis with an IL12-Expressing Maraba Virus Cellular Vaccine. *Cancer Immunology Research.* **5**(3), pp.211-221.
Alvaro-Naranjo, T., Jaen-Martinez, J., Guma-Padro, J., Bosch-Princep, R. and Salvado-Usach, M.T. 2003. CD20-negative DLBCL transformation after rituximab treatment in follicular lymphoma: a new case report and review of the literature. *Ann Hematol.* **82**(9), pp.585-588.
American Cancer Society. 2017. Types of Non-Hodgkin Lymphoma.
Amini, R.M., Berglund, M., Rosenquist, R., Von Heideman, A., Lagercrantz, S., Thunberg, U., Bergh, J., Sundstrom, C., Glimelius, B. and Enblad, G. 2002. A novel B-cell line (U-2932) established from a patient with diffuse large B-cell lymphoma following Hodgkin lymphoma. *Leuk Lymphoma.* **43**(11), pp.2179-2189.
Anatomyorgan. 2017. Mouse Anatomy Diagram.

Andrews, P.S.a.P., Fiona and Sampson, Adam T. and Scott, Lisa and Coles, Mark. 2008. Simulating biology: towards understanding what the simulation shows. *Proceedings of the 2008 Workshop on Complex Systems Modelling and Simulation, York, UK, September 2008.*
Andtbacka, R.H., Curti, B.D., Hallmeyer, S., Feng, Z., Paustian, C., Bifulco, C., Fox, B., Grose, M. and Shafren, D. 2015. Phase II calm extension study: Coxsackievirus A21 delivered intratumorally to patients with advanced melanoma induces immune-cell infiltration in the tumor microenvironment. *Journal for ImmunoTherapy of Cancer.* **3**(2), pP343.
Angelova, A.L., Witzens-Harig, M., Galabov, A.S. and Rommelaere, J. 2017. The Oncolytic Virotherapy Era in Cancer Management: Prospects of Applying H-1 Parvovirus to Treat Blood and Solid Cancers. *Front Oncol.* **7**, p93.
Ann W. Silk, H.L.K., Mark Faries, Steven O'Day, Nashat Gabrail, Janice Mehnert, Jennifer Bryan, Jacqueline Norrell, Azra Haider, Praveen K. Bommareddy, Darren Shafren, Mark Grose and Andrew Zloza. 2017. CAPRA: A Phase Ib study of intratumoral oncolytic Coxsackievirus A21 (CVA21) and systemic pembrolizumab in advanced melanoma patients. *Society for Immunotherapy of Cancer – 32nd Annual Meeting.*
Annels, N.E., Arif, M., Simpson, G.R., Denyer, M., Moller-Levet, C., Mansfield, D., Butler, R., Shafren, D., Au, G., Knowles, M., Harrington, K., Vile, R., Melcher, A. and Pandha, H. 2018. Oncolytic Immunotherapy for Bladder Cancer Using Coxsackie A21 Virus. *Molecular Therapy - Oncolytics.* **9**, pp.1-12.
Ansell, S.M. 2015. Non-Hodgkin Lymphoma: Diagnosis and Treatment. *Mayo Clin Proc.* **90**(8), pp.1152-1163.
Arase, H., Arase, N. and Saito, T. 1996. Interferon gamma production by natural killer (NK) cells and NK1.1+ T cells upon NKR-P1 cross-linking. *J Exp Med.* **183**(5), pp.2391-2396.
Arellano-Garcia, M.E., Misuno, K., Tran, S.D. and Hu, S. 2014. Interferon-γ Induces Immunoproteasomes and the Presentation of MHC I-Associated Peptides on Human Salivary Gland Cells. *PLOS ONE.* **9**(8), pe102878.
Armitage, J.O. and Weisenburger, D.D. 1998. New approach to classifying non-Hodgkin's lymphomas: clinical features of the major histologic subtypes. Non-Hodgkin's Lymphoma Classification Project. *J Clin Oncol.* **16**(8), pp.2780-2795.
ATCC. 2017. Human Coxsackievirus A 21 (ATCC® VR-850™)
Atzeni, F., Schena, M., Ongari, A.M., Carrabba, M., Bonara, P., Minonzio, F. and Capsoni, F. 2002. Induction of CD69 activation molecule on human neutrophils by GM-CSF, IFN-gamma, and IFN-alpha. *Cell Immunol.* **220**(1), pp.20-29.
Au, G.G., Lincz, L.F., Enno, A. and Shafren, D.R. 2007. Oncolytic Coxsackievirus A21 as a novel therapy for multiple myeloma. *Br J Haematol.* **137**(2), pp.133-141.
Au, G.G., Lindberg, A.M., Barry, R.D. and Shafren, D.R. 2005. Oncolysis of vascular malignant human melanoma tumors by Coxsackievirus A21. *Int J Oncol.* **26**(6), pp.1471-1476.
Aurelian, L. 2016. Oncolytic viruses as immunotherapy: progress and remaining challenges. *Onco Targets Ther.* **9**, pp.2627-2637.
Baig, S., Seevasant, I., Mohamad, J., Mukheem, A., Huri, H.Z. and Kamarul, T. 2016. Potential of apoptotic pathway-targeted cancer therapeutic research: Where do we stand? *Cell Death & Disease.* **7**(1), pe2058.

Bajenoff, M., Breart, B., Huang, A.Y., Qi, H., Cazareth, J., Braud, V.M., Germain, R.N. and Glaichenhaus, N. 2006. Natural killer cell behavior in lymph nodes revealed by static and real-time imaging. *J Exp Med.* **203**(3), pp.619-631.
Barnes, J.A., Lacasce, A.S., Feng, Y., Toomey, C.E., Neuberg, D., Michaelson, J.S., Hochberg, E.P. and Abramson, J.S. 2011. Evaluation of the addition of rituximab to CODOX-M/IVAC for Burkitt's lymphoma: a retrospective analysis. *Ann Oncol.* **22**(8), pp.1859-1864.
Bartee, E., Bartee, M.Y., Bogen, B. and Yu, X.Z. 2016. Systemic therapy with oncolytic myxoma virus cures established residual multiple myeloma in mice. *Mol Ther Oncolytics.* **3**, p16032.
Basso, K. and Dalla-Favera, R. 2012. Roles of BCL6 in normal and transformed germinal center B cells. *Immunol Rev.* **247**(1), pp.172-183.
Batenchuk, C., Le Boeuf, F., Stubbert, L., Falls, T., Atkins, H.L., Bell, J.C. and Conrad, D.P. 2013. Non-replicating rhabdovirus-derived particles (NRRPs) eradicate acute leukemia by direct cytolysis and induction of antitumor immunity. *Blood Cancer Journal.* **3**, pe123.
Bauzon, M. and Hermiston, T. 2014. Armed therapeutic viruses - a disruptive therapy on the horizon of cancer immunotherapy. *Front Immunol.* **5**, p74.
Beider, K., Ribakovsky, E., Abraham, M., Wald, H., Weiss, L., Rosenberg, E., Galun, E., Avigdor, A., Eizenberg, O., Peled, A. and Nagler, A. 2013. Targeting the CD20 and CXCR4 pathways in non-hodgkin lymphoma with rituximab and high-affinity CXCR4 antagonist BKT140. *Clin Cancer Res.* **19**(13), pp.3495-3507.
Bellesso, M., Xavier, F.D., Costa, R.O., Pereira, J., Siqueira, S.A. and Chamone, D.A. 2011. Disease progression after R-CHOP treatment associated with the loss of CD20 antigen expression. *Rev Bras Hematol Hemoter.* **33**(2), pp.148-150.
Benlahrech, A., Donaghy, H., Rozis, G., Goodier, M., Klavinskis, L., Gotch, F. and Patterson, S. 2009. Human NK Cell Up-regulation of CD69, HLA-DR, Interferon gamma Secretion and Cytotoxic Activity by Plasmacytoid Dendritic Cells is Regulated through Overlapping but Different Pathways. *Sensors (Basel).* **9**(1), pp.386-403.
Beretta, L., Svitkin, Y.V. and Sonenberg, N. 1996. Rapamycin stimulates viral protein synthesis and augments the shutoff of host protein synthesis upon picornavirus infection. *J Virol.* **70**(12), pp.8993-8996.
Berget, E., Helgeland, L., Liseth, K., Lokeland, T., Molven, A. and Vintermyr, O.K. 2014. Prognostic value of bone marrow involvement by clonal immunoglobulin gene rearrangements in follicular lymphoma. *J Clin Pathol.* **67**(12), pp.1072-1077.
Bernard Mach, Viktor Steimle, Eduardo Martinez-Soria, a. and Reith, W. 1996. REGULATION OF MHC CLASS II GENES: Lessons from a Disease. *Annual Review of Immunology.* **14**(1), pp.301-331.
Berry, L.J., Au, G.G., Barry, R.D. and Shafren, D.R. 2008. Potent oncolytic activity of human enteroviruses against human prostate cancer. *Prostate.* **68**(6), pp.577-587.
Beuneu, H., Deguine, J., Breart, B., Mandelboim, O., Di Santo, J.P. and Bousso, P. 2009. Dynamic behavior of NK cells during activation in lymph nodes. *Blood.* **114**(15), pp.3227-3234.

Bhat, R., Dempe, S., Dinsart, C. and Rommelaere, J. 2011. Enhancement of NK cell antitumor responses using an oncolytic parvovirus. *Int J Cancer.* **128**(4), pp.908-919.
Bhat, R. and Rommelaere, J. 2015. Emerging role of Natural killer cells in oncolytic virotherapy. *Immunotargets Ther.* **4**, pp.65-77.
Bhatt, A.P., Bhende, P.M., Sin, S.H., Roy, D., Dittmer, D.P. and Damania, B. 2010. Dual inhibition of PI3K and mTOR inhibits autocrine and paracrine proliferative loops in PI3K/Akt/mTOR-addicted lymphomas. *Blood.* **115**(22), pp.4455-4463.
Black, L.R. and Aiken, C. 2010. TRIM5alpha disrupts the structure of assembled HIV-1 capsid complexes in vitro. *J Virol.* **84**(13), pp.6564-6569.
Borge, M., Belen Almejun, M., Podaza, E., Colado, A., Fernandez Grecco, H., Cabrejo, M., Bezares, R.F., Giordano, M. and Gamberale, R. 2015. Ibrutinib impairs the phagocytosis of rituximab-coated leukemic cells from chronic lymphocytic leukemia patients by human macrophages. *Haematologica.* **100**(4), pp.e140-142.
Bos, J.L. 1989. ras oncogenes in human cancer: a review. *Cancer Res.* **49**(17), pp.4682-4689.
Bottino, C., Castriconi, R., Pende, D., Rivera, P., Nanni, M., Carnemolla, B., Cantoni, C., Grassi, J., Marcenaro, S., Reymond, N., Vitale, M., Moretta, L., Lopez, M. and Moretta, A. 2003. Identification of PVR (CD155) and Nectin-2 (CD112) as cell surface ligands for the human DNAM-1 (CD226) activating molecule. *J Exp Med.* **198**(4), pp.557-567.
Bradley, S., Jakes, A.D., Harrington, K., Pandha, H., Melcher, A. and Errington-Mais, F. 2014. Applications of coxsackievirus A21 in oncology. *Oncolytic Virother.* **3**, pp.47-55.
Brady, G., MacArthur, G.J. and Farrell, P.J. 2007. Epstein-Barr virus and Burkitt lymphoma. *J Clin Pathol.* **60**(12), pp.1397-1402.
Brandstadter, J.D. and Yang, Y. 2011. Natural killer cell responses to viral infection. *J Innate Immun.* **3**(3), pp.274-279.
Breitbach, C.J., De Silva, N.S., Falls, T.J., Aladl, U., Evgin, L., Paterson, J., Sun, Y.Y., Roy, D.G., Rintoul, J.L., Daneshmand, M., Parato, K., Stanford, M.M., Lichty, B.D., Fenster, A., Kirn, D., Atkins, H. and Bell, J.C. 2011. Targeting tumor vasculature with an oncolytic virus. *Mol Ther.* **19**(5), pp.886-894.
Bruu, D.A.L. 2013. Enteroviruses: Polioviruses, Coxsackieviruses, Echoviruses and Newer Enteroviruses. *A Practical Guide to Clinical Virology.*
Buchmeier, N.A. and Schreiber, R.D. 1985. Requirement of endogenous interferon-gamma production for resolution of Listeria monocytogenes infection. *Proceedings of the National Academy of Sciences.* **82**(21), pp.7404-7408.
Bundscherer, A., Hafner, C., Maisch, T., Becker, B., Landthaler, M. and Vogt, T. 2008. Antiproliferative and proapoptotic effects of rapamycin and celecoxib in malignant melanoma cell lines. *Oncol Rep.* **19**(2), pp.547-553.
Cai, J., Lin, Y., Zhang, H., Liang, J., Tan, Y. and Cavenee, W.K. 2017. Selective replication of oncolytic virus M1 results in a bystander killing effect that is potentiated by Smac mimetics. **114**(26), pp.6812-6817.
Campbell, J.A., Schelling, P., Wetzel, J.D., Johnson, E.M., Forrest, J.C., Wilson, G.A., Aurrand-Lions, M., Imhof, B.A., Stehle, T. and Dermody, T.S. 2005. Junctional adhesion molecule a serves as a receptor for prototype and field-isolate strains of mammalian reovirus. *J Virol.* **79**(13), pp.7967-7978.

Castleton, A., Dey, A., Beaton, B., Patel, B., Aucher, A., Davis, D.M. and Fielding, A.K. 2014. Human mesenchymal stromal cells deliver systemic oncolytic measles virus to treat acute lymphoblastic leukemia in the presence of humoral immunity. *Blood.* **123**(9), pp.1327-1335.
Chao, M.P. 2013. Treatment challenges in the management of relapsed or refractory non-Hodgkin's lymphoma - novel and emerging therapies. *Cancer Manag Res.* **5**, pp.251-269.
Chawla-Sarkar, M., Lindner, D.J., Liu, Y.F., Williams, B.R., Sen, G.C., Silverman, R.H. and Borden, E.C. 2003. Apoptosis and interferons: role of interferon-stimulated genes as mediators of apoptosis. *Apoptosis.* **8**(3), pp.237-249.
Cheema, T.A., Wakimoto, H., Fecci, P.E., Ning, J., Kuroda, T., Jeyaretna, D.S., Martuza, R.L. and Rabkin, S.D. 2013. Multifaceted oncolytic virus therapy for glioblastoma in an immunocompetent cancer stem cell model. *Proceedings of the National Academy of Sciences.* **110**(29), pp.12006-12011.
Chen, Z., Yang, L., Liu, Y., Tang, A., Li, X., Zhang, J. and Yang, Z. 2014. LY294002 and Rapamycin promote coxsackievirus-induced cytopathic effect and apoptosis via inhibition of PI3K/AKT/mTOR signaling pathway. *Mol Cell Biochem.* **385**(1-2), pp.169-177.
Cheng, X., Wang, W., Xu, Q., Harper, J., Carroll, D., Galinski, M.S., Suzich, J. and Jin, H. 2016. Genetic Modification of Oncolytic Newcastle Disease Virus for Cancer Therapy. *J Virol.* **90**(11), pp.5343-5352.
Choo, A.Y., Yoon, S.O., Kim, S.G., Roux, P.P. and Blenis, J. 2008. Rapamycin differentially inhibits S6Ks and 4E-BP1 to mediate cell-type-specific repression of mRNA translation. *Proc Natl Acad Sci U S A.* **105**(45), pp.17414-17419.
Ciobanu, A., Stanca, O., Triantafyllidis, I. and Lupu, A. 2013. Indolent lymphoma: diagnosis and prognosis in medical practice. *Maedica (Buchar).* **8**(4), pp.338-342.
ClinicalTrials.gov. 2014. Intratumoral CAVATAK (CVA21) and Ipilimumab in Patients With Advanced Melanoma (VLA-013 MITCI) (MITCI).
ClinicalTrials.gov. 2015a. Intratumoral CAVATAK (CVA21) and Pembrolizumab in Patients With Advanced Melanoma (VLA-011 CAPRA) (CAPRA).
ClinicalTrials.gov. 2015b. Study of Pembrolizumab With REOLYSIN® and Chemotherapy in Patients With Advanced Pancreatic Adenocarcinoma.
ClinicalTrials.gov. 2015c. Wild-Type Reovirus, Bortezomib, and Dexamethasone in Treating Patients With Relapsed or Refractory Multiple Myeloma.
ClinicalTrials.gov. 2016. Pembrolizumab + CVA21 in Advanced NSCLC.
ClinicalTrials.gov. 2017a. A Phase I/II Study of Pexa-Vec Oncolytic Virus in Combination With Immune Checkpoint Inhibition in Refractory Colorectal Cancer.
ClinicalTrials.gov. 2017b. A Study of Recombinant Vaccinia Virus in Combination With REGN2810 for Renal Cell Carcinoma.
ClinicalTrials.gov. 2017c. Viral Immunotherapy in Relapsed/Refractory Multiple Myeloma (MUKeleven).
Clodi, K., Asgary, Z., Zhao, S., Kliche, K.O., Cabanillas, F., Andreeff, M. and Younes, A. 1998a. Coexpression of CD40 and CD40 ligand in B-cell lymphoma cells. *Br J Haematol.* **103**(1), pp.270-275.

Clodi, K., Snell, V., Zhao, S., Cabanillas, F., Andreeff, M. and Younes, A. 1998b. Unbalanced expression of Fas and CD40 in mantle cell lymphoma. *Br J Haematol.* **103**(1), pp.217-219.
Colamonici, O.R., Domanski, P., Sweitzer, S.M., Larner, A. and Buller, R.M. 1995. Vaccinia virus B18R gene encodes a type I interferon-binding protein that blocks interferon alpha transmembrane signaling. *J Biol Chem.* **270**(27), pp.15974-15978.
Comins, C., Simpson, G.R., Rogers, W., Relph, K., Harrington, K., Melcher, A., Roulstone, V., Kyula, J. and Pandha, H. 2018. Synergistic antitumour effects of rapamycin and oncolytic reovirus. *Cancer Gene Therapy.* **25**(5), pp.148-160.
Comins, C., Spicer, J., Protheroe, A., Roulstone, V., Twigger, K., White, C.M., Vile, R., Melcher, A., Coffey, M.C., Mettinger, K.L., Nuovo, G., Cohn, D.E., Phelps, M., Harrington, K.J. and Pandha, H.S. 2010. REO-10: a phase I study of intravenous reovirus and docetaxel in patients with advanced cancer. *Clin Cancer Res.* **16**(22), pp.5564-5572.
Compagno, M., Lim, W.K., Grunn, A., Nandula, S.V., Brahmachary, M., Shen, Q., Bertoni, F., Ponzoni, M., Scandurra, M., Califano, A., Bhagat, G., Chadburn, A., Dalla-Favera, R. and Pasqualucci, L. 2009. Mutations of multiple genes cause deregulation of NF-kappaB in diffuse large B-cell lymphoma. *Nature.* **459**(7247), pp.717-721.
Correia, C., Schneider, P.A., Dai, H., Dogan, A., Maurer, M.J., Church, A.K., Novak, A.J., Feldman, A.L., Wu, X., Ding, H., Meng, X.W., Cerhan, J.R., Slager, S.L., Macon, W.R., Habermann, T.M., Karp, J.E., Gore, S.D., Kay, N.E., Jelinek, D.F., Witzig, T.E., Nowakowski, G.S. and Kaufmann, S.H. 2015. BCL2 mutations are associated with increased risk of transformation and shortened survival in follicular lymphoma. *Blood.* **125**(4), pp.658-667.
Critchley-Thorne, R.J., Simons, D.L., Yan, N., Miyahira, A.K., Dirbas, F.M., Johnson, D.L., Swetter, S.M., Carlson, R.W., Fisher, G.A., Koong, A., Holmes, S. and Lee, P.P. 2009. Impaired interferon signaling is a common immune defect in human cancer. *Proc Natl Acad Sci U S A.* **106**(22), pp.9010-9015.
CRUK. 2018. Non-Hodgkin lymphoma incidence statistics.
Davis, R.E., Brown, K.D., Siebenlist, U. and Staudt, L.M. 2001. Constitutive nuclear factor kappaB activity is required for survival of activated B cell-like diffuse large B cell lymphoma cells. *J Exp Med.* **194**(12), pp.1861-1874.
De Paepe, P. and De Wolf-Peeters, C. 2007. Diffuse large B-cell lymphoma: a heterogeneous group of non-Hodgkin lymphomas comprising several distinct clinicopathological entities. *Leukemia.* **21**(1), pp.37-43.
de Souza, A.P., de Freitas, D.N., Antuntes Fernandes, K.E., D'Avila da Cunha, M., Antunes Fernandes, J.L., Benetti Gassen, R., Fazolo, T., Pinto, L.A., Scotta, M., Mattiello, R., Pitrez, P.M., Bonorino, C. and Stein, R.T. 2016. Respiratory syncytial virus induces phosphorylation of mTOR at ser2448 in CD8 T cells from nasal washes of infected infants. *Clin Exp Immunol.* **183**(2), pp.248-257.
Deng, H., Tang, N., Stief, A.E., Mehta, N., Baig, E., Head, R., Sleep, G., Yang, X.Z., McKerlie, C., Trudel, S., Stewart, A.K. and McCart, J.A. 2008. Oncolytic virotherapy for multiple myeloma using a tumour-specific double-deleted vaccinia virus. *Leukemia.* **22**(12), pp.2261-2264.
Deonarain, R., Cerullo, D., Fuse, K., Liu, P.P. and Fish, E.N. 2004. Protective Role for Interferon-β in Coxsackievirus B3 Infection. *Circulation.* **110**(23), pp.3540-3543.

Devasthanam, A.S. 2014. Mechanisms underlying the inhibition of interferon signaling by viruses. *Virulence.* **5**(2), pp.270-277.
Diacovo, T.G., Blasius, A.L., Mak, T.W., Cella, M. and Colonna, M. 2005. Adhesive mechanisms governing interferon-producing cell recruitment into lymph nodes. *J Exp Med.* **202**(5), pp.687-696.
Diaz-San Segundo, F., Moraes, M.P., de Los Santos, T., Dias, C.C. and Grubman, M.J. 2010. Interferon-induced protection against foot-and-mouth disease virus infection correlates with enhanced tissue-specific innate immune cell infiltration and interferon-stimulated gene expression. *J Virol.* **84**(4), pp.2063-2077.
Ding, Y., Shan, L., Nai, W., Lin, X., Zhou, L., Dong, X., Wu, H., Xiao, M., Zhou, X., Wang, L., Li, T., Fu, Y., Lin, Y., Jia, C., Dai, M. and Bai, X. 2018. DEPTOR Deficiency-Mediated mTORc1 Hyperactivation in Vascular Endothelial Cells Promotes Angiogenesis. *Cell Physiol Biochem.* **46**(2), pp.520-531.
Dock, G., Brothers, L. and Company. 1904. *The Influence of Complicating Diseases Upon Leukaemia.* Lea Brothers & Company.
Donnelly, O.G., Errington-Mais, F., Steele, L., Hadac, E., Jennings, V., Scott, K., Peach, H., Phillips, R.M., Bond, J., Pandha, H., Harrington, K., Vile, R., Russell, S., Selby, P. and Melcher, A.A. 2013. Measles virus causes immunogenic cell death in human melanoma. *Gene therapy.* **20**(1), pp.7-15.
Dorff, T.B. and Crawford, E.D. 2013. Management and challenges of corticosteroid therapy in men with metastatic castrate-resistant prostate cancer. *Ann Oncol.* **24**(1), pp.31-38.
Dormond, O., Contreras, A.G., Meijer, E., Datta, D., Flynn, E., Pal, S. and Briscoe, D.M. 2008. CD40-induced signaling in human endothelial cells results in mTORC2- and Akt-dependent expression of vascular endothelial growth factor in vitro and in vivo. *J Immunol.* **181**(11), pp.8088-8095.
Dotzauer, A. and Kraemer, L. 2012. Innate and adaptive immune responses against picornaviruses and their counteractions: An overview. *World J Virol.* **1**(3), pp.91-107.
Douville, R.N., Su, R.C., Coombs, K.M., Simons, F.E. and Hayglass, K.T. 2008. Reovirus serotypes elicit distinctive patterns of recall immunity in humans. *J Virol.* **82**(15), pp.7515-7523.
Downward, J. 2003. Targeting RAS signalling pathways in cancer therapy. *Nat Rev Cancer.* **3**(1), pp.11-22.
Drakos, E., Singh, R.R., Rassidakis, G.Z., Schlette, E., Li, J., Claret, F.X., Ford, R.J., Jr., Vega, F. and Medeiros, L.J. 2011. Activation of the p53 pathway by the MDM2 inhibitor nutlin-3a overcomes BCL2 overexpression in a preclinical model of diffuse large B-cell lymphoma associated with t(14;18)(q32;q21). *Leukemia.* **25**(5), pp.856-867.
Duan, X., Lu, J., Wang, H., Liu, X., Wang, J., Zhou, K., Jiang, W., Wang, Y. and Fang, M. 2017. Bidirectional factors impact the migration of NK cells to draining lymph node in aged mice during influenza virus infection. *Exp Gerontol.* **96**, pp.127-137.
Duncan, M.R., Stanish, S.M. and Cox, D.C. 1978. Differential sensitivity of normal and transformed human cells to reovirus infection. *Journal of Virology.* **28**(2), pp.444-449.
Eigl, B.J., Winquist, E., Tu, D., Hotte, S.J., Canil, C.M., Gregg, R.W., Zulfiqar, M., North, S.A., Ellard, S., Ruether, J.D., Le, L.H., Kakumanu, A.S., Theis, A., Booth, C.M., Potvin, K.R., Chi, K.N. and Seymour, L. 2017. A randomized

phase II study of pelareorep (REO) plus docetaxel vs. docetaxel alone in patients with metastatic castration resistant prostate cancer (mCRPC): Canadian Cancer Trials Group study IND 209. *Journal of Clinical Oncology.* **35**(15_suppl), pp.5021-5021.
El-Serafi, I., Abedi-Valugerdi, M., Potacova, Z., Afsharian, P., Mattsson, J., Moshfegh, A. and Hassan, M. 2014. Cyclophosphamide alters the gene expression profile in patients treated with high doses prior to stem cell transplantation. *PLoS One.* **9**(1), pe86619.
Elankumaran, S., Chavan, V., Qiao, D., Shobana, R., Moorkanat, G., Biswas, M. and Samal, S.K. 2010. Type I interferon-sensitive recombinant newcastle disease virus for oncolytic virotherapy. *J Virol.* **84**(8), pp.3835-3844.
Elgueta, R., Benson, M.J., de Vries, V.C., Wasiuk, A., Guo, Y. and Noelle, R.J. 2009. Molecular mechanism and function of CD40/CD40L engagement in the immune system. *Immunol Rev.* **229**(1), pp.152-172.
Elmore, S. 2007. Apoptosis: A Review of Programmed Cell Death. *Toxicologic pathology.* **35**(4), pp.495-516.
Errington, F., White, C.L., Twigger, K.R., Rose, A., Scott, K., Steele, L., Ilett, L.J., Prestwich, R., Pandha, H.S., Coffey, M., Selby, P., Vile, R., Harrington, K.J. and Melcher, A.A. 2008. Inflammatory tumour cell killing by oncolytic reovirus for the treatment of melanoma. *Gene Ther.* **15**(18), pp.1257-1270.
Erum Naqvi, I.-O.N. 2013. Reolysin.
Esfandyari, T., Tefferi, A., Szmidt, A., Alain, T., Zwolak, P., Lasho, T., Lee, P.W. and Farassati, F. 2009. Transcription factors down-stream of Ras as molecular indicators for targeting malignancies with oncolytic herpes virus. *Mol Oncol.* **3**(5-6), pp.464-468.
Faller, W.J., Jackson, T.J., Knight, J.R., Ridgway, R.A., Jamieson, T., Karim, S.A., Jones, C., Radulescu, S., Huels, D.J., Myant, K.B., Dudek, K.M., Casey, H.A., Scopelliti, A., Cordero, J.B., Vidal, M., Pende, M., Ryazanov, A.G., Sonenberg, N., Meyuhas, O., Hall, M.N., Bushell, M., Willis, A.E. and Sansom, O.J. 2015. mTORC1-mediated translational elongation limits intestinal tumour initiation and growth. *Nature.* **517**(7535), pp.497-500.
Federica, Z., Paolo, M., Roberta, B., Daniele, S., Roberto, M. and Francesco, T. 2005. Controlling complement resistance in cancer by using human monoclonal antibodies that neutralize complement-regulatory proteins CD55 and CD59. *European Journal of Immunology.* **35**(7), pp.2175-2183.
Ferguson, M.S., Lemoine, N.R. and Wang, Y. 2012. Systemic delivery of oncolytic viruses: hopes and hurdles. *Adv Virol.* **2012**, p805629.
Fields, P.A. and Wrench, D.J. 2015. Assessing risk and improving survival in lymphoma. *Br J Gen Pract.* **65**(634), pp.220-221.
Filley, A.C. and Dey, M. 2017. Immune System, Friend or Foe of Oncolytic Virotherapy? *Front Oncol.* **7**, p106.
Fiola, C., Peeters, B., Fournier, P., Arnold, A., Bucur, M. and Schirrmacher, V. 2006. Tumor selective replication of Newcastle disease virus: association with defects of tumor cells in antiviral defence. *Int J Cancer.* **119**(2), pp.328-338.
Fiore, F., Von Bergwelt-Baildon, M.S., Drebber, U., Beyer, M., Popov, A., Manzke, O., Wickenhauser, C., Baldus, S.E. and Schultze, J.L. 2006. Dendritic cells are significantly reduced in non-Hodgkin's lymphoma and express less CCR7 and CD62L. *Leukemia & Lymphoma.* **47**(4), pp.613-622.
Fitzgerald-Bocarsly, P. 2002. Natural interferon-alpha producing cells: the plasmacytoid dendritic cells. *Biotechniques.* **Suppl**, pp.16-20, 22, 24-19.

Fitzsimmons, L., Boyce, A.J., Wei, W., Chang, C., Croom-Carter, D., Tierney, R.J., Herold, M.J., Bell, A.I., Strasser, A., Kelly, G.L. and Rowe, M. 2017. Coordinated repression of BIM and PUMA by Epstein–Barr virus latent genes maintains the survival of Burkitt lymphoma cells. *Cell Death And Differentiation.* **25**, p241.
Fogel, L.A., Sun, M.M., Geurs, T.L., Carayannopoulos, L.N. and French, A.R. 2013. Markers of Nonselective and Specific NK Cell Activation. *The Journal of Immunology.* **190**(12), pp.6269-6276.
Forsyth, P., Roldan, G., George, D., Wallace, C., Palmer, C.A., Morris, D., Cairncross, G., Matthews, M.V., Markert, J., Gillespie, Y., Coffey, M., Thompson, B. and Hamilton, M. 2008. A phase I trial of intratumoral administration of reovirus in patients with histologically confirmed recurrent malignant gliomas. *Mol Ther.* **16**(3), pp.627-632.
Gagez, A.L. and Cartron, G. 2014. Obinutuzumab: a new class of anti-CD20 monoclonal antibody. *Curr Opin Oncol.* **26**(5), pp.484-491.
Galanis, E., Markovic, S.N., Suman, V.J., Nuovo, G.J., Vile, R.G., Kottke, T.J., Nevala, W.K., Thompson, M.A., Lewis, J.E., Rumilla, K.M., Roulstone, V., Harrington, K., Linette, G.P., Maples, W.J., Coffey, M., Zwiebel, J. and Kendra, K. 2012. Phase II trial of intravenous administration of Reolysin((R)) (Reovirus Serotype-3-dearing Strain) in patients with metastatic melanoma. *Mol Ther.* **20**(10), pp.1998-2003.
Galizia, G., Lieto, E., De Vita, F., Orditura, M., Castellano, P., Troiani, T., Imperatore, V. and Ciardiello, F. 2007. Cetuximab, a chimeric human mouse anti-epidermal growth factor receptor monoclonal antibody, in the treatment of human colorectal cancer. *Oncogene.* **26**(25), pp.3654-3660.
Godeny, E.K. and Gauntt, C.J. 1987. Interferon and natural killer cell activity in coxsackie virus B3-induced murine myocarditis. *European Heart Journal.* **8**(suppl_J), pp.433-435.
Gollamudi, R., Ghalib, M.H., Desai, K.K., Chaudhary, I., Wong, B., Einstein, M., Coffey, M., Gill, G.M., Mettinger, K., Mariadason, J.M., Mani, S. and Goel, S. 2010. Intravenous administration of Reolysin, a live replication competent RNA virus is safe in patients with advanced solid tumors. *Invest New Drugs.* **28**(5), pp.641-649.
Good, D.J. and Gascoyne, R.D. 2008. Classification of non-Hodgkin's lymphoma. *Hematol Oncol Clin North Am.* **22**(5), pp.781-805, vii.
Groninger, E., Meeuwsen-De Boer, G.J., De Graaf, S.S., Kamps, W.A. and De Bont, E.S. 2002. Vincristine induced apoptosis in acute lymphoblastic leukaemia cells: a mitochondrial controlled pathway regulated by reactive oxygen species? *Int J Oncol.* **21**(6), pp.1339-1345.
Grote, D., Russell, S.J., Cornu, T.I., Cattaneo, R., Vile, R., Poland, G.A. and Fielding, A.K. 2001. Live attenuated measles virus induces regression of human lymphoma xenografts in immunodeficient mice. *Blood.* **97**(12), pp.3746-3754.
Gu, L., Xie, L., Zuo, C., Ma, Z., Zhang, Y., Zhu, Y. and Gao, J. 2015. Targeting mTOR/p70S6K/glycolysis signaling pathway restores glucocorticoid sensitivity to 4E-BP1 null Burkitt Lymphoma. *BMC Cancer.* **15**, p529.
Gu, Y., Albuquerque, C.P., Braas, D., Zhang, W., Villa, G.R., Bi, J., Ikegami, S., Masui, K., Gini, B., Yang, H., Gahman, T.C., Shiau, A.K., Cloughesy, T.F., Christofk, H.R., Zhou, H., Guan, K.L. and Mischel, P.S. 2017. mTORC2 Regulates Amino Acid Metabolism in Cancer by Phosphorylation of the Cystine-Glutamate Antiporter xCT. *Mol Cell.* **67**(1), pp.128-138.e127.

Guertin, D.A. and Sabatini, D.M. 2009. The pharmacology of mTOR inhibition. *Sci Signal.* **2**(67), ppe24.
Guglielmelli, T., Giugliano, E., Brunetto, V., Rapa, I., Cappia, S., Giorcelli, J., Rrodhe, S., Papotti, M. and Saglio, G. 2015. mTOR pathway activation in multiple myeloma cell lines and primary tumour cells: pomalidomide enhances cytoplasmic-nuclear shuttling of mTOR protein. *Oncoscience.* **2**(4), pp.382-394.
Gujar, S., Dielschneider, R., Clements, D., Helson, E., Shmulevitz, M., Marcato, P., Pan, D., Pan, L.Z., Ahn, D.G., Alawadhi, A. and Lee, P.W. 2013. Multifaceted therapeutic targeting of ovarian peritoneal carcinomatosis through virus-induced immunomodulation. *Mol Ther.* **21**(2), pp.338-347.
Gujar, S.A., Pan, D.A., Marcato, P., Garant, K.A. and Lee, P.W. 2011. Oncolytic virus-initiated protective immunity against prostate cancer. *Mol Ther.* **19**(4), pp.797-804.
Guri, Y., Colombi, M., Dazert, E., Hindupur, S.K., Roszik, J., Moes, S., Jenoe, P., Heim, M.H., Riezman, I., Riezman, H. and Hall, M.N. 2017. mTORC2 Promotes Tumorigenesis via Lipid Synthesis. *Cancer Cell.* **32**(6), pp.807-823.e812.
Hadac, E.M. and Russell, S.J. 2006. 436. Coxsackievirus A21 Has Potent Oncolytic Activity in Multiple Myeloma. *Molecular Therapy.* **13**, pS168.
Hall, K., Scott, K.J., Rose, A., Desborough, M., Harrington, K., Pandha, H., Parrish, C., Vile, R., Coffey, M., Bowen, D., Errington-Mais, F. and Melcher, A.A. 2012. Reovirus-mediated cytotoxicity and enhancement of innate immune responses against acute myeloid leukemia. *Biores Open Access.* **1**(1), pp.3-15.
Hansmann, L., Groeger, S., von Wulffen, W., Bein, G. and Hackstein, H. 2008. Human monocytes represent a competitive source of interferon-alpha in peripheral blood. *Clin Immunol.* **127**(2), pp.252-264.
Hardy, R.R. and Hayakawa, K. 2001. B Cell Development Pathways. *Annual Review of Immunology.* **19**(1), pp.595-621.
Hashiro, G., Loh, P.C. and Yau, J.T. 1977. The preferential cytotoxicity of reovirus for certain transformed cell lines. *Arch Virol.* **54**(4), pp.307-315.
Hastie, E. and Grdzelishvili, V.Z. 2012. Vesicular stomatitis virus as a flexible platform for oncolytic virotherapy against cancer. *J Gen Virol.* **93**(Pt 12), pp.2529-2545.
Hausch, F., Kozany, C., Theodoropoulou, M. and Fabian, A.-K. 2013. FKBPs and the Akt/mTOR pathway. *Cell Cycle.* **12**(15), pp.2366-2370.
Hernandez-Ilizaliturri, F.J., Jupudy, V., Ostberg, J., Oflazoglu, E., Huberman, A., Repasky, E. and Czuczman, M.S. 2003. Neutrophils contribute to the biological antitumor activity of rituximab in a non-Hodgkin's lymphoma severe combined immunodeficiency mouse model. *Clin Cancer Res.* **9**(16 Pt 1), pp.5866-5873.
Hiddemann, W. and Cheson, B.D. 2014. How we manage follicular lymphoma. *Leukemia.* **28**(7), pp.1388-1395.
Ho, A.D., Moritz, T., Rensch, K., Hunstein, W. and Kirchner, H. 1988. Deficiency in interferon production of peripheral blood leukocytes from patients with non-Hodgkin lymphoma. *J Interferon Res.* **8**(4), pp.405-413.
Ho, A.D., Moritz, T., Rensch, K., Hunstein, W. and Kirchner, H. 1992. Deficiency in interferon production of peripheral blood leukocytes from patients with non-Hodgkin lymphoma. *J Interferon Res.* **Spec No**, pp.61-69.
Hoelzer, D., Walewski, J., Döhner, H., Schmid, M., Hiddemann, W., Baumann, A., Serve, H., Dührsen, U., HÃ¼ttmann, A., Thiel, E., Dengler, J., Kneba, M., Schuler, M., Schmidt-Wolf, I., Beck, J., Hertenstein, B., Reichle, A., Domanska-

Czyz, K., Fietkau, R., Horst, H.-A., Rieder, H., Schwartz, S., Burmeister, T. and Goekbuget, N. 2012. Substantially Improved Outcome of Adult Burkitt Non-Hodgkin Lymphoma and Leukemia Patients with Rituximab and a Short-Intensive Chemotherapy; Report of a Large Prospective Multicenter Trial. *Blood.* **120**(21), pp.667-667.
Holland, J. and Owens, T. 1997. Signaling through Intercellular Adhesion Molecule 1 (ICAM-1) in a B Cell Lymphoma Line: THE ACTIVATION OF Lyn TYROSINE KINASE AND THE MITOGEN-ACTIVATED PROTEIN KINASE PATHWAY. *Journal of Biological Chemistry.* **272**(14), pp.9108-9112.
Hollender, A., Kvaloy, S., Nome, O., Skovlund, E., Lote, K. and Holte, H. 2002. Central nervous system involvement following diagnosis of non-Hodgkin's lymphoma: a risk model. *Ann Oncol.* **13**(7), pp.1099-1107.
Homicsko, K., Lukashev, A. and Iggo, R.D. 2005. RAD001 (everolimus) improves the efficacy of replicating adenoviruses that target colon cancer. *Cancer Res.* **65**(15), pp.6882-6890.
Horwitz, M.S., Krahl, T., Fine, C., Lee, J. and Sarvetnick, N. 1999. Protection from lethal coxsackievirus-induced pancreatitis by expression of gamma interferon. *J Virol.* **73**(3), pp.1756-1766.
Howells, A., Marelli, G., Lemoine, N.R. and Wang, Y. 2017. Oncolytic Viruses-Interaction of Virus and Tumor Cells in the Battle to Eliminate Cancer. *Front Oncol.* **7**, p195.
Hubbard, A.K. and Rothlein, R. 2000. Intercellular adhesion molecule-1 (ICAM-1) expression and cell signaling cascades. *Free Radic Biol Med.* **28**(9), pp.1379-1386.
Hwang, H.Y., Kim, J.Y., Lim, J.Y., Chung, S.K., Nam, J.H. and Park, S.I. 2007. Coxsackievirus B3 modulates cell death by downregulating activating transcription factor 3 in HeLa cells. *Virus Res.* **130**(1-2), pp.10-17.
Hwang, M.H., Li, X.J., Kim, J.E., Jeong, S.Y., Lee, S.W., Lee, J. and Ahn, B.C. 2015. Potential Therapeutic Effect of Natural Killer Cells on Doxorubicin-Resistant Breast Cancer Cells In Vitro. *PLoS One.* **10**(8), pe0136209.
Ilett, E.J., Prestwich, R.J., Kottke, T., Errington, F., Thompson, J.M., Harrington, K.J., Pandha, H.S., Coffey, M., Selby, P.J., Vile, R.G. and Melcher, A.A. 2009. Dendritic cells and T cells deliver oncolytic reovirus for tumour killing despite pre-existing anti-viral immunity. *Gene Ther.* **16**(5), pp.689-699.
Ilkow, C.S., Marguerie, M., Batenchuk, C., Mayer, J., Ben Neriah, D., Cousineau, S., Falls, T., Jennings, V.A., Boileau, M., Bellamy, D., Bastin, D., de Souza, C.T., Alkayyal, A., Zhang, J., Le Boeuf, F., Arulanandam, R., Stubbert, L., Sampath, P., Thorne, S.H., Paramanthan, P., Chatterjee, A., Strieter, R.M., Burdick, M., Addison, C.L., Stojdl, D.F., Atkins, H.L., Auer, R.C., Diallo, J.S., Lichty, B.D. and Bell, J.C. 2015. Reciprocal cellular cross-talk within the tumor microenvironment promotes oncolytic virus activity. *Nat Med.* **21**(5), pp.530-536.
Iqbal, J., Sanger, W.G., Horsman, D.E., Rosenwald, A., Pickering, D.L., Dave, B., Dave, S., Xiao, L., Cao, K., Zhu, Q., Sherman, S., Hans, C.P., Weisenburger, D.D., Greiner, T.C., Gascoyne, R.D., Ott, G., Muller-Hermelink, H.K., Delabie, J., Braziel, R.M., Jaffe, E.S., Campo, E., Lynch, J.C., Connors, J.M., Vose, J.M., Armitage, J.O., Grogan, T.M., Staudt, L.M. and Chan, W.C. 2004. BCL2 translocation defines a unique tumor subset within the germinal center B-cell-like diffuse large B-cell lymphoma. *Am J Pathol.* **165**(1), pp.159-166.

Israelsson, S., Jonsson, N., Gullberg, M. and Lindberg, A.M. 2011. Cytolytic replication of echoviruses in colon cancer cell lines. *Virol J.* **8**, p473.
Izumi, T. and Ozawa, K. 2000. [Clinical staging classification of non-Hodgkin's lymphoma]. *Nihon Rinsho.* **58**(3), pp.598-601.
Janeway CA Jr, T.P., Walport M, et al. 2001. B-cell activation by armed helper T cells. *Immunobiology: The Immune System in Health and Disease.* **5th edition**.
Jazirehi, A.R., Vega, M.I., Chatterjee, D., Goodglick, L. and Bonavida, B. 2004. Inhibition of the Raf-MEK1/2-ERK1/2 signaling pathway, Bcl-xL down-regulation, and chemosensitization of non-Hodgkin's lymphoma B cells by Rituximab. *Cancer Res.* **64**(19), pp.7117-7126.
Jennifer, A., John, L.R., Andrea, B., Iñaki, S. and Fay, Y. 2003. Down-regulation of CD20 on B cells upon CD40 activation. *European Journal of Immunology.* **33**(9), pp.2398-2409.
Jhawar, S.R., Thandoni, A., Bommareddy, P.K., Hassan, S., Kohlhapp, F.J., Goyal, S., Schenkel, J.M., Silk, A.W. and Zloza, A. 2017. Oncolytic Viruses-Natural and Genetically Engineered Cancer Immunotherapies. *Front Oncol.* **7**, p202.
Jiang, Z.K., Johnson, M., Moughon, D.L., Kuo, J., Sato, M. and Wu, L. 2013. Rapamycin enhances adenovirus-mediated cancer imaging and therapy in pre-immunized murine hosts. *PLoS One.* **8**(9), pe73650.
Johansson, E.S., Xing, L., Cheng, R.H. and Shafren, D.R. 2004. Enhanced cellular receptor usage by a bioselected variant of coxsackievirus a21. *J Virol.* **78**(22), pp.12603-12612.
Jordan, M.A. and Wilson, L. 2004. Microtubules as a target for anticancer drugs. *Nature Reviews Cancer.* **4**, p253.
Jurianz, K., Ziegler, S., Garcia-Schuler, H., Kraus, S., Bohana-Kashtan, O., Fishelson, Z. and Kirschfink, M. 1999. Complement resistance of tumor cells: basal and induced mechanisms. *Mol Immunol.* **36**(13-14), pp.929-939.
Kahn, S.T., Flowers, C.R., Lechowicz, M.J., Hollenbach, K. and Johnstone, P.A. 2005. Refractory or relapsed Hodgkin's disease and non-Hodgkin's lymphoma: optimizing involved-field radiotherapy in transplant patients. *Cancer J.* **11**(5), pp.425-431.
Karapanagiotou, E.M., Roulstone, V., Twigger, K., Ball, M., Tanay, M., Nutting, C., Newbold, K., Gore, M.E., Larkin, J., Syrigos, K.N., Coffey, M., Thompson, B., Mettinger, K., Vile, R.G., Pandha, H.S., Hall, G.D., Melcher, A.A., Chester, J. and Harrington, K.J. 2012. Phase I/II trial of carboplatin and paclitaxel chemotherapy in combination with intravenous oncolytic reovirus in patients with advanced malignancies. *Clin Cancer Res.* **18**(7), pp.2080-2089.
Karnad, A.B., Haigentz, M., Miley, T., Coffey, M., Gill, G. and Mita, M. 2011. Abstract C22: A phase II study of intravenous wild-type reovirus (Reolysin®) in combination with paclitaxel plus carboplatin in patients with platinum refractory metastatic and/or recurrent squamous cell carcinoma of the head and neck. *Molecular Cancer Therapeutics.* **10**(11 Supplement), pp.C22-C22.
Kater, A.P., Evers, L.M., Remmerswaal, E.B., Jaspers, A., Oosterwijk, M.F., van Lier, R.A., van Oers, M.H. and Eldering, E. 2004. CD40 stimulation of B-cell chronic lymphocytic leukaemia cells enhances the anti-apoptotic profile, but also Bid expression and cells remain susceptible to autologous cytotoxic T-lymphocyte attack. *Br J Haematol.* **127**(4), pp.404-415.
Kaufman, H.L., Kim, D.W., DeRaffele, G., Mitcham, J., Coffin, R.S. and Kim-Schulze, S. 2010. Local and distant immunity induced by intralesional

vaccination with an oncolytic herpes virus encoding GM-CSF in patients with stage IIIc and IV melanoma. *Ann Surg Oncol.* **17**(3), pp.718-730.
Kaufman, H.L., Kohlhapp, F.J. and Zloza, A. 2015. Oncolytic viruses: a new class of immunotherapy drugs. *Nat Rev Drug Discov.* **14**(9), pp.642-662.
Kawauchi, K., Ogasawara, T. and Yasuyama, M. 2002. Activation of extracellular signal-regulated kinase through B-cell antigen receptor in B-cell chronic lymphocytic leukemia. *Int J Hematol.* **75**(5), pp.508-513.
Kelly, E. and Russell, S.J. 2007. History of oncolytic viruses: genesis to genetic engineering. *Mol Ther.* **15**(4), pp.651-659.
Kennedy, N.D., Le, G.N., Kelly, M.E., Harding, T., Fadalla, K. and Winter, D.C. 2018. Surgical management of splenic marginal zone lymphoma. *Ir J Med Sci.* **187**(2), pp.343-347.
Kepp, O., Senovilla, L., Vitale, I., Vacchelli, E., Adjemian, S., Agostinis, P., Apetoh, L., Aranda, F., Barnaba, V., Bloy, N., Bracci, L., Breckpot, K., Brough, D., Buqué, A., Castro, M.G., Cirone, M., Colombo, M.I., Cremer, I., Demaria, S., Dini, L., Eliopoulos, A.G., Faggioni, A., Formenti, S.C., Fučíková, J., Gabriele, L., Gaipl, U.S., Galon, J., Garg, A., Ghiringhelli, F., Giese, N.A., Guo, Z.S., Hemminki, A., Herrmann, M., Hodge, J.W., Holdenrieder, S., Honeychurch, J., Hu, H.-M., Huang, X., Illidge, T.M., Kono, K., Korbelik, M., Krysko, D.V., Loi, S., Lowenstein, P.R., Lugli, E., Ma, Y., Madeo, F., Manfredi, A.A., Martins, I., Mavilio, D., Menger, L., Merendino, N., Michaud, M., Mignot, G., Mossman, K.L., Multhoff, G., Oehler, R., Palombo, F., Panaretakis, T., Pol, J., Proietti, E., Ricci, J.-E., Riganti, C., Rovere-Querini, P., Rubartelli, A., Sistigu, A., Smyth, M.J., Sonnemann, J., Spisek, R., Stagg, J., Sukkurwala, A.Q., Tartour, E., Thorburn, A., Thorne, S.H., Vandenabeele, P., Velotti, F., Workenhe, S.T., Yang, H., Zong, W.-X., Zitvogel, L., Kroemer, G. and Galluzzi, L. 2014. Consensus guidelines for the detection of immunogenic cell death. *Oncoimmunology.* **3**(9), pe955691.
Kern, D.J., James, B.R., Blackwell, S., Gassner, C., Klein, C. and Weiner, G.J. 2013. GA101 induces NK-cell activation and antibody-dependent cellular cytotoxicity more effectively than rituximab when complement is present. *Leuk Lymphoma.* **54**(11), pp.2500-2505.
Kheirallah, S., Caron, P., Gross, E., Quillet-Mary, A., Bertrand-Michel, J., Fournie, J.J., Laurent, G. and Bezombes, C. 2010. Rituximab inhibits B-cell receptor signaling. *Blood.* **115**(5), pp.985-994.
Kim, M., Williamson, C.T., Prudhomme, J., Bebb, D.G., Riabowol, K., Lee, P.W., Lees-Miller, S.P., Mori, Y., Rahman, M.M., McFadden, G. and Johnston, R.N. 2010. The viral tropism of two distinct oncolytic viruses, reovirus and myxoma virus, is modulated by cellular tumor suppressor gene status. *Oncogene.* **29**(27), pp.3990-3996.
Kinoshita, T. 1998. Decay-Accelerating Factor (CD55) A2 - Delves, Peter J. *Encyclopedia of Immunology (Second Edition).* Oxford: Elsevier, pp.735-736.
Kitada, S., Zapata, J.M., Andreeff, M. and Reed, J.C. 1999. Bryostatin and CD40-ligand enhance apoptosis resistance and induce expression of cell survival genes in B-cell chronic lymphocytic leukaemia. *Br J Haematol.* **106**(4), pp.995-1004.
Klein, K.A. and Jackson, W.T. 2011. Picornavirus subversion of the autophagy pathway. *Viruses.* **3**(9), pp.1549-1561.
Klimpel, G.R., Infante, A.J., Patterson, J., Hess, C.B. and Asuncion, M. 1990. Virus-induced interferon alpha/beta (IFN-alpha/beta) production by T cells and

by Th1 and Th2 helper T cell clones: a study of the immunoregulatory actions of IFN-gamma versus IFN-alpha/beta on functions of different T cell populations. *Cell Immunol.* **128**(2), pp.603-618.
Kober, C., Weibel, S., Rohn, S., Kirscher, L. and Szalay, A.A. 2015. Intratumoral INF-gamma triggers an antiviral state in GL261 tumor cells: a major hurdle to overcome for oncolytic vaccinia virus therapy of cancer. *Mol Ther Oncolytics.* **2**, p15009.
Kohlhapp, F.J., Zloza, A. and Kaufman, H.L. 2015. Talimogene laherparepvec (T-VEC) as cancer immunotherapy. *Drugs Today (Barc).* **51**(9), pp.549-558.
Korniluk, A., Kemona, H. and Dymicka-Piekarska, V. 2014. Multifunctional CD40L: pro- and anti-neoplastic activity. *Tumour Biol.* **35**(10), pp.9447-9457.
Koues, O.I., Oltz, E.M. and Payton, J.E. 2015. Short-Circuiting Gene Regulatory Networks: Origins of B Cell Lymphoma. *Trends in Genetics.* **31**(12), pp.720-731.
Kratky, W., Reis e Sousa, C., Oxenius, A. and Sporri, R. 2011. Direct activation of antigen-presenting cells is required for CD8+ T-cell priming and tumor vaccination. *Proc Natl Acad Sci U S A.* **108**(42), pp.17414-17419.
Kuo, S.-H., Hsu, C.-H., Chen, L.-T., Lu, Y.-S., Lin, C.-H., Yeh, P.-Y., Jeng, H.-J., Gao, M., Yeh, K.-H. and Cheng, A.-L. 2011. Lack of compensatory pAKT activation and eIF4E phosphorylation of lymphoma cells towards mTOR inhibitor, RAD001. *European Journal of Cancer.* **47**(8), pp.1244-1257.
Kurland, J.F., Voehringer, D.W. and Meyn, R.E. 2003. The MEK/ERK pathway acts upstream of NF kappa B1 (p50) homodimer activity and Bcl-2 expression in a murine B-cell lymphoma cell line. MEK inhibition restores radiation-induced apoptosis. *J Biol Chem.* **278**(34), pp.32465-32470.
Labiotech.eu. 2015. The First Ever Oncolytic Immunotherapy is Set to Reach the European Market.
Le Sage, V., Cinti, A., Amorim, R. and Mouland, A.J. 2016. Adapting the Stress Response: Viral Subversion of the mTOR Signaling Pathway. *Viruses.* **8**(6).
Lee, J.W., Yoo, N.J., Soung, Y.H., Kim, H.S., Park, W.S., Kim, S.Y., Lee, J.H., Park, J.Y., Cho, Y.G., Kim, C.J., Ko, Y.H., Kim, S.H., Nam, S.W., Lee, J.Y. and Lee, S.H. 2003. BRAF mutations in non-Hodgkin's lymphoma. *Br J Cancer.* **89**(10), pp.1958-1960.
Lee, S.W., Cho, H.Y., Na, G., Yoo, M.R., Seo, S.K., Hur, D.Y., Han, J., Lee, C.K. and Choi, I. 2012. CD40 stimulation induces vincristine resistance via AKT activation and MRP1 expression in a human multiple myeloma cell line. *Immunol Lett.* **144**(1-2), pp.41-48.
Lehmann, C., Lafferty, M., Garzino-Demo, A., Jung, N., Hartmann, P., Fatkenheuer, G., Wolf, J.S., van Lunzen, J. and Romerio, F. 2010. Plasmacytoid dendritic cells accumulate and secrete interferon alpha in lymph nodes of HIV-1 patients. *PLoS One.* **5**(6), pe11110.
Lei, X., Sun, Z., Liu, X., Jin, Q., He, B. and Wang, J. 2011. Cleavage of the adaptor protein TRIF by enterovirus 71 3C inhibits antiviral responses mediated by Toll-like receptor 3. *J Virol.* **85**(17), pp.8811-8818.
Lennette, E.H., Fox, V.L., Schmidt, N.J. and Culver, J.O. 1958. The Coe virus: an apparently new virus recovered from patients with mild respiratory disease. *Am J Hyg.* **68**(3), pp.272-287.
Leopoldo, S.A., Ikuri, A.M., Héctor, R.R. and Leopoldo, F.R. 2001. Enforced and prolonged CD40 ligand expression triggers autoantibody production in vivo. *European Journal of Immunology.* **31**(12), pp.3484-3492.

Leroy, K., Haioun, C., Lepage, E., Le Métayer, N., Berger, F., Labouyrie, E., Meignin, V., Petit, B., Bastard, C., Salles, G., Gisselbrecht, C., Reyes, F. and Gaulard, P. 2002. p53 gene mutations are associated with poor survival in low and low-intermediate risk diffuse large B-cell lymphomas. *Annals of Oncology.* **13**(7), pp.1108-1115.
Lesokhin, A.M., Ansell, S.M., Armand, P., Scott, E.C., Halwani, A., Gutierrez, M., Millenson, M.M., Cohen, A.D., Schuster, S.J., Lebovic, D., Dhodapkar, M., Avigan, D., Chapuy, B., Ligon, A.H., Freeman, G.J., Rodig, S.J., Cattry, D., Zhu, L., Grosso, J.F., Bradley Garelik, M.B., Shipp, M.A., Borrello, I. and Timmerman, J. 2016. Nivolumab in Patients With Relapsed or Refractory Hematologic Malignancy: Preliminary Results of a Phase Ib Study. *J Clin Oncol.* **34**(23), pp.2698-2704.
Levine, B. 2005. Eating oneself and uninvited guests: autophagy-related pathways in cellular defense. *Cell.* **120**(2), pp.159-162.
Li, X., Wang, P., Li, H., Du, X., Liu, M., Huang, Q., Wang, Y. and Wang, S. 2017. The Efficacy of Oncolytic Adenovirus Is Mediated by T-cell Responses against Virus and Tumor in Syrian Hamster Model. *Clin Cancer Res.* **23**(1), pp.239-249.
Li, Z.S., Shao, Z.H., Fu, R., Wang, J., Li, L.J., Zhang, T., Wang, H.Q., Wu, Y.H., Ruan, E.B., Song, J., Qu, W., Liu, H., Xing, L.M., Wang, X.M., Liang, Y., Guan, J. and Wang, G.J. 2011. [Percentages and functions of natural killer cell subsets in peripheral blood of patients with severe aplastic anemia]. *Zhonghua Yi Xue Za Zhi.* **91**(16), pp.1084-1087.
Lichty, B.D., Breitbach, C.J., Stojdl, D.F. and Bell, J.C. 2014. Going viral with cancer immunotherapy. *Nat Rev Cancer.* **14**(8), pp.559-567.
Lichty, B.D., Stojdl, D.F., Taylor, R.A., Miller, L., Frenkel, I., Atkins, H. and Bell, J.C. 2004. Vesicular stomatitis virus: a potential therapeutic virus for the treatment of hematologic malignancy. *Hum Gene Ther.* **15**(9), pp.821-831.
Lim, S.H., Beers, S.A., French, R.R., Johnson, P.W., Glennie, M.J. and Cragg, M.S. 2010. Anti-CD20 monoclonal antibodies: historical and future perspectives. *Haematologica.* **95**(1), pp.135-143.
Lind, K., Svedin, E., Domsgen, E., Kapell, S., Laitinen, O., Moll, M. and Flodstrom-Tullberg, M. 2016. Coxsackievirus counters the host innate immune response by blocking type III interferon expression. *J Gen Virol.* **97**(6), pp.1-12.
Liu, Y.-P., Suksanpaisan, L., Steele, M.B., Russell, S.J. and Peng, K.-W. 2013. Induction of antiviral genes by the tumor microenvironment confers resistance to virotherapy. *Scientific Reports.* **3**, p2375.
Ljunggren, H.G. and Karre, K. 1990. In search of the 'missing self': MHC molecules and NK cell recognition. *Immunol Today.* **11**(7), pp.237-244.
Lolkema, M.P., Arkenau, H.T., Harrington, K., Roxburgh, P., Morrison, R., Roulstone, V., Twigger, K., Coffey, M., Mettinger, K., Gill, G., Evans, T.R. and de Bono, J.S. 2011. A phase I study of the combination of intravenous reovirus type 3 Dearing and gemcitabine in patients with advanced cancer. *Clin Cancer Res.* **17**(3), pp.581-588.
Lopez, M., Aoubala, M., Jordier, F., Isnardon, D., Gomez, S. and Dubreuil, P. 1998. The human poliovirus receptor related 2 protein is a new hematopoietic/endothelial homophilic adhesion molecule. *Blood.* **92**(12), pp.4602-4611.
Lord, S.J., Rajotte, R.V., Korbutt, G.S. and Bleackley, R.C. 2003. Granzyme B: a natural born killer. *Immunol Rev.* **193**, pp.31-38.

Lukes, R.J. and Collins, R.D. 1975. New approaches to the classification of the lymphomata. *Br J Cancer Suppl.* **2**, pp.1-28.
Lun, X., Alain, T., Zemp, F.J., Zhou, H., Rahman, M.M., Hamilton, M.G., McFadden, G., Bell, J., Senger, D.L. and Forsyth, P.A. 2010. Myxoma Virus Virotherapy for Glioma in Immunocompetent Animal Models: Optimizing Administration Routes and Synergy with Rapamycin. *Cancer Research.* **70**(2), pp.598-608.
Magnuson, B., Ekim, B. and Fingar, D.C. 2012. Regulation and function of ribosomal protein S6 kinase (S6K) within mTOR signalling networks. *Biochem J.* **441**(1), pp.1-21.
Mahauad-Fernandez, W.D. and Okeoma, C.M. 2016. The role of BST-2/Tetherin in host protection and disease manifestation. *Immun Inflamm Dis.* **4**(1), pp.4-23.
Maitra, R., Augustine, T., Dayan, Y., Chandy, C., Coffey, M. and Goel, S. 2017. Toll like receptor 3 as an immunotherapeutic target for KRAS mutated colorectal cancer. *Oncotarget.* **8**(21), pp.35138-35153.
Marcato, P., Shmulevitz, M., Pan, D., Stoltz, D. and Lee, P.W. 2007. Ras transformation mediates reovirus oncolysis by enhancing virus uncoating, particle infectivity, and apoptosis-dependent release. *Mol Ther.* **15**(8), pp.1522-1530.
Marsh, M. and Helenius, A. 2006. Virus Entry: Open Sesame. *Cell.* **124**(4), pp.729-740.
Medina, D.J., Sheay, W., Osman, M., Goodell, L., Martin, J., Rabson, A.B. and Strair, R.K. 2005. Adenovirus infection and cytotoxicity of primary mantle cell lymphoma cells. *Exp Hematol.* **33**(11), pp.1337-1347.
Menon, M.P., Pittaluga, S. and Jaffe, E.S. 2012. The histological and biological spectrum of diffuse large B-cell lymphoma in the World Health Organization classification. *Cancer J.* **18**(5), pp.411-420.
Miller, C.G. and Fraser, N.W. 2003. Requirement of an integrated immune response for successful neuroattenuated HSV-1 therapy in an intracranial metastatic melanoma model. *Mol Ther.* **7**(6), pp.741-747.
Minuk, G.Y., Paul, R.W. and Lee, P.W. 1985. The prevalence of antibodies to reovirus type 3 in adults with idiopathic cholestatic liver disease. *J Med Virol.* **16**(1), pp.55-60.
Mita, A.C., Argiris, A., Coffey, M., Gill, G. and Mita, M. 2013. Abstract C70: A phase 2 study of intravenous administration of REOLYSIN® (reovirus type 3 dearing) in combination with paclitaxel (P) and carboplatin (C) in patients with squamous cell carcinoma of the lung. *Molecular Cancer Therapeutics.* **12**(11 Supplement), pp.C70-C70.
Miyamoto, S., Inoue, H., Nakamura, T., Yamada, M., Sakamoto, C., Urata, Y., Okazaki, T., Marumoto, T., Takahashi, A., Takayama, K., Nakanishi, Y., Shimizu, H. and Tani, K. 2012. Coxsackievirus B3 is an oncolytic virus with immunostimulatory properties that is active against lung adenocarcinoma. *Cancer Res.* **72**(10), pp.2609-2621.
Moody, C.A., Scott, R.S., Amirghahari, N., Nathan, C.O., Young, L.S., Dawson, C.W. and Sixbey, J.W. 2005. Modulation of the cell growth regulator mTOR by Epstein-Barr virus-encoded LMP2A. *J Virol.* **79**(9), pp.5499-5506.
Morin, R.D., Mendez-Lago, M., Mungall, A.J., Goya, R., Mungall, K.L., Corbett, R.D., Johnson, N.A., Severson, T.M., Chiu, R., Field, M., Jackman, S., Krzywinski, M., Scott, D.W., Trinh, D.L., Tamura-Wells, J., Li, S., Firme, M.R.,

Rogic, S., Griffith, M., Chan, S., Yakovenko, O., Meyer, I.M., Zhao, E.Y., Smailus, D., Moksa, M., Chittaranjan, S., Rimsza, L., Brooks-Wilson, A., Spinelli, J.J., Ben-Neriah, S., Meissner, B., Woolcock, B., Boyle, M., McDonald, H., Tam, A., Zhao, Y., Delaney, A., Zeng, T., Tse, K., Butterfield, Y., Birol, I., Holt, R., Schein, J., Horsman, D.E., Moore, R., Jones, S.J., Connors, J.M., Hirst, M., Gascoyne, R.D. and Marra, M.A. 2011. Frequent mutation of histone-modifying genes in non-Hodgkin lymphoma. *Nature.* **476**(7360), pp.298-303.
Morris, D., Tu, D., Tehfe, M.A., Nicholas, G.A., Goffin, J.R., Gregg, R.W., Shepherd, F.A., Murray, N., Wierzbicki, R., Lee, C.W., Kuruvilla, S., Keith, B., Ahmed, A., Blais, N., Goss, G.D., Korpanty, G., Sederias, J., Laurie, S.A., Seymour, L. and Bradbury, P.A. 2016. A Randomized Phase II study of Reolysin in Patients with Previously Treated Advanced or Metatstatic Non Small Cell Lung Cancer (NSCLC) receiving Standard Salvage Chemotherapy – Canadian Cancer Trials Group IND 211. *Journal of Clinical Oncology.* **34**(15_suppl), pp.e20512-e20512.
Mortola, E., Endo, Y., Ohno, K., Watari, T., Tsujimoto, H. and Hasegawa, A. 1998. The use of two immunosuppressive drugs, cyclosporin A and tacrolimus, to inhibit virus replication and apoptosis in cells infected with feline immunodeficiency virus. *Vet Res Commun.* **22**(8), pp.553-563.
Mounier, N., Briere, J., Gisselbrecht, C., Emile, J.F., Lederlin, P., Sebban, C., Berger, F., Bosly, A., Morel, P., Tilly, H., Bouabdallah, R., Reyes, F., Gaulard, P. and Coiffier, B. 2003. Rituximab plus CHOP (R-CHOP) overcomes bcl-2--associated resistance to chemotherapy in elderly patients with diffuse large B-cell lymphoma (DLBCL). *Blood.* **101**(11), pp.4279-4284.
Mukherjee, A., Morosky, S.A., Delorme-Axford, E., Dybdahl-Sissoko, N., Oberste, M.S., Wang, T. and Coyne, C.B. 2011. The coxsackievirus B 3C protease cleaves MAVS and TRIF to attenuate host type I interferon and apoptotic signaling. *PLoS Pathog.* **7**(3), pe1001311.
Muro, S., Wiewrodt, R., Thomas, A., Koniaris, L., Albelda, S.M., Muzykantov, V.R. and Koval, M. 2003. A novel endocytic pathway induced by clustering endothelial ICAM-1 or PECAM-1. *J Cell Sci.* **116**(Pt 8), pp.1599-1609.
Muster, T., Rajtarova, J., Sachet, M., Unger, H., Fleischhacker, R., Romirer, I., Grassauer, A., Url, A., Garcia-Sastre, A., Wolff, K., Pehamberger, H. and Bergmann, M. 2004. Interferon resistance promotes oncolysis by influenza virus NS1-deletion mutants. *Int J Cancer.* **110**(1), pp.15-21.
Newcombe, N.G., Johansson, E.S., Au, G., Lindberg, A.M., Barry, R.D. and Shafren, D.R. 2004. Enterovirus capsid interactions with decay-accelerating factor mediate lytic cell infection. *J Virol.* **78**(3), pp.1431-1439.
Nicola E Annels, G.S., Mehreen Arif, Mick Denyer, Attya Iqbal, David Mansfield, Sarbjinder Sandhu, Alan Melcher, Kevin Harrington, Gough Au, Mark Grose, Darren Shafren, Hugh Mostafid, and Hardev Pandha. 2015. Oncolytic immunotherapy for the treatment of non-muscle invasive bladder cancer using intravesical coxsackievirus A21. *Journal for Immunotherapy of Cancer.* **3**.
Noonan, A.M., Farren, M.R., Geyer, S.M., Huang, Y., Tahiri, S., Ahn, D., Mikhail, S., Ciombor, K.K., Pant, S., Aparo, S., Sexton, J., Marshall, J.L., Mace, T.A., Wu, C.S., El-Rayes, B., Timmers, C.D., Zwiebel, J., Lesinski, G.B., Villalona-Calero, M.A. and Bekaii-Saab, T.S. 2016. Randomized Phase 2 Trial of the Oncolytic Virus Pelareorep (Reolysin) in Upfront Treatment of Metastatic Pancreatic Adenocarcinoma. *Mol Ther.* **24**(6), pp.1150-1158.

O'Shea, C., Klupsch, K., Choi, S., Bagus, B., Soria, C., Shen, J., McCormick, F. and Stokoe, D. 2005. Adenoviral proteins mimic nutrient/growth signals to activate the mTOR pathway for viral replication. *Embo j.* **24**(6), pp.1211-1221.
Ochiai, H., Campbell, S.A., Archer, G.E., Chewning, T.A., Dragunsky, E., Ivanov, A., Gromeier, M. and Sampson, J.H. 2006. Targeted therapy for glioblastoma multiforme neoplastic meningitis with intrathecal delivery of an oncolytic recombinant poliovirus. *Clin Cancer Res.* **12**(4), pp.1349-1354.
Ochiai, K., Kagami, M., Nakazawa, T., Sugiyama, T., Sueishi, M., Ito, M. and Tomioka, H. 2000. Regulation of CD69 expression on eosinophil precursors by interferon-gamma. *Int Arch Allergy Immunol.* **122 Suppl 1**, pp.28-32.
Oflazoglu, E. and Audoly, L.P. 2010. Evolution of anti-CD20 monoclonal antibody therapeutics in oncology. *MAbs.* **2**(1), pp.14-19.
Omar, A.R., Ideris, A., Ali, A.M., Othman, F., Yusoff, K., Abdullah, J.M., Wali, H.S., Zawawi, M. and Meyyappan, N. 2003. An overview on the development of newcastle disease virus as an anti-cancer therapy. *Malays J Med Sci.* **10**(1), pp.4-12.
Oncozine. 2013. Reolysin Meets Primary Endpoint for First Stage of Phase II Metastatic Melanoma Trial.
Ong, S.T. and Le Beau, M.M. 1998. Chromosomal abnormalities and molecular genetics of non-Hodgkin's lymphoma. *Semin Oncol.* **25**(4), pp.447-460.
Osinska, I., Popko, K. and Demkow, U. 2014. Perforin: an important player in immune response. *Cent Eur J Immunol.* **39**(1), pp.109-115.
Pandha, H., Harrington, K., Ralph, C., Melcher, A., Grose, M. and Shafren, D. 2015a. Phase I/II storm study: Intravenous delivery of a novel oncolytic immunotherapy agent, Coxsackievirus A21, in advanced cancer patients. *Journal for ImmunoTherapy of Cancer.* **3**(2), pP341.
Pandha, H., Harrington, K., Ralph, C., Melcher, A. and Shafren, D.R. 2015b. Abstract CT205: Intravenous delivery of a novel oncolytic immunotherapy agent, CAVATAK, in advanced cancer patients. *Cancer Research.* **75**(15 Supplement), pp.CT205-CT205.
Parameswaran, R., Ramakrishnan, P., Moreton, S.A., Xia, Z., Hou, Y., Lee, D.A., Gupta, K., deLima, M., Beck, R.C. and Wald, D.N. 2016. Repression of GSK3 restores NK cell cytotoxicity in AML patients. *Nature Communications.* **7**, p11154.
Park, M.S., Garcia-Sastre, A., Cros, J.F., Basler, C.F. and Palese, P. 2003. Newcastle disease virus V protein is a determinant of host range restriction. *J Virol.* **77**(17), pp.9522-9532.
Parker, A.K., Parker, S., Yokoyama, W.M., Corbett, J.A. and Buller, R.M. 2007. Induction of natural killer cell responses by ectromelia virus controls infection. *J Virol.* **81**(8), pp.4070-4079.
Parrish, C., Scott, G.B., Migneco, G., Scott, K.J., Steele, L.P., Ilett, E., West, E.J., Hall, K., Selby, P.J., Buchanan, D., Varghese, A., Cragg, M.S., Coffey, M., Hillmen, P., Melcher, A.A. and Errington-Mais, F. 2015. Oncolytic reovirus enhances rituximab-mediated antibody-dependent cellular cytotoxicity against chronic lymphocytic leukaemia. *Leukemia.* **29**(9), pp.1799-1810.
Pasqualucci, L. and Dalla-Favera, R. 2014. SnapShot: diffuse large B cell lymphoma. *Cancer Cell.* **25**(1), pp.132-132.e131.
Pedersen, I.M., Buhl, A.M., Klausen, P., Geisler, C.H. and Jurlander, J. 2002. The chimeric anti-CD20 antibody rituximab induces apoptosis in B-cell chronic

lymphocytic leukemia cells through a p38 mitogen activated protein-kinase-dependent mechanism. *Blood.* **99**(4), pp.1314-1319.
Perry, A.M., Mitrovic, Z. and Chan, W.C. 2012. Biological prognostic markers in diffuse large B-cell lymphoma. *Cancer Control.* **19**(3), pp.214-226.
Phillips, D.C., Xiao, Y., Lam, L.T., Litvinovich, E., Roberts-Rapp, L., Souers, A.J. and Leverson, J.D. 2015. Loss in MCL-1 function sensitizes non-Hodgkin's lymphoma cell lines to the BCL-2-selective inhibitor venetoclax (ABT-199). *Blood Cancer J.* **5**, pe368.
Pineda, A., Sancho, J.-M., Garcia, O., Esteve, J., Tormo, M., Martinez, P., Vall-llovera, F., Martino, R., Montesinos, P., Gonzalez-Campos, J., Bergua, J., Calbacho, M., Gil, C., Vicent, A., Cladera, A., Hernandez, J., Moreno, M.-J., Serrano, A., Alonso, N., García, R., Barba, P., Fernandez, A., Miralles, P., Novo, A., Moraleda, J.M., Hernández, J.Á., Abella, E., Sanchez, M., Lopez, M.-E., Bernal, T., Mateos, M.C., Lavilla, E. and Ribera, J.-M. 2015. Incidence, Treatment and Prognosis of Patients with Relapsed Burkitt Lymphoma/Leukemia Treated with Specific Chemotherapy or Immunochemotherapy in Spain. *Blood.* **126**(23), pp.2723-2723.
Press, O.W., Unger, J.M., Rimsza, L.M., Friedberg, J.W., LeBlanc, M., Czuczman, M.S., Kaminski, M., Braziel, R.M., Spier, C., Gopal, A.K., Maloney, D.G., Cheson, B.D., Dakhil, S.R., Miller, T.P. and Fisher, R.I. 2013. Phase III randomized intergroup trial of CHOP plus rituximab compared with CHOP chemotherapy plus (131)iodine-tositumomab for previously untreated follicular non-Hodgkin lymphoma: SWOG S0016. *J Clin Oncol.* **31**(3), pp.314-320.
Prestwich, R.J., Errington, F., Ilett, E.J., Morgan, R.S., Scott, K.J., Kottke, T., Thompson, J., Morrison, E.E., Harrington, K.J., Pandha, H.S., Selby, P.J., Vile, R.G. and Melcher, A.A. 2008. Tumor infection by oncolytic reovirus primes adaptive antitumor immunity. *Clin Cancer Res.* **14**(22), pp.7358-7366.
Prestwich, R.J., Ilett, E.J., Errington, F., Diaz, R.M., Steele, L.P., Kottke, T., Thompson, J., Galivo, F., Harrington, K.J., Pandha, H.S., Selby, P.J., Vile, R.G. and Melcher, A.A. 2009. Immune-Mediated Antitumor Activity of Reovirus Is Required for Therapy and Is Independent of Direct Viral Oncolysis and Replication. *Clinical Cancer Research.* **15**(13), pp.4374-4381.
Qian, W., Liu, J., Tong, Y., Yan, S., Yang, C., Yang, M. and Liu, X. 2008. Enhanced antitumor activity by a selective conditionally replicating adenovirus combining with MDA-7/interleukin-24 for B-lymphoblastic leukemia via induction of apoptosis. *Leukemia.* **22**(2), pp.361-369.
Qiao, J., Dey, M., Chang, A.L., Kim, J.W., Miska, J., Ling, A., D, M.N., Han, Y., Zhang, L. and Lesniak, M.S. 2015. Intratumoral oncolytic adenoviral treatment modulates the glioma microenvironment and facilitates systemic tumor-antigen-specific T cell therapy. *Oncoimmunology.* **4**(8), pe1022302.
Rahman, A. and Fazal, F. 2009. Hug tightly and say goodbye: role of endothelial ICAM-1 in leukocyte transmigration. *Antioxid Redox Signal.* **11**(4), pp.823-839.
Rahmani, M., Aust, M.M., Benson, E.C., Wallace, L., Friedberg, J. and Grant, S. 2014. PI3K/mTOR inhibition markedly potentiates HDAC inhibitor activity in NHL cells through BIM- and MCL-1-dependent mechanisms in vitro and in vivo. *Clin Cancer Res.* **20**(18), pp.4849-4860.
Rai, S.S. and Wolff, J. 1996. Localization of the vinblastine-binding site on beta-tubulin. *J Biol Chem.* **271**(25), pp.14707-14711.

Randazzo, B.P., Tal-Singer, R., Zabolotny, J.M., Kesari, S. and Fraser, N.W. 1997. Herpes simplex virus 1716, an ICP 34.5 null mutant, is unable to replicate in CV-1 cells due to a translational block that can be overcome by coinfection with SV40. *J Gen Virol.* **78 (Pt 12)**, pp.3333-3339.
Reed, J.C. 2017. Bcl-2 on the brink of breakthroughs in cancer treatment. *Cell Death And Differentiation.* **25**, p3.
Reed, L.J. and Muench, H. 1938. A SIMPLE METHOD OF ESTIMATING FIFTY PER CENT ENDPOINTS12. *American Journal of Epidemiology.* **27**(3), pp.493-497.
Ribas, A., Puzanov, I., Dummer, R., Schadendorf, D., Hamid, O., Robert, C., Hodi, F.S., Schachter, J., Pavlick, A.C., Lewis, K.D., Cranmer, L.D., Blank, C.U., O'Day, S.J., Ascierto, P.A., Salama, A.K., Margolin, K.A., Loquai, C., Eigentler, T.K., Gangadhar, T.C., Carlino, M.S., Agarwala, S.S., Moschos, S.J., Sosman, J.A., Goldinger, S.M., Shapira-Frommer, R., Gonzalez, R., Kirkwood, J.M., Wolchok, J.D., Eggermont, A., Li, X.N., Zhou, W., Zernhelt, A.M., Lis, J., Ebbinghaus, S., Kang, S.P. and Daud, A. 2015. Pembrolizumab versus investigator-choice chemotherapy for ipilimumab-refractory melanoma (KEYNOTE-002): a randomised, controlled, phase 2 trial. *Lancet Oncol.* **16**(8), pp.908-918.
Robinson, M., Li, B., Ge, Y., Ko, D., Yendluri, S., Harding, T., VanRoey, M., Spindler, K.R. and Jooss, K. 2009. Novel immunocompetent murine tumor model for evaluation of conditionally replication-competent (oncolytic) murine adenoviral vectors. *J Virol.* **83**(8), pp.3450-3462.
Romano, M.F., Lamberti, A., Tassone, P., Alfinito, F., Costantini, S., Chiurazzi, F., Defrance, T., Bonelli, P., Tuccillo, F., Turco, M.C. and Venuta, S. 1998. Triggering of CD40 Antigen Inhibits Fludarabine-Induced Apoptosis in B Chronic Lymphocytic Leukemia Cells. *Blood.* **92**(3), pp.990-995.
Rosen, L., Hovis, J.F., Mastrota, F.M., Bell, J.A. and Huebner, R.J. 1960. Observations on a newly recognized virus (Abney) of the reovirus family. *Am J Hyg.* **71**, pp.258-265.
Rudnicka, D., Oszmiana, A., Finch, D.K., Strickland, I., Schofield, D.J., Lowe, D.C., Sleeman, M.A. and Davis, D.M. 2013. Rituximab causes a polarization of B cells that augments its therapeutic function in NK-cell-mediated antibody-dependent cellular cytotoxicity. *Blood.* **121**(23), pp.4694-4702.
Runkel, L., Pfeffer, L., Lewerenz, M., Monneron, D., Yang, C.H., Murti, A., Pellegrini, S., Goelz, S., Uze, G. and Mogensen, K. 1998. Differences in activity between alpha and beta type I interferons explored by mutational analysis. *J Biol Chem.* **273**(14), pp.8003-8008.
Sadler, A.J. and Williams, B.R. 2007. Structure and function of the protein kinase R. *Curr Top Microbiol Immunol.* **316**, pp.253-292.
Salles, G.A. 2007. Clinical features, prognosis and treatment of follicular lymphoma. *Hematology Am Soc Hematol Educ Program.* pp.216-225.
Samson, A., Bentham, M.J., Scott, K., Nuovo, G., Bloy, A., Appleton, E., Adair, R.A., Dave, R., Peckham-Cooper, A., Toogood, G., Nagamori, S., Coffey, M., Vile, R., Harrington, K., Selby, P., Errington-Mais, F., Melcher, A. and Griffin, S. 2018. Oncolytic reovirus as a combined antiviral and anti-tumour agent for the treatment of liver cancer. **67**(3), pp.562-573.
Sangfelt, O., Erickson, S. and Grander, D. 2000. Mechanisms of interferon-induced cell cycle arrest. *Front Biosci.* **5**, pp.D479-487.

Sarkar, S., Sabhachandani, P., Ravi, D., Potdar, S., Purvey, S., Beheshti, A., Evens, A.M. and Konry, T. 2017. Dynamic Analysis of Human Natural Killer Cell Response at Single-Cell Resolution in B-Cell Non-Hodgkin Lymphoma. *Frontiers in Immunology.* **8**, p1736.
Sasaki, O., Karaki, T. and Imanishi, J. 1986. Protective effect of interferon on infections with hand, foot, and mouth disease virus in newborn mice. *J Infect Dis.* **153**(3), pp.498-502.
Saunders, R.N., Metcalfe, M.S. and Nicholson, M.L. 2001. Rapamycin in transplantation: a review of the evidence. *Kidney Int.* **59**(1), pp.3-16.
Sawicki, M.W., Dimasi, N., Natarajan, K., Wang, J., Margulies, D.H. and Mariuzza, R.A. 2001. Structural basis of MHC class I recognition by natural killer cell receptors. *Immunol Rev.* **181**, pp.52-65.
Saxton, R.A. and Sabatini, D.M. 2017. mTOR Signaling in Growth, Metabolism, and Disease. *Cell.* **169**(2), pp.361-371.
Sborov, D.W., Nuovo, G.J., Stiff, A., Mace, T., Lesinski, G.B., Benson, D.M., Jr., Efebera, Y.A., Rosko, A.E., Pichiorri, F., Grever, M.R. and Hofmeister, C.C. 2014. A phase I trial of single-agent reolysin in patients with relapsed multiple myeloma. *Clin Cancer Res.* **20**(23), pp.5946-5955.
Schatz, J.H. 2011. Targeting the PI3K/AKT/mTOR pathway in non-Hodgkin's lymphoma: results, biology, and development strategies. *Curr Oncol Rep.* **13**(5), pp.398-406.
Schneider, W.M., Chevillotte, M.D. and Rice, C.M. 2014. Interferon-stimulated genes: a complex web of host defenses. *Annu Rev Immunol.* **32**, pp.513-545.
Schreiber, K.H., Ortiz, D., Academia, E.C., Anies, A.C., Liao, C.Y. and Kennedy, B.K. 2015. Rapamycin-mediated mTORC2 inhibition is determined by the relative expression of FK506-binding proteins. *Aging Cell.* **14**(2), pp.265-273.
Scott, D.W. and Gascoyne, R.D. 2014. The tumour microenvironment in B cell lymphomas. *Nature Reviews Cancer.* **14**, p517.
Sehn, L.H. and Gascoyne, R.D. 2015. Diffuse large B-cell lymphoma: optimizing outcome in the context of clinical and biologic heterogeneity. *Blood.* **125**(1), pp.22-32.
Senac, J.S., Doronin, K., Russell, S.J., Jelinek, D.F., Greipp, P.R. and Barry, M.A. 2010. Infection and killing of multiple myeloma by adenoviruses. *Hum Gene Ther.* **21**(2), pp.179-190.
Shafren, D., Quah, M., Wong, Y., Andtbacka, R.H., Kaufman, H.L. and Au, G.G. 2014. Combination of a novel oncolytic immunotherapeutic agent, CAVATAK (coxsackievirus A21) and immune-checkpoint blockade significantly reduces tumor growth and improves survival in an immune competent mouse melanoma model. *Journal for ImmunoTherapy of Cancer.* **2**(3), pP125.
Shafren, D.R., Au, G.G., Nguyen, T., Newcombe, N.G., Haley, E.S., Beagley, L., Johansson, E.S., Hersey, P. and Barry, R.D. 2004. Systemic therapy of malignant human melanoma tumors by a common cold-producing enterovirus, coxsackievirus a21. *Clin Cancer Res.* **10**(1 Pt 1), pp.53-60.
Shafren, D.R., Dorahy, D.J., Greive, S.J., Burns, G.F. and Barry, R.D. 1997a. Mouse cells expressing human intercellular adhesion molecule-1 are susceptible to infection by coxsackievirus A21. *J Virol.* **71**(1), pp.785-789.
Shafren, D.R., Dorahy, D.J., Ingham, R.A., Burns, G.F. and Barry, R.D. 1997b. Coxsackievirus A21 binds to decay-accelerating factor but requires intercellular adhesion molecule 1 for cell entry. *J Virol.* **71**(6), pp.4736-4743.

Shafren, D.R., Sylvester, D., Johansson, E.S., Campbell, I.G. and Barry, R.D. 2005. Oncolysis of human ovarian cancers by echovirus type 1. *Int J Cancer.* **115**(2), pp.320-328.
Sharp, D.W. and Lattime, E.C. 2016. Recombinant Poxvirus and the Tumor Microenvironment: Oncolysis, Immune Regulation and Immunization. *Biomedicines.* **4**(3).
Shatkin, A.J., Sipe, J.D. and Loh, P. 1968. Separation of ten reovirus genome segments by polyacrylamide gel electrophoresis. *J Virol.* **2**(10), pp.986-991.
Shi, Y., He, X., Zhu, G., Tu, H., Liu, Z., Li, W., Han, S., Yin, J., Peng, B. and Liu, W. 2015. Coxsackievirus A16 elicits incomplete autophagy involving the mTOR and ERK pathways. *PLoS One.* **10**(4), pe0122109.
Shinde, S., Wu, Y., Guo, Y., Niu, Q., Xu, J., Grewal, I.S., Flavell, R. and Liu, Y. 1996. CD40L is important for induction of, but not response to, costimulatory activity. ICAM-1 as the second costimulatory molecule rapidly up-regulated by CD40L. *The Journal of Immunology.* **157**(7), pp.2764-2768.
Showkat, M., Beigh, M.A. and Andrabi, K.I. 2014. mTOR Signaling in Protein Translation Regulation: Implications in Cancer Genesis and Therapeutic Interventions. *Mol Biol Int.* **2014**, p686984.
Singh, P.K., Doley, J., Kumar, G.R., Sahoo, A.P. and Tiwari, A.K. 2012. Oncolytic viruses & their specific targeting to tumour cells. *Indian J Med Res.* **136**(4), pp.571-584.
Skelding, K.A., Barry, R.D. and Shafren, D.R. 2009. Systemic targeting of metastatic human breast tumor xenografts by Coxsackievirus A21. *Breast Cancer Res Treat.* **113**(1), pp.21-30.
Sokolowski, N.A., Rizos, H. and Diefenbach, R.J. 2015. Oncolytic virotherapy using herpes simplex virus: how far have we come? *Oncolytic Virother.* **4**, pp.207-219.
Solal-Celigny, P., Roy, P., Colombat, P., White, J., Armitage, J.O., Arranz-Saez, R., Au, W.Y., Bellei, M., Brice, P., Caballero, D., Coiffier, B., Conde-Garcia, E., Doyen, C., Federico, M., Fisher, R.I., Garcia-Conde, J.F., Guglielmi, C., Hagenbeek, A., Haioun, C., LeBlanc, M., Lister, A.T., Lopez-Guillermo, A., McLaughlin, P., Milpied, N., Morel, P., Mounier, N., Proctor, S.J., Rohatiner, A., Smith, P., Soubeyran, P., Tilly, H., Vitolo, U., Zinzani, P.L., Zucca, E. and Montserrat, E. 2004. Follicular lymphoma international prognostic index. *Blood.* **104**(5), pp.1258-1265.
Solimando, A.G., Brandl, A., Mattenheimer, K., Graf, C., Ritz, M., Ruckdeschel, A., Stuhmer, T., Mokhtari, Z., Rudelius, M., Dotterweich, J., Bittrich, M., Desantis, V., Ebert, R., Trerotoli, P., Frassanito, M.A., Rosenwald, A., Vacca, A., Einsele, H., Jakob, F. and Beilhack, A. 2018. JAM-A as a prognostic factor and new therapeutic target in multiple myeloma. *Leukemia.* **32**(3), pp.736-743.
Springer, T.A. 1995. Traffic signals on endothelium for lymphocyte recirculation and leukocyte emigration. *Annu Rev Physiol.* **57**, pp.827-872.
Stojdl, D.F., Lichty, B., Knowles, S., Marius, R., Atkins, H., Sonenberg, N. and Bell, J.C. 2000. Exploiting tumor-specific defects in the interferon pathway with a previously unknown oncolytic virus. *Nature Medicine.* **6**, p821.
Strong, J.E., Coffey, M.C., Tang, D., Sabinin, P. and Lee, P.W. 1998. The molecular basis of viral oncolysis: usurpation of the Ras signaling pathway by reovirus. *Embo j.* **17**(12), pp.3351-3362.
Sugano, Y., Takeuchi, M., Hirata, A., Matsushita, H., Kitamura, T., Tanaka, M. and Miyajima, A. 2008. Junctional adhesion molecule-A, JAM-A, is a novel cell-

surface marker for long-term repopulating hematopoietic stem cells. *Blood.* **111**(3), pp.1167-1172.
Sun, S., Zhang, X., Tough, D.F. and Sprent, J. 1998. Type I interferon-mediated stimulation of T cells by CpG DNA. *J Exp Med.* **188**(12), pp.2335-2342.
Tacar, O., Sriamornsak, P. and Dass, C.R. 2013. Doxorubicin: an update on anticancer molecular action, toxicity and novel drug delivery systems. *J Pharm Pharmacol.* **65**(2), pp.157-170.
Takeuchi, O. and Akira, S. 2010. Pattern recognition receptors and inflammation. *Cell.* **140**(6), pp.805-820.
Tan, V.P. and Miyamoto, S. 2016. Nutrient-sensing mTORC1: Integration of metabolic and autophagic signals. *J Mol Cell Cardiol.* **95**, pp.31-41.
Terstappen, L.W., Nguyen, M., Lazarus, H.M. and Medof, M.E. 1992. Expression of the DAF (CD55) and CD59 antigens during normal hematopoietic cell differentiation. *J Leukoc Biol.* **52**(6), pp.652-660.
Terui, Y., Sakurai, T., Mishima, Y., Mishima, Y., Sugimura, N., Sasaoka, C., Kojima, K., Yokoyama, M., Mizunuma, N., Takahashi, S., Ito, Y. and Hatake, K. 2006. Blockade of bulky lymphoma-associated CD55 expression by RNA interference overcomes resistance to complement-dependent cytotoxicity with rituximab. *Cancer Sci.* **97**(1), pp.72-79.
The Human Protein Atlas. 2017. ICAM1.
Thirukkumaran, C.M., Luider, J.M., Stewart, D.A., Cheng, T., Lupichuk, S.M., Nodwell, M.J., Russell, J.A., Auer, I.A. and Morris, D.G. 2003. Reovirus oncolysis as a novel purging strategy for autologous stem cell transplantation. *Blood.* **102**(1), pp.377-387.
Thirukkumaran, C.M., Nodwell, M.J., Hirasawa, K., Shi, Z.Q., Diaz, R., Luider, J., Johnston, R.N., Forsyth, P.A., Magliocco, A.M., Lee, P., Nishikawa, S., Donnelly, B., Coffey, M., Trpkov, K., Fonseca, K., Spurrell, J. and Morris, D.G. 2010. Oncolytic viral therapy for prostate cancer: efficacy of reovirus as a biological therapeutic. *Cancer Res.* **70**(6), pp.2435-2444.
Thirukkumaran, C.M., Shi, Z.Q., Luider, J., Kopciuk, K., Gao, H., Bahlis, N., Neri, P., Pho, M., Stewart, D., Mansoor, A. and Morris, D.G. 2012. Reovirus as a viable therapeutic option for the treatment of multiple myeloma. *Clin Cancer Res.* **18**(18), pp.4962-4972.
Thirukkumaran, C.M., Shi, Z.Q., Luider, J., Kopciuk, K., Gao, H., Bahlis, N., Neri, P., Pho, M., Stewart, D., Mansoor, A. and Morris, D.G. 2013. Reovirus modulates autophagy during oncolysis of multiple myeloma. *Autophagy.* **9**(3), pp.413-414.
Thorley-Lawson, D., Deitsch, K.W., Duca, K.A. and Torgbor, C. 2016. The Link between Plasmodium falciparum Malaria and Endemic Burkitt's Lymphoma-New Insight into a 50-Year-Old Enigma. *PLoS Pathog.* **12**(1), pe1005331.
Touitou, V.r., Daussy, C.c., Bodaghi, B., Camelo, S., de Kozak, Y., Lehoang, P., Naud, M.-C., Varin, A., Thillaye-Goldenberg, B., Merle-Béral, H.l.n., Fridman, W.H., Sautès-Fridman, C. and Fisson, S. 2007. Impaired Th1/Tc1 Cytokine Production of Tumor-Infiltrating Lymphocytes in a Model of Primary Intraocular B-Cell Lymphoma. *Investigative Ophthalmology & Visual Science.* **48**(7), pp.3223-3229.
Traub, S., Nikonova, A., Carruthers, A., Dunmore, R., Vousden, K.A., Gogsadze, L., Hao, W., Zhu, Q., Bernard, K., Zhu, J., Dymond, M., McLean, G.R., Walton, R.P., Glanville, N., Humbles, A., Khaitov, M., Wells, T., Kolbeck, R., Leishman, A.J., Sleeman, M.A., Bartlett, N.W. and Johnston, S.L. 2013. An

Anti-Human ICAM-1 Antibody Inhibits Rhinovirus-Induced Exacerbations of Lung Inflammation. *PLoS Pathogens.* **9**(8), pe1003520.
Triantafilou, K., Orthopoulos, G., Vakakis, E., Ahmed, M.A., Golenbock, D.T., Lepper, P.M. and Triantafilou, M. 2005. Human cardiac inflammatory responses triggered by Coxsackie B viruses are mainly Toll-like receptor (TLR) 8-dependent. *Cell Microbiol.* **7**(8), pp.1117-1126.
Tsang, J.J. and Atkins, H.L. 2015. The ex vivo purge of cancer cells using oncolytic viruses: recent advances and clinical implications. *Oncolytic Virother.* **4**, pp.13-23.
Tsang, R.W. and Gospodarowicz, M.K. 2005. Radiation therapy for localized low-grade non-Hodgkin's lymphomas. *Hematol Oncol.* **23**(1), pp.10-17.
Tumilasci, V.F., Oliere, S., Nguyen, T.L., Shamy, A., Bell, J. and Hiscott, J. 2008. Targeting the apoptotic pathway with BCL-2 inhibitors sensitizes primary chronic lymphocytic leukemia cells to vesicular stomatitis virus-induced oncolysis. *J Virol.* **82**(17), pp.8487-8499.
Uchida, J., Hamaguchi, Y., Oliver, J.A., Ravetch, J.V., Poe, J.C., Haas, K.M. and Tedder, T.F. 2004. The innate mononuclear phagocyte network depletes B lymphocytes through Fc receptor-dependent mechanisms during anti-CD20 antibody immunotherapy. *J Exp Med.* **199**(12), pp.1659-1669.
UniProt. 2008. UniProtKB - P22055 (POLG_CXA21).
Vaha-Koskela, M. and Hinkkanen, A. 2014. Tumor Restrictions to Oncolytic Virus. *Biomedicines.* **2**(2), pp.163-194.
Valaperti, A., Nishii, M., Liu, Y., Naito, K., Chan, M., Zhang, L., Skurk, C., Schultheiss, H.P., Wells, G.A., Eriksson, U. and Liu, P.P. 2013. Innate immune interleukin-1 receptor-associated kinase 4 exacerbates viral myocarditis by reducing CCR5(+) CD11b(+) monocyte migration and impairing interferon production. *Circulation.* **128**(14), pp.1542-1554.
van den Broek, M.F., Muller, U., Huang, S., Aguet, M. and Zinkernagel, R.M. 1995. Antiviral defense in mice lacking both alpha/beta and gamma interferon receptors. *J Virol.* **69**(8), pp.4792-4796.
Veres, G., Helin, T., Arato, A., Färkkilä, M., Kantele, A., Suomalainen, H. and Savilahti, E. 2001. Increased Expression of Intercellular Adhesion Molecule-1 and Mucosal Adhesion Molecule α4β7 Integrin in Small Intestinal Mucosa of Adult Patients with Food Allergy. *Clinical Immunology.* **99**(3), pp.353-359.
Veuillen, C., Aurran-Schleinitz, T., Castellano, R., Rey, J., Mallet, F., Orlanducci, F., Pouyet, L., Just-Landi, S., Coso, D., Ivanov, V., Carcopino, X., Bouabdallah, R., Collette, Y., Fauriat, C. and Olive, D. 2012. Primary B-CLL resistance to NK cell cytotoxicity can be overcome in vitro and in vivo by priming NK cells and monoclonal antibody therapy. *J Clin Immunol.* **32**(3), pp.632-646.
Vidal, L., Pandha, H.S., Yap, T.A., White, C.L., Twigger, K., Vile, R.G., Melcher, A., Coffey, M., Harrington, K.J. and DeBono, J.S. 2008. A phase I study of intravenous oncolytic reovirus type 3 Dearing in patients with advanced cancer. *Clin Cancer Res.* **14**(21), pp.7127-7137.
Villalona-Calero, M.A., Lam, E., Otterson, G.A., Zhao, W., Timmons, M., Subramaniam, D., Hade, E.M., Gill, G.M., Coffey, M., Selvaggi, G., Bertino, E., Chao, B. and Knopp, M.V. 2016. Oncolytic reovirus in combination with chemotherapy in metastatic or recurrent non-small cell lung cancer patients with KRAS-activated tumors. *Cancer.* **122**(6), pp.875-883.
Viralyitics. 2016. Disease Control Rate of 78 Percent Shown in Phase 1b MITCI Clinical Trial.

ViralZone. 2015. Enterovirus.
Voorzanger-Rousselot, N., Alberti, L. and Blay, J.Y. 2006. CD40L induces multidrug resistance to apoptosis in breast carcinoma and lymphoma cells through caspase independent and dependent pathways. *BMC Cancer.* **6**, p75.
Voorzanger-Rousselot, N., Favrot, M. and Blay, J.Y. 1998. Resistance to cytotoxic chemotherapy induced by CD40 ligand in lymphoma cells. *Blood.* **92**(9), pp.3381-3387.
Walker, K.B., Potter, J.M. and House, A.K. 1987. Interleukin 2 synthesis in the presence of steroids: a model of steroid resistance. *Clin Exp Immunol.* **68**(1), pp.162-167.
Walsh, D., Mathews, M.B. and Mohr, I. 2013. Tinkering with translation: protein synthesis in virus-infected cells. *Cold Spring Harb Perspect Biol.* **5**(1), pa012351.
Walsh, D. and Mohr, I. 2006. Assembly of an active translation initiation factor complex by a viral protein. *Genes Dev.* **20**(4), pp.461-472.
Wang, F., Liu, J., Robbins, D., Morris, K., Sit, A., Liu, Y.Y. and Zhao, Y. 2011. Mutant p53 exhibits trivial effects on mitochondrial functions which can be reactivated by ellipticine in lymphoma cells. *Apoptosis.* **16**(3), pp.301-310.
Wang, J. and Ke, X.-Y. 2011. The Four types of Tregs in malignant lymphomas. *Journal of Hematology & Oncology.* **4**(1), p50.
Wang, J., Li, F., Zheng, M., Sun, R., Wei, H. and Tian, Z. 2012. Lung natural killer cells in mice: phenotype and response to respiratory infection. *Immunology.* **137**(1), pp.37-47.
Wang, J.P., Asher, D.R., Chan, M., Kurt-Jones, E.A. and Finberg, R.W. 2007. Cutting Edge: Antibody-mediated TLR7-dependent recognition of viral RNA. *J Immunol.* **178**(6), pp.3363-3367.
Ward, J.M., Ratliff, M.L., Dozmorov, M.G., Wiley, G., Guthridge, J.M., Gaffney, P.M., James, J.A. and Webb, C.F. 2016. Human effector B lymphocytes express ARID3a and secrete interferon alpha. *J Autoimmun.* **75**, pp.130-140.
Waterhouse, N.J., Sutton, V.R., Sedelies, K.A., Ciccone, A., Jenkins, M., Turner, S.J., Bird, P.I. and Trapani, J.A. 2006. Cytotoxic T lymphocyte-induced killing in the absence of granzymes A and B is unique and distinct from both apoptosis and perforin-dependent lysis. *J Cell Biol.* **173**(1), pp.133-144.
Weiner, G.J. 2010. Rituximab: mechanism of action. *Semin Hematol.* **47**(2), pp.115-123.
Weledji, E.P. and Orock, G.E. 2015. Surgery for Non-Hodgkin's Lymphoma. *Oncol Rev.* **9**(1), p274.
Wendel, M., Galani, I.E., Suri-Payer, E. and Cerwenka, A. 2008. Natural killer cell accumulation in tumors is dependent on IFN-gamma and CXCR3 ligands. *Cancer Res.* **68**(20), pp.8437-8445.
Wenzel, S.S., Grau, M., Mavis, C., Hailfinger, S., Wolf, A., Madle, H., Deeb, G., Dorken, B., Thome, M., Lenz, P., Dirnhofer, S., Hernandez-Ilizaliturri, F.J., Tzankov, A. and Lenz, G. 2013. MCL1 is deregulated in subgroups of diffuse large B-cell lymphoma. *Leukemia.* **27**(6), pp.1381-1390.
Westin, J.R. 2014. Status of PI3K/Akt/mTOR pathway inhibitors in lymphoma. *Clin Lymphoma Myeloma Leuk.* **14**(5), pp.335-342.
White, C.L., Twigger, K.R., Vidal, L., De Bono, J.S., Coffey, M., Heinemann, L., Morgan, R., Merrick, A., Errington, F., Vile, R.G., Melcher, A.A., Pandha, H.S. and Harrington, K.J. 2008. Characterization of the adaptive and innate immune

response to intravenous oncolytic reovirus (Dearing type 3) during a phase I clinical trial. *Gene Ther.* **15**(12), pp.911-920.
Willard-Mack, C.L. 2006. Normal structure, function, and histology of lymph nodes. *Toxicol Pathol.* **34**(5), pp.409-424.
Woller, N., Gurlevik, E., Ureche, C.I., Schumacher, A. and Kuhnel, F. 2014. Oncolytic viruses as anticancer vaccines. *Front Oncol.* **4**, p188.
Wollmann, G., Robek, M.D. and van den Pol, A.N. 2007. Variable deficiencies in the interferon response enhance susceptibility to vesicular stomatitis virus oncolytic actions in glioblastoma cells but not in normal human glial cells. *J Virol.* **81**(3), pp.1479-1491.
Wongthida, P., Diaz, R.M., Galivo, F., Kottke, T., Thompson, J., Pulido, J., Pavelko, K., Pease, L., Melcher, A. and Vile, R. 2010. Type III IFN interleukin-28 mediates the antitumor efficacy of oncolytic virus VSV in immune-competent mouse models of cancer. *Cancer Res.* **70**(11), pp.4539-4549.
Workman, P., Aboagye, E.O., Balkwill, F., Balmain, A., Bruder, G., Chaplin, D.J., Double, J.A., Everitt, J., Farningham, D.A., Glennie, M.J., Kelland, L.R., Robinson, V., Stratford, I.J., Tozer, G.M., Watson, S., Wedge, S.R. and Eccles, S.A. 2010. Guidelines for the welfare and use of animals in cancer research. *Br J Cancer.* **102**(11), pp.1555-1577.
Wu, D., Sanin, D.E., Everts, B., Chen, Q., Qiu, J., Buck, M.D., Patterson, A., Smith, A.M., Chang, C.-H., Liu, Z., Artyomov, M.N., Pearce, E.L., Cella, M. and Pearce, E.J. 2016. Type 1 interferons induce changes in core metabolism that are critical for immune function. *Immunity.* **44**(6), pp.1325-1336.
Xiang, Z., Li, L., Lei, X., Zhou, H., Zhou, Z., He, B. and Wang, J. 2014. Enterovirus 68 3C protease cleaves TRIF to attenuate antiviral responses mediated by Toll-like receptor 3. *J Virol.* **88**(12), pp.6650-6659.
Xiao, C., Bator, C.M., Bowman, V.D., Rieder, E., He, Y., Hebert, B., Bella, J., Baker, T.S., Wimmer, E., Kuhn, R.J. and Rossmann, M.G. 2001. Interaction of coxsackievirus A21 with its cellular receptor, ICAM-1. *J Virol.* **75**(5), pp.2444-2451.
Xu-Monette, Z.Y., Wu, L., Visco, C., Tai, Y.C., Tzankov, A., Liu, W.M., Montes-Moreno, S., Dybkaer, K., Chiu, A., Orazi, A., Zu, Y., Bhagat, G., Richards, K.L., Hsi, E.D., Zhao, X.F., Choi, W.W., Zhao, X., van Krieken, J.H., Huang, Q., Huh, J., Ai, W., Ponzoni, M., Ferreri, A.J., Zhou, F., Kahl, B.S., Winter, J.N., Xu, W., Li, J., Go, R.S., Li, Y., Piris, M.A., Moller, M.B., Miranda, R.N., Abruzzo, L.V., Medeiros, L.J. and Young, K.H. 2012. Mutational profile and prognostic significance of TP53 in diffuse large B-cell lymphoma patients treated with R-CHOP: report from an International DLBCL Rituximab-CHOP Consortium Program Study. *Blood.* **120**(19), pp.3986-3996.
Xu, P.P., Sun, Y.F., Fang, Y., Song, Q., Yan, Z.X., Chen, Y., Jiang, X.F., Fei, X.C., Zhao, Y., Leboeuf, C., Li, B., Wang, C.F., Janin, A., Wang, L. and Zhao, W.L. 2017. JAM-A overexpression is related to disease progression in diffuse large B-cell lymphoma and downregulated by lenalidomide. *Sci Rep.* **7**(1), p7433.
Yang, H., Rudge, D.G., Koos, J.D., Vaidialingam, B., Yang, H.J. and Pavletich, N.P. 2013. mTOR kinase structure, mechanism and regulation. *Nature.* **497**(7448), pp.217-223.
Yang, Z.Z., Novak, A.J., Stenson, M.J., Witzig, T.E. and Ansell, S.M. 2006a. Intratumoral CD4+CD25+ regulatory T-cell-mediated suppression of infiltrating CD4+ T cells in B-cell non-Hodgkin lymphoma. *Blood.* **107**(9), pp.3639-3646.

Yang, Z.Z., Novak, A.J., Ziesmer, S.C., Witzig, T.E. and Ansell, S.M. 2006b. Attenuation of CD8(+) T-cell function by CD4(+)CD25(+) regulatory T cells in B-cell non-Hodgkin's lymphoma. *Cancer Res.* **66**(20), pp.10145-10152.
Yashiro, M. 2008. ICAM1 (intercellular adhesion molecule 1 (CD54), human rhinovirus receptor).
Yeganeh, B., Ghavami, S., Rahim, M.N., Klonisch, T., Halayko, A.J. and Coombs, K.M. 2018. Autophagy activation is required for influenza A virus-induced apoptosis and replication. *Biochim Biophys Acta.* **1865**(2), pp.364-378.
Younes, A., Snell, V., Consoli, U., Clodi, K., Zhao, S., Palmer, J.L., Thomas, E.K., Armitage, R.J. and Andreeff, M. 1998. Elevated levels of biologically active soluble CD40 ligand in the serum of patients with chronic lymphocytic leukaemia. *Br J Haematol.* **100**(1), pp.135-141.
Yuan, J., Liu, Z., Lim, T., Zhang, H., He, J., Walker, E., Shier, C., Wang, Y., Su, Y., Sall, A., McManus, B. and Yang, D. 2009. CXCL10 inhibits viral replication through recruitment of natural killer cells in coxsackievirus B3-induced myocarditis. *Circ Res.* **104**(5), pp.628-638.
Zamai, L., Ahmad, M., Bennett, I.M., Azzoni, L., Alnemri, E.S. and Perussia, B. 1998. Natural killer (NK) cell-mediated cytotoxicity: differential use of TRAIL and Fas ligand by immature and mature primary human NK cells. *J Exp Med.* **188**(12), pp.2375-2380.
Zemp, F.J., Lun, X., McKenzie, B.A., Zhou, H., Maxwell, L., Sun, B., Kelly, J.J.P., Stechishin, O., Luchman, A., Weiss, S., Cairncross, J.G., Hamilton, M.G., Rabinovich, B.A., Rahman, M.M., Mohamed, M.R., Smallwood, S., Senger, D.L., Bell, J., McFadden, G. and Forsyth, P.A. 2013. Treating brain tumor–initiating cells using a combination of myxoma virus and rapamycin. *Neuro-Oncology.* **15**(7), pp.904-920.
Zeyaullah, M., Patro, M., Ahmad, I., Ibraheem, K., Sultan, P., Nehal, M. and Ali, A. 2012. Oncolytic viruses in the treatment of cancer: a review of current strategies. *Pathol Oncol Res.* **18**(4), pp.771-781.
Zhao, C., Lu, F., Chen, H., Zhao, X., Sun, J. and Chen, H. 2014. Dysregulation of JAM-A plays an important role in human tumor progression. *Int J Clin Exp Pathol.* **7**(10), pp.7242-7248.
Zhao, X., Rajasekaran, N., Chester, C., Yonezawa, A., Dutt, S., Coffey, M. and Kohrt, H.E. 2015. Reovirus activated NK cells show enhanced cetuximab mediated antibody-dependent cellular cytotoxicity against colorectal cancer cells. *Journal for ImmunoTherapy of Cancer.* **3**(2), pP340.
Zhao, Y.M., Zhou, Q., Xu, Y., Lai, X.Y. and Huang, H. 2008. Antiproliferative effect of rapamycin on human T-cell leukemia cell line Jurkat by cell cycle arrest and telomerase inhibition. *Acta Pharmacol Sin.* **29**(4), pp.481-488.
Zhou, G., Ye, G.J., Debinski, W. and Roizman, B. 2002. Engineered herpes simplex virus 1 is dependent on IL13Ralpha 2 receptor for cell entry and independent of glycoprotein D receptor interaction. *Proc Natl Acad Sci U S A.* **99**(23), pp.15124-15129.
Zhu, J. and Mohan, C. 2010. Toll-like receptor signaling pathways--therapeutic opportunities. *Mediators Inflamm.* **2010**, p781235.
Ziegler, S.F., Ramsdell, F. and Alderson, M.R. 1994. The activation antigen CD69. *Stem Cells.* **12**(5), pp.456-465.
Zimmermann, M., Oehler, C., Mey, U., Ghadjar, P. and Zwahlen, D.R. 2016. Radiotherapy for Non-Hodgkin's lymphoma: still standard practice and not an outdated treatment option. *Radiat Oncol.* **11**(1), p110.